

ABSTRACT

This study investigates the applicability of conceptual monthly water balance models (MWBM) originally developed for humid climates to semi-arid and arid regions. These models are based on a simplified representation of the hydrological processes and the balances of incoming and outgoing water from the catchment on a monthly time base. Based on the experience of the monthly water balance models, two new models, the 10-day Water Balance Models (DWBM) and Parsimonious Daily Rainfall-Runoff Model (PDRRM) are developed. The time step of modelling is reduced to 10 days and one day to account for the high temporal variability of hydrological variables such as rainfall and soil moisture for semi-arid and arid catchments. A stepwise parameter optimization procedure is implemented to obtain base flow parameters from hydrograph analysis. Parameter optimization is achieved by using two optimization algorithms: the VA05A (Harwell Subroutine Library, 1974) and the Shuffled Complex Algorithm (Duan, *et al.*, 1992).

A total of 20 catchments from West Africa, North East and South Africa and China are used for testing the models. The catchments used are characterized by having an extended dry period followed by short rainy period. For most catchments, the potential evaporation exceeds the amount of rainfall received for a large period of the year. Though for some catchments the annual rainfall is as high as 1000 mm, due to the short duration of the rainfall and high potential evaporation, the runoff that reaches the outlet is only 10-20 % of the rainfall.

The study of the monthly water balance models showed that a slight modification of the structure of the model concerning the temporal variability of the hydrological improves the performance of the models. Moreover, it is shown that a particular representation of the evaporation equation is justified and some of the discrete parameters were narrowed to a definite range of values, indicating the possible regionalization of the forms of the general equations governing the models.

The investigation on the 10 days and daily models shows that a relatively small number of parameters are sufficient to represent the rainfall-runoff relations. Further, it demonstrates that a routine devised to compute the recession coefficient for 10-days and daily rainfall-runoff model is useful to incorporate *a priori* knowledge of a catchment in hydrological modelling. The stepwise parameter optimization can be extended to daily rainfall runoff models by

hierarchically determining parameters such as the recession coefficient from hydrograph analysis and evaporation parameters from long-term water balance models. This will ease the competition of numerous parameters in the minimization of the objective function in standard optimization procedures.

Further, the developed models are implemented to extend flow data from meteorological data, to study influences of variability of flow regimes, determination of low-flow-duration curves and reservoir designs and operations.

The developed models are implemented in a software package (*VUBMOD for Windows*) for data entering, model calibration and simulation. The package facilitates the visualization of both numerical and graphical outputs for analyses. The package runs on personal computers in Windows (95/98) and Microsoft Windows NT operating systems.

ACKNOWLEDGMENTS

I would like to express my gratitude to my promoter Prof. W. Bauwens for his consistent guidance and invaluable suggestions without which the realization of this work would have been difficult.

This work has been a continuation of the research, which has been undertaken at the Laboratory of Hydrology Vrije Universiteit Brussel to develop conceptual monthly water balance models. The works of Prof. A. Van der Beken, Prof. G. Vandewiele, Dr. Xu-Yu-Chong Dr. Ni-Lar-Win and many others have been a springboard for this research. My acknowledgement extends to all of them.

I am very grateful to Prof. A. Van der Beken Director of Laboratory of Hydrology and Prof. F. De Smedt, Chairman of the IUPWARE for their keen interest academically and also for giving me an opportunity to work as a part-time at the Laboratory. My thanks also go to Mr. O. Batelaan for his friendship and encouragement. I have been very happy working with them, supporting the logistic and program co-ordination for the IUPWARE (Inter-University Programme of Water Resources Engineering) and also in the organization of four series of summer courses (1994-1997) in Microcomputer Application in Water resources Engineering.

I am indebted to Prof. J.J. Peters, Prof. G. Vandewiele, Prof. J. Marien and Dr. G. Demaree for their excellent lectures and personal discussions on various scientific topics. I am grateful to Dr. Z. Wang and Mr. A. Debebe for their valuable suggestions and discussions on this research and above all for their friendship.

I wish to acknowledge the support I received from all the technical staff of the Laboratory of Hydrology: Mrs J.Vermeulen (former secretary), Mr. E. Verbeken, Mr. E. Van den Storm, Mr. L. Dode, Mr. J. Debruyne, and Ms. Peggy Reniers. I am also grateful to Ms. Howson Louise for her time reading and correcting this manuscript. I wish to express my gratitude to Mrs C. Fronteau, Dr. F. Mwanuzi, Ms. Gemma Manache, Mr. A. Sbai, Mr. T. Belayneh Mr. T. Abebe and all former and present IUPHY/IUPWARE alumni from the different corners of the world for their valuable friendship.

I am thankful to the member of the jury: Prof. A. Van der Beken, Prof. F. De Smedt, Prof. J.Marien, Prof. J. Feyen, (Catholic University Leuven) Prof. J.W. Delleur, Purdue University, USA. for their willingness to read and evaluate this thesis.

I would like to thank the Ethiopian Ministry of Water Resources and the Zambian Government Department of Water Affairs and the Meteorological Department for providing data of the Awash and the Kafu catchments respectively. I would like to thank Prof. D. A Hughes (Rhodes University South Africa) for the data of the Tati catchment in Botswana. I wish to express my thanks to Dr. E. Servat, l'Institut Français de Recherche Scientifique pour le Développement et Coopération (ORSTOM) for the data on West African catchments and discussions on the validity of the models. Thanks are also due to Dr Q. Duan, Department of Hydrology and Water Resources, University of Arizona, Tucson, for making available the subroutines of the Shuffled Complex Evolution Algorithm.

The financial support to attend international conferences by the Research and Development Office, Vrije Universiteit Brussels, is gratefully acknowledged. The last year of my study was also sponsored by an award from the Rector-scholarship.

My earnest appreciation goes to friends and families I met in Brussels for their understanding, continuous support and advise. Having life time friends from home, who have extended their moral support for such a long time regardless of the distance has been a great help for the success of this work.

Finally, my heartfelt thanks goes to my beloved parents Mr. Moreda Game and Mrs. Walala Joro for their prayers, love and care. I am also thankful to my brothers: Eshetu, Berhan, Tesfaye, Addisu, and sisters: Aberash, Tadelech, Mulunesh, Asnakech, Tigist, Mekdes and my little niece Lelise for their true love. I am grateful to my brother in-law Dr. Mesret Yazachew for his moral support and above all, making himself available for the family during my long absence.

Fekadu Moreda

Brussels, July 1999.

TABLE OF CONTENTS

Abstract	I
Acknowledgement	iii
Table of contents	v
List of figures	x
List of tables	xiv
Abbreviations and symbols	xvi

CHAPTER 1 INTRODUCTION

1.1	General	1
1.2	Problem definition	2
1.3	Objectives of the research	4
1.4	Structure of the thesis	5

CHAPTER 2 LITERATURE REVIEW ON RAINFALL RUNOFF MODELLING

2.1	Components of the hydrological cycle	6
2.1.1	Precipitation	8
2.1.2	Evaporation and transpiration	8
2.1.3	Interception	9
2.1.4	Infiltration	9
2.1.5	Stream Flow	9
2.1.6	Hydrological characteristics of semi-arid and arid areas	10
2.2	System approach in catchment modelling	14
2.2.1	The system	14
2.2.2	Modelling concept and classification	15
2.3	Historical development of rainfall - runoff modelling	18
2.4	Time resolution of modelling	21
2.4.1	Common monthly water balance models	22
2.5	Review of the VUB monthly water balance models	24
2.5.1	Model hypothesis	24
2.5.2	Models for different input levels	29
2.5.3	Regional study of monthly water balance models	30
2.6	Summary	30

CHAPTER 3 MODEL STRUCTURES FOR DIFFERENT MODELLING TIME STEPS

3.1	Introduction	34
3.2	The monthly water balance model for semi-arid catchments	35
3.2.1	Structure of the model	35
3.2.2	Models for rainfall and temperature inputs	49
3.2.3	Parameter description	50
3.2.4	Initial soil moisture storage	51
3.3	A 10-day water balance model (DWBM)	52
3.3.1	Background	52
3.3.2	Description of the 10-day water balance model	53
3.3.3	Infiltration component	54
3.3.4	Evapotranspiration component	56
3.3.5	Percolation component	57
3.3.6	Flow components	58
3.3.7	The water balance	58
3.3.8	Parameter sets	59
3.3.9	Base flow recession parameter estimation	60
3.4	A parsimonious daily rainfall - runoff model	64
3.4.1	Background	64
3.4.2	Model structure	64
3.4.3	Properties of linear reservoirs	66
3.4.4	The Nash-Unit Hydrograph	67
3.4.5	Parameter sets	69
3.5	Data requirement and scope of application of the developed models	71

CHAPTER 4 STATISTICAL METHODS

4.1	Introduction	74
4.2	Data checking	74
4.3	Parameter estimation	77
4.3.1	Objective function	78
4.3.2	Optimization Algorithms	80
4.3.3	The VAO5A algorithm	84
4.3.4	The shuffled complex evolution algorithm	86
4.4	Model validation	90

4.4.1	Checks on significance of a parameter	92
4.4.2	Graphical comparison of simulated and observed flows	92
4.4.3	Comparison of monthly means of observed and computed flow	92
4.4.4	Model Efficiency	93
4.4.5	Model Quality factor	93
4.4.6	Residual Analysis	95
4.4.7	Sensitivity to calibration period	96

CHAPTER 5 CASE STUDIES OF MONTHLY WATER BALANCE MODELS FOR SEMI-ARID AND ARID CATCHMENTS

5.1	Introduction	98
5.2	Data description	98
5.2.1	Ethiopian catchments	98
5.2.2	Chinese catchments	105
5.2.3	West African Catchments	107
5.2.4	Tanzanian catchments	109
5.2.5	Zambian catchments	109
5.2.6	Botswana catchment	111
5.2.7	Common characteristics of the test catchments	112
5.3	Monthly model application	115
5.3.1	Initial soil moisture index	115
5.3.2	Parameter optimization	116
5.3.3	Selection of the forms of the model	116
5.3.4	Summary of the results for the test catchments	129
5.3.5	Reproducing flow regimes	132
5.3.6	Water balance variables	134
5.3.7	Sensitivity of the parameters for the calibration period and extrapolation test	137
5.4	Conclusions	138

CHAPTER 6 CASE STUDIES OF THE 10-DAY WATER BALANCE MODEL

6.1	Introduction	140
6.2	Data description	140
6.3	Detailed model tests with an example catchment	143
6.3.1	Parameter optimization	143
6.3.2	Comparison of observed and computed flow	145
6.3.3	Flow components	147
6.3.4	Intermediate water balance variables	149
6.3.5	Residual analyses	150
6.4	Summary of the results for the test catchments	154
6.4.1	General performance of the models	154
6.4.1	Reproducing flow regimes	154
6.4.2	Water Balance components	156
6.5	Concluding remarks	158

CHAPTER 7 CASE STUDIES OF DAILY RAINFALL RUNOFF MODELS

7.1	Introduction	160
7.2	Models from literature	161
7.2.1	The XNJ model	161
7.2.2	The Soil Moisture Accounting and Routing (SMAR) model.	161
7.2.3	The NAM model	163
7.3	Application of the rainfall-runoff models	164
7.3.1	Calibration of the models	164
7.3.2	Comparison of performance of the models	166
7.4	Comparison of the PDRRM with the 10 days and monthly models	173
7.5	Concluding remarks	175

CHAPTER 8 PRACTICAL APPLICATION OF THE DEVELOPED MODEL

8.1	Introduction	176
8.2	Influences of the variability of rainfall on flow regimes	179
8.2.1	Introduction	179
8.2.2	Annual rainfall variability	180
8.2.3	Influence of rainfall timing on flow regimes	182
8.2.4	Influence of long -term rainfall variability on flow regimes	183
8.2.5	Conclusions	185
8.3	Low flow - duration - return period curves	186
8.4	Reservoir capacity design	188

CHAPTER 9 SUMMARY CONCLUSIONS AND RECOMMENDATIONS

9.1	Summary	190
9.2	Conclusions	191
9.2.1	Monthly water balance models	191
9.2.2	10 days water balance models	192
9.2.3	Daily rainfall runoff models	192
9.2.4	Practical application of the models	193
9.3	Recommendations	194

REFERENCES

APPENDIX A THE VUBMOD FOR WINDOWS

APPENDIX B ORDERS OF MAGNITUDE OF THE MODEL PARAMETERS

LIST OF FIGURES

Figure 2.1 Elements of the hydrologic cycle (Chow <i>et al.</i> , 1988)	7
Figure 2.2 Schematic representation of the land phase of the water Cycle (after Starosolszky, 1987)	10
Figure 2.3 Diagrammatic representation of a system	14
Figure 2.4 Model classification according to <i>a priori</i> knowledge. (after Todini, 1988).	16
Figure 2.5 Classification of models (Chow et al 1988)	17
Figure 2. 6 Diagrammatic representation of the VUB monthly water balance model.	25
Figure 3.1 Conceptual representation of the monthly water balance variables.	36
Figure 3.2 Conceptual representation of the monthly water balance model.	36
Figure 3.3 Influences of evaporation parameter for evaporation equation 3.1.	40
Figure 3.4 Influences of evaporation parameter for evaporation equation 3.2	40
Figure 3.5 Typical monthly rainfall series of humid climate (e.g. from KleineNete catchment, Belgium)	43
Figure 3. 6 Typical evolution of soil moisture storage in response to humid climate precipitation. (e.g. from Kleine Nete catchment, Belgium)	43
Figure 3.7 Typical monthly rainfall series. (E.g. of Faleme River, Senegal)	44
Figure 3. 8 Typical evolution of soil moisture storage in response to strong contrast between rainy and dry season (E.g. of Faleme River, Senegal)	44
Figure 3.9 Physical description of the flow components (Xu, 1988)	46
Figure 3.10 Conceptual representation of the 10-day water balance model.	54
Figure 3.11 Evolution of the infiltration rate	55
Figure 3.12 Relationship between infiltration and soil moisture storage.	56
Figure 3.13 Example of parallel recession curves (Mwambashi catchment, Zambia).	62
Figure 3.14 Example of normalized recession hydrographs (Mwambashi catchment, Zambia)	62
Figure 3.15 Flow-chart for recession parameter estimation	63
Figure 3.16 Conceptual representation of the daily rainfall runoff model.	65
Figure 4.1 Response surface A: one parameter model; B: two-parameter mode	181
Figure 5.1 Location of Awash River Basin	100
Figure 5.2 10-days moving average of rainfall at Addis Ababa and Sebeta stations.	102
Figure 5.3 Typical comparison of hydrograph of Awash River at Melka Kuntre and Hombole stations (1988)	106
Figure 5.4 Over estimation of rating curves in extrapolation (Modjo River at Modjo)	106
Figure 5.5 Location of West African basins under study	108

Figure 5.6 Location of Ruaha Catchment (Tanzania)	110
Figure 5.7 Location of Kafu catchments. (Zambia)	110
Figure 5.8 Location of Tati catchment, (Botswana).	111
Figure 5.9 Location of the study areas in Africa.	112
Figure 5.10 Long term monthly pan evaporation, precipitation and flow for some of the study catchments	114
Figure 5.11 Time series of Input data (Boa Catchment, Ivory Coast)	117
Figure 5.12 Plot of the parameter and the sum of squares of error in the neighborhood of the optimum value. (Boa catchment -modeled with MWBM-B)	121
Figure 5.13 Comparison of observed and modeled flow with the two variants of monthly water balance models (Boa catchment)	122
Figure 5.14 Residual versus rainfall MWBM-A. (Boa Catchment, Ivory Coast)	124
Figure 5.15 Residual versus rainfall MWBM-B (Boa Catchment, Ivory Coast)	124
Figure 5.16 Residual versus computed flow MWBM-A. (Boa Catchment, Ivory Coast)	125
Figure 5.17 Residual versus computed flow MWBM-B. (Boa Catchment, Ivory Coast)	125
Figure 5.18 Residual versus Potential evapotranspiration MWBM-A. (Boa Catchment, Ivory Coast)	126
Figure 5.19 Residual versus Potential evapotranspiration MWBM-B. (Boa Catchment, Ivory Coast)	126
Figure 5.20 Auto correlation of residuals from MWBM-A. (Boa Catchment, Ivory Coast)	127
Figure 5.21 Time series plot of residuals. (Boa Catchment, Ivory Coast)	127
Figure 5.22 Comparison soil moisture evolution flow with the two variants of monthly water balance models (Boa Catchment, Ivory Coast)	128
Figure 5.23 Comparison of the actual evaporation with the two variants of monthly water balance models. (Boa Catchment, Ivory Coast)	128
Figure 5.24 Flow components using MWBM-A. (Boa Catchment, Ivory Coast).	129
Figure 5.25 Flow components using MWBM-B. (Boa Catchment, Ivory Coast).	129
Figure 5.26 Ranges of estimates of parameter for MWBM-A (left) and MWBM-B (right)	132
Figure 5.27 Comparison of seasonal observed and simulated monthly flows using MWBM-A and MWBM-B.	133
Figure 5.28 Proportion of water balances variables for East African catchments	135
Figure 5.29 Proportion of water balances for West African catchments	135
Figure 5.30 Proportion of water balances for South African catchments	136
Figure 5.31 Proportion of water balances for Chines catchments	136
Figure 5.32 Comparison of observed and computed flow for the calibration period (Awash -Hombole)	138
Figure 5.33 Comparison of observed and computed flow for the verification period	

(Awash -Hombole)	138
Figure 6.1 10-day long-term mean of rainfall and flow for the study catchments	142
Figure 6.2 Time series of rainfall, evaporation and flow data for calibration (Awash -Hombole)	143
Figure 6.3 Plot of the parameter and the sum of squares of error in the neighborhood of optimum value. (left: MWBM-B, and right DWBM).	146
Figure 6.4 Comparison of observed and modeled flow with MWBM and DWBM (Awash-Hombole)	147
Figure 6.5 Flow components using MWBM-B. (Awash-Hombole)	148
Figure 6.6 Flow components using DWBM (Awash-Hombole)	148
Figure 6.7 Comparison of soil moisture storage evolution with MWBM-B and DWBM. (Awash-Hombole)	149
Figure 6. 8 Comparison of 10-day actual evaporation with MWBM-B and DWBM. (Awash-Hombole)	149
Figure 6.9 Residual versus rainfall using MWBM-B.(Awash-Hombole)	150
Figure 6.10 Residual versus rainfall using DWBM. (Awash-Hombole)	150
Figure 6.11 Residual versus potential evapotranspiration using MWBM-B. (Awash-Hombole)	151
Figure 6.12 Residual versus potential evapotranspiration DWBM. (Awash-Hombole)	151
Figure 6.13 Residual versus computed flow using MWBM-B. (Awash-Hombole)	152
Figure 6.14 Residual versus computed flow using DWBM. (Awash-Hombole).	152
Figure 6.15 Time series plot of residuals. (Awash-Hombole)	153
Figure 6.16 Autocorrelation of residuals for DWBM. (Awash-Hombole)	153
Figure 6.17 Comparison of long-term 10 day mean observed and computed flow using MWBM-A and DWBAM.	156
Figure 6.18 Proportion of water balance s using DWBM.	157
Figure 6.19 Comparison of monthly observed and computed flow using the MWBAM and the DWBM. (Awash -Hombole)	159
Figure 7.1 A comparison of scatter plots of the observed and computed flow for the four models (Awash River at Hombole).	169
Figure 7.2 Comparison of observed and computed hydrographs for the Awash-Hombole catchment. (Typical year 1986.)	171
Figure 7.3 Comparison of observed and estimated flows for Awash-Melka catchment	172
Figure 7.4 Comparison of observed and estimated flows Berga catchment	172
Figure 7.5 Comparison of the daily rainfall-runoff and the 10-day water balance models (Awash-Hombole)	174
Figure 7.6 Comparison of the daily rainfall-runoff, the 10-day and monthly water balance models (Awash-Hombole)	174

Figure 8.1 Schematic representation of extension of flow.	177
Figure 8.2 Relationship between areal and Addis Ababa monthly rainfall.	178
Figure 8.3 Time series comparison of long –term rainfall series and modeled annual flows	179
Figure 8.4 Annual variability of rainfall at Addis Ababa station.	181
Figure 8.5 Annual variability of Awash River flow at Hombole	182
Figure 8.6 Departure of annual and summer rainfall from long term means on decade basis.	184
Figure 8.7 Departure of annual and summer flow from long-term means on decade basis.	184
Figure 8.8 Departure of annual base flow and low flow from long term means on decade basis.	185
Figure 8.9 Low flow duration -return period relationships for Awash River at Hombole (1963-1992)	187
Figure 8.10 Low flow duration -return period relationships for Awash River at Hombole. (1900-1995)	187
Figure 8.11 Return period versus reservoir capacity using the extended flow series for given demands. (Awash River at Hombole).	189

LIST OF TABLES

Table 2.1 Relationship between time step of modelling and area of catchment	22
Table 2.2 Common monthly water balance models	24
Table 2.3 model types and input requirements	30
Table 3.1 Description of parameters of monthly water balance model.	50
Table 3.2 Ranges of values of hydraulic conductivity	55
Table 3.3 Parameters of the 10-days water balance model	60
Table 3.4 Description of parameters of the daily rainfall-runoff model	71
Table 4.1 Inputs of the VA05A optimization method	86
Table 4.2 Inputs of the Shuffled complex optimization method	89
Table 4.3 Some 5 % points of the Chi-square distribution with n degrees of freedom.	97
Table 5.1 Description of daily rainfall data in upper Awash River Basin	101
Table 5.2 Cross-correlation between monthly rainfall data of stations in the upper Awash River Basin	102
Table 5.3 Pan evaporation daily data	103
Table 5.4 Daily River flow data	103
Table 5.5 Stage-discharge relationships rating curves for different periods	103
Table 5.6 Characteristics of the test catchments and available data on monthly time step	112
Table 5.7 Representation of different warming up period	115
Table 5.8 Influences of length of warming period on initial soil moisture storage using MWBM-A ($IR=2$, $b_1=2$, $b_2=2$)	116
Table 5.9 Example application of the MWBM-A	117
Table 5.10 Example application of the MWBM-B	118
Table 5.11 Summary of results for all 18 variants of the model WBAM-A. (Boa Catchment, Ivory Coast)	119
Table 5.12 Summary of results for all 18 variants of the WBAM-B. (Boa Catchment, Ivory Coast)	119
Table 5.13 Parameter estimates for MWBM-A ($IR=2$, $b_1=b_2=2.0$)	131
Table 5.14 Parameter estimates for MWBM-B ($IR=2$, $b_1=b_2=2.0$)	131
Table 5.15 Comparison of parameter estimates and water balance variables for the three sets of data (Awash catchment the discrete parameters: $b_1=2$, $b_2=2$)	137

Table 6.1 Test catchments for 10-day time step modelling	141
Table 6.2 Parameter estimates of the MWBM-B and DWBM for Awash -Hombole)	145
Table 6.3 Table Parameter estimates for the MWBM-B with 10-day time step	155
Table 6.4 Parameter estimates for the DWBM	155
Table 7.1 Description of XNJ model parameters (Zhao <i>et al.</i> , 1980)	162
Table 7.2 Description of SMAR model parameters (O’Connell <i>et al.</i> , 1970)	163
Table 7.3 Parameters of the NAM model (Ref. Danish Hydraulic Institute, 1982)	164
Table 7.4 Calibration periods	164
Table 7.5 Model parameters: The XNJ Model	165
Table 7.6 The SMAR Model parameters	165
Table 7.7 The NAM Model parameters	166
Table 7.8 The PDRRM Model parameters	166
Table 7.9 Comparison of statistics of the studied models	168
Table 8.1 Rainfall Variability during the last 9 decades based on Addis Ababa observations.	181
Table 8.2 Cross correlation coefficients of rainfall and flow regimes	183

Abbreviations

Bias	Bias of the residual series
DWBM	Decade (10-day) water balance model
CI	Confidence interval
Ef.	Model Efficiency as defined by Nash and Sutcliffe, (1970)
HMLE	Heteroscedastic Maximum Likelihood Estimator
HWCI	Half width of confidence interval
MQ	Model quality factor
MWBM	Monthly water balance model
MWBM-A	Monthly water balance model variant A (without upper limit for soil moisture storage)
MWBM-B	Monthly water balance model variant B (without upper limit for soil moisture storage)
NAM	Danish Hydraulic Institute rainfall-runoff model
PDRRM	Parsimonious daily rainfall -runoff model
RMSE	Root mean square error
SHU-CA	Shuffled complex Algorithm
SMAR	Soil Moisture Accounting and Routing
VAO5A	Optimization algorithm from Harwell Subroutine Library (1974)
XNJ	XINJIANG Daily rainfall-runoff model

Symbols

$(a_1, a_2...)$	continuous parameters
b_t	base flow
b_1, b_2	discrete parameters
c_t	temperature
d_t	computed total flow
e_t	Potential evaporation
f_t	fast flow
g_t	groundwater storage
h_t	humidity
h_f	ordinates fast flow unit hydrograph
h_s	ordinates of slow flow unit hydrograph
I_t	infiltration
k	recession coefficient
l_t	percolation
m_t	soil moisture storage
n_t	net rain
p_t	precipitation
q_t	observed flow
r_t	actual evaporation
s_t	slow flow
w_t	available water

Chapter 1

1. INTRODUCTION

1.1	General	1
1.2	Problem definition.....	2
1.3	Objectives of the research	4
1.4	Structure of the thesis	5

1.1 General

Water resources are essential renewable resources that are the basis for existence and development of a society. Proper utilization of these resources requires assessment and management of the quantity and quality of the water resources both spatially and temporally.

Water crises caused by shortages, floods and diminishing water quality, among others, are increasing in all parts of the world. The growth of population demands for increased domestic water supplies and, at the same time, results with a higher consumption of water due to expansion in agriculture and industry. Mismanagement and lack of knowledge about existing water resources and the changing climatic conditions have consequences of an imbalance of supply and demand of water. The problem is pronounced in semi-arid and arid areas where the resources are limited.

Surface water being easy, direct and therefore less expensive to exploit in comparison to other sources like groundwater or desalinization makes it the major source of water supply for irrigation, industry and domestic uses. The surface water, in the form of lakes and river discharge (runoff) is predominately obtained from rainfall after being generated by the rainfall -

runoff processes. In order to make decisions for planning, design and control of water resource systems, long runoff series are required. The latter are not often available with reasonable length. On the other hand, for flood control and reservoir regulation future, flows shall be forecasted with rainfall runoff models. A number of rainfall runoff models exist for generation of flow, forecasting and other purposes.

Establishing a rainfall-runoff relationship is the central focus of hydrological modelling from its simple form of unit hydrograph to rather complex models based on fully dynamic flow equations. As the computing capabilities are increasing, the use of these models to simulate a catchment became a standard. Models are generally used as utility in various areas of water resource development, in assessing the available resources, in studying the impact of human interference in an area such as land use change, deforestation and other hydraulic structure such as dams and reservoirs.

1.2 Problem definition

Traditional lumped, conceptual rainfall-runoff models attempt to represent hydrological processes by mathematical equations and multiple layers of storage. These equations involve a large number of parameters, e.g., the Stanford Watershed Model IV (Crawford and Linsley, 1966) has 16 parameters, the SACRAMENTO model (Burnash *et al.*, 1973) has 21 parameters, and the XINANJIANG model (Zhao *et al.*, 1980) has 15 parameters. In applying such models, a modeler always faces the difficulty of obtaining a unique set of parameters that satisfies a certain objective, usually minimizing the sum of squares of errors between measured and model outputs. Moreover, high correlations between parameters hinder identification and result in individual parameters that lack (statistical) significance. The numerous parameters make it impossible to relate catchment characteristics to parameter values for regionalization of parameters and application of the models to ungauged catchments. This prompts researchers to develop physically based models such as the SHE model (Abott, 1986a, 1986b). Data availability for model calibration remains the bottleneck for development in this direction.

For the reasons previously described, simple conceptual rainfall-runoff models that use readily available data are applied for water resources assessment and management in areas where hydrological data are limited. Monthly water balance models (Vandewiele *et al.*, 1992) are

examples of parsimonious models that are pragmatic for application. The models developed have conceptual structures and inputs are monthly precipitation and evaporation or (mean temperature and/or mean relative humidity). The outputs are typically monthly flow and soil moisture index. The models are described with few parameters (3 to 6) and the inputs are relatively easily available at catchment scales. These models have been successfully applied in humid climate and for a few semi-arid catchments (see Xu, 1992, 1995, 1996, Vandewiele and Ni-Lar-Win, 1998).

This study focuses in extending the application of these models to semi-arid and arid catchments and also to reduce the time resolution of modelling from monthly to 10 days and one day.

Compared to humid climate there are a lot of problems in modelling hydrological process of arid and semi-arid regions, which cover a large part of the world. In general the two interrelated underpinning problems in hydrological modelling in such region are: (1) the feebleness of the model assumptions and simplifications which are inherent to any modelling in any region but lead to over simplification of the variability in arid and semi-arid areas, (2) the limitation of data availability as opposed to the temporal and spatial variability of the input to any physical or conceptual (distributed or lumped) models. Therefore there is a need of research which compromises the two problems by developing models which are not too simple to ignore the processes and yet not requiring very much detail of data that are not available in real life application.

Time resolution of modelling determines the complexity of modelling as much as the spatial resolution of modelling. One can argue that if it is possible to model with a smaller time step, the larger time steps can always be reconstructed by aggregations. Perhaps the very objectives of modelling with larger time spans are to simplify the processes prevailing in a catchment and availability of data to calibrate and eventually apply the model. Moreover, the time step of modelling depends on the potential uses of a model. A flood warning scheme of a small catchment requires modelling over shorter time spans such as minutes and hours where as a monthly water balance model would be much more handy to extend a runoff series for the purpose of reservoir capacity design. A decade model would also be good enough to study the water availability of a river flow for irrigation diversion and to study the soil water evolution in a soil, to manage crop water requirements.

1.3 Objectives of the research

The objectives of this thesis are to investigate the applicability of the models originally developed for humid climates to semi-arid and arid regions. Further, to study the peculiar hydrological phenomena in such regions, either by modification of the existing model or establishing new ones. The research also attempts to address the problem of data deficiency in such regions and hence the models developed require readily available data on a catchment scale.

The specific objectives are:

- (1) Modifying the existing models for application to different climatic and basin characteristics.
- (2) Developing a conceptual 10-day water balance model and a daily rainfall-runoff model by keeping the modelling philosophy as the monthly water balance models i.e. the model being simple and parsimonious.
- (3) Introducing step-wise parameter optimization by inferring some parameters from hydrograph analysis.
- (4) Coupling the models with modern parameter optimization techniques
- (5) Testing the models
- (6) Application of the model to real problems such as runoff extension for studies of long term changes in flow regimes, low flow analysis and reservoir capacity design.
- (7) Packaging the three models in a software system. This allows not only model calibration and simulation but also graphical visualization with formats compatible for exporting to other systems.

The present models are intended to satisfy the following guidelines for building conceptual rainfall runoff models (Van der Beken, 1977)

- The models should be representative of the regimes of a wide variety of streams
- The models should be easily applicable to different basins with existing hydrological data

- The models should be physically sound so that, in addition to stream flows, estimates of surface runoff, actual evaporation, soil moisture can be made
- The calibration procedure should be automatic or, at least, fully reproducible without ambiguity.

1.4 Structure of the thesis

This dissertation is subdivided into 9 chapters including introduction and the last chapter, which present summary, conclusions and recommendations. The first four chapters will discuss the general development of the models. Following this introduction a brief review of rainfall modelling is given in Chapter 2. Also, a historical development of rainfall runoff modelling and concepts of the VUB monthly water balance models are discussed in this chapter to lay a background of the study. The core of the thesis is presented in Chapter 3, which treats the Monthly Water Balance Model, (MWBm) for the semi-arid and arid case and gives the full development of the Decade (10-day) Water Balance Model (DWBM). Finally, it introduces the Parsimonious Daily Rainfall- Runoff Model, (PDRRM). The later two models have evolved from the concepts of the monthly water balance models. The justifications and pitfalls of the models developed are discussed. The fourth chapter discusses statistical methods applied in parameter optimization and evaluation of results.

The next three chapters present the case studies to validate the models developed in Chapter 3. Chapter 5 gives applications of the monthly water balance model to 20 catchments from 8 countries in Africa and Asia. Chapter 6 gives applications of the 10 days Water Balance model to 8 catchments from Africa. In Chapter 7, the daily models are applied to a few catchments. The results are compared to three classical conceptual rainfall runoff models namely XNJ, (Zhao *et al.*, 1980), SMAR (O'Connell *et al.*, 1970) and NAM (Danish Hydraulic Institute, 1982)

Chapter 8 presents the practical application of the developed model in three aspects: extension of flow time series for studying long term variability of flow regimes, low flow analysis and reservoir capacity design. Lastly, the summary and conclusions drawn from the study are given in chapter 9.

Chapter 2

LITERATURE REVIEW ON RAINFALL RUNOFF MODELLING

2.1	Components of the hydrological cycle.....	6
2.2	System approach in catchment modelling.....	14
2.3	Historical development of rainfall - runoff modelling.....	18
2.4	Time resolution of modelling.....	21
2.5	Review of the VUB monthly water balance models.....	24
2.6	Summary.....	30

2.1 Components of the hydrological cycle

The central focus of any hydro-meteorological study is the hydrological cycle shown in Figure 2.1. The hydrological cycle has no beginning or end and its many processes occur continuously (Chow *et al.*, 1988). In describing the cycle, the water evaporates from ocean and land surface to become part of atmosphere; water vapour is transported and lifted in the atmosphere until it condenses and precipitates on the land or the oceans. Precipitated water may be intercepted by vegetation, becomes overland flow over the ground surface, infiltrate into the ground, flow through the soil as subsurface flow and discharges into streams as surface runoff. The infiltrated water may percolate deeper to recharge groundwater, later emerging as spring and seeping into streams to form surface runoff and finally flowing into the sea or evaporating into the atmosphere as the hydrological cycle continues.

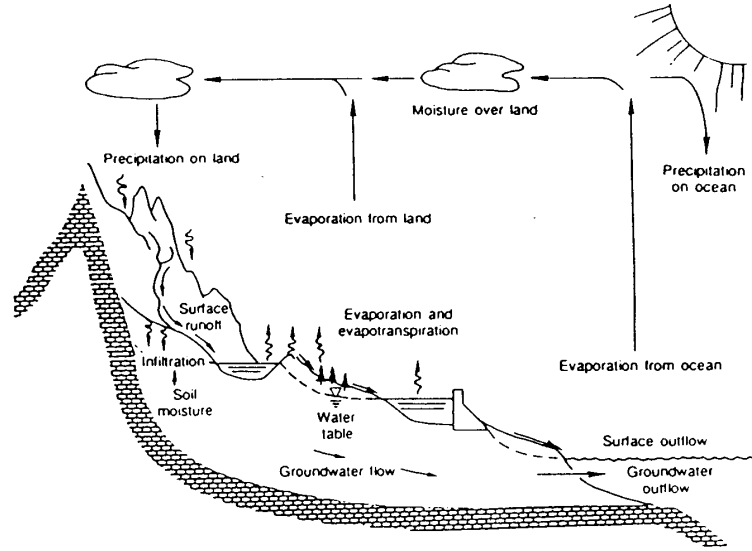


Figure 2.1 Elements of the hydrologic cycle (Chow *et al.*, 1988)

It is noted that though the concept of the cycle seems simple, the phenomena are enormously complex and intricate. It is not just one large cycle but it is rather composed of many interrelated cycles of continental, regional and local extent. The major achievement and objectives of the rainfall runoff modelling is thus to study a part (section) of the hydrological cycle, namely the land phase of the hydrological cycle on a catchment scale. Then the problem becomes to express the runoff from the catchment as a function of the rainfall and other catchment characteristics.

Considering the land phase of the hydrological cycle, any conceptual model predicates its effort on an expansion of the basic water balance or continuity equation that is:

$$I - O = \frac{ds}{dt} \quad (2.1)$$

where I is the input to the system (Precipitation), and O is output from the system (evaporation, stream and groundwater flow) and the ds/dt is the change in soil moisture. The main processes encompassed are precipitation, evapotranspiration, interception, infiltration, subsurface flow and streamflow. It is evident that before any modelling effort can be performed, one has to

understand the above physical processes, their extent of effect on the abstraction from or addition of water to a catchment.

2.1.1 Precipitation

Precipitation is the input to the system of catchment, which may have different forms, rainfall, storms, dew or any form of water landing from atmosphere. The amount of precipitation can be defined as an accumulated total volume for any selected period. Precipitation as a function of time and space is highly variable. Systematic averaging methods such as Thiessen polygon, isohyte and reciprocal distance methods have been developed to account for variations in space to obtain a representation of areal precipitation values from point observation. Singh and Chowdhury, (1986) after comparing the various methods for calculating areal averages, concluded that all methods give comparable results, especially when the time period is long. For short time step records, the conversion of a point observation to an areal rainfall has a large influence.

2.1.2 Evaporation and transpiration

Catchment evaporation demand is generally defined as that evaporation which would occur if there were no deficiencies in the availability of moisture for evapotranspiration by that area's particular plant regime. The two main factors influencing evaporation from an open water surface are the supply of energy to provide latent heat of vaporization and the ability to transport the vapour away from the evaporative surface: solar radiation and wind. Evapotranspiration from land surface comprises evaporation directly from the soil and vegetation surface and transpiration through plant leaves, in which water is abstracted from the sub soil. The third factor is the supply of moisture at evaporative surface, which brought about the definition of potential and actual evaporation. Evaporation involves a highly complex set of processes, which themselves are influenced by factors dependent on the local conditions (land use, vegetation cover, and meteorological variables). Mostly the potential evaporation is the quantity obtained either by using some simple empirical formula such as Thornthwaite, (1948), Penman formula (Penman, 1948) and a process-based model of Penman-Monteith (Monteith, 1965).

Since potential evaporation and evaporation from pans are governed by the same meteorological factors they have strong correlation. The relation between them is often give as a simple ratio.

Burnash (1995) suggests using seasonal coefficients for converting pan data to potential evaporation rather than a single coefficient. In conceptual rainfall runoff modelling one of the two terms, pan evaporation and potential evapotranspiration are equally used as input, which exerts energy to extract water from open surface or soil moisture storage.

2.1.3 Interception

The portion of rainfall intercepted by the vegetation and roofs before reaching the ground is referred to as interception. The water, which is intercepted by the leaves of vegetation and roofs eventually evaporates into atmosphere. The amount of interception could be significant in densely vegetated areas such as tropical rainforests. Such forests maintain a relatively consistent canopy and do not generally exhibit the seasonal range of interception encountered in areas where deciduous trees are dominant. It is commonly understood that if the density of the vegetation cover is sparse then this loss is insignificant.

2.1.4 Infiltration

The precipitation, which is not intercepted or evaporated from the land, will eventually infiltrate into the soil or flow as overland flow. Infiltration is one of the most difficult hydrological processes to quantify. The difficulty arises due to many physical factors affecting the rate of infiltration such as rainfall intensity, initial moisture content, soil property, etc. Some experimental and empirical formulas such as Horton (1939), Philip (1957), and others are available to compute infiltration rates during a rainfall event. Depending on the soil strata, the infiltrated water gradually percolates to the groundwater or either flows as subsurface flow supplying river or springs within the catchment.

2.1.5 Stream Flow

The rainfall that exceeds the interception requirement and infiltration starts to accumulate on the surface. Initially the excess water collects to fill depressions, until the surface detention requirement is satisfied. There after when water begins to move down slope as a thin film and tiny streams which eventually join to form bigger and bigger channels. This part of the stream flow is termed as surface runoff. The infiltrated part of the rain may sometimes come as subsurface runoff, which combined with the surface runoff, constitutes the direct runoff. Hence

the direct runoff is the result of the immediate response of a catchment to the input rainfall. The stream flow consists of the direct runoff (which lasts for hours or days depending upon the catchment size) and the base flow (that emerges from groundwater resources and also delayed subsurface runoff). The above description of the processes at catchment scale is schematically represented in Figure 2.2.

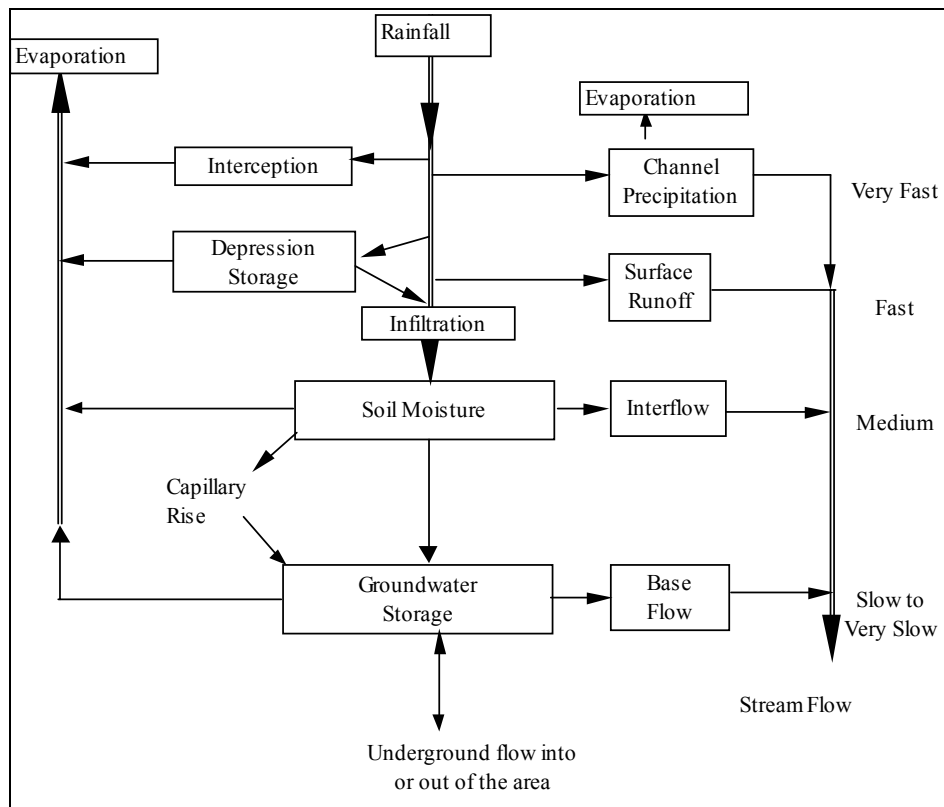


Figure 2.2 Schematic representation of the land phase of the water Cycle (after Starosolszky, 1987)

2.1.6 Hydrological characteristics of semi-arid and arid areas

In the past, several hydrologists attempted to classify zones of the world in to humid, semi arid and arid according to the climatological characteristics. One of the earliest indexes (Chow, 1964) used for classification is based upon the adequacy of precipitation in relation to the needs of plants whereby the precipitation analyzed month by month is just adequate to supply all the water for maximum evaporation and transpiration in the course of a year. UNESCO (1979) attributes the arid and semiarid zones as the dry areas associated with annual potential evaporation over 1000mm and further classifies according to the amount of annual rainfall they

receive to hyper-arid, arid semiarid and humid. Chow, (1964) suggests that in addition to climatic characteristics other features of the land surface may also be used to delimit arid zones, since the geomorphology, soils and vegetation have their own distinctive characteristics. The objective of these classifications is mainly to study the peculiar characteristics common to a region, which would help generalization and inference for climatological and hydrological processes prevailing in these regions.

The hydrological processes operating in rainfall runoff transformation for the semi-arid and arid areas differ from those in humid temperate. Some of the distinct properties manifested in semi-arid and arid catchments are pointed out below.

2.1.6.1 Variability in time

The rainfall in semi-arid and arid catchments is characterized by a high variability of the small amount received in space and time (Moore, 1989). A high percentage (about 80 percent of the annual rainfall) is received within the rainy seasons during 3 to 6 months. Individual rainfall events generally occur with high intensity and short duration storms. Verma (1979) points out some of the particular features of the semiarid and arid hydrological processes as:

- The marked seasonal variation in semiarid climates may require segregation of data by season. A combination of hydrological factors common in one season of the year may be virtually non-existent during another season.
- A particular combination of factors may exist for only a few days in several years and may render hydrological computation based on average values grossly erroneous.

Actual evaporation from semi-arid zones is a highly transient phenomenon with extreme variation within a day because of the available water but not over a season. The transient nature of evaporation is also controlled by the rapid growth of vegetation to climax followed by rapid die-off (Moore, 1989).

2.1.6.2 Variability in space

In contrast to humid climate, hydrological processes in semiarid and arid regions often vary greatly over different parts of a catchment. Especially in large catchments, the contributing area could be localized at the upper part of the catchment. In such cases, computation of areal rainfall in a lumped conceptual model leads to unrealistic average distribution over the whole area. More over, the sparse vegetation cover and its sharp response to the first rain have an impact on the evaporation process prevailing in such regions. The rivers in such regions are generally characterized by having long periods of low flow regime.

Another distinct characteristic of such regions is that in some cases infiltration could be very small due to outcropped rocks on the slopes of valleys whereas it could be high in areas with fractured bedrock channels. There could also be the possibility of channel infiltration from the bed of the rivers supplying the groundwater in lower valleys of the river (Sami, 1992). This fact implies that especially during low flow regime the stream flow that originates from upstream will be depleted by the channel bed before it reaches the outlet. Hence this phenomenon should be accounted for in formulating models based on the water balance of a catchment

2.1.6.3 Hydrological modelling inadequacy

In arid regions, an important feature of the water balance is the high proportion of incoming water which is returned to the atmosphere by evaporation from soil surface. In contrast to the humid regions, where evaporation is limited by available energy (e.g. net radiation), in the arid zone water availability is the dominant control over evaporation rates. Because of the sparse density of vegetation, direct evaporation of water from the soil is of enhanced importance, and frequently as much as half of the annual rainfall can be lost in this manner (Chow, 1964).

It is noted that the prevailing rainfall and evaporation mechanism in semi-arid and arid catchments, associated with the thin and sparse vegetation cover, alter the runoff generation of these regions in contrast to the humid regions. The runoff generated is mainly controlled by infiltration excess and is frequently localized. The runoff generated on some of the slopes and first order catchments may not always survive to contribute to the flow at the outlet of catchments of sufficient size. Hughes (1995) numerates the possible reasons why deterministic models can fail as tools for water resources estimation purposes, where failure implies the model imperfection. Apart from erroneous data inputs and poor interpretation of model results,

the problems associated with the application of rainfall- runoff models to arid and semiarid areas are:

- Inadequate or inappropriate model representation of the prevailing catchment processes
- Inadequate representation of the spatial variability of runoff generation response to runoff. While this problem can be masked by spatial lumping, it may be important if the effects are non-linear and non-stationary
- Inadequate representation of the spatial variability in rainfall input, either through lumping or lack of spatial resolution in the available data.
- Inadequate representation of the temporal variability in rainfall input through the use of a coarse time interval model. This is not always a serious problem as long as the rainfall mechanisms are reasonably consistent and the durations and intensities of the major rainfall events are similar.
- Inadequate estimation of parameter values. This problem may relate to the length of the records available for calibration (Görgens, 1983) and the extent to which the rainfall-runoff relationships reflected in the observed data are sufficiently representative to allow a suitable parameter set to be quantified

In general the two interrelated underpinning problems in hydrological modelling in such regions are:

1. the model assumptions and simplifications which are not always justified in modelling in any region but over simplification of the variability in such areas,
2. The limitation of data availability as opposed to the temporal and special variability of the input to any physical or conceptual (distributed or lumped) models.

This implies that any effort in modelling such region should consider and compromise the two underlying problems that on one hand the model has to address the peculiar phenomena and at the same time it should require limited input as only limited data are available.

2.2 System approach in catchment modelling

2.2.1 The system

The detailed processes that link the rainfall over the catchment to the stream flow, may be studied by applying physical laws that are reasonably well known. However, the complexity of the boundary conditions (i.e. the physical description of the catchment and the initial conditions and distribution of the variables) makes a solution based on the direct application of the laws of physics impracticable. Moreover, direct application of these laws requires subdividing the catchment into homogenous and isotropic regions. The sub division depends on catchment characteristics (soil type, land use, slope, vegetation cover, etc.) and these factors may also vary in space and time. For these reasons, instead of exact representation of the processes effort is directed to the construction of a model by using system concepts relating input and outputs.

A hydrologic system is defined as a structure or volume in a space, surrounded by a boundary that accepts water and other inputs, operates on them internally, and produces them as outputs. (Chow *et al.*, 1988). Schematic representation of the system operation is shown in Figure 2.3 where the symbol Ω represents a transformation between the input and the output.

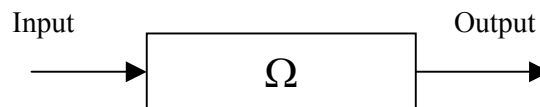


Figure 2.3 Diagrammatic representation of a system

The objective of the hydrologic system analysis is to study the system operation and to predict its output. A hydrological system model is an approximation of the actual system. Its input and output are measurable hydrological variables and its structure is the concept of the system transformation.

The system analysis approach depends on the prior supposition of a general, flexible, relationship (e.g. linear time invariant) whose expression may be obtained by the application of systems analysis methods to the records. Examples in the hydrological context include the unit hydrograph method, the linear difference equation models (Box and Jenkins, 1976), the

constrained linear system model (Natale, and Todini, 1976), the linear perturbation model (Nash, and Barsi, 1983) and many similar models are found in literature.

2.2.2 Modelling concept and classification

Based on the assumptions and concepts formulating the structure of the transformation (Operator) the resulting models may have different forms. According to Clarke, 1973 mathematical models may be classified in to four main groups.

- 1) Stochastic - Conceptual
- 2) Stochastic - Empirical
- 3) Deterministic - Conceptual
- 4) Deterministic - Empirical

Any of which may be classified as *linear* or *non-linear* in the *system theory sense*. Group 1 and 2 may be *linear* or *non-linear* in the *statistical regression sense*. The models in any group may further be classified as *lumped*, *probability distributed* or *geometrically distributed*.

If any of the variables is a random variable having a probability distribution, then the model is stochastic rather than statistical. Conversely, if all the variables are free from random variations, then the model is deterministic. The hydrological models are described as conceptual or empirical according to whether the form of the model equation is, or is not suggested by consideration of the physical processes acting up on the input variable to produce the output variables. This distinction is, however artificial since many physical laws contain empirical constants. Despite the artificiality of the distinction, it is one widely drawn in the literature, the difference between 'conceptual' and 'empirical' corresponding approximately to the O' Connell's (1966) terms 'synthetic' and 'analytic' whilst the term 'black box' used by some writers, corresponds to 'empirical'.

Linearity and non-linearity in the system analysis sense is based on the principle of superposition (Clarke 1973). A model is linear in the system analyses sense if the principle of superposition holds. The model is linear in statistical regression sense if it is linear function of the parameters to be estimated.

A lumped model ignores the spatial distribution of the input variables and parameters, which characterises the physical process. A probability-distributed model describes the spatial variation of the input variables without geometrical references to the point at which the input is measured or estimated. On the other hand a geometrically distributed model expresses the spatial variability in terms of the orientation of the network points relative to each other and their spacing.

Todini (1988) classified models based on the level of the priori knowledge on the system under study in terms of both model structure and parameters. Accordingly the recent classification groups the model in the increasing level of a priori knowledge as: 1) purely stochastic, 2) lumped integral, 3) distributed integral and 4) distributed differential. (See Figure 2.4) Chow *et al.* (1988) give classification of model based on three objectives, model account for randomness, time and space. Figure 2.5 shows possible combination of the model types.

A priori Knowledge

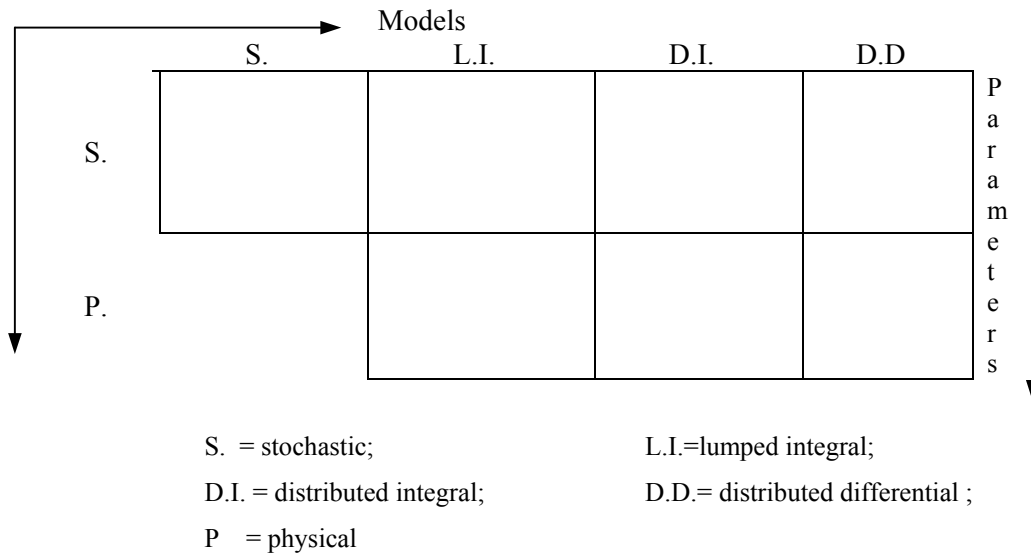


Figure 2.4 Model classification according to *a priori* knowledge. (after Todini,1988).

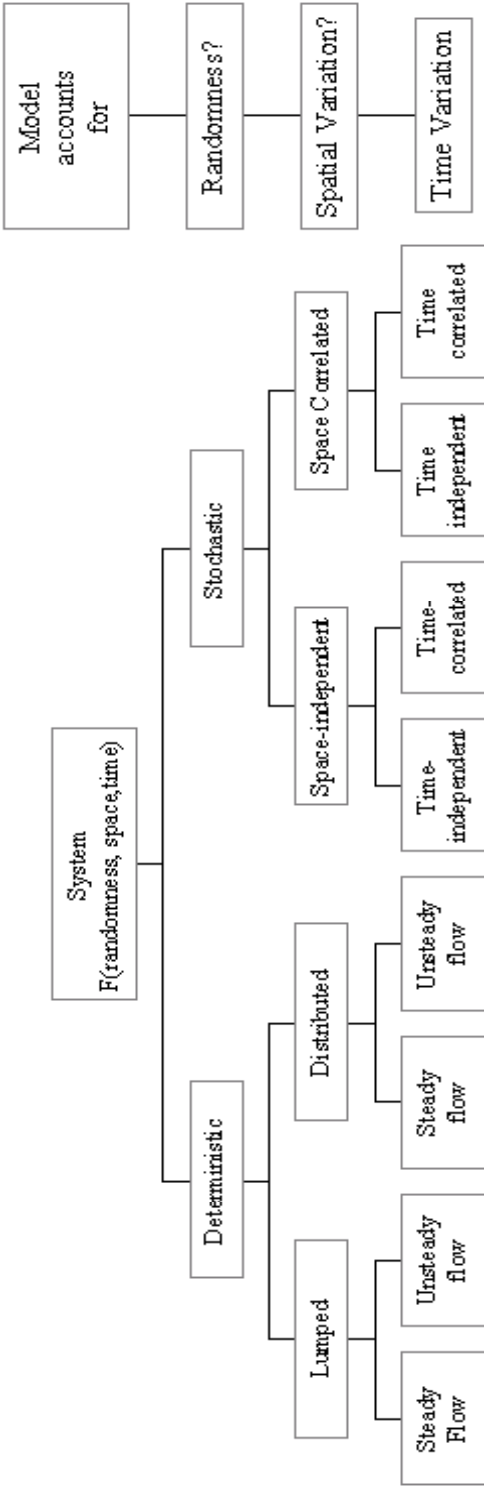


Figure 2.5 Classification of models (Chow et al., 1988)

2.3 Historical development of rainfall - runoff modelling

In this section a brief historical development of rainfall runoff modelling is discussed. It is obvious that a large number of models have been developed and used both as research and as operational tools. An exhaustive list and account is not the purpose of this study. We try to evince the trend of development and the causes for such evolution. Therefore only some of the models pertinent to the development of the conceptual modelling are discussed.

Though the speculation and awareness of hydrological cycle is dated BC, modern methodologies relating rainfall to runoff originated during the last half of the 19th century. The main objectives at that time was to determine the design discharges for sewerage design, land reclamation and reservoir spillway design.

According to Dooge (1957, 1973), during the last part of the 19th century and earlier part of the 20th century, most engineers used empirical formulas derived for particular cases and applied them to the other cases under the assumption that condition were similar enough. The engineers at that time also used the 'rational method' which may be seen as the first attempt to approach practically the problem of predicting runoff from rainfall. The methods were derived only for small mountainous catchments. Later during 1920s many modifications were introduced to extend the applicability of the rational formula to larger catchments.

The modified rational method based on the concept of isochrones, or lines of equal travel time, can be seen as the first rainfall-runoff model based on a transfer function. The model parameters were derived by means of topographic maps and the use of Mannings formula to evaluate the different travel times.

Sherman (1932) introduced the concept of the unit hydrograph on the basis of the principle of superposition. Although not yet known at that time, the superposition principle implied many assumptions, i.e. the catchment behaves like a causative, linear time invariant system with respect to the rainfall/surface runoff transformation.

At the end of 1930s and during 1940s a number of techniques were proposed in order to improve the objectivity of methods and results, the techniques of statistical analysis were invoked.

The real break through came in the fifties when hydrologists became aware of system engineering approaches used for the analysis of complex dynamic systems. They realized that the unit hydrographs was the solution of a causative, linear time invariant system and the response functions could be derived from input and output data by use of mathematical techniques. Prior to the development of computer models, the Antecedent Index approach (Kohler and Linsley, 1951) was a popular technique to determine runoff from rainfall. The Antecedent Index system correlates prior precipitation and a second variable, generally a week number to determine a "runoff curve". The "runoff curve" provides a technique for determining the quantity of runoff, which would be produced from storm rainfall totals. By comparing rainfall and runoff totals at fixed times throughout a storm, period volumes can be computed. A unit graph is then applied to the period runoff volumes, an estimate of base flow is added, and estimates of catchment streamflow are obtained.

The derivation of the unit hydrograph in the discrete form from input and output still remained a big problem, due to the assumed linear behavior of the system and errors in the data. Shape and volume constrained unit hydrograph with a smaller number of parameters was introduced to overcome these problems (Nash, 1958, 1959, 1960).

Box and Jenkins (1976) provided hydrologists with alternative methods of expressing the unit hydrograph in terms of autoregressive moving average (ARMA). This school of thought brought about the use of Artificial Neural Network (ANN) approach a method applied widely in other fields of science and engineering to represent non-linear and dynamic system. An example in the field of hydrology includes the recent work of Hsu *et al.*, (1995). They made a comparison of the ARMAX, the ANN and a conceptual model (the Sacramento soil moisture accounting model, SAC-SMA). The comparison of the three models shows the superiority of the performance of the ANN approach over the three others for a medium sized Leaf River Basin near Collins Mississippi. However, the transportability of the model and internal structure of the ARMA and ANN model and their relation to the physical process in a catchment remains ambiguous.

In the 1960s, in search for more physical understanding of the rainfall runoff processes other approaches were considered. With the advent of the computer capability the search for an improved rainfall-runoff methodology accelerated rapidly. Several models, which represent the

single hydrologic cycle at catchment level by using interconnected conceptual elements, were developed. Among the more widely used and reported lumped watershed models are Stanford model IV (Crawford and Linsley, 1966), Sacramento River (Burnash *et al.*, 1973), HEC-1 U.S. Army Corps of Engineers (Rockwood and Nelson, 1966), Tank and so on (WMO, 1975). These models are designed to approximate within their structures (in some physical realistic manner) the general internal sub-processes and physical mechanisms which govern the hydrological cycle. The main problem of these models was the fact that they have a large number of parameters, which have to be optimized.

During the late seventies and beginning of the eighties, the real time forecasting model which are based on recent updating and calibrating techniques. The Theoretical concepts used were due to Kalman, (1960), Kalman and Bucy, (1961); Todini, (1978); O' Connell, (1985) and etc.

The lack of a one to-one relationship between the model and the reality gave rise to a development of a so-called physical based models such as SHE (Syst \blacksquare m Hydrologique Europ \blacksquare en) (Abbot, 1986). This model is believed to be the state-art of the physically based model. A fourth generation model MIKE SHE (Refsgaard and Storm, 1995) is now being developed to apply for integrated water resource management. Typical areas of applications of this model are river basin planing, water supply, irrigation and drainage, effects of change of land use, and other ecological factors influencing surface and groundwater system.

To minimize the uncertainty of the parameters, lumped conceptual models are extended to handle catchments as composites of sub catchments, which are divided according to homogeneity in topography and land use. A good example of such development are TOPMODEL (Beven *et al.*, 1979, Beven *et al.*, 1995) and ARINO (Todini, 1996). The main concept behind these models is to give detailed account of very important topographic and hydraulic characteristics of a watershed. The TOPMODEL is developed on the basis that the catchment storage is related to the local water table in which the main factor is the topographic index known as Kirkby index (Beven and Kirkby, 1979). Therefore a basin is subdivided in to segments according to topographic index. Segments with a similar value of index are assumed to have the same response irrespective of their location in a catchment. One can argue that though the topography or slope plays great role in flow generation there is still a gap of understanding whether the effect of adjacent planes in catchment subdivision dominates how flows are transferred from one subdivision to the other. At this stage it is interesting to consider

the subdivision of a catchment used in the ARNO model (Todini, 1995) which looks more realistic. In the latter model, the catchment is divided into series of subbasins to each of which the rainfall-runoff model is applied; this division takes place according to the natural subbasin boundaries so that the subbasin closing section coincides with the cross-sections of interest along the river and its tributary.

There is still a point of argument that once the model is described with a number of parameters, they are mostly calibrated with the judgement of the model ability to reproduce observed quantities (such as flow at the outlet). The problem is that when one has several subbasins, the number of parameters to be optimized is multiplied by the number of subbasins. Optimizing these parameters always solely depends on one time series (observed flow). Therefore the parameters determined are very much correlated and competition among them is also very high. One possible attempt to solve these problems is to obtain all the parameters from physical properties of a catchment as for example in the SHE model. Which of course requires detailed spatially distributed information over the catchment.

The availability and use of digital elevation model (DEM), geographical information system (GIS) and remotely sensed data for inferring (soil moisture and vegetation index) somewhat moderate the problems huge data requirement of distributed models.

In this study we focus on areas where even major water balance variables such as rainfall and evaporation time series are sparsely and scarcely available. The scarcity of data in most of developing countries are so alarming that one gets a single station for a catchment as large as 1000 km². It is also possible a station from neighboring catchment should be considered for those catchments, which have no observation at all. For such areas the pragmatic solution is to apply conceptually sound lumped rainfall-runoff models with fewer parameters.

2.4 Time resolution of modelling

Hydrological processes occur at a wide range of scales, from unsaturated flow 1m soil profile to floods in river system of a million square kilometers; from flashfloods of several minutes duration to flow in aquifers over hundreds of years (Blöschl and Sivapalan, 1995). There exist rainfall runoff models which represents these processes using time spans a few minutes, hours, days or even up to one year. Selection of a time step of modelling depends on:

- Catchment input characteristics such as dominant storms in the area. An area with commonly conventional type of storms with separate rainfall storms can only be modeled with time steps less than a day.
- The model structure in representing the time scale of hydrological processes. A model, which accounts for infiltration rate of loose soil, should have computation in terms of minutes. The time step is interrelated with the area of the catchment under study. Starosolszky (1987) gives an approximate representation of this relationship (Table 2.1)
- The scope (purpose) of the model

Table 2.1 Relationship between time step of modelling and area of catchment (Adapted from Starosolszky (1987))

Average size of basin (km ²)		$0,5 \cdot 10^2$	10^2	10^3	10^4	$>10^4$
Time (log t)	Hours	5	10	20	30	
	Days			1	3	5
	Weeks				1	3
	Months					1

2.4.1 Common monthly water balance models

The main structure of a monthly water balance model attempts to model the hydrological processes by conceptualizing the catchment as interconnected storages, through which the water passes from input as rainfall to output as stream flow. The models at this scale do not reflect implicitly the hydraulic part of the catchment process but rather depend on the empirical relationship between storage and extraction rates and water balances

Monthly water balance models have been in hydrologic research as early as 1940s. The first monthly water balance models were developed by Thornthwaite (1948) and later revised by Thornthwaite and Mather (1955, 1957). A review of water balance model in common use is given by Alley (1984) and recently by Xu and Singh, (1998). The models discussed are summarized in Table 2. 2.

The available models use rainfall, temperature or evaporation either on monthly or daily time step. Most of the models have few parameters compared to the daily rainfall runoff models. One of the common features of these models is that most of the parameters (if not all) are estimated by fitting the observed hydrologic data such as rainfall and stream flow (Xu and Singh, 1998).

The models that use rainfall and evaporation as input are usually found to be more realistic, especially in reproducing seasonal flows and intermediate water balance variables. Attempts at developing models with input of rainfall and temperature resulted either with over parameterization or non-realistic storages as reported by Alley (1984). The VUB monthly water balance models have been tested by more than 100 catchments in different climatic regions and proved to satisfy most of the requirement at this scale (See Xu, 1992, 1995, 1996 Vandewiele and Ni-Larwin, 1998). Compared to the other monthly water balance model with almost same complexity the VUB monthly water balance models are reported performing better (Xu, 1994). The overview of the VUB monthly water balance model is given in the following section.

Table 2. 2 Common monthly water balance models

Input	Name/Reference	Number of Storages	Number of Parameters
Monthly rainfall, Temperature	T-model Thornthwaite and Mather (1955)	2	2
	T α -Model Alley (1984)	2	3
	abcd-Model Thomas (1981)	2	4
Monthly Rainfall and Evaporation	Pitman (1973,1978)	2	12
	Roberts (1979)	2	8
	Hughs (1982)	1	8
	Salas <i>et al.</i> (1986)		11
	VUBMOD Vandewiele <i>et al.</i> (1992)	1	3
	Makhlouf and Michel (1994)	1	2
Daily Rainfall and Evaporation	Haan (1972)	2	4
	Kuczera (1983)	2	9
	McMahon and Mein, Bouhton (1973)model	3	10

2.5 Review of the VUB monthly water balance models

This section reviews the development of a parsimonious water balance model and describes the basic hypothesis and principles. Discussions on the applicability of the model to different climatic regions and highlights of further room for improvement of the structure of the model for the given time step are highlighted.

2.5.1 Model hypothesis

The VUB monthly water balance model was designed based on the conceptualization of a river basin as a system and book keeping the water balance of various processes on a monthly time base. The model is intended to be rather simple and requires readily available hydrometeorological data. A water balance model on a monthly basis with a single reservoir (Figure 2. 6) uses precipitation and evaporation rate as input and has flow of the river as output. All the water balance terms are on monthly basis and expressed in mm. The model is generally described with three basic equations.

- 1) Computation of the actual evaporation r_t as a function of rainfall and soil moisture m_t of month t ,
- 2) Computation of stream flow as a function of the amount of rainfall, p_t and soil moisture storage m_t .
- 3) Computation of the water balance, at the end of the month.

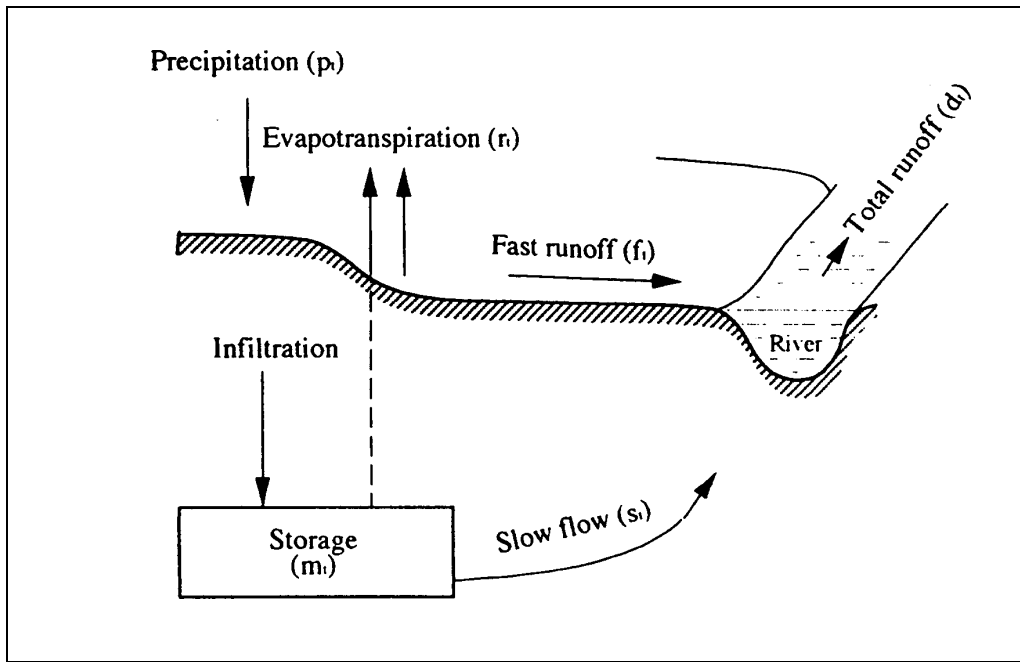


Figure 2. 6 Diagrammatic representation of the VUB monthly water balance model.

Originally, Van der Beken (1977) proposed the above three relationships with the following set of equations.

$$r_t = e_t(1 - e^{-a_1 m_t}) \quad a_1 > 0 \quad (2.2)$$

where e_t is potential evapotranspiration and a_1 is a parameter.

Here the actual evapotranspiration r_t is represented as a function of potential evaporation or pan-evaporation which ever is available. The actual evaporation increases as the soil moisture,

m_t increases. The actual evaporation approaches potential evaporation, as the soil moisture is very large. The values of parameter a_1 are high for sandy texture soils.

The surface outflow, d_t is represented as follows

$$d_t = a_2 m_{t-1} + a_3 N_t \quad 0 \leq a_2, a_3 \leq 1 \quad (2.3)$$

The first term of the right side of Equation 2.3 represents the slow flow component and the second term represents the fast flow component which is proportional to the net rainfall $N_t = P_t - r_t$. The parameter a_2 is expected to increase when the soil texture is more sandy and parameter a_3 is expected to increase with degree of urbanization and average basin slope.

The water balance equation is written as:

$$m_{t+1} = m_t + P_t - r_t - d_t - R_t - T_t \quad (2.4)$$

R_t is a variable that takes care of the unaccounted inflow and outflow from the catchment if little is known about this component it may be represented as

$$R_t = a_4 m_t - a_5 \quad 0 \leq a_4 \leq 1 \quad a_5 > 0 \quad (2.5)$$

The variable T_t represents the known amount of water supply or abstraction from the catchment. Optimization of the above parameters was performed by minimizing the sum of error squares i.e. the deviation of the observed discharge q_t from the computed discharge d_t . This model was reported successfully applied to the catchments Grote Nete and Zwalm, located in North Belgium (see Van der Beken, 1977 and Van der Beken and Byloos, 1977)

Based on the above general structure of the model, several researchers either applied the model directly to new catchments or modified some of the equations. Among others Quasim, (1984) introduced another evaporation equation whereby the actual evaporation is computed as a fraction of the potential evaporation, depending on a ratio of the amount of rainfall to the potential evaporation.

$$r_t = e_t (1 - e^{-a_1 p_t / e_t}) \quad a_1 > 0 \quad (2.6)$$

According to the above equation, for months without rainfall the actual evaporation is zero, which is not necessarily true because evaporation from the soil moisture and transpiration from plants may take place. This type of model may be limited to regions where rainfall in a month is always greater than zero. Hassan (1984) suggested different forms of evaporation equations which are based on the principle that the actual evaporation is a fraction of the potential evaporation and represent the relationship which accounts for soil moisture, and the available rainfall.

Substantial improvements of the monthly water balance model were carried out by, Vandewiele *et al.* (1993), where a methodology for model formulation, parameter estimation and model testing are developed.

After comparing different equations they suggested the following two equations for the computation of the actual evapotranspiration.

$$r_t = \min[e_t (1 - a_1^{w_t / e_t}), w_t] \quad 0 \leq a_1 < 1 \quad (2.7)$$

$$r_t = \min[w_t (1 - e^{-e_t a_1}), e_t] \quad 0 \leq a_1 \quad (2.8)$$

In here the available water during the month, w_t , is defined as the sum of the moisture storage and precipitation during that month i.e.

$$w_t = m_{t-1} + p_t \quad (2.9)$$

It is pointed out that the difference between the above two equation is that in second equation the actual evaporation approaches to total available water when evaporation is very high which is not the case in first equation. These two equations seem to combine both the influences of the available water and also the available energy for evaporation.

According to the evapotranspiration equations 2.7 and 2.8 the computation of the actual evapotranspiration holds a time invariant parameter a_1 . In reality, because of the seasonal variation of the level of vegetation growth and cover, this parameter should vary. Ni-Lar-Win (1994) proposed to account for such variation and the parameter a_1 to have a variable value represented as:

$$a_t = a_1 + a_4 \sin\left[\frac{2\pi}{12}(t - a_5)\right] \quad (2.10)$$

Note that this increases the number of parameters from 3 to 5. A comparison between the results of evaporation equation with constant and time varying parameter for 88 catchment from (Belgium, China, Burma, and West Africa) showed a slight improvement of the model performance for models with variable evaporation parameter. Dias (1993) applied Dissociated models with the exponential function of evaporation equations in 7 West African and 3 Srilanka catchments (Semi-arid catchments) and reported that the results are only as good as the previous rather simple models.

The flow equation is also modified by introducing discrete parameters to relate flow with soil moisture. Xu (1988), based on the concept of variable source area, showed that the fast flow component is not only a function of effective rainfall but also the wetness of the soil. Hence the flow equation is adjusted as follows:

$$d_t = a_2 m_{t-1}^{b_1} + a_3 m_{t-1}^{b_2} N_t \quad 0 \leq a_2, a_3 \leq 1 \quad (2.11)$$

and N_t is also redefined as:

$$N_t = P_t - r_t (1 - e^{-P_t / r_t}) \quad (2.12)$$

Due to the high correlation between the pairs (a_1, b_1) and (a_2, b_2) , specific discrete values were assigned to $(b_1=0.5, 1, 2)$ and $(b_2=0.5, 1, 2)$. Each of these combinations would result with a specific model for a catchment. The physical significance of these parameters and computation of the initial values from catchment properties are studied by Xu (1988) and where a_2 is found

to depend upon the transmissivity of the aquifer of the catchment and a_3 depends mainly on the slope and imperviousness of the catchment.

2.5.2 Models for different input levels

Owing to the lack of evapotranspiration data the monthly water balance models were modified or augmented for different input levels. What is really modified in this cases is that the driving force for water extraction from the catchment e_t is represented as a function. The first attempt is to represent the e_t input series as a function of monthly mean temperature, c_t and mean humidity, h_t which are the dominant factors for evaporation process. The function used is

$$e_t = a_4 (c_t^+)^2 h_t \quad (2.13)$$

where a_4 is a positive valued parameter.

c_t =temperature in degree Celsius (the plus sign is to indicate that zero values are taken for temperatures below freezing.

h_t =relative humidity in per cent

If data on relative humidity is not available e_t may be written as

$$e_t = a_4 (c_t^+)^2 \quad (2.14)$$

If only rainfall data is available,

$$e_t = a_6 + a_4 \sin\left[\frac{2\pi}{12}(t - a_5)\right] \quad (2.15)$$

Equation 2.15 is justified since the e_t series generally varies regularly in most region of the world and it is nearly a periodic function with a more or less sinusoidal function.

The e_t series generated by one of the equations 2.13, 2.14 and 2.15 is not intended to compute a physically relevant potential evaporation, therefore these are only intermediate driving forces computation for the water balance model.

Table 2. 3 model types and input requirements

MODEL TYPE	INPUT DATA	PARAMETERS
1	Precipitation and Potential evapotranspiration	a_1, a_2, a_3
2	Precipitation, Temperature, and Relative humidity	a_1, a_2, a_3, a_4
3	Precipitation and Temperature	a_1, a_2, a_3, a_4
4	Precipitation	$a_1, a_2, a_3, a_4, a_5, a_6$

2.5.3 Regional study of monthly water balance models

Along with the development of the monthly water balance models efforts were also directed to relate parameter values to catchment properties. The model parameters could be linked to physical basin characteristics such as for example lithology (Xu, 1988, Vandewiele *et al.*, 1991).

In the context of Belgium (Vandewiele and Atlabachew, 1995) the monthly water balance model parameters could be regionalized, which enables deriving flows for ungauged catchment. A method of Kriging and parameters from few neighbouring basins were used to obtain the parameters for ungauged catchments. Further research along this line is necessary to analyze the possibility for regionalization of the water balance models in other climatic regions.

2.6 Summary

In order to select among the plethora of different mathematical models available today, it is possible to identify models according to a priori knowledge. The latter ranges from total ignorance (pure stochastic models) to the full description of system dynamics based upon differential equations describing the balance of mass and momentum. The final choice on which model to use mainly depends on the purpose of application, the accuracy desired, the available data and economics.

Conceptual models are widely used in water balance studies and chosen in this study particularly due to:

- their ability in representing the system in terms of parameters.
- their potential to correlate the few parameters with hydrometeorological and physiographical characteristics.
- their ability to carry out computations on time scales varying from hours to years. The time step chosen depends on the application of the model. Daily and monthly time steps are common in water balance models for basins. Important to note is that the smaller the time step, the more complicated the model becomes and the more stringent are requirements on the data.
- their use of readily available hydrometeorological data (as mean or totals of daily, weekly or monthly values).

The physical based distributed models are appropriate to study land use change impacts on the catchment system and also to investigate test catchments to prove hydrological hypotheses. There are a number of sophisticated and detailed models appearing in the field of hydrology but, for many catchments, the available data are far from the requirements of these models. In addition arid and semi-arid catchments are very difficult to model as compared to humid areas due to the large temporal variation of the variables and the limited data.

Therefore, the focal point of the ongoing research is to develop conceptual rainfall - runoff models on a catchment scale and at different time steps. Hereby it will be attempted to incorporate the specific features of semi-arid and arid catchments.

Since 1977, in an effort to develop simple conceptual models for limited available data, monthly water balance models have been developed and tested for over 100 catchments from 8 countries at the Laboratory of Hydrology of the Vrije Universiteit Brussel. Most of the test catchments lie in humid climatic regions and a few in arid and semi-arid regions. The result of the study could be summarized as follows:

- 1) the models perform satisfactorily in humid regions

- 2) model parameters of a few regions from Belgium could be related to lithology and also geographically regionalized.
- 3) application to some arid catchments resulted with high correlation of residuals
- 4) the models show a low performance for intermittent flows.

Further areas of improvement addressed in this study are:

- In semi-arid catchments, it is known that the potential evaporation is higher than the actual evaporation. In all cases, the limiting factor for actual evaporation is the available water rather than the potential evaporation. Model structures, which include this phenomenon, should be investigated.
- In the model formulation, flow components are expressed as a fraction of the soil moisture storages of the previous month. This leads to under estimation of the runoff generation during the transition from a very long dry period to a rainy period. This phenomenon often prevails in semi-arid and arid climates. Therefore, a means of accounting this transitional period should be investigated.
- The model structure does not have an upper limit for the storage of the catchment. In reality, the storages are limited to a saturated condition. Hence an upper limit should be included in the structure.
- In dealing with semi-arid and arid regions, due to the high variability of input variables, there is a need for smaller time step of modelling. A 10- day time step can be considered as a homogeneous time span for example for the soil moisture content. Hence a 10-day water balance models can be developed based on the experience of the previous studies.
- Further, the concept of the water balance can be extended to develop a parsimonious daily rainfall runoff model at catchment scale. Smaller time step models are applicable in water resources structure operation and also in flood forecasting.

Chapter 3

3 MODEL STRUCTURES FOR DIFFERENT MODELLING TIME STEPS

3.1	Introduction	34
3.2	The monthly water balance model for semi-arid catchments	35
3.3	A 10-day water balance model (DWBM).....	52
3.4	A parsimonious daily rainfall - runoff model	64
3.5	Data requirement and scope of application of the developed models	71

3.1 Introduction

Conceptual monthly water balance models have been developed and tested for a number of catchments in humid climates and few arid and semi-arid regions at the Laboratory of Hydrology, Free University of Brussels. These models are based on a simplified representation of the hydrological processes and the balances of incoming and outgoing water from the catchment on a monthly time step. This chapter presents further developments and improvements of the model structure to extend their applicability to semi-arid and arid catchments. Secondly, the chapter discusses the development of a new 10-day Water Balance Model (DWBM) and of a Parsimonious Daily Rainfall-Runoff Model (PDRRM).

The last two models have evolved from the long experience obtained from the monthly time step model as applied to different climatic regions. The methodology of parameter optimization and the main philosophy of modelling are kept as for previous VUB monthly water balance models.

3.2 The monthly water balance model for semi-arid catchments

3.2.1 Structure of the model

The models have generally three components.

- (1) Computation of actual evapotranspiration, r_t which is empirically related to the areal potential evaporation, e_t and the available water in the catchment expressed as the storage index m_t .
- (2) Computation of flow, d_t which is partitioned as fast flow, f_t (a function of excess rainfall and wetness of the catchment) and the slow flow, s_t as a function of catchment storage.
- (3) The water balance of the single storage certainly augmented by rainfall p_t and depleted by the flow of the river and evaporation.

All variables are in the same unit and are normally expressed as mm of water depth over the surface area. The subscript t is used to represent the time horizon. For the variables: rainfall, evaporation and flows the subscript t indicates the total amount of the variables during time t . For the soil moisture storage variable m_{t-1} indicates the state at the beginning of the particular time (month in this case) and m_t indicates the state at the end of the t . Figure 3.1 shows the schematized water balance variables.

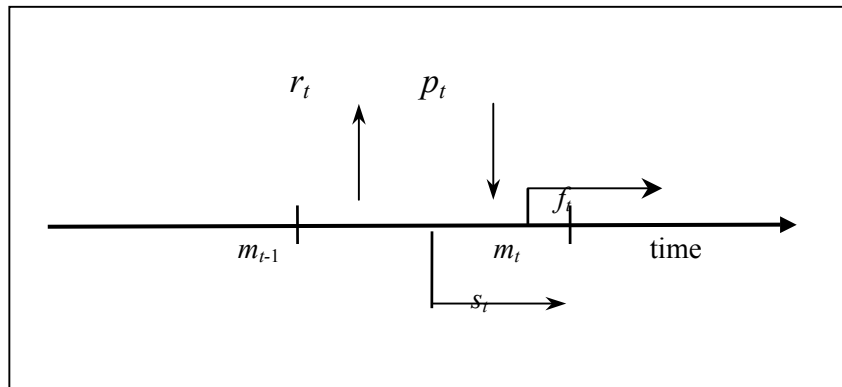


Figure 3.1 Conceptual representation of the monthly water balance variables.

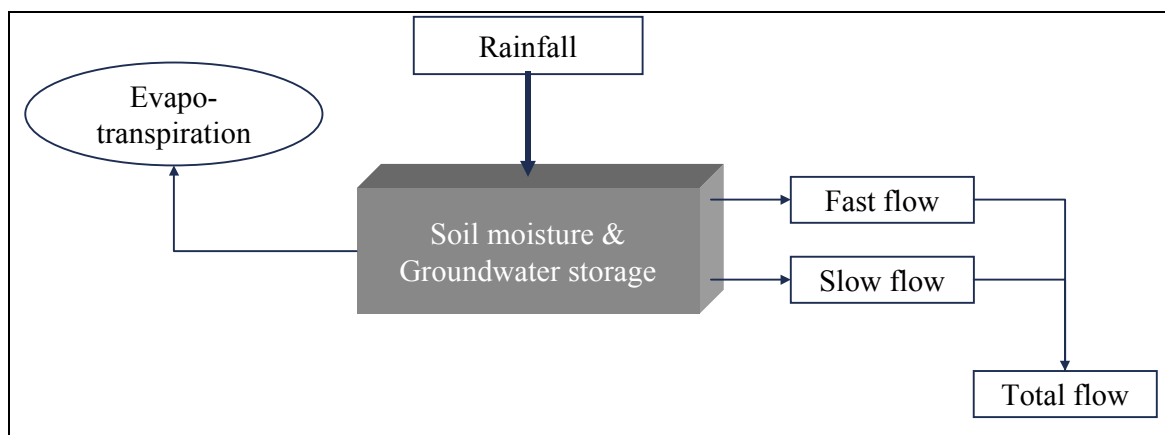


Figure 3.2 Conceptual representation of the monthly water balance model.

Actual Evapotranspiration

Evaporation of water from a soil is dependent on many physical parameters of the soil and hydrometeorological variables. On annual basis, evaporation extracts as much as 40 per cent to 90 percent of the water in humid and dry regions respectively. Practically, the actual evaporation from a natural surface is the most difficult to measure. Two existing methods of estimating the evaporation from land surfaces are based upon changes of the water content of the soil. This can be done by periodically measuring the soil moisture profile and by comparing successive profiles. The second method is by using a Lysimeter, a tank filled with soils in which all conditions inside and around the tank are reproduced as exactly as possible. Note that

the first method has limitations because the computed difference can comprise drainage to the bottom or lateral strata of the soil in addition to evaporation. The second method gives relatively accurate data for a specific local condition. However installing, such an instrument to cover a large heterogeneous catchment is not practical from economical point of view.

The obvious fact is that the actual evaporation from a heterogeneous land cover depends on a) the climatological factors b) the land cover and c) the moisture availability. At present the theoretical studies and observations, regarding explicit relationship among the factors are not sufficient to adapt them to catchment studies because they are microscale and time span oriented. This leads to incorporating the actual evaporation calculation as an intermediate step in conceptual rainfall runoff models.

To compute actual evapotranspiration from known water balance variables, the following basic assumptions are necessary:

- a) the superimposed effect of climatological driving forces (factors) can be represented by the potential evapotranspiration or pan evaporation;
- b) for fairly sparse vegetation cover and rural catchments, the effect of interception may be neglected.
- c) at the larger scale of time step (decade and monthly) the actual evaporation is considered to be that amount of water extracted from the soil moisture which has been filled with not only rainfall of the current month but also the previous months. This overcomes the problem of deficiency of water (rain-potential evaporation) due to a large value of the potential evaporation, as compared to the rainfall amount during the time step. Further it can be justified that rainfall events are rather short compared to continuous process of extraction of water. Hence there should be a mechanism of delaying the water in storage.

Following the above assumptions, empirical relationships between the actual evaporation (r_i) and the other water balance variables (e , p , m) have to be established. In most of moisture accounting models such as the Soil Moisture Accounting and Routing Model known as Layer model (O' Connell *et al.*, 1970) evaporation is allowed to extract water at potential rate from the most upper stack of soil layers. After the exhaustion of the upper layer, evaporation takes place from the second layer at the potential rate multiplied by a parameter whose value is less than unity. If the potential evaporation is not satisfied at the exhaustion of the second layer the

evaporation takes place at the potential rate multiplied by the square of the parameter and so on. A similar approach is used by Xinanjiang model (Zhao *et al.*, 1980).

At least for the monthly water balance model considered here, the layers are amalgamated to a single storage. This assumption is fairly valid for a shallow unconfined aquifer beneath the root zone. In the next section the necessity of sub-dividing this storage into two namely the soil moisture and the deep groundwater storage is discussed with respect to smaller time step resolutions.

Any empirical relation between actual evaporation and known variables should satisfy the following requirements. Let the available water in the soil storage at time t be $w_t = m_{t-1} + p_t$, the potential evaporation e_t , and actual evaporation during the month $t = r_t$,

- a) r_t increases with e_t and w_t
- b) $r_t = 0$ when $w_t = 0$ or $e_t = 0$.
- c) $r_t \leq e_t$ and $r_t \leq w_t$
- d) $r_t \rightarrow e_t$ when $w_t \rightarrow \infty$.

Xu, (1992) tested seven equations (from Roberts, 1978) and two equations from the VUB monthly water balance model. All the tested equations satisfy the above requirements. He concluded that the latter two equations are overwhelmingly good. Though some variants of the seven equations also perform well for the monthly water balance model, the two equations - hereafter also refereed as evaporation IR=1 (Equation 3.1) and IR=2 (Equation 3.2) are used in this study.

$$r_t = \min[e_t(1 - a_1^{w_t/e_t}), w_t] \quad 0 \leq a_1 \leq 1 \quad (3.1)$$

$$r_t = \min[w_t(1 - e^{-e_t a_1}), e_t] \quad 0 \leq a_1 \quad (3.2)$$

where a_1 is a time invariant parameter, which represents the characteristics of a catchment under study.

Basically in evaporation equation (3.1) the actual evaporation r_t is computed as a portion of potential evaporation which is bound by the available water in the catchment during month t . Alternatively the actual evaporation may be computed as a portion of the available water which

in this case is limited to the potential evaporation equation (3.2). Their behavior in the range of possible values and influences of the corresponding parameters are shown in Figure 3.3 and Figure 3.4 for the first and second evaporation equations respectively.

It is evident that in semiarid and arid catchment, the potential evaporation is higher than the actual evaporation for a large period of the year. Hence, the limiting factor for evaporation in this region is the available water rather than the potential evaporation. Relations such as equation (3.2) have therefore a better background since the actual evaporation is a fraction of the available water rather than being a fraction of potential evaporation. Comparison of the model outputs for most of the test catchments shows that equation (3.2) resulted with mostly better and in a few cases equal model performance compared to equation (3.1).

Ni-Lar-Win (1994), and Vandewiele and Ni-Lar-Win (1998) proposed to vary the parameters of evaporation seasonally with a sinusoidal function. Hughes (1997) and Hughes and Metzler (1998) also introduced a potential vegetation growth factor as a function of the last two months and current soil moisture states in the Pitman monthly rainfall runoff model. The modifications are necessitated from the fact that a single wet month preceded by two dry months will therefore have less effect than as sequence of moderately wet months. These different studies came however to the conclusion that separation of the vegetation factor and soil moisture storage led to difficulties in calibrating the models with more additional parameters.

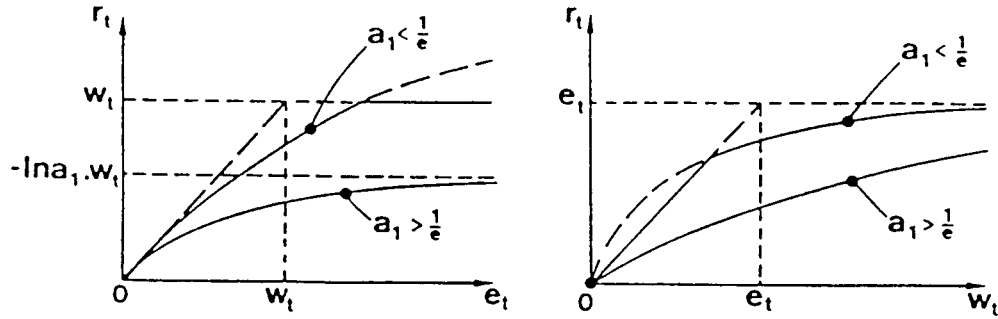


Figure 3.3 Influences of evaporation parameter for evaporation equation 3.1. The left diagram shows curves with $w_t = \text{constant}$. The right diagram shows curves with $e_t = \text{constant}$. (Vandewiele *et al.*, 1993)

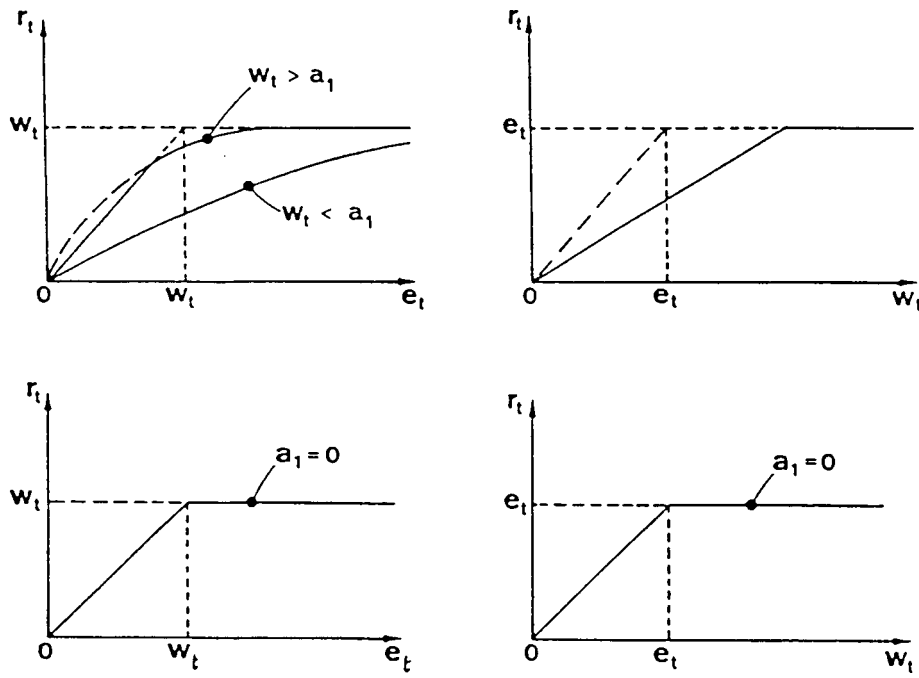


Figure 3.4 Influences of evaporation parameter for evaporation equation 3.2. The left diagram shows curves with $w_t = \text{constant}$. The right diagram shows curves with $e_t = \text{constant}$. (Vandewiele *et al.*, 1993)

Empirical equations relating the actual evapotranspiration with soil moisture storage and potential evaporation are used for all the three types of models. The effect of growth of vegetation has not been considered explicitly. It is assumed that this phenomenon is well represented by the soil moisture available in a catchment.

Flow components

River flow is composed of several components such as, channel flow, surface runoff, interflow and base flow. Modelling each component in a catchment scale is rather complicated and requires a detailed representation. Especially in large time scale modelling, it is often impossible to make a clear distinction between each component. In the present study, the flow components are conceptually grouped in to two main domains namely the fast and slow flows. The fast flow may be defined as the part of precipitation that reaches the outlet within the time step of modeling, in this case a month. It is comprised of channel flow and surface flow and part of the interflow. The slow flow, which is gradually released from the groundwater storage, may be regarded as the "base flow" component.

The fast flow component

Fast flow is considered as the immediate response of a catchment to a given precipitation and hence can be represented as the difference between rainfall and actual evaporation. The equivalent term to the so-called net rainfall or effective rain n is given as:

$$n_t = p_t - r_t(1 - e^{-p_t/r_t}) \quad (3.3)$$

The flow generated depends on the evaporation, excess rainfall and also the wetness of a catchment, which is expressed as m_{t-1} . The (+) sign indicates that m_{t-1} is restricted to non-negative value. One of the efficient relationships tested for different climatic regions is

$$f_t = a_3(m_{t-1}^+)^{b_1} n_t \quad (3.4)$$

where a_3 and b_1 are parameters. It was observed that parameters a_3 and b_1 are highly correlated. Hence it was suggested to limit the later parameter to fixed values (0.5, 1.0, 2.0) Experience showed that one of the discrete values fits a given catchment.

The consequence of this equation is that a precipitation, which occurs after several dry months, would produce a fairly lower magnitude of fast flow compared to that occurring in the middle of the wet season. In essence this is a sort of variable source area concept, i.e. the wetter the catchment the higher will be the generated surface runoff.

Referring to equation (3.4) the fast flow component is a function of the soil moisture storage at the beginning of a month. In a temperate area where these formulations are proved to be working efficiently, the moisture index rarely drops to a value of zero (see for e.g. Figure 3. 6). Whereas in semiarid and arid regions since the dry seasons last for longer periods the index can have a value about zero for more than one month (see for e.g. Figure 3.7). It is noted that in these equation if the soil moisture storage at the beginning of a month is zero we would have no fast flow for the next month for whatever amount of rainfall.

The rainfall of semi-arid and arid areas is associated with high intensity. Also, at the beginning of the rainy season, the vegetation is normally dry and scarce which reduces the retention of the rain. Though the initial infiltration rate is high, because of the larger intensity of the rain it is more likely that it produces some fast flow. This process is not well represented by equation (3.4) i.e. regardless of the amount of effective rain, the fast flow component is not generated if the soil moisture index is zero. Hence for the fast flow equation (3.4) an average soil moisture index of the month is used instead of the storage index at the beginning of the month. Therefore Equation 3.4 is rewritten as:

$$f_t = a_3 \bar{m}_t^{b_1} n_t \quad (3.5)$$

where $\bar{m}_t = \frac{m_{t-1} + m_t}{2}$

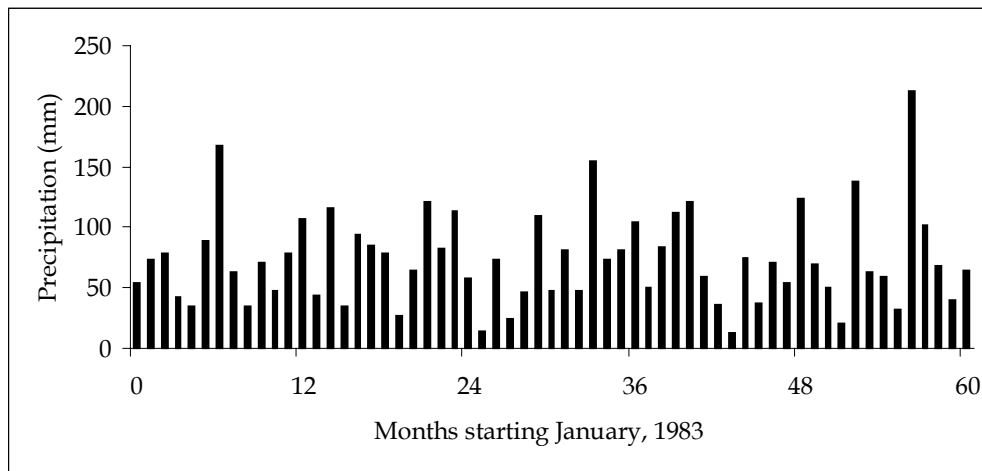


Figure 3.5 Typical monthly rainfall series of humid climate (e.g. from Kleine Nete catchment, Belgium)

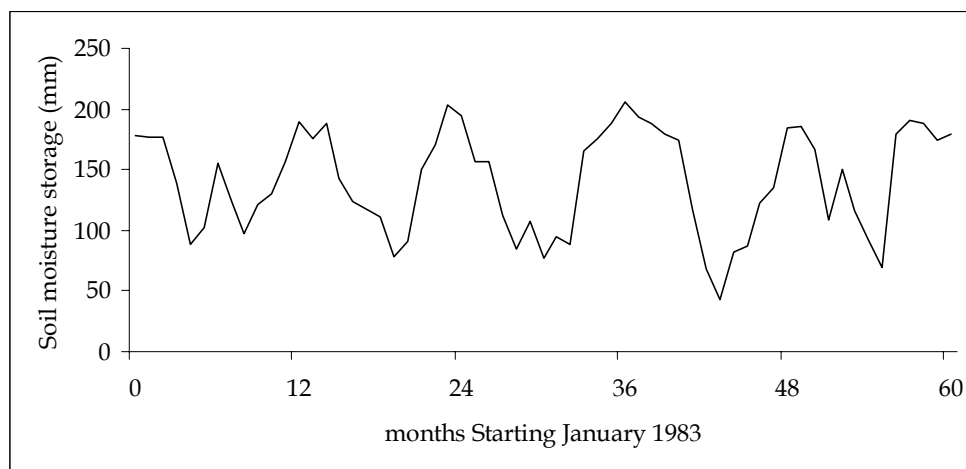


Figure 3. 6 Typical evolution of soil moisture storage in response to humid climate precipitation. (e.g. from Kleine Nete catchment, Belgium)

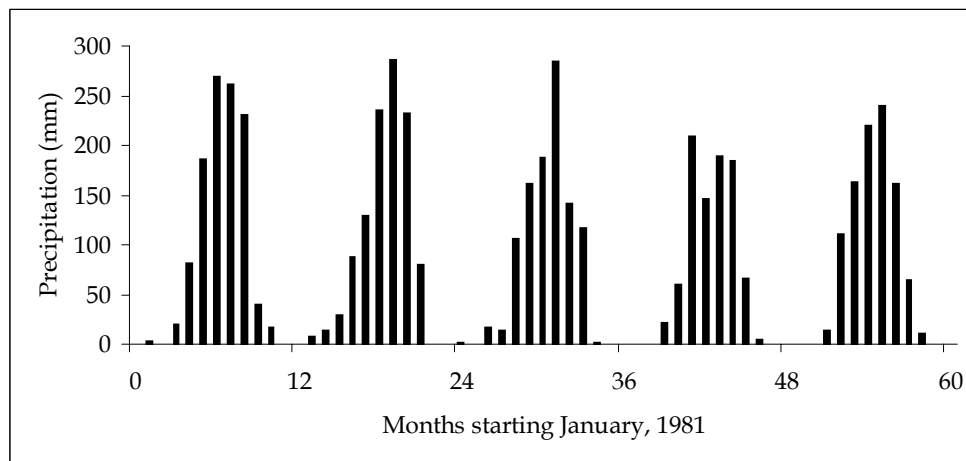


Figure 3.7 Typical monthly rainfall series. (e.g. of Faleme River, Senegal)

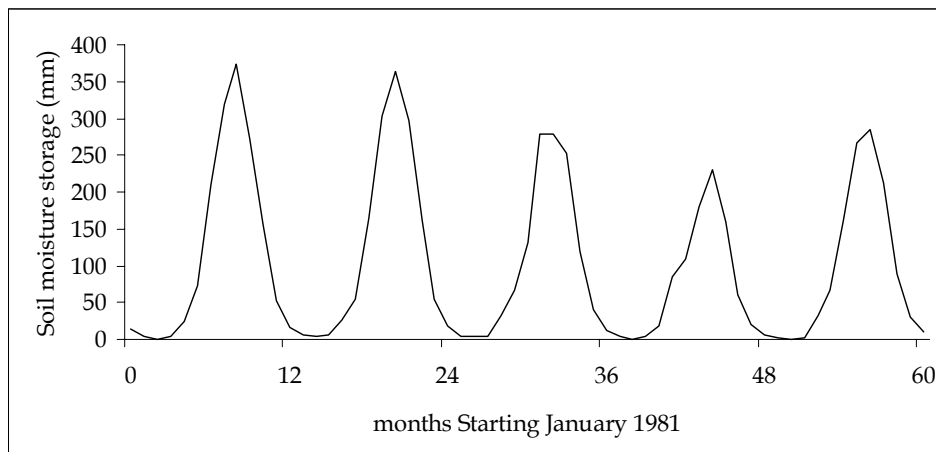


Figure 3. 8 Typical evolution of soil moisture storage in response to strong contrast between rainy and dry season (e.g. of Faleme River, Senegal)

To obtain the average soil moisture an iterative method is introduced which is performed for every computation step. Firstly the initial \bar{m}_i is assumed to be m_{i-1} , then all computations are executed and the resulting final storage, m_i is computed. Next the average is computed and compared with the previous value and the iteration will continue until the difference between the two consecutive mean storages is smaller than the defined accuracy (0.01mm). This modification does not add any other parameter but the computation time during calibration will take more time since the iteration is done for the individual time steps of the computation. This is not considered to be a limiting factor with the modern fast computing facilities.

The slow flow component

Let us consider the steady state of groundwater flow for schematic representation of a catchment of Figure 3.9. From Darcy's law and Dupuit's assumptions, the groundwater flow component of the river is proportional to the transmissivity and the hydraulic gradient. For the total flow during a period of one month per unit area, this becomes:

$$Q_b = \frac{T(h - h_o) / (\frac{L}{2})}{L} \Delta_t \quad (3.6)$$

where: T is the transmissivity: the hydraulic conductivity times the average thickness of the ground layer

Δ_t = time step

h is the average water table elevation

h_o is the average water level in the river channel

L is the average width of a cross section and $L/2$ is assumed to be the average distance between the groundwater and the river.

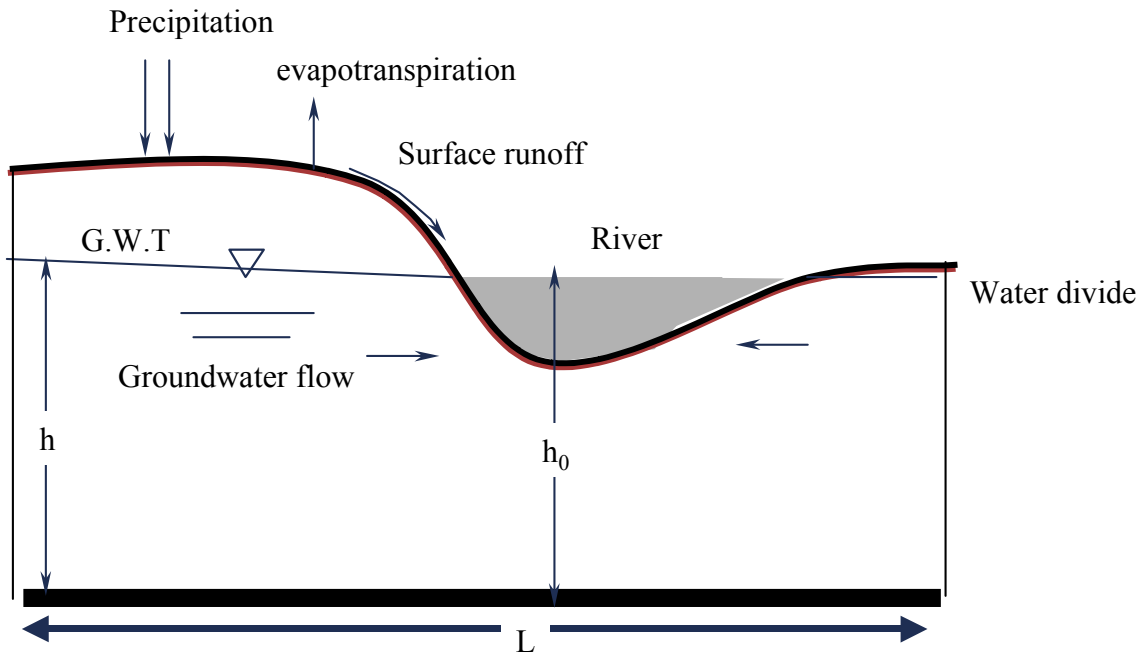


Figure 3.9 Physical description of the flow components (Xu, 1988)

From Figure 3.9 it is clear that the groundwater per unit area that can drain to the river system is proportional to the difference between the two heads ($h-h_0$). The total amount of water available in this layer is then:

$$m = \varepsilon(h - h_0) \quad (3.7)$$

where m is the storage and ε is average effective porosity. Hence we have:

$$Q_b = \frac{2T\Delta_t}{L^2\varepsilon} m \quad (3.8)$$

It follows that the groundwater contribution is largely a function of water table changes reflected in T and other physical characteristics of the catchment. Two extremes can be considered. First, if we assume water level fluctuations are very small compared to the thickness, then T can be considered as constant and

$$Q_b = a_2 m \quad \text{with} \quad a_2 = \frac{2T\Delta_t}{L^2 \varepsilon} \quad (3.9)$$

On the other hand if the thickness of the groundwater layer below the river h_o is much smaller than the water table drop $h-h_o$, then

$$T = K(h - h_o) = Km / \varepsilon \quad (3.10)$$

where K is hydraulic conductivity of the layer.

$$Q_b = a_2 m^2 \quad \text{with} \quad a_2 = \frac{2K\Delta_t}{L^2 \varepsilon^2} \quad (3.11)$$

This analysis shows that for the intermediate conditions one has to look for optimum values by changing all possible values. The factor L can be calculated as the catchment area divided by the total length of the river. Therefore, for general condition the low flow component is represented as :

$$s_t = a_2 (\overline{m}_t)^{b_2} \quad (3.12)$$

Like b_1 , b_2 is also restricted to have values of (0.5, 1.0 and 2.0). Note also that the average storage in a month is used here also for the same reasoning as for the fast flow case.

The total flow

Eventually the total flow during the month t , d_t is given as the sum of the previous two components equation (3.13). No delay of flows is considered, which limits the model to apply to catchments with a concentration time not more than a month. As a rule of thumb, the upper area limit is considered to be about 5000 km². This is a very hypothetical limit, since other factors such as the shape of the catchment and slope also affects the concentration time. A major limiting factor is also the homogeneity of rainfall and evaporation inputs over the catchment considered as a unit.

$$d_t = f_t + s_t \quad (3.13)$$

The water balance

The water balances of the catchment i.e. the input to and the output from the catchment is computed for month to obtain the soil moisture available at the end of each computation.

$$m_t = m_{t-1} + p_t - r_t - d_t \quad (3.14)$$

Maximum soil moisture storage

Though the described model is not a physical model whereby all the complex processes are strictly represented, one would expect the storage index to have an upper limit by analogy: the field capacity of the soil or, for shallow groundwater tables, the ground surface. An additional parameter a_4 (maximum soil moisture storage) may be introduced whereby storage values exceeding a_4 augment directly the fast flow and the soil moisture at the end of the month will have the value of the upper limit, a_4 . Consequently considering the later modification, Equation (3.5) may be written again as:

$$f_t = a_3 (\overline{m}_t)^{b_1} \left\{ p_t - r_t \left[1 - \exp(-p_t / r_t) \right] \right\} + (m_t - a_4)^+ \quad (3.15)$$

This is to be considered as the second variant of the described model. The (+) sign indicates that only non-negative values are considered. This modification also costs one additional parameter. One should pay attention to the values of this parameter because of the fact that if very low values are obtained by optimization and in situations where we have consecutive rainfall events, the storage would likely be exceeded and the fast flow generated is going to be unrealistic. In such cases, one has to gradually increase this value to obtain realistic upper limits. On the other hand, if one starts with very high upper limits, there will not be any influence on the flow generation. More explanation will be provided in the case study (Chapter 5).

3.2.2 Models for rainfall and temperature inputs

Previous studies on these types of modelling have shown that any attempt of computation of evaporation from other meteorological data such as temperature and humidity within the model structure adds one or two more parameters. It often results with unrealistic intermediate variables.

In this study we recommend that in the case of an absence of longer potential evaporation:

- a) If data for a number of years are available, calculate the mean monthly evaporation for the 12 months of the year, and use these values for all the calibration period.
- b) If data of evaporation for few years and longer data of temperature and/ or relative humidity are available establish a simple relationship on a monthly basis. Use this relationship to derive potential evaporation, which eventually would be the input to the models.
- c) If there is no data on evaporation but there is a time series of temperature, a simple formula can be applied to derive potential evaporation which does not require many variables. One of the earliest formulas are those proposed by Thornthwaite (1948) and Blaney and Criddle (1950) several other formulas are available with different input requirements. Recently Singh and Xu, (1997) have evaluated and generalized them into seven categories.

The Thornthwaite equation is applied here because of fewer data requirements. The method computes the potential evaporation from series of mean temperature and average monthly sunshine hours.

The equation calculates monthly potential evaporation as

$$e_t = 1.6 \frac{l_d}{12} \frac{N_d}{30} \left(\frac{10c_t}{I} \right)^a \quad (3.16)$$

where e_t = potential evaporation (mm),
 l_d = actual day length in hours,
 N_d = the number of days in the month,
 c_t = mean monthly air temperature ($^{\circ}\text{C}$),

$$I = \sum_{t=1}^{12} (c_t / 5)^{1.514} \quad \text{and} \quad a = (0.657I^3 - 77.1I^2 + 492390)10^{-6} \quad (3.17)$$

The factors in the formula can be easily obtained from tables. The advantage of using this equation is to reduce the number of inter-related parameters in hydrological models.

3.2.3 Parameter description

The first variant of the monthly water balance model, which is denoted as MWBM-A, has three parameters. The second variant, which is denoted as MWBM-B, has one more parameter, the upper limit of soil moisture storage in addition to the three parameters.

Taking average values of water balance variables and substituting them in model equations one can obtain reasonable orders of magnitudes of the parameters. The Order of magnitudes of the four parameters are shown in Table 3.1. For detailed explanation on the scale of parameters see Appendix B.

Table 3.1 Description of parameters of monthly water balance model.

Parameter	Description	Initial values		recommended range
a_1	evaporation parameter	$IR=1$	0.4	0.1-0.9
		$IR=2$	0.004	0.0001-0.009
a_2	slow flow Parameter	$b_1=0.5$	0.4	0.01-0.9
		$b_1=1.0$	0.04	0.001-0.1
		$b_1=2.0$	0.0004	0.00001-0.001
a_3	fast flow parameter	$b_2=0.5$	0.04	0.01-0.1
		$b_2=1.0$	0.004	0.001-0.01
		$b_2=2.0$	0.0004	0.0001-0.001
a_1 for (MWBM-B)	max. soil moisture storage	400		100-1000

3.2.4 Initial soil moisture storage

The soil moisture storage at every time step is calculated using the other known water balance variables and hence is known as an intermediate variable. But while calibrating or simulating the model one has to start from known soil moisture storage. In fact this value is not measurable because it is a conceptual variable of the whole catchment. Two possible solutions are available to handle this problem. The first solution is to consider the initial soil moisture as an additional parameter and obtain the optimum value through optimization methods along the other model parameters. This of course is against the major objectives towards developing parsimonious models.

The other solution which is adopted as a standard in modelling practice in this field of conceptual rainfall-runoff modelling is to start with a reasonable assumption of the initial soil moisture storage and run the model for a few years referred to as a 'warming up period'. The idea is that the model performance should not be accounted for during this period and at the end of the warming period it is assumed that the effect of the initial value would disappear and the catchment start to respond naturally. The length of the warming up period depends upon a) the availability of data and b) the memory of a catchment. In case of short data, mean monthly values of input variables (precipitation and potential evaporation) can be appended to the beginning of the data, which would be used as a warming up period. It is recommended that at least one year of actual inputs should be used as a part of the warming up period.

3.3 A 10-day water balance model (DWBM)

3.3.1 Background

This model is based on the experiences gained from the extensive application of the monthly water balance models discussed in section 3.2. The objective of this study is generally to reduce the time step of the model to account for the high variability of hydrological variables such as rainfall and soil moisture in a month for semi-arid and arid catchments. The first logical attempt was to use the same model structure as for the monthly time step, which has resulted with unsatisfactory results.

Further attention was given to the use of this model in catchments where there is a contrast between the wet and the dry season. Semi-arid and arid regions are characterized by having at least two distinct seasons: the rainy season and the dry season where no rainfall (insignificant) but still flow is available in smaller magnitude. It is then possible to treat the two situations separately, or this feature may be used as an indication of some processes governing the two seasons. This prompted us in modifying the existing model. Most of the methodologies would be adopted from the parent model and new concepts specific to this model are detailed in the following sections.

The other peculiarity of this study is that among the parameters describing the model, the base flow parameter is obtained by hydrograph analysis. This model is especially suitable for regions where two seasons, rainy and dry seasons, are easily identified to obtain the base flow parameter through hydrograph analysis.

3.3.2 Description of the 10-day water balance model

A Parsimonious (5 parameters) lumped conceptual rainfall-runoff model for a time step of 10-day is described. The new features of the actual model deal with the reduction of the time step to 10-day and with the introduction of two distinct storages: a soil moisture storage and a groundwater storage. The time step of the model is reduced to 10-day to account to some extent for the temporal variability of rainfall. Obviously, the variability of separate storms can not be handled neither by the 10-day time step and requires modelling with shorter time steps such as hourly or daily. However, a 10-day time step could be sufficient to represent the uniform state of a catchment.

The separation of the storages is necessitated by the fact that the upper soil moisture storage controls the processes during the rainy season and the lower part predominantly controls the gradual release of water during the dry season. The upper storage is augmented by rainfall (infiltration) and depleted by evapotranspiration, interflow and percolation to the underlying groundwater storage. The groundwater storage is augmented by percolation and depleted by base flow. The actual evaporation and flow components are calculated on a 10-day time step using empirical equations, which relate the rainfall and the average states of storage. The river flow is represented as the sum of three-flow components: surface runoff (infiltration excess), interflow and base flow. The diagrammatic representation of the structure of the model is shown in

Figure 3.10. The mathematical formulation of the components of the model is described in the following sections.

All the water balance variables considered are described in (mm) of depth of water over the surface area of the catchment. The subscript t designates the time step where $t=1, 2, 3, \dots$ corresponds to the first, second and third decades (10-day) etc. All quantities are assumed to be uniform over the catchment.

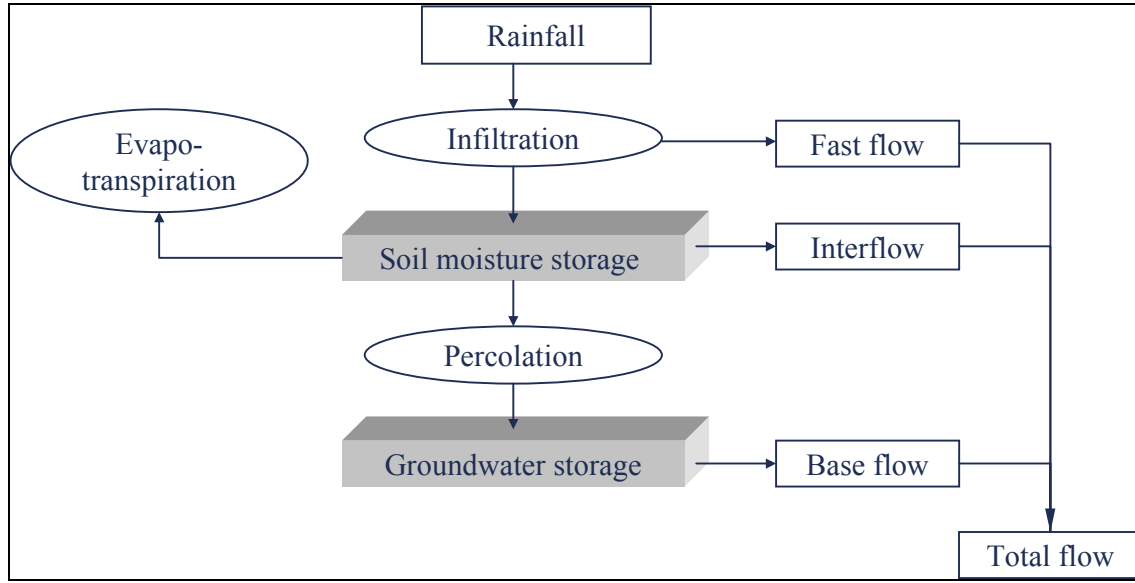


Figure 3.10 Conceptual representation of the 10-day water balance model.

3.3.3 Infiltration component

Generally the infiltration rate depends on soil characteristics, vegetation cover, initial moisture content of the soil and intensity of the rain. Horton (1939) represents rate of infiltration as a decaying function starting at a rate i_o until it reaches a constant rate i_c .

$$i_t = i_c + (i_o - i_c)e^{-k_h t} \quad (3.18)$$

where k_h is a decay constant. Similar observations are noted by Philip (1957) who proposes the following evolution of the infiltration rate.

$$i_t = \frac{1}{2}\phi t^{-1/2} + k_h \quad (3.19)$$

where ϕ is the sorptivity parameter and k_h is hydraulic conductivity. The above and other theoretical derivations of the infiltration process imply that under favorable conditions where there is enough water supply from the surface, there will be at least a minimum value of infiltration rate taking place. The minimum value corresponds to the saturated hydraulic conductivity of the soil (Figure 3.11). The problems that arise in applying the above hypothesis

in water balance models for larger time steps (10-day or monthly) are: within the time step of computation one can have several such curves during sequences of storms separated by one or more dry days. Moreover, if the infiltration rate is integrated over a time step, a large amount of potential infiltration is expected which would not be satisfied with rainfall within the time step. One can see from Table 3.2 that the total potential infiltration in one day is very high for all soil types (except clay). Daily rainfall could not satisfy even the lowest integrated infiltration amount using the saturated hydraulic conductivity.

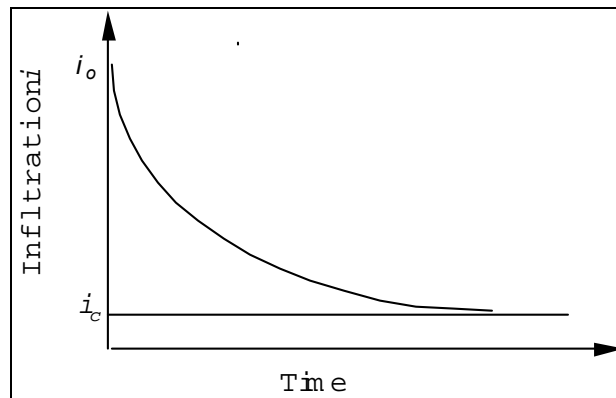


Figure 3.11 Evolution of the infiltration rate

Table 3.2 Ranges of values of hydraulic conductivity: (Todd, 1980)

Soil Type	m/day	m/10day
Sand course	45	450
Sand	12	120
Sand fine	2.5	25
Silt	0.08	0.8
Clay	0.0002	0.002

Hence using one of the common infiltration equations at this time step is not justified. In this study we preserve the decay of the infiltration rate through the control of the storage of the soil. We assume that the amount of rain infiltrated to the subsoil at a given time step is equal to the soil moisture deficit defined as the difference between the storage capacity and the current soil moisture content.

$$i_t = \min(p_t, (a_4 - m_{t-1})) \quad a_4 > 0 \quad (3.20)$$

where i_t is actual infiltration in mm per time step, a_4 is the storage capacity of the upper storage and m_{t-1} represents the soil moisture content at the beginning of time step t . The actual amount is always the minimum of the deficit and the rainfall p_t . The effect of antecedent rainfall is taken care of by the soil moisture storage i.e. the deficit calculated will be lower in cases the catchment is already wet. The graphical explanation of the above concept is shown in Figure 3.12. The available rainfall p_t controls the actual amount.

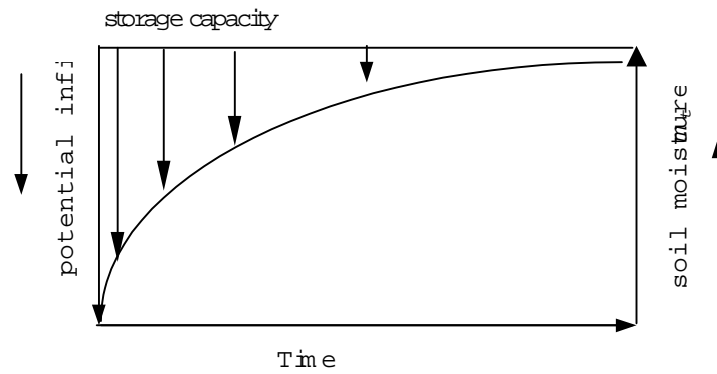


Figure 3.12 Relationship between infiltration and soil moisture storage.

3.3.4 Evapotranspiration component

The actual evaporation r_t is computed as a portion of the available water, while limited to the potential evaporation. In this model the average soil moisture is introduced as described in section 3.2. The same second evaporation equation of monthly water balance model is used with a 10-day time step with a slight modification. Instead of the available water w_t in the previous case, the average soil moisture storage is used in the equation. This is intended to consider the influence of variability of the soil moisture storage as in the flow computations.

$$r_t = \min[\bar{m}_t(1 - e^{-e_t a_1}), e_t] \quad a_1 \geq 1 \quad (3.21)$$

$$\text{where } \bar{m}_t = \frac{m_{t-1} + m_t}{2}$$

and a_1 is a time invariant parameter, which represents the characteristics of the catchment under study. e_t is the potential evaporation. It is evident that the predominant factor for evaporation in semi-arid and arid regions is the available water rather than the potential evaporation (Moore, 1989). Hence the above equation is applicable to catchments where the potential evaporation is very high during long periods and where mainly the available water controls the actual evaporation

3.3.5 Percolation component

Percolation, l_t , from the upper storage, to the groundwater is proportional to the upper soil moisture storage. The maximum percolation will be obtained when the upper storage is saturated. In some models such as the Stanford watershed IV Model (Crawford et al., 1966) percolation between layers is assumed to be not only function of the upper storage but also to the storage in the underlying layer. This will only make a difference when we consider the detail of the unsaturated zone between the two layers as capillary fringes, which account for very small part of the total storage.

The following empirical equation is used to represent the percolation at time t .

$$l_t = a_2 \bar{m}_t \quad 0 \leq a_2 \leq 1 \quad (3.22)$$

where a_2 is a percolation parameter when the upper storage is saturated.

An alternative to the above formulation was proposed by Moreda and Bauwens (1998). Hereby, the percolation was expressed as a function the ratio of the available moisture storage and the maximum capacity of the storage *i.e.* $l_t = a_2 m_t / a_4$. This results in a physically meaningful relation that when the available water is approaches the upper limit of the moisture storage, the percolation rate would be a_2 . It follows that parameter a_2 is analogous to the saturated hydraulic conductivity. This model structure was tested for two catchments and reported to show good performance. However this structure leads to problems for the parameter optimization, due to a high correlation between a_2 and a_4 .

3.3.6 Flow components

Three flow components are identified. The fast flow component f_t generated whenever the rainfall exceeds the infiltration rate within a time step considered.

$$f_t = p_t - i_t \quad (3.23)$$

The interflow s_t is calculated as a function of the infiltrated water and the product of the wetness of the upper storage expressed as m_t and parameter a_3 .

$$s_t = a_3 \bar{m}_t i_t \quad 0 \leq a_3 \leq 1 \quad (3.24)$$

The base flow component is computed as the release of the lower storage g_t which is controlled by base flow parameter a_5 .

$$b_t = a_5 \bar{g}_t \quad 0 \leq a_5 \leq 1 \quad (3.25)$$

$$\text{where } \bar{g}_t = \frac{g_{t-1} + g_t}{2}$$

The total flow d_t is then,

$$d_t = f_t + s_t + b_t \quad (3.26)$$

3.3.7 The water balance

At each time step, the water balance is computed for the two storages. The water balance of the upper soil moisture storage is computed at each time step as:

$$m_t = m_{t-1} + i_t - s_t - l_t - r_t \quad (3.27)$$

and the groundwater balance is computed as,

$$g_t = g_{t-1} + l_t - b_t \quad (3.28)$$

For medium sized catchments no delay of the flow components are considered, however for large catchments delay of flow (routing) may be necessary.

In the equations the average storages are used. To obtain the average storages, a similar iterative method as previously discussed for the monthly water balance models is adopted. The iteration is extended for both the soil moisture storage and the groundwater storages.

3.3.8 Parameter sets

Table 3.3 lists the parameter set of the 10-day water balance model. The table also gives the initial values for parameter optimization and approximate ranges of possible values for each parameter. The ranges are obtained by considering the order of magnitude of different components the water balance. Full description on the order of magnitude of parameters is provided in Appendix B.

Table 3.3 Parameters of the 10-days water balance model.

Parameter	Description	Initial values	Range
a_1	evaporation	0.004	0.001-0.01
a_2	percolation	0.04	0.001-0.01
a_3	interflow parameter	0.004	0.001-0.01
a_4	max. soil moisture storage	400	100-1000
a_5	base flow recession	0.04	0.01- 0.9

The optimum value of the first four parameters is obtained by minimizing the sum of squares of errors. For the last parameter, *a priori* knowledge on the catchment is used. The following section explains the methodology developed and coupled to the model.

3.3.9 Base flow recession parameter estimation

During low flow periods, the discharge of a river may be represented by an exponential decay function (Chow et al. 1988):

$$q_t = q_{t_0} e^{-k(t-t_0)} \quad (3.29)$$

It can be shown that applying the continuity equation for a linear reservoir, the flow of the river is given as:

$$q(t) = a_5 g_t \quad (3.30)$$

where $a_5 = -k$ is a decay coefficient and g_t is the groundwater storage. To determine the recession coefficient, the recession limbs of hydrographs are analyzed in such a way that during these periods it is assumed that only groundwater storage contributes to the flow. A routine for the estimation of the recession coefficient is included in the model. The method simultaneously traverses the rainfall and the flow series to obtain the recession hydrographs. The procedure to do this is:

- 1) *Locate a point on hydrograph when the recession starts.* A point (t_0, q_{t_0}) on the recession curve will be chosen as starting point if there are $n=3$ consecutive dry decades before t_0 . A dry decade may be defined as the decade with a rainfall less than a given limit, $RLIM$, that is not able to generate flow of the river. For 10-day time step $RLIM = 30$ mm can be taken. It has to be noted that this amount of rainfall is assumed to be evenly distributed over the ten days period.
- 2) *Check if the flow of the next decade is on recession hydrograph.* The flows at time t_0+1 , is selected if the decade is dry and the flow is less than q_{t_0} . If these conditions are not met go to step 4.
- 3) *Hold the pairs, time from the start of the recession point $(t-t_0)$ and the corresponding flows q_t . Repeat step 2.*
- 4) *Terminate a recession limb and start to look for the next recession limb until the flow series is exhausted (go to Step1.)*

This selection will result with a list of pairs of flows and time after the starting point t_0 . The recession curves for different years will normally also be different. An example of the result of the procedure for Mwambashi catchment is shown in Figure 3.14. To normalize the series each series is divided by the corresponding initial q_0 . Taking the natural logarithm of the ratio we have:

$$\ln \frac{q_t}{q_{t_0}} = -a_5 (t - t_0) \quad (3.31)$$

The above equation simply shows that a_5 is the slope of the average line relating the logarithm transformed ratio of flow plotted against the time delay $(t-t_0)$ (Figure 3.14). The unit of a_5 is 1/time step. Therefore the value of this parameter can be determined right before going to the model to ease the competition of multiple parameters in representing the general hydrograph. The flow cart that describes this procedure is given in Figure 3.15

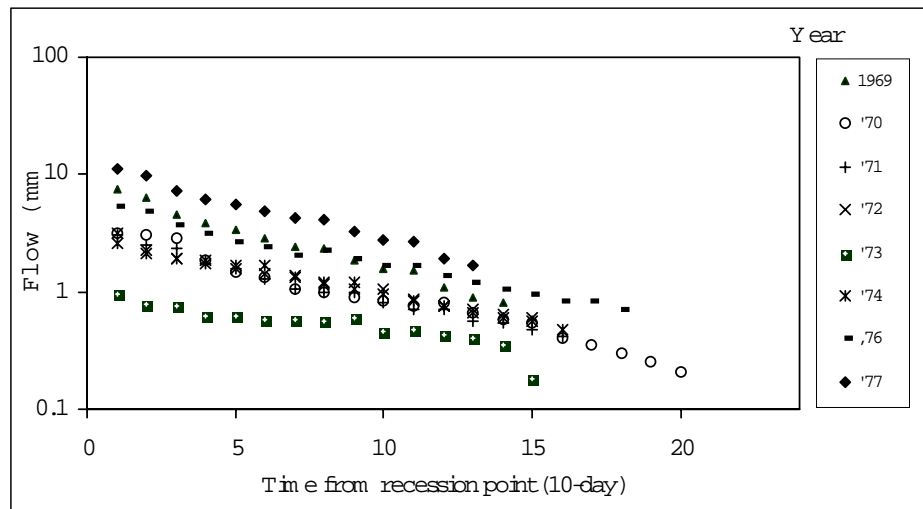


Figure 3. 13 Example of parallel recession curves (Mwambashi catchment, Zambia).

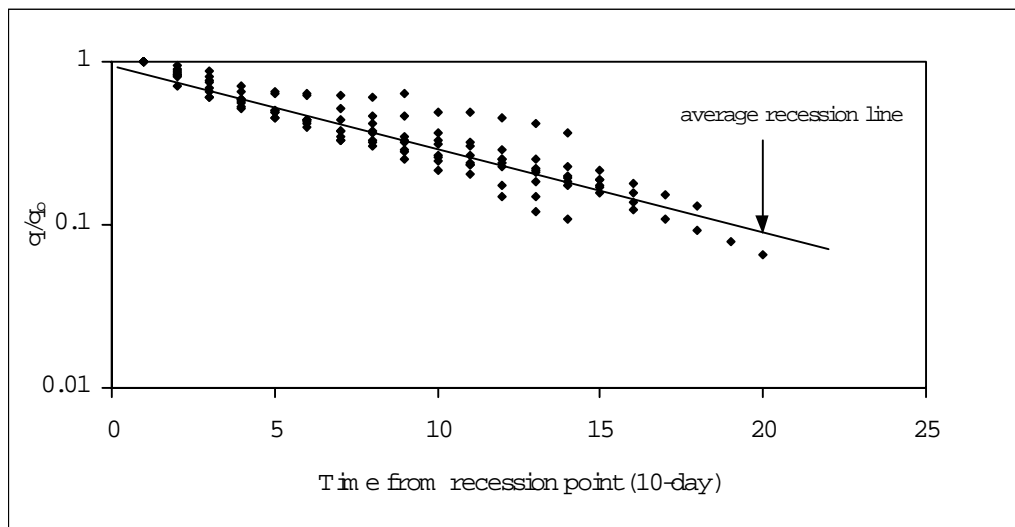


Figure 3.14 Example of normalized recession hydrographs (Mwambashi catchment, Zambia)

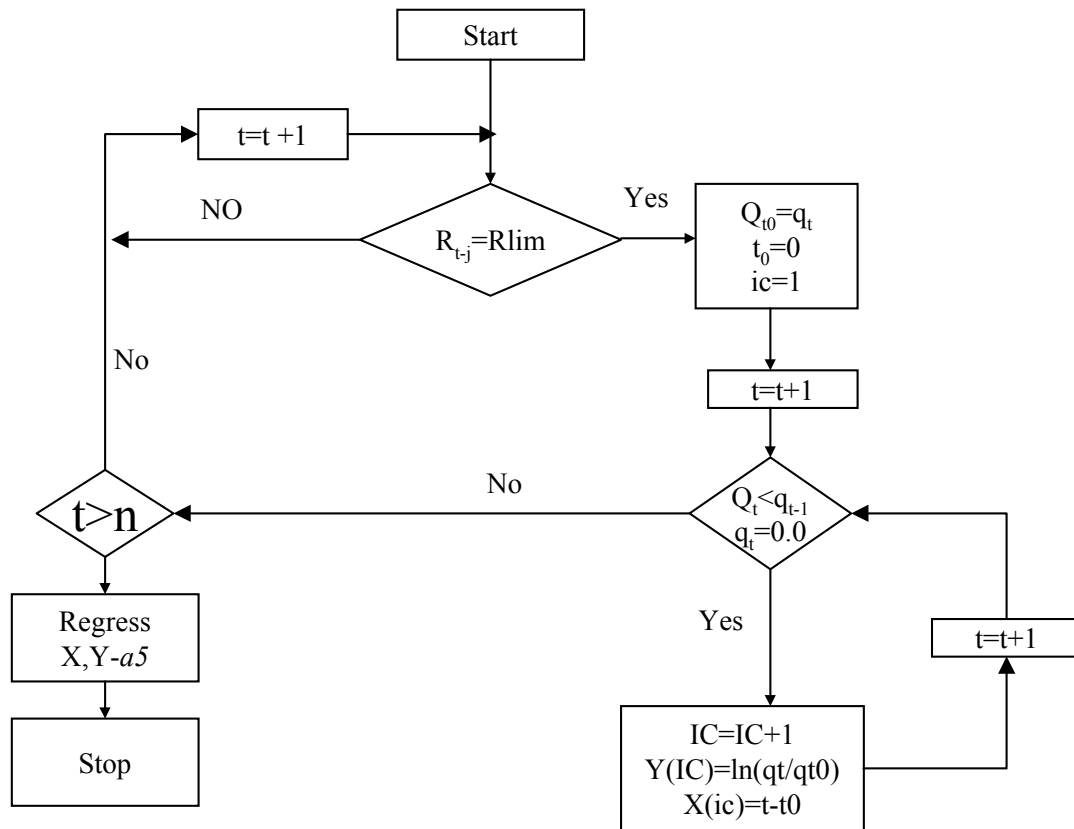


Figure 3.15 Flow-chart for recession parameter estimation

3.4 A parsimonious daily rainfall - runoff model

3.4.1 Background

The objective of this section is to extend the approach of conceptualization of the rainfall-runoff processes at catchment scale considered in the previous sections to daily time step.

Conceptual rainfall-runoff models consist of two main components: the first represents the soil water balance and the second represents the transfer of water to the closure section of the catchment. The water balance component is the most important aspect that characterizes a model. This component expresses the balance between the moisture content of the soil, generally divided into several zones and the incoming (precipitation) and outgoing (evaporation and runoff) quantities (Franchini and Pacciani, 1991). The earlier models described in this study deal only with the first component. Due to the coarse time step of computation attention was given only to the volume of water that could be proportioned to runoff and evaporation. Diminishing the time step to daily requires to also routing the generated volume of runoffs from each point in the catchment to the outlet in to account.

3.4.2 Model structure

The daily time step model proposed here (Figure 3.16) has the same structure as the 10-day time step model at the water-soil level. In addition the fast flow and the interflow are subjected to a transfer operation using linear reservoirs.

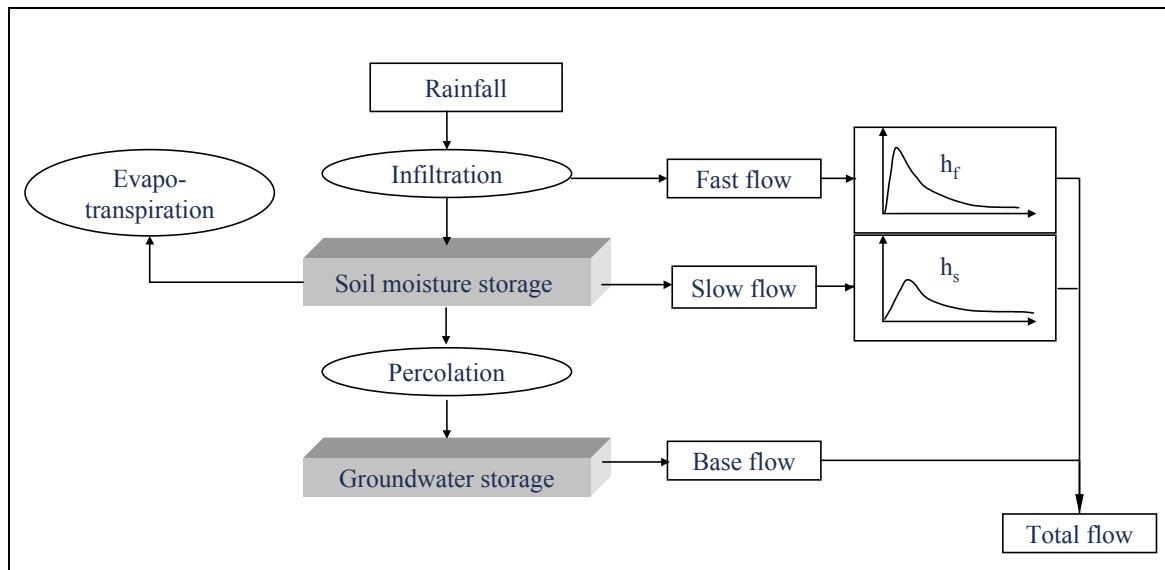


Figure 3.16 Conceptual representation of the daily rainfall runoff model.

In daily or smaller time step the runoff generated at a point in the catchment should be subjected to a transfer operation. Singh (1992) describes the runoff processes in two phases: (1) the overland flow phase, or the land phase, and (2) the channel phase. The transformation undergone by the inflow at a point until it reaches the outlet is due to a translation and a storage effect consisting of a time lag, and a shape modification. Some examples of flow routings used in conceptual-rainfall runoff models are described below.

In the SACRAMENTO (Burnash *et al.*, 1973) model, four components of flow (direct runoff, surface runoff, interflow, and base flow) are produced separately. The sum of the first three is transferred to the outlet section of the catchment using a unit hydrograph. The base flow on the other hand is added directly to the amount obtained from the transfer of the above mentioned three components.

In the SSARR (Rockwood *et al.*, 1972) model, each of the three components of flow (surface, interflow and base flow) is transferred to the outlet section separately by means of an algorithm based on the linear reservoir scheme.

In the XINANJIANG (Zhao *et al.*, 1980) model, the runoff is divided into two parts representing the surface component and the base flow component separately. The surface

component is transferred to the outlet section using a unit hydrograph. The base flow component is transferred using a linear reservoir scheme.

The ARNO (Todini, 1995) model has peculiarity that the three components (the direct runoff, the surface runoff, the interflow and the base flow) are added together and transferred to the outlet section by a double application of the parabolic unitary hydrograph. This unit hydrograph is obtained through analytical solution of the diffusive-convective flow equation (parabolic partial differential equation with the boundary condition that the input is uniformly distributed along the length of the drainage net (Franchini and Todini, 1988). Propagation towards the closure section of a succeeding sub-basin is also performed by means of a parabolic unit hydrograph (Todini and Bossi, 1986).

Among the various ways of routing, the Nash unit hydrograph based on a cascade of linear reservoirs is the most commonly used in hydrological modelling. The details of the derivation of the Nash unit hydrograph are available in a series of papers by Nash (1958,1959,1960) and summarized by Singh (1992).

In the proposed model, the fast and the interflow components are transferred to the outlet using a unit hydrograph described by a series of linear reservoirs. Similar to the SACRAMENTO model, the base flow is directly added to the routed components since the base flow is already described as a release from a linear reservoir considered in the water balance level, namely the groundwater storage.

3.4.3 Properties of linear reservoirs

The continuity equation for a reservoir is given by

$$I = Q + \frac{dS}{dt} \quad (3.32)$$

where I is the rate of inflow, Q is the rate of out flow, and S is the storage. These quantities are all functions of time. For the daily model (DRRM), the fast flow and interflow components, which are generated by the water balance level of the model are considered as separate inputs. The corresponding outflows are the delayed and routed response of each of the flow components at the catchment outlet. The fast flow is expected to respond in short period of time

compared to the interflow and for this reason two separate unit hydrographs are implemented which differ with their parameters. The highlight of the derivation of the unit hydrograph is given below. Detailed derivations are available in any hydrology books.

Using a simple linear relationship between discharge and storage

$$S = kQ \quad (3.33)$$

where k is the storage parameter, we have

$$I - Q = k \frac{dQ}{dt} \quad (3.34)$$

By utilizing the operator notation $D=d/dt$,

$$Q = \frac{1}{1 + kD} I(t) \quad (3.35)$$

Mathematically this is equivalent to

$$Q = e^{-t/k} \int e^{t/k} I \cdot dt \quad (3.36)$$

The operator $1/(1+kD)$ represents its effect on the inflow. The instantaneous unit hydrograph of the linear reservoir obtained by replacing $I(t)$ by a unit impulse input $\delta(t)$ in equation (3.36) is given as:

$$h(t) = \frac{e^{-t/k}}{k} \quad (3.37)$$

3.4.4 The Nash-Unit Hydrograph

The Nash model is based on a cascade of identical linear reservoirs. When the instantaneous unit effective rainfall, given by $\delta(t)$, is fed into the first reservoir, then equation 3.34 becomes.

$$h + k \frac{dh}{dt} = \delta(t) \quad (3.38)$$

Taking the Laplace transform of both sides of the above equation the outflow from the first reservoir due to an instantaneous inflow is: (Singh, 1992)

$$h_1(s) = \frac{1}{k(\frac{1}{k} + s)} \quad (3.39)$$

Where s is Laplace transform term that indicates the order of differences. Thus h_1 will be the inflow to the second reservoir, and the continuity equation for the second reservoir is given as

$$h_2 + k \frac{dh}{dt} = h_1 \quad (3.40)$$

Similarly Laplace transform gives

$$h_2(s) = \frac{1}{k(\frac{1}{k} + s)^2} \quad (3.41)$$

Generally for the n th reservoir we can write

$$h_{n(s)} = \frac{1}{k^n (\frac{1}{k} + s)^n} \quad (3.42)$$

By taking the inverses of the Laplace transform the Nash model is expressed as

$$h_{n(t)} = \frac{1}{k} \left(\frac{t}{k} \right)^{n-1} \frac{e^{-t/k}}{\Gamma(n)} \quad (3.43)$$

where $\Gamma(n) = \int_0^{\infty} e^{-x} x^{n-1} dx$ is the gamma function of n . Equation (3.43) expresses the impulse.

With the flexibility obtained by allowing n to take fraction values, the impulse response of this equation has the ability to represent adequately almost all impulse response of shapes commonly encountered in the hydrological context.

If the input is represented as a series of pulses (block of uniform input over duration T) and the output is similarly expressed as ordinate at intervals T , then the linear relationship is most conveniently expressed through the pulse response. For the system whose impulse response is given by a gamma function given as in equation (3.43), the corresponding pulse response can be obtained numerically by

$$h(T, t) = \frac{G(t) - G(t - T)}{T} \quad (3.44)$$

where

$$G(t) = \int_0^t h(t) dt = \frac{1}{k\Gamma(n)} \int_0^t e^{\tau/k} (\tau/k)^{n-1} d\tau \quad (3.45)$$

and τ is a dummy variable given as $t-T$. From Equation 3.44 one can see that the ordinates of the unit hydrographs can be obtained once the number of reservoirs, n and the storage parameter k , are fixed. These parameters are obtained by optimization. The parameter pair, n and nk , should however be chosen rather than n and k , because n is a shape parameter and the product nk is a scale parameter. In this way the two parameters are likely to be more independent than would n and k , both of which contribute to the scale.

Normally to set appropriate memory length one starts with a longer time and checks the significance of the ordinates at the tail of the hydrograph. The memory length for the catchment depends on the size and shape of the catchments. For the fast flow components a couple of weeks are necessary while for the interflow component longer memory length from a month to two month can be used.

3.4.5 Parameter sets

The set of parameters for the daily model can then sub-divided into two levels: The water balance and the flow routing parameters. To keep the number of parameters to be optimized as low as possible and for practical purposes, the parameter n which stands for the number of reservoirs can be fixed to integer values 1, 2, 3... etc. For the fast flow component, a starting value $n=1$ and for interflow $n=2$ are suggested. Thus the set of optimized parameters are $(a_1, a_2, a_3, a_4, a_5, a_6, a_7)$. As previously described, a_5 can be determined from daily hydrograph analysis hence the set of parameters to be optimized consists of $(a_1, a_2, a_3, a_4, a_6, a_7)$.

Table 3. 4 Description of parameters of the daily rainfall-runoff model

Parameter	Description	Initial value	Range
<i>Water balance</i>			
a_1	Evaporation parameter	0.04	0.01-0.1
a_2	Percolation parameter	0.004	0.001-0.01
a_3	Inter flow Parameter	0.004	0.0001-0.01
a_4	Max. soil moisture storage	400	100 -1000
a_{5*}	Base flow recession parameter.	0.01	0.01-0.001
<i>flow routing</i>			
a_6	Storage parameter for fast flow, k_f	1.0	1.0-30.0
a_7	Storage parameter for interflow k_s	2.0	1.0-100.0
<i>fixed parameters</i>			
n_f	Number of storage for fast flow	1	
n_s	Number of storage for interflow	2	
m_f	Memory length for fast flow	1-30 days	
m_s	Memory length for interflow	10-100 days	

- a_5 is possibly determined using hydrograph analysis.

3.5 Data requirement and scope of application of the developed models

The models developed here are intended to address the limited data availability in some regions of the world and hence require the following hydrological inputs on a daily, 10-day and monthly time steps. For calibrating these models a length of about 10 years of data is sufficient. For daily time step model rather short period of data up to 3 years may be enough to obtain optimum parameters.

- Areal precipitation
- Areal potential evaporation / mean temperature
- River flow at outlet of a catchment
- Catchment area

Since the models are strictly based on the water balance at a catchment scale any water taken from or come in to a catchment from an adjacent catchment has to be taken care of separately.

The potential uses of these models are to extend flow data from precipitation and evaporation data and filling missing flow data. They can also be used to separate fast and slow flow components. Moreover the models also provide some intermediate variables such as the soil moisture fluctuation during the season which can be used for observing soil moisture deficits for agricultural purposes. The daily rainfall runoff model developed may also be used for flood forecasting if coupled with a rainfall forecasting scheme.

Limitations

One of the limitations of the present models is the area of the catchment because of the assumption of homogeneous distribution of rainfall and evaporation. If there is high spatial variation of rainfall the model will not perform efficiently. On the other hand, too small catchments will also give difficulties in that the groundwater and the topographic divides may not coincide. Hence there would be a considerable loss of water to adjacent catchments and the water balance would be violated.

The models are not applicable if there are large water bodies such as lakes in the catchment and if significant frost and snow occur. For the latter problem, an extension of the model was proposed by introducing one additional storage, which takes care of the snow storage (Ni-Lar - Win, 1994). For such models temperature inputs are mandatory.

Chapter 4

4 STATISTICAL METHODS

4.1	Introduction	74
4.2	Data checking.....	74
4.3	Parameter estimation	77
4.4	Model validation	90

4.1 Introduction

With the increasing number of models in literature, efforts are devoted to developing a statistical methodology to the evaluation of the quality of input data, estimation of initial conditions, to parameter optimization techniques and to the validation of the performance of a model. This chapter formulates the methodology that will be followed in this research.

4.2 Data checking

Advances in scientific hydrology and practice of engineering hydrology depend on good, reliable and continuous measurements of hydrological variables. Model calibration more than anything relies on the quality of data available. Hydrological data must be cleaned from random and systematic error for erroneous data leads to either non-veritable rejection of a model or wrong calibration that affects the usefulness of a model. Different types of error that encountered in hydrological data are due to:

- Instrument errors
- Change of measuring sites and techniques

- Data inputting and computation errors
- Flow computation errors.

Instrument errors and change of measuring site

The first two types of errors can be identified using known methodologies such as mass curve and double mass curve analysis. Inter comparison plots of the same variables measured at adjacent stations can help to verify the consistency of the data series.

Another interesting procedure to check the stationarity of long records is to split the data set in to two periods and to test the elementary statistics for the two periods. This test can be done if there are long data series to observe and if there are general changes of the hydrological variables due to the reasons listed above.

Let $X_{1j}, j=1, 2, \dots, n_1$ and $X_{2j}, j=1, 2, \dots, n_2$ be two time subseries of a very large hydrological data series with the sample means \bar{X}_1 and \bar{X}_2 respectively. The t-statistic is mostly used for testing whether the difference of the two means of the subseries is significant, that is

$$t = \frac{\bar{X}_1 - \bar{X}_2}{s \sqrt{\frac{n_1 + n_2}{n_1 n_2}}} \quad (4.1)$$

where

$$s = \sqrt{\frac{\sum_{i=1}^{n_1} (X_i - \bar{X}_1)^2 + \sum_{i=1}^{n_2} (X_i - \bar{X}_2)^2}{n_1 + n_2 - 2}} \quad (4.2)$$

The variable t of Equation 4.1 is compared with the table value of the Student t-distribution with $(n_1 + n_2 - 2)$ degrees of freedom and 5% significance level. Helsel and Hirsh, (1992) state that the above test is valid if the two subseries are independent and the series under study are normally distributed.

Data inputting and computation errors

Data inputting and gross computational errors are those which generate random errors and it is very difficult to detect them. Time series plot and visual inspection of the graphs may reveal large errors such as decimal point shift and addition of digits. Quick annual water balance of observed components may also reveal some gross errors.

Flow computation errors

The quality of discharge data plays a central role in the development of a model and also in calibrating and applying it. However, the discharge records are often less accurate than desirable. Discharges are computed from continuous stage records using an established rating curve (Stage-Discharge relationship) at a gauging site on a river. Some of the causes of errors in discharge computation include the unstability of the cross-section (the riverbanks and bed) so that the discharge translation from stage can be corrupted. The complexity of a rating curve with hysteresis also reduces the accuracy of flow. High flows are normally approximated by extrapolation of rating curves and debris or sedimentation of a channel easily corrupts low flows. Despite these and many other problems associated with obtaining an effective record of stream discharge, the stream flow record is generally considered to be the most accurate element of a catchment's hydrologic history (Burnash, 1995)

Most of the river gauging sites in the world are located on the natural cross-section of rivers. Ideally, the sites (the banks and bed of a channel) should be stable and there should be a control section downstream such as fall to avoid backwater effect. However, it is often impossible to locate such a site which should also be accessible for daily reading and regular supervision. As a result a reasonably good site is identified and instruments are installed. It is advisable in such instances to investigate the cross-section of the gauging site and calculate indicative discharges using Manning or Chezy formulas to avoid extrapolation errors that could occur by applying the rating curves. An example of such problem is discussed in Section 5.2 for a river gauging station in Ethiopia.

Since stream flow data are continuous in time and correlated in space it is possible for the reliability of the observation to be checked by interpolation and statistical methods. WMO (1994) outlines means of checking for internal consistency between observed discharges as follows:

- a) Qualitative assessment of the correspondence between discharges at adjacent stations;
- b) Qualitative assessment of the relationship between the discharges and the value during the previous measure;
- c) Approximate check of the value of the discharge by seeing that it falls within the range of the previous value for the given phase in the regime of the river; and
- d) Approximate assessment of correspondence between the measured value and the regular variation during the previous period.

4.3 Parameter estimation

Sorooshian, and Gupta (1995) classify parameters into two groups: physical and process parameters. A physical parameter represents physically measurable properties of the watershed (e.g. areas of the catchment, fraction of impervious area and surface area of water bodies, surface slope etc). Process parameters represents properties of the watershed which are not directly measurable e.g. average or effective depth of surface soil moisture storage, the effective lateral inflow rate, the coefficient of non linearity controlling the rate of percolation to the groundwater and so on. In fact the division between the two groups depends on the spatial distribution and structure of a model. In a conceptual rainfall-runoff models almost all of the parameters are of the second type where the optimum values are obtained by calibrating the model using historical data.

Model calibration is one of the most important aspects of hydrologic modelling. Conceptually realistic models can produce erroneous results if they are not properly calibrated. When calibrating catchment models the following questions are frequently asked (Gan, 1988):

- a) Which calibration approach should be used, manual or automatic?
- b) For automatic calibration, how many parameters should be optimized and which ones?
- c) When calibrating manually, what parameters should be changed and by how much?
- d) How to determine if optimality has been reached and that any further adjustment would only yield marginal returns?
- e) What guidelines to use to determine if parameters are final or not?

In dealing with the questions above, the skill, experience and intuition of the hydrologist and his/her knowledge of the hydrologic model play an important role. This is particularly true when manual calibration is employed. It is recommended that a combination of manual and automatic procedure be adopted for the model calibration (*Gan, 1988*). Manual calibration alone is very tedious, time consuming, and requires the experience of the hydrologist. Because of the time-consuming nature of the manual model calibration, there has been a number of researches towards development of automated calibration methods. Automatic calibration on the other hand relies heavily on the optimization algorithm and the specified objective function. The following section summarizes some of the usual objective functions and techniques of optimization algorithms.

4.3.1 Objective function

An objective function is an equation that is used to compute a numerical measure of the deviation between the model calculated output and the observed catchment output. Typical outputs used in hydrological modelling are stream flow hydrographs and groundwater levels. Objective functions that have been shown to work well in practice include the least square and maximum likelihood estimates.

Least square method

The least square method (LS) determines the parameter value for which the sum of squared deviations between the observations and their expectations is as small as possible.

$$F(X) = \sum_{t=1}^n w_t [q_t - d_t(X)]^2 \quad (4.3)$$

where:

q_t	= observed streamflow value at time t ;
$d_t(X)$	= model calculated flow value at time t ;
X	= vector of model parameters;
n	= the number of data points.
w_t	= weight at time t

The method implicitly assumes that the differences of observed and calculated quantities have equal weights throughout the data points. In practice, a weight factor can be introduced to indicate the importance of particular hydrological values such as high flow regime. If all weights are equal then one has the Simple Least Square (SLS), and if different weights are introduced the Weighted Least Square (WLS). In case where the variance of the deviations exhibits a large variation, a transformation of the observed and calculated quantities would be necessary. Vandewiele *et al.* (1993) suggest square root transformation, which is believed to have less computation difficulties than the logarithmic transformation. In the present study due to large variation of flow, the square root transformation of the computed and observed flows is used to compute the objective function.

Maximum Likelihood Methods

The maximum likelihood method (ML) determines the parameter value, for which the probability of the deviation is as maximum as possible. Hence the method estimates the parameters set that maximizes the probability of the observation. The Maximum Likelihood is reduced to the SLS if the following two assumptions hold true:

the deviations are normally distributed with mean zero and variance σ^2

the deviations are independent of each other.

In reality, these assumptions are often violated and hence methods that account for non-stationary variance in streamflow errors are developed (Sorooshian and Dracup, 1980; Sorooshian, 1981). One of the forms of the maximum likelihood criteria called HMLE (Heteroscedastic Maximum Likelihood Estimator) is defined as:

$$\max_{X, \lambda} HMLE = \frac{\frac{1}{n} \sum_{t=1}^n w_t \varepsilon_t^2}{\left[\prod_{t=1}^n w_t \right]^{1/n}} \quad (4.4)$$

where $\varepsilon_t = q_{t, \text{obs}} - d_t(X)$ is the model residual at time t ; w_t is the weight assigned to time t , computed as:

$$w_t = f_t^{2(\lambda-1)} \quad (4.5)$$

where f_t is the expected value of the simulated flow at time t . Recently Yapo *et al.* (1996) suggest the use of the observed flow as a factor to obtain a stable estimator. Further they confirmed that this estimator provides consistent performance across all flow ranges.

4.3.2 Optimization Algorithms

Once the objective function is identified, the next step is to obtain the parameter set, which results in the extreme value of the function. The surface described by the set of parameter is known as the response surface.

Figure 4.1 shows a surface described by one and two parameter models.

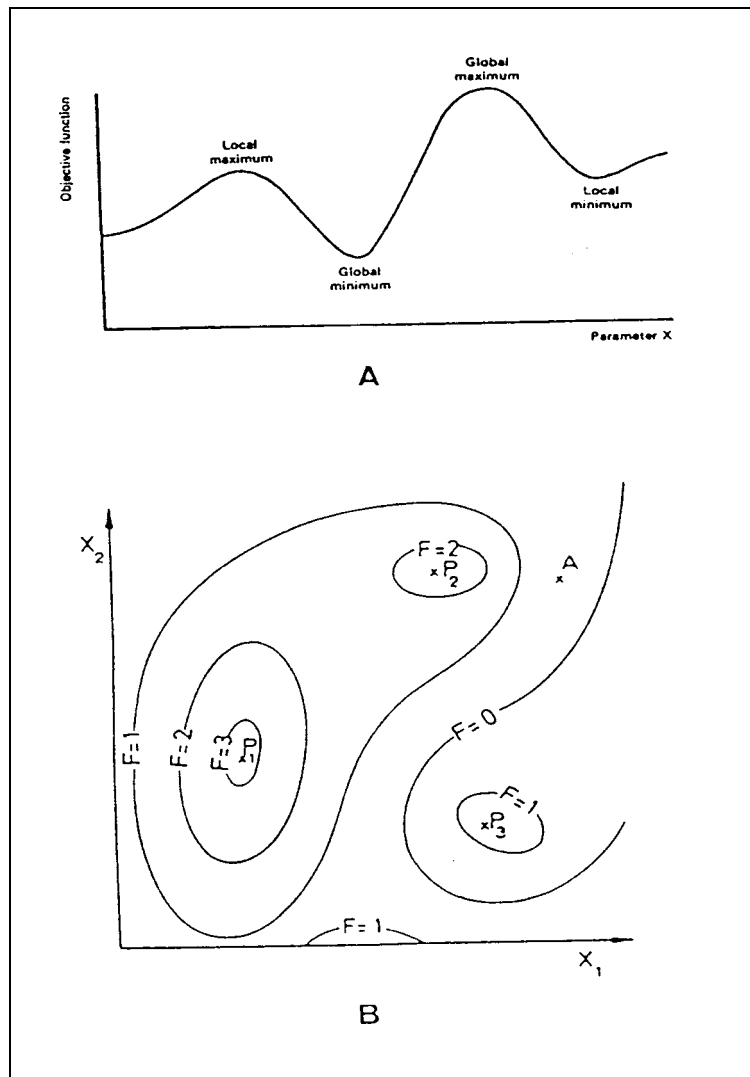


Figure 4.1 Response surface A: one parameter model; B: two-parameter model

The gradient G of the objective function is given as:

$$G(X) = \left(\frac{\partial F(X)}{\partial x_1}, \frac{\partial F(X)}{\partial x_2}, \dots, \frac{\partial F(X)}{\partial x_n} \right) \quad (4.6)$$

One obtains the second derivative, which is often called Hessian matrix as:

$$H(x) = \begin{vmatrix} \frac{\partial^2 F(X)}{\partial x_1^2} & \frac{\partial^2 F(X)}{\partial x_1 \partial x_2} & \dots & \frac{\partial^2 F(X)}{\partial x_1 \partial x_n} \\ \frac{\partial^2 F(X)}{\partial x_2 \partial x_1} & \frac{\partial^2 F(X)}{\partial x_2^2} & \dots & \frac{\partial^2 F(X)}{\partial x_2 \partial x_n} \\ \dots & \dots & \dots & \dots \\ \frac{\partial^2 F(X)}{\partial x_n \partial x_1} & \frac{\partial^2 F(X)}{\partial x_n \partial x_2} & \dots & \frac{\partial^2 F(X)}{\partial x_n^2} \end{vmatrix} \quad (4.7)$$

Under general conditions this matrix is symmetrical i.e.

$$\frac{\partial^2 F(X)}{\partial x_1 \partial x_2} = \frac{\partial^2 F(X)}{\partial x_2 \partial x_1} \quad (4.8)$$

Let $F_0 = F(X_0)$, $G_0 = G(X_0)$, $H_0 = H(X_0)$ then one can write the Taylor expansions as:

$$F(X) = F_0 + G_0 \cdot (X - X_0)^T + \frac{1}{2} (X - X_0)^T H_0 \cdot (X - X_0)^T + \dots \quad (4.9)$$

and for the gradient we have

$$G(X) = G_0 + (X - X_0) \cdot H_0 + \dots \quad (4.10)$$

If F is twice differentiable, the necessary condition for \tilde{X} to be associated with a global or local minimum value of F is that $G(\tilde{X})=0$, and that $H(\tilde{X})$ be positive definite. Due to the non-linearity nature of the system, the assumptions mentioned above are seldom realized. In reality the objective function for the rainfall runoff models are not analytically differentiable. The values are normally discrete values for each time step considered. The immediate solution at this instance is using the differences. For instance if X is an n -parameters vector $\{a'_1, a'_2 \dots a'_n\}$, the first element of the Hessian matrix, i.e. second derivative with respect of the same parameter can be estimated as:

$$\frac{\partial^2 F}{\partial a'_1 \partial a'_1} = \frac{F(a'_1 + \Delta a'_1, a'_2 \dots a'_n) - 2F(a'_1, a'_2 \dots a'_n) + F(a'_1 - \Delta a'_1, a'_2 \dots a'_n)}{(\Delta a'_1)^2} \quad (4.11)$$

A similar formula can be used to estimate the diagonal of the matrix. For the other elements,

$$\frac{\partial^2 F}{\partial a'_1 \partial a'_2} = \frac{1}{4\Delta a'_1 \Delta a'_2} \left\{ \begin{aligned} & \left(F(a'_1 + \Delta a'_1, a'_2 + \Delta a'_2, \dots, a'_n) - F(a'_1 + \Delta a'_1, a'_2 - \Delta a'_2, \dots, a'_n) \right) \\ & - \left(F(a'_1 - \Delta a'_1, a'_2 + \Delta a'_2, \dots, a'_n) + F(a'_1 - \Delta a'_1, a'_2 - \Delta a'_2, \dots, a'_n) \right) \end{aligned} \right\} \quad (4.12)$$

In calculating the Hessian matrix it is better to use scaled parameters instead of the parameter itself to obtain a well-conditioned matrix for inversion.

Different optimization algorithms are available for solving this problem with varying efficiency, depending on the level of complexity of the problem such as number of parameters, computation capacity etc. The major characteristics complicating the optimization problem in conceptual rainfall-runoff modelling summarised by Duan *et al.* (1992).

- a) regions of attraction, where more than one main convergence region exists;
- b) minor local optima, where there are small peaks in each region;
- c) roughness, when the response surface is rough with discontinuous derivatives;
- d) sensitivity, poor and varying sensitivity of the response surface in the region of optimum and non-linear parameter interaction; and
- e) shape, resulting from a non convex response surface with long curved ridges.

Search algorithms are broadly classified into two groups, the local and global search methods. The difference between these two methods is mainly the way they advance from one solution point on the surface of the response to the next feasible point. A local search algorithm tries to find the minimum point from a certain given point by investigating all possible ways and then continues until it reaches a point where further move does not improve the solution. On the other hand the global search algorithms attempt to exhaust all possible local minimum points by starting from different initial points and then evolving following different of selection criteria from the set of the points.

Local Search algorithms are further classified as direct search method and gradient methods. Direct methods just use information of the function value to arrive at the optimal (evaluating objective function in successive neighbor points). These algorithms select the best new direction and best step to achieve improvement as fast as possible. Rosenbrock method (Rosenbrock, 1960), the Pattern Search Method (Hook and Jeeves, 1961) and the Simplex Method (Nelder and Mead, 1965) are some examples of direct search method.

Gradient algorithms use the function value and additionally information coming from the gradient in order to determine direction and step to reach the local minimum. Gradient methods are based on a truncation of the Taylor Series expansion in the domain of the parameters (Sorooshian 1995).

In this study two optimization methods are coupled with the developed models: the VAO5A method (Harwell subroutine library, 1974) which has been recommended as a better optimization method for rainfall-runoff modelling by Demaree (1982) and the more recent Shuffled Complex optimization method developed by Duan *et al.* (1992). The following two sections briefly describe the two optimization methods.

4.3.3 The VAO5A algorithm

The VAO5A program is originally taken from the Harwell subroutine library (1974). The method is based on the compromise between three different classical algorithms for minimizing the sum of squares of errors, namely Newton Raphson, Steepest Descent and Marquardt. It automatically obtains and improves an approximation of the Jacobian matrix G and the Hessian Matrix H . From the inverse of the Hessian matrix H , the covariance matrix, Λ , of the continuous filter parameters is obtained by

$$\Lambda = 2\sigma^2 H^{-1} \quad (4.13)$$

where σ is the standard deviation which is obtained as:

$$\sigma = \sqrt{\frac{\min(ssq)}{N - n}} \quad (4.14)$$

where

N = number of data points

n = number of parameters to be optimized

From the covariance matrix, the correlation between two parameters a_i and a_j can be calculated

$$\text{Corr}(a_i, a_j) = \frac{\lambda_{ij}}{\sqrt{\lambda_{ii}\lambda_{jj}}} \quad (4.15)$$

Where λ_{ij} is the $(i,j)^{th}$ element of the covariance matrix, Λ . It follows that the standard deviation of parameter a_i is

$$\sigma = \sqrt{\lambda_{ii}} \quad (4.16)$$

The program is supplemented with subroutines that provide key statistics such as standard deviation of a parameter and correlation matrix among the parameter. These statistics are not given much attention in other methods such as shuffled complex algorithm.

The algorithm requires a predetermined order of magnitude of the parameters to scale them down to values between 0.0 to 1.0. This is to allow using the same step of increment while searching the direction. The other limitation of this method is that the parameters can not be constrained. A user has to specifically define the parameter constraints in the structure of the model to avoid unrealistic computation. For example for the models described in section 3.2, the parameters a_2 and a_3 are bounded by zero and 1. The final values of parameters obtained from this optimization method should be inspected, to see whether they fall within the specified range. The definition of the constants and default setting used in the method are given Table 4.1.

Table 4.1 Inputs of the VA05A optimization method.

No.	Symbol	Definition	Recommended value
1	DSTEP	initial increment of parameters	0.01
2	ACC	stop criterion difference between consecutive sum of squares of error.	0.001
3	MAXFUN	Maximum number of iterations to obtain optimal vales.	10000

4.3.4 The shuffled complex evolution algorithm

The shuffled complex evolution algorithm (SCE-UA) is a global technique that can be applied in a broad range of optimization problems. This method is classified as probabilistic because it evaluates the objective function at randomly spaced points in the feasible parameter space. The SCE-UA combines advantages and strategies of the Simplex procedure (Nelder and Mead, 1965), Controlled Random Search (Price, 1987), Competitive Evolution (Holland, 1975) and the newly developed complex shuffling (Duan *et.al*, 1992). "The strategy in this optimization method is analogous to giving the same difficult problem to 12 identically capable people and asking them to solve it without conferring with each other. Clearly, a more efficient strategy would be for them to spend some time working independently or in small groups and to get together now and then to share information about their progress"

SCE-UA treats the searching process as a natural biological evolution course. The method begins with a population of points randomly chosen from the feasible space. Then the population is partitioned into several communities, referred to as complexes, each containing $2n+1$ points; where n is the dimension of the problem (number of optimized parameters). Each community is made to evolve based on a statistical "reproduction" process that uses simplex geometric shape to direct the search in an improvement direction. It ensures sharing information by periodically shuffling the entire community (Duan *et al.*, 1992).

The SCE-UA algorithm consists the following steps (Duan et al, 1992).

1. To initialize the process, select $p \geq 1$ and $m \geq n+1$, where p is the number of complexes, m is the number of points in each complex, and n is the dimension of the problem. Compute the sample size $s = pm$
2. Then generate a sample as follows. Sample s points $x_1 \dots x_s$ in the feasible space $\Omega \subset R^n$. Compute the function value F_i at each point x_i . In the absence of prior information, use a uniform sampling distribution.
3. Rank the points as follows. Sort the s points in order of increasing function value. Store them in an array $D = \{x_i, F_i, i=1 \dots s\}$. So that $i=1$ represents the point with the smallest function value.
4. Partition D into p complexes $A^1 \dots A^p$, each containing m points, such that $A^k = \{x_j^k, F_j^k / x_j^k = x_{k+p(j-1)}, F_j^k = F_{k+p(j-1)}, j=1 \dots m\}$.
5. Evolve each complex A^k , $k=1 \dots p$, according to the complex evolution (CCE) algorithm outlined separately.
6. Shuffle the complexes as follows. Replace $A^1 \dots A^p$ into D , such that $D = \{A^k, k=1 \dots p\}$. Sort D in order of increasing function value
7. Check convergence. If the convergence criteria are satisfied or maximum number of trials is exceeded. stop. Otherwise return to step 4. The convergence criteria is expressed as the difference between the successive F values, and which should be smaller than a given accuracy limit.

The competitive complex evolution (CCE) algorithm required for the evolution of each complex in step 5 is outlined as follows.

1. To initialize the process, select q , α , and β , where $2 \leq q \leq m$, $\alpha \geq 1$ and $\beta \geq 1$.
2. Assign weights as follows. Assign a trapezoidal probability distribution to A^k , i.e.,

$$\rho_i = \frac{2(m+1-i)}{m(m+1)}, \quad i = 1 \dots m \quad (4.17)$$

The point x_1^k has the highest probability $\rho_1=2/m+1$. The point x_m^k has the lowest probability $\rho_m=2/m(m+1)$.

3. Select parents randomly choosing q distinct points $u_1 \dots u_q$ from A^k according to the probability distribution specified above (the q points define a ‘subcomplex’). Store them in array $B=\{u_i, v_i, i=1..q\}$, where v_i is the function value associated with point u_i . Store in L the locations of A^k , which are used to construct B .
4. Generate offspring’s according to the following procedure:
 - a) Sort B and L so that the q points are arranged in order of increasing function value and compute the centroid g using the expression:

$$g = \frac{1}{q-1} \sum_{j=1}^{q-1} u_j \quad (4.18)$$

- b) Compute the new point $r=2g-u_q$ (reflection step).
- c) If r is within the feasible space Ω , compute the function value f_r and go to step d ; otherwise compute the smallest hypercube $H \subset \mathbb{R}^n$ that contains A^k , randomly generate a point z within H . Compute f_z set $r=z$ and set $f_r=f_z$ (mutation step).
- d) If $f_r < f_q$, replace u_q by r , go to step f ; otherwise compute $c=(g+u_q)/2$ and f_c (contraction step).
- e) If $f_c < f_q$ replace u_q by c , go to step f ; otherwise randomly generate a point z within H and compute f_z (mutation step). Replace u_q by z .
- f) Repeat steps a-e α times, where $\alpha \geq 1$ is a user-specified parameter. This value can be set to unity.

5. Replace parents by offspring as fallow. Replace B into A^k using the original locations stored in L . Sort A^k in order of increasing function value.

6. Iterate by repeating steps 2-5 β times, where $\beta \geq 1$ is a user-specified parameter that determines how many offspring should be generated (how far each complex should evolve).

The FORTRAN coded program is available from the Authors. The user should provide an input file that contains some of the constants and the range of parameters. Table 4.2 summarizes the input required. The choice of the objective function is left for the user. This allows adapting the optimization method to any kind of model involving parameter optimization.

The authors claim that the method developed is efficient in a wide range of problems. Recent application of this method by Gan *et al.*, (1996), and Franchini *et al.*, (1998) also confirm the method mostly guarantees the global optimization for conceptual rainfall-runoff models. The main advantage of this method is that once the range of a parameter (lower bound and upper bound) is identified from experience or from physical interpretation of a component of models, it allows investigating a wider range of points in such a manner that the global optimum will be obtained.

Unlike the first optimization method VA05A, this method does not require scaling of parameters. This endows one of the advantages since in some cases prior identification of scales of parameter can be difficult.

It is obvious from the description of the method, that it explores exhaustively in the space of the feasible region bounded by the upper and lower limits of parameters. Hence it ensures the global optimization. On the other hand the method does not give any statistics about the inter-relationship that exists between parameters nor of sensitivity of the objective function. In the present study, the parameters are optimized using either of the two methods. To obtain the statistics related to the parameter optimization, the final solutions obtained by the Shuffled complex algorithm are input to the VAO5A method. From the latter method the essential statistics such as standard deviation of parameter, correlation matrix and sensitivity of the objective function to individual parameter in a periphery of the optimal point are obtained.

Table 4.2 Inputs of the Shuffled complex optimization method.

No.	Symbol	Definition	Recommended value

1	MAXN	Maximum number of trials	10000
2	KSTOP	Number of Shuffling loops in which the criterion value must change in a the specified percentage or else optimization will be terminated	5
3	PCENTO	Percentage by which criterion value must change in the specified number of shuffling loops or else optimization is terminated	
4	NGS (p)	Number of complexes used for optimization search	2-20
5	ISEED	Random seed in optimization search	
6	NPG (m)	Number of points in each complex	$2n_{opt}+1$
7	NPS (q)	Number of points in each sub-complex	$N_{opt}+1$
8	NSPL (β)	Number of evolution steps taken by each complex before next shuffling	$2n_{opt}+1$
9	MINGS	Minimum number of complexes required for optimization search, if the number of complexes is allowed to reduce as the optimization search proceeds.	2-20
10**	INIT	Initial estimate of the parameter to be optimized	
11	LOWER-B	Lower bound of the parameter to be optimized	
12	UPPER-B	Upper bound of the parameter to be optimized	

* N_{opt} = Number of parameters to be optimized; ** Inputs 10, 11, 12 are provided for each parameter to be optimized.

4.4 Model validation

Selection of a 'good' model requires both subjective and objective judgements to determine whether the results provide adequate information for answering the question facing decision-makers. The results may be influenced by a variety of causes. Common problems in calibration are among others;

- errors in the data used in calibration
- use of a period of record that does not contain enough of the physical processes needed to calibrate key parameters

After the model has been chosen and parameters estimated, its merits have to be judged. This testing or validation can be considered as an important stage of the model analysis. If the model is good enough, then application proceeds. If not, the whole process starts again by changing one or more working hypotheses. The criteria considered to judge on the performance of the models developed in this study are as follows.

- 1) The significance of the parameters (confidence intervals)
- 2) Graphical comparison of simulated and observed flows
- 3) Comparison of monthly means of observed and computed flow
- 4) Model Efficiency: the percentage of explained variance
- 5) Model Quality factor (see Vandewiele *et al.*, 1992).
- 6) Residual Analysis (variance, seasonality and auto-correlation of residuals)

4.4.1 Checks on significance of a parameter

The question to be answered at this step is if all parameters are really necessary in the model to describe the physical processes occurring. The hypothesis is tested that parameters a_i are significantly different from zero. This is examined by checking whether the zero value belongs to the 95% confidence interval, CI.

$$CI = (\hat{a}_i - 1.96\sigma_i, \hat{a}_i + 1.96\sigma_i) \quad (4.19)$$

and the half width of confidence interval (HWCI) is given as:

$$HWCI(\hat{a}_i) = 1.96\sigma_i \quad (4.20)$$

If the hypotheses $a_i = 0$ is acceptable, then parameter a_i can be set equal to zero without diminishing the explanatory power of the model. The model then has to be recalibrated either with by setting the value of this parameters to zero. Care must be taken at this stage that the hypothesis suggests the superfluous parameter considering all the rest of the parameters at optimum value.

4.4.2 Graphical comparison of simulated and observed flows

Graphical display of simulated and observed flows is very important because the traditional method of evaluating model performance by statistical measures has limitations. Statistical indices are not effective in communicating qualitative information such as trends, types of errors and distribution patterns. In fact one should not depend on only single statistical measures of model performance. These are sometimes misleading because of the high possibility of compensation of errors from season to season or over years in long-term calibration. In this research we propose that in cases of highly variable input cases the quality measures should also account for this variation and hence seasonal means have to be compared.

4.4.3 Comparison of monthly means of observed and computed flow

The seasonal means are computed as follows. Let q_{ij} denote the observed flow during year i and season j , where $j=1,2,..P$ and P is the number of seasons in the year. For example $P=12$ and $P=36$ for monthly and decade time series respectively. The seasonal mean is given as:

$$\bar{q}_j = \frac{1}{Y} \sum_{i=1}^Y q_{ij} \quad (4.21)$$

where Y is the length of the data in years. Similarly long term seasonal means of all input and output variables are computed using equation 4.21. Graphical or numerical display of these values gives a summary of results on the water balance of a catchment. Moreover it depicts the success or failure of the model in reproducing the expected values along the whole period of the year.

4.4.4 Model Efficiency

The statistical index of modelling efficiency (E_f) was defined by (Nash and Sutcliffe, 1970) as:

$$E_f = \frac{\sum (q_o - \bar{q}_o)^2 - \sum (q_c - q_o)^2}{\sum (q_o - \bar{q}_o)^2} \quad (4.22)$$

where q_o = observed flow,
 \bar{q}_o = mean observed flow and
 q_c = calculated flow.

The sum is taken over the whole period of the data used for calibration. The closer this value to unity, the better the model explains the variance. A negative modelling efficiency means that the model prediction is worse than simply using the mean of the observed flows. This measure is highly affected by a few extreme errors and can be biased if a wide range of flow events is experienced.

4.4.5 Model Quality factor

The model quality is a check on whether the model gives a computed output that is a sufficiently close reproduction of the observed output. When the standard deviation, σ of the random component is small, the unexplained part of runoff is small and the model fits observed runoff very nearly. Therefore, σ is an inverse measure of quality. It is better to use the variation coefficient $vcf\ q_t$, which is a dimensionless quantity expressed as standard deviation divided by expectation. Vandewiele et al., (1993) provides different expression for the vcf for transformed flows. For square root transformed flows It can be shown that

$$vcf\ q_t = \frac{\sigma \sqrt{4d_t + 2\sigma^2}}{d_t + \sigma^2} \approx \frac{2\sigma}{\sqrt{d_t}} \quad (4.23)$$

where d_t is the computed flow. The approximated expressions are valid for small σ . The inverse measure of the quality depends on d_t , that is on time. Therefore the model variation coefficient for d_t equal to its mean \bar{d} is considered as;

$$mvcf = \frac{\sigma \sqrt{4\bar{d} + 2\sigma^2}}{\bar{d} + \sigma^2} \approx \frac{2\sigma}{\sqrt{\bar{d}}} \quad (4.24)$$

When the observed variation coefficient of runoff is small in a given basin, it can be expected that the model variation coefficient will be small also and vice versa. This leads to the comparison of these two variations by taking their quotient and to a definition of an 'absolute' model quality measure, MQ.

$$MQ = \frac{\text{observed vcf of runoff}}{\text{model vcf for mean runoff}} = \frac{ovcf}{mvcf} \quad (4.25)$$

For judging whether a difference in quality of two models is important, a confidence interval of MQ is computed. Since MQ is approximately inversely proportional to σ , the HWCI of σ and MQ are approximately proportional to σ and MQ respectively. With the expression of HWCI (σ) leads to an approximate expression of the half width of a 95% confidence interval as;

$$HWCI(MQ) = \frac{1.38MQ}{\sqrt{N-n}} \quad (4.26)$$

Where N is the number of data points and n is number of optimized parameters.

4.4.6 Residual Analysis

The computed runoff is only an approximation of the expected value of q_t (Eq_t). The difference between the transformed observed and computed flows gives the residuals as:

$$u_t = \sqrt{q_t} - \sqrt{d_t} \quad (4.27)$$

Residual analysis is carried out to determine whether the residuals u_t behave as required by the model hypotheses, especially whether they are independent, homoscedastic and normally distributed with zero expectation. Independence of residuals is checked by computing their autocorrelations, ρ_k with time lag k ;

$$\rho_k = \frac{\sum_{t=1}^{N-K} (u_t - \bar{u})(u_{t+k} - \bar{u})}{\sum_{t=1}^N (u_t - \bar{u})^2} \quad (4.28)$$

where \bar{u} is the mean residual and N is the length of the time series (in case there are no gaps in the runoff data series). The half width of 95% critical interval (5% significance level) is approximately;

$$HWCI(\rho_k) = \frac{1.96}{\sqrt{N}} \sqrt{1 + 2 \sum_{i=1}^{k-1} \rho_i^2} \quad (4.29)$$

The hypotheses $\rho_k = 0$ is true at 5% significance level when;

$$|\rho_k| \leq HWCI(\rho_k) \quad (4.30)$$

These expressions are bad estimates when $k > N/5$. It is sufficient to compute them for $k = 24$ up to two years for monthly time step.

4.4.7 Sensitivity to calibration period

If the input and output data are assumed to be time homogeneous, the results of application of a given model to two different calibration periods of the same catchment have to be the same. The different calibration periods can be defined by splitting long observed time series. Let

$$\dot{A} = (\dot{a}_1, \dot{a}_2, \dots, \dot{a}_n) \quad (4.31)$$

and

$$\ddot{A} = (\ddot{a}_1, \ddot{a}_2, \dots, \ddot{a}_n) \quad (4.32)$$

be the estimates of vector $A = (a_1, a_2, \dots, a_n)$ of filter parameters obtained from two calibration periods, where n is the number of parameters. Then \dot{A} and \ddot{A} are stochastically independent and approximately normally distributed. A level 5 % test on identity of the two models is Vandewiele *et al*, 1993 proposes that at a level of 5%

$$(\dot{A} - \ddot{A})(\Lambda' + \Lambda'')^{-1}(\dot{A} - \ddot{A})^T \sim \chi_n^2(5\%) \quad (4.33)$$

where Λ' and Λ'' are the corresponding covariance matrices, T is transpose and χ_n^2 is chi-square distributed with n degrees of freedom. The $\chi_n^2(5\%)$ is the 5% point of χ_n^2 (see Table 4.3). Practically the individual confidence interval of parameters should be investigated to contain the optimum parameters estimates obtained using two calibration periods.

Table 4.3 Some 5 % points of the Chi-square distribution with n degrees of freedom.

degrees of freedom, n	2	3	4	5	6	7
5% χ_n^2 -value	5.991	7.815	9.488	11.070	12.592	14.067

Equality of model standard deviations $\hat{\sigma}$ and $\hat{\sigma}'$ can similarly be tested at the 5% level by checking whether;

$$\frac{|\hat{\sigma}' - \hat{\sigma}|}{\sqrt{\frac{\hat{\sigma}'^2}{2(N' - K)} + \frac{\hat{\sigma}^2}{2(N'' - K)}}} \leq 1.96 \quad (4.34)$$

where N' and N'' are the numbers of data in the two calibration periods. Besides these formal tests, the general behaviour of residuals is compared.

Chapter 5

5 CASE STUDIES OF MONTHLY WATER BALANCE MODELS FOR SEMI- ARID AND ARID CATCHMENTS

5.1	Introduction	98
5.2	Data description.....	98
5.3	Monthly model application	115
5.4	Conclusions	138

5.1 Introduction

This chapter begins with the description of the test catchments used in this study. The hydrometeorological data are examined with regard to the quality and sufficiency for the model calibration and verification. Then the conceptual monthly water balance models developed in Section 3.2 are applied to the test catchments. Although originally developed for humid regions, improvement of the performance of the models for arid areas is aimed at due to incorporation concepts that account for the hydrological characteristics of the arid and semiarid conditions.

5.2 Data description

5.2.1 Ethiopian catchments

Four catchments located within the Upper Awash River Basin are used in this study. The Awash River Basin is one of the major river basins in Ethiopia with a total catchment area of 112,697 km². The Awash basin is narrow in the upper part and widens towards the north of the catchment. The catchment is characterized by its closed river system (no outlet to the sea).

The catchments are located upstream of Koka dam (see Figure 5.1). The average annual areal rainfall is 1000 mm for the upper part of the catchment and decreases to the 500 mm for the lower basin. The major rainy season is between June and mid September with a short monsoon rain in March to April. The annual minimum and maximum temperatures are 14°C and 32°C respectively.

The topography of the catchment is characterized by highlands ranging from 2000- 3000m above sea level for the upper part of the catchment and lowlands for the lower part of the basin. There are two major soil types in the catchment; the deep red clay soil, Nitosol, and the dark clay soil, Vertisol (Alem, 1989). The Nitosols are found in the upland areas, whereas the Vertisols are found in lowland areas with slopes ranging from 2 to 8%. Agrarian farmers practicing rain fed agriculture populate the upper part of the catchment (upstream of the Koka Dam). Farmers practicing pastoral farming and mixed farming sparsely populate the lower part, which is flat lowland. The existing water resources are mainly used for development of hydropower and irrigation schemes with the water being regulated by the two dams, Koka and Tendaho, on the main river. Figure 5.1 shows location of the rainfall and discharge gauging stations in the Upper Awash River Basin.

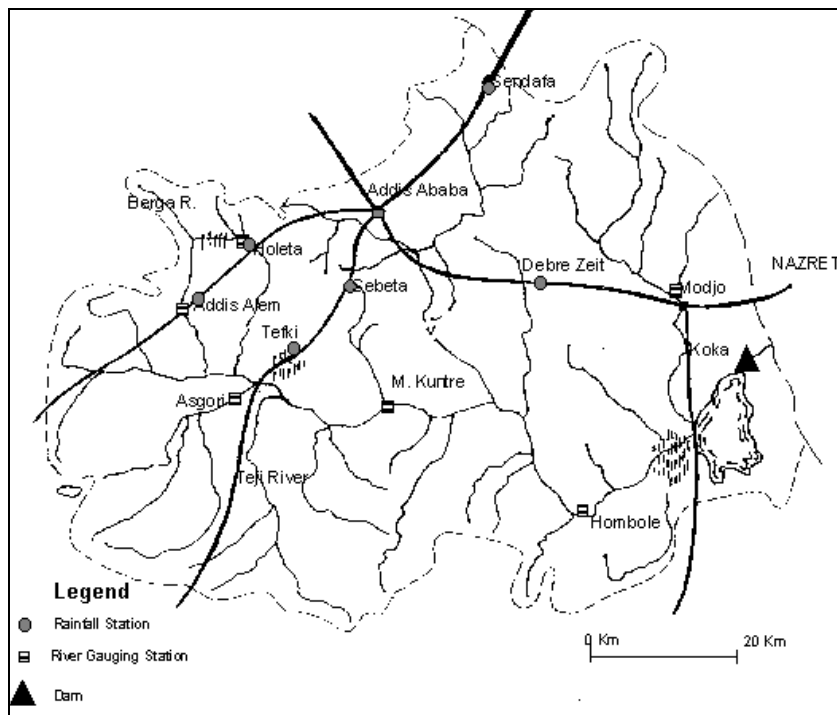
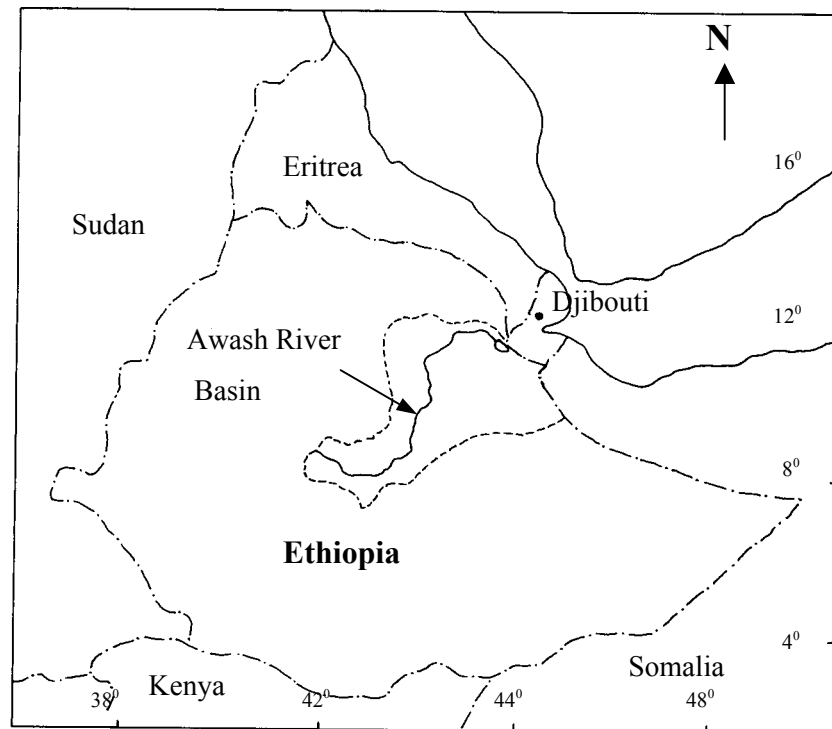


Figure 5.1 Location of Awash River Basin

Meteorological data

The rainfall and evaporation data are collected from the National Meteorological Agency. Hard copies of daily data were edited in digital form. A total of seven stations within the interest area are available (Table 5.1). From the location of the stations one can see that the distribution of the raingauge stations is not uniform across the watershed but fair enough compared to the data availability in the country.

Table 5.1 Description of daily rainfall data in upper Awash River Basin

STATION	Lat.	Long	Elve. a.s.l (m)	Period	Annual Rainfall (mm)
Addis Ababa	09 ⁰ 02'	38 ⁰ 43'	2408	1900-1996	1192
Addis Alem	09 ⁰ 03'	38 ⁰ 24'	2340	1980-1996	1117
Holeta	09 ⁰ 05'	38 ⁰ 30'	2000	1980-1995	1061
Sebeta *	08 ⁰ 55'	38 ⁰ 30'	2379	1980-1994	2347
Sendafa	09 ⁰ 10'	39 ⁰ 02'	2550	1980-1995	890
Debrezeit	08 ⁰ 26'	39 ⁰ 01'	1900	1980-1995	781
Modjo	08 ⁰ 37'	39 ⁰ 08'	1870	1980-1995	853

* Erroneous data

The stations at Sebeta showed extremely high rainfall records that do not accord with the other stations. The annual rainfall record of this station reaches more than 3000 mm compared to 1200 mm of the others. The station is located about 40 km from Addis Ababa station and this amount of variation is not explained. Comparison of the 10 days moving average of data of Sebeta and Addis Ababa shows the same trend but multiplied by different factor at different times hence hinders correction of the data. Due to the possible erroneous data this station is excluded and only the remaining 6 stations are considered.

The general quality of the other data of rainfall data is checked by inter comparison between the stations. The correlation coefficient among the stations on monthly rainfall amount ranges from 0.647 to 0.874 (Table 5.2). This shows fairly good agreement on the monthly rainfall series. Daily rainfall data variation between the stations is pronounced due to localized storms. Missing data of a few days at stations Debrezeit, Modjo and Holeta are encountered. The gaps are filled using the data of the nearest station, which has a record for the missing periods.

Data on evaporation are only available for the station at Addis Ababa, for a continuous period of two years (1988-89). To have the seasonal variation of evaporation, the monthly mean evaporation rates (for the 12 months) are computed using these two years record (Table 5.3).

The data of this station is used for modelling for the four catchments in the Awash River Basin.

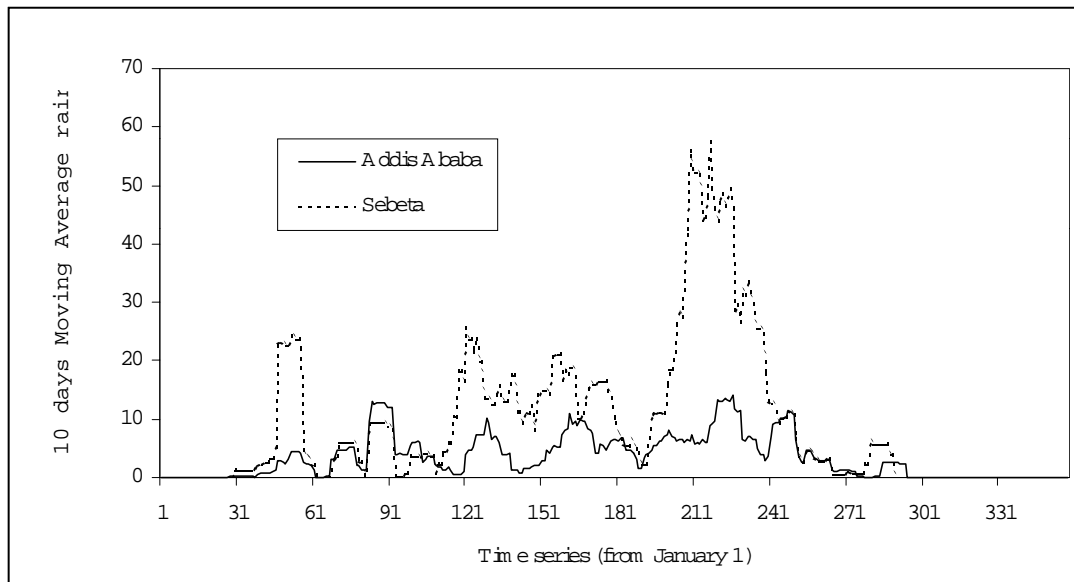


Figure 5.2 10-days moving average of rainfall at Addis Ababa and Sebeka stations.

Table 5.2 Cross-correlation between monthly rainfall data of stations in the upper Awash River Basin

Station	Addis A.	Addis Alem	Holeta	Sendafa	Debrezeit	Modjo
Addis A.	1.000					
Addis Alem	0.875	1.000				
Holeta	0.927	0.968	1.00			
Sendafa	0.805	0.765	0.805	1.000		
Debrezeit	0.828	0.812	0.884	0.753	1.000	
Modjo	0.815	0.791	0.866	0.749	0.814	1.000

Table 5.3 Pan evaporation daily data

Addis Ababa : 1987-1988												
Month	Jan	Feb	Mar	Apr	May	Jun	Jul	Aug	Sep	Oct	Nov	Dec
Evap. (mm)	158	150	155	104	152	106	75	77	94	164	189	114

Hydrological data

Daily stage readings of three rivers at four stations with corresponding rating curve equations were obtained from the Hydrology Department of the Ministry of Water Resources of Ethiopia (Table 5.4). Daily discharge values are computed using the rating curves, which were developed for specific periods. The availability of the raw data enabled us to check the reliability and quality of the data. Among the stations considered gauging site of Awash Melka Kuntre and Modjo at Modjo are located in a very stable cross-section and hence have unique rating curve for the entire record. Berga station exhibits morphological change. Three stage-discharge relationships are developed which are valid in specific period (Table 5.5).

The gauging station at Hombole has also a stable channel but distinct relationships are available flow depths less and greater than 0.72 m up to 1987. Afterwards it appears that a single relationship is adequate for all stages.

Table 5.4 Daily River flow data

STATION	Area (km ²)	Period	Rainfall Station
Berga -Addis Alem	4456	1986-1990	Addis Alem , Holeta
Modjo - Modjo	7656	1985-1989	Modjo, Sendafa
Awash - M. Kuntre	248	1985-1992	Holeta, Addis Alem
Awash - Hombole	1264	1963-1992	Addis Alem, Holeta, Addis A., Modjo Debrezeit, Sendafa

Table 5.5 Stage-discharge relationships rating curves for different periods. (h =Stage (m), and Q = flow m^3/s)

River	Valid during		Rating curve equations
	From	To	

Berga	Jan. 01, 1985	Aug. 02, 1986	$Q = 9.56(h - 0.44)^{1.77}$
	Aug. 03, 1986	Aug. 27, 1987	$Q = 11.29(h - 0.66)^{2.12}$
	Aug. 28, 1987	Dec. 31, 1990	$Q = 9.64(h - 0.52)^{1.98}$
Awash M.Kuntre	Jan. 01, 1980	Dec. 31, 1990	$Q = 22.03(h - 0.04)^{2.104}$
Awash Hombole	Jan. 01, 1962	Dec. 31, 1987	$Q = 10.32(h + 0.26)^{1.582} \quad h \leq 0.72\text{m}$ $Q = 19.67(h - 0.04)^{1.754} \quad h \geq 0.72\text{m}$
	Jan. 01, 1988	Dec. 31, 1990	$Q = 3.195(h + 0.78)^{2.73}$
Modjo	Jan. 01, 1984	Dec. 31, 1990	$Q = 4.636(h - 0.1)^{5.168}$

Data quality checking

The stages are checked through time series plots, which revealed a number of inconsistencies due to data entry error. The flow data at a station are validated by simultaneously examining the rainfall time series and the flow of the other rivers.

For example the consistency of the flow data of Awash River at two stations is verified using correlation and time series plots. The cross correlation coefficients for these two stations are 0.92 and 0.89 for lag 0 and lag 1 day respectively. Figure 5.3 shows a typical hydrograph of the two stations on the Awash River. Comparing the two hydrographs, one can see that the contribution of the drainage area below the Melka Hombole is not only large but also highly variable diurnally during the rainy season.

The major errors found during data checking deal with the high flows computed using the rating curves. Several of these errors are observed. For example considering the Modjo station the record shows that the stage readings of August 8 and August 9, 1985 are 2.08 m and 3.04 m respectively. Using the rating curve the corresponding discharges are 260 m³/s and 1715 m³/s. The later flow is extremely large, with an equivalent of 110 mm of rainfall over the whole catchment area. The rainfall record at Modjo on that particular day is only 15 mm and no rain on August 7 1985. Similarly over estimation is seen also on 15 August 1985.

This overestimation is due to (at least for this station) the nature of the equation of the rating curve which is derived from pure regression analysis of the measured stage and discharge. For example the rating curve equation for Modjo is:

$$Q = 4.636(h + 0.1)^{5.168}$$

Where Q = discharge of the river in m³/s
 h = Stage (water level) in m

From a theoretical point of view the value of the exponent should be in the range of 1.5 to 2.5 for wide trapezoidal cross-section. In this case the value of the exponent, as determined from the curve fitting is 5.168, which explodes the computed discharge for a small increase of stage. The limitation of the rating curves is mostly in the extrapolation of high flow regimes. Hence due care must be taken in the use of the relationships for extreme stages. For this catchment, the overestimated points are quite few. They are replaced by the mean of either the previous or the following day. When the stage of the following day is smaller, the stage of the previous day is taken. It is advisable in such instances to investigate the cross-section of the gauging site and calculate the maximum capacity of the river channel discharges using the Manning or Chezy formulas.

5.2.2 Chinese catchments

Two catchments from the Shanxi Province of China are used. The data are obtained from (Li, 1995). The region has semi-arid climate with an average annual precipitation between 500 and 600 mm. The maximum precipitation in a wet year reaches about 900-1300 mm and the minimum precipitation in a dry year can be as low as 200-250 mm. Most of the precipitation is received during the rainy season (July to September). The annual potential evaporation is about 900 mm.

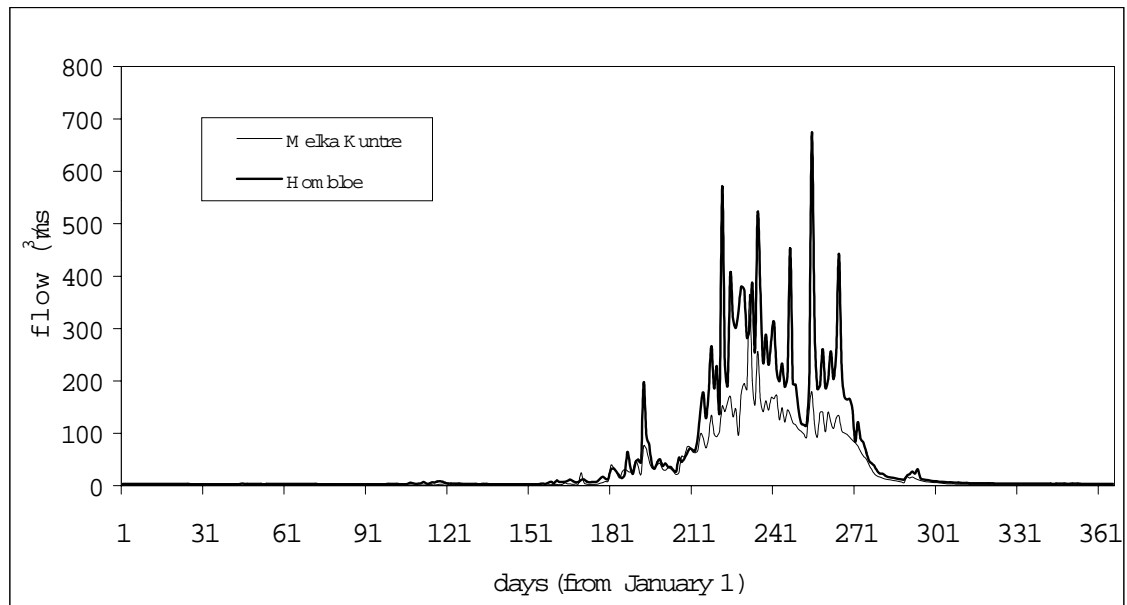


Figure 5.3 Typical comparison of hydrograph of Awash River at Melka Kuntre and Hombole stations (1988)

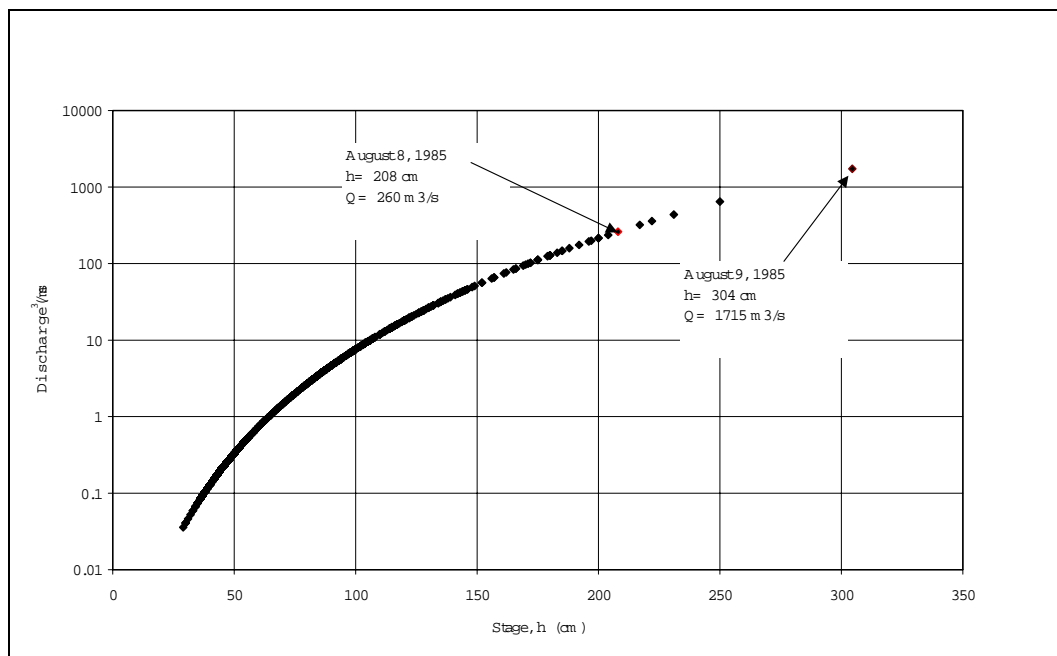


Figure 5.4 Over estimation of rating curves in extrapolation (Modjo River at Modjo)

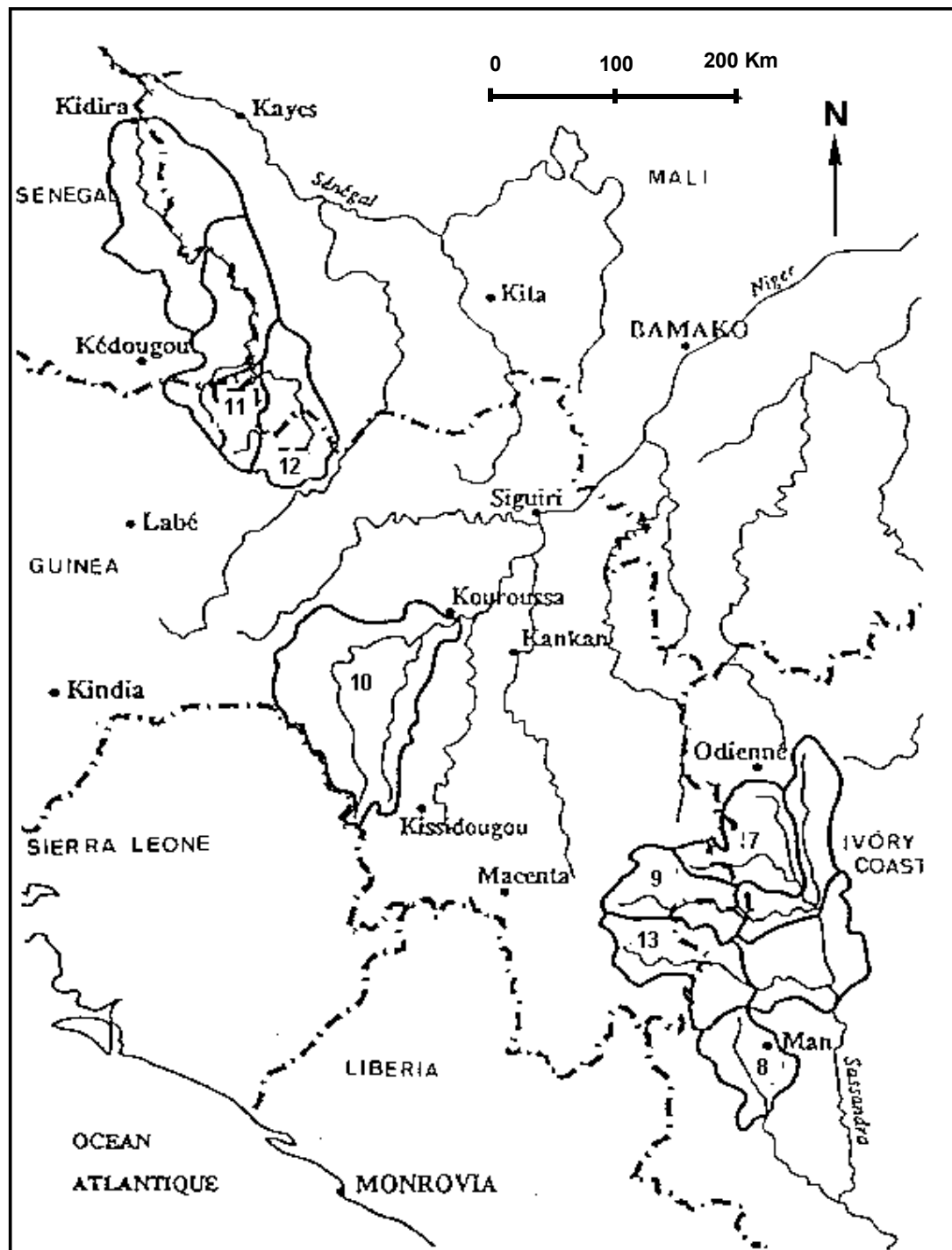
5.2.3 West African Catchments

The two basins on Faleme River are tributaries of the Senegal River. The other catchments Boa, N'zo, and Ferdougouba are tributary of Sassandra river. One catchment is the upper part of the Niger River basin. The location of the basins is given in Figure 5.5. The detailed description of the catchments can be found in Ni-Lar-Win (1994).

The upper Senegal basin is characterized by its tropical climate. The basin receives most of its rainfall during July - October. The geology of the basin is composed of schist, micaschist, quartzite cut by volcanic rocks (metaandesite and metabasite) and plutonic (granite and granodiorite). To the south, the plutonic intrusion creates a succession of subtabular morphologies covered by lateritic terrain within which rivers have dissected V shape valleys. The vegetation cover of the two basins on Falem is savannah with trees and bushes, cultivated area, savannah densely covered with trees and dry forest.

The Niger basin lies on the transition of the tropical region. The duration of the rainy season is about four months (July - September) and the dry season is less severe than the in the tropical region. The geology of the basin is composed of strongly metamorphosed and recrystallized granites, that appears as Gnesis in many cases. The vegetation cover of the Niger basin is densely covered with trees, dry forest, cultivation, and fallow land.

The geology of the Sassandra basin is somewhat similar to the upper basin of Niger. The climate and vegetation covers of the four basins are different from one another. Boa and Ferdougouba lie in the tropical transition region with one rainy season during the months of July-September. The Boa basin is densely covered with Savannah trees while Ferdougouba is covered with sparse trees and bushes. The climatic region of Bafing is tropical transition and equatorial transition. It is covered by evergreen forest and secondary forest. The N'Zo basin lies in the equatorial transition region characterized by scarce rain from march to June, and much rain in September and October. It is covered with evergreen forest and secondary forest.



- | | | | |
|----------|----------|---------------|----------|
| 7 Boa | 8 N'Zo | 9 Ferdougouba | 10 Niger |
| 11 Falem | 12 Falem | 13 Bafinga | |

Figure 5.5 Location of West African basins under study

5.2.4 Tanzanian catchments

Tanzania is a semi-arid country transversed on average by a line of 6 degree below the equator. Hydrometeorological data of Little Ruaha catchment from Tanzania (Figure 5.6) at the outlet of Makalala and Ihimbu station were available. The area covered up to Makalala is 759 km² and for Ihimbu is 2480 km². The catchment has on average an annual historical rainfall of 1000 mm/yr. There are six rainfall-gauging stations in the catchment with continuous data for 9 years (1966-1975). Discharges at Ihimbu and Makalala are available from 1966 to 1975. The catchment has only one evaporation station at Madibira with data from 1966 to 1975. The data for these catchments were obtained from University of Dar Es Salaam, Tanzania.

5.2.5 Zambian catchments

Data of five catchments from Zambia were available for the study. Information on the catchment was obtained from the country report prepared by Mott MacDonald and Partners, (1990). All the five catchments are located in the upper part of the Kafue River Basin (Figure 5.7). The basin encompasses a very large area (155 000 km²) which is about 20 % of Zambia's total land area. The mean annual rainfall over the catchment ranges from 700 mm in the south to over 1200 mm in the north and has an areal mean rainfall of 1050 mm. The mean annual flow at the outlet at Kasaka is about 350 m³/s, equivalent to 71 mm. The average runoff coefficient at this large basin scale is only 0.06, which implies that more than 90 percent of the rainfall disappears mainly as evaporation. The rainy season is well defined, occurring in during the months of November to April.

According to Hughes, (1997) the Kafu river is underlain by shales, sandstones, dolmites and quartzites of the Katanga system and some areas of basement complex comprising gneisses, schists and micaceous quartzites. The associated soils vary from clay to sandy clay loams and are generally quite deep. Vegetation and land use consists of natural woodland, forest reserves, cultivated land and urban/industrial areas associated with mining.

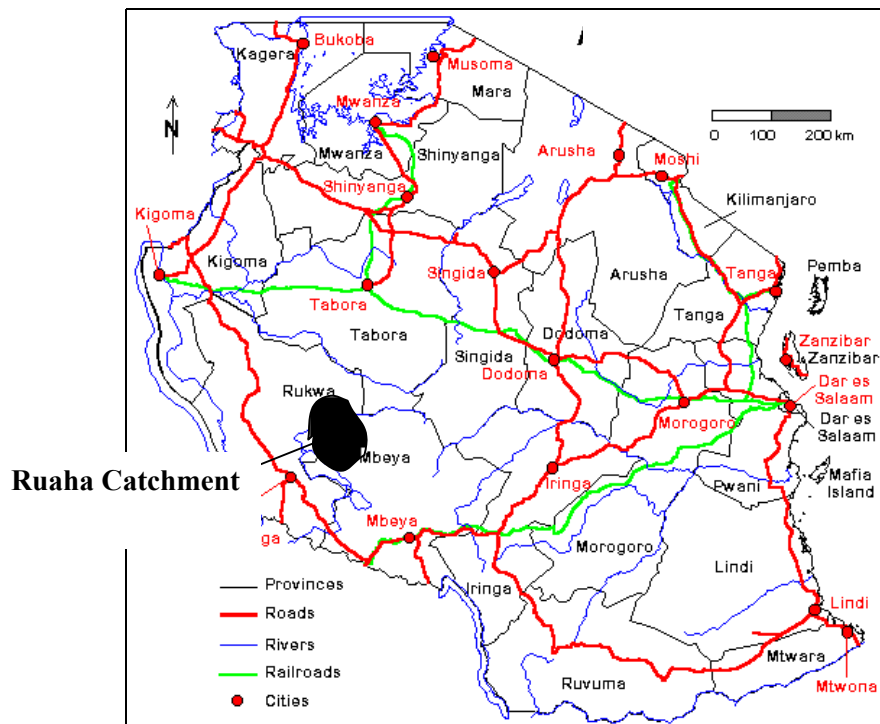


Figure 5.6 Location of Ruaha Catchment (Tanzania)

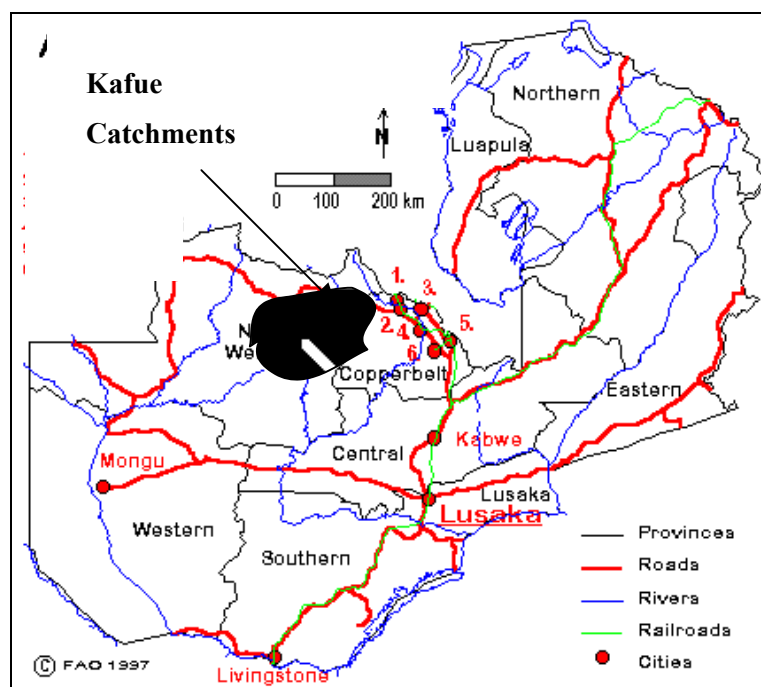


Figure 5.7 Location of Kafu catchments. (Zambia)

The data available for the study in the basin are the monthly discharge, precipitation and pan evaporation. For Mwambashi and Baluba daily data were available. These meteorological and hydrological data are obtained from the Zambian Government Department of Water Affairs and the Meteorological Department respectively.

5.2.6 Botswana catchment

Only data for one catchment was available from Botswana for this study. The brief description for this catchment is taken from Hughes (1997). Tati river basin is located in the east part of Botswana. The vegetation cover is savanna bush and trees, while the soils are predominantly loamy sands to coarse sandy loams with 10 to 20 % clay contents and approximately 800 mm in depth. In some areas of the upper catchments, the soils are sandy clay loams and sandy clays that can be up to 2m deep. Six rainfall stations are used to calculate areal rainfall for the catchment. Only mean monthly evaporation data are available for the study. The data were obtained from Southern African "Friend" project.

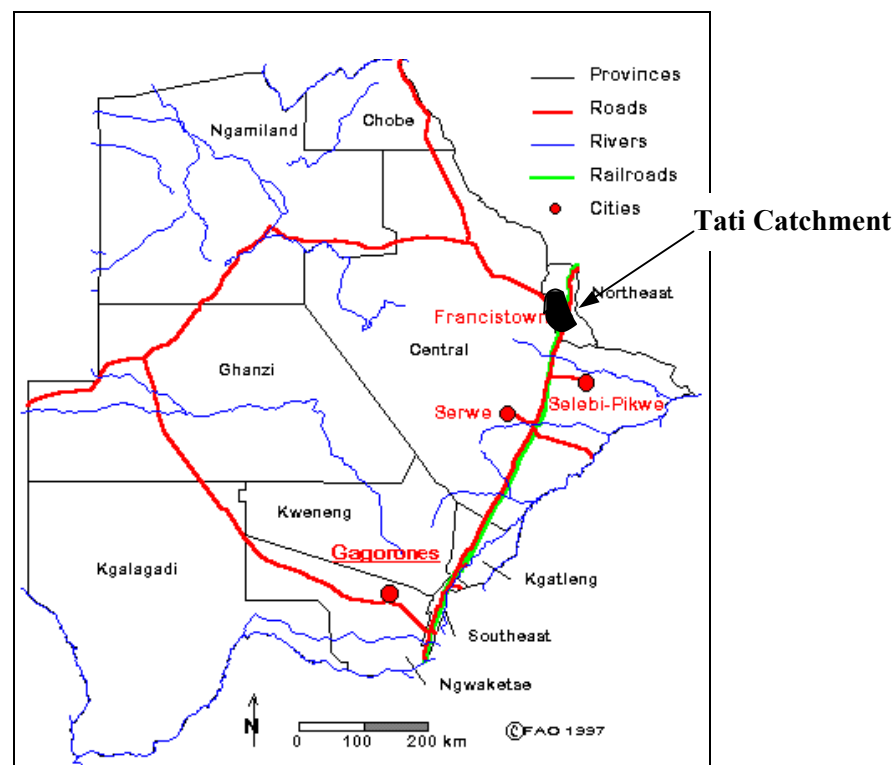


Figure 5. 8 Location of Tati catchment, (Botswana).

5.2.7 Common characteristics of the test catchments

A total of 20 catchments from West Africa, North East and South Africa and China were used in this study. The catchment areas range from 248 to 16820 km². Seasonal variation of rainfall, evaporation and flow characteristics are shown in Figure 5.10. Though for some of the catchments the amount of rainfall seems high, its concentration within a short period of the year causes low flow and in some years even zero river flows. On an annual basis, only up to 10-20% of the rainfall reaches the outlets as river flow for the East and West African catchments and 40 % for the Chinese catchments.

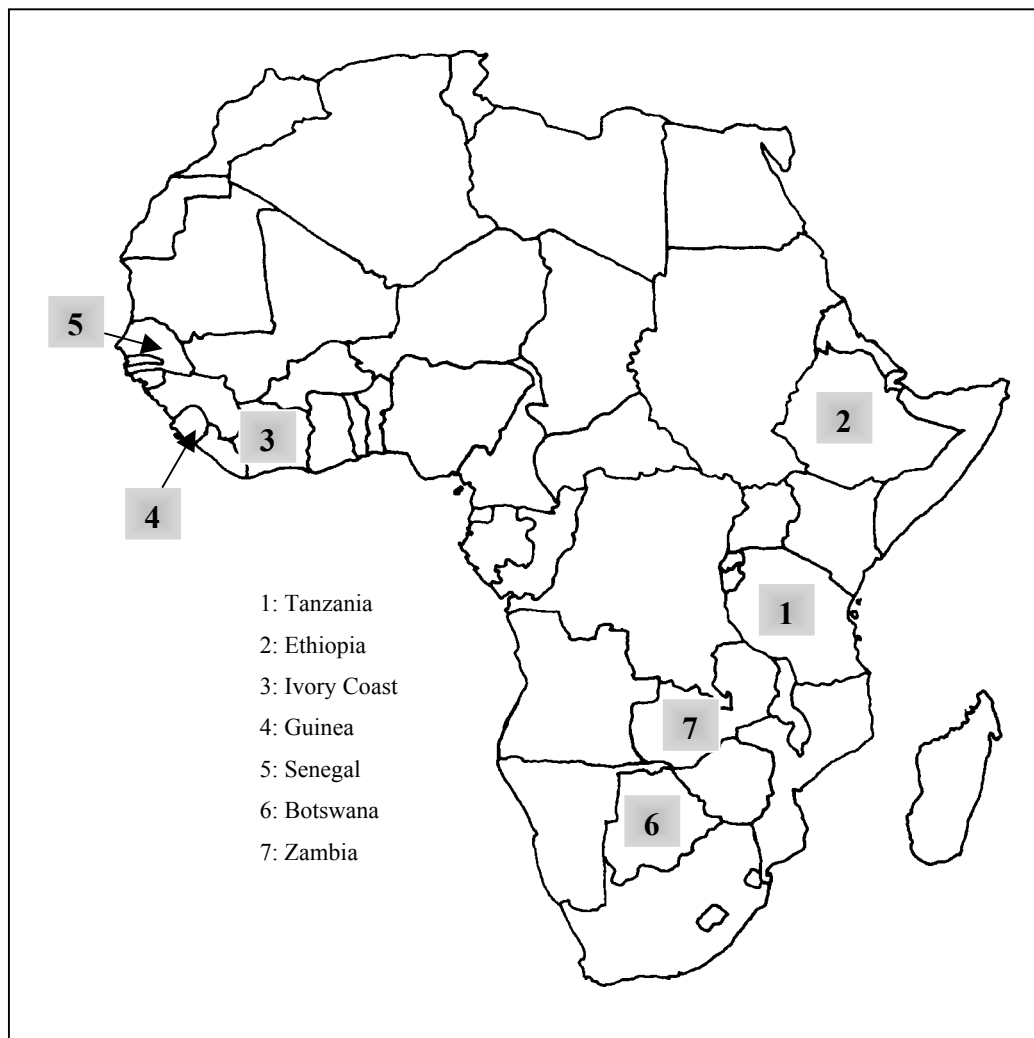


Figure 5. 9 Location of the study areas in Africa.

Table 5.6 Characteristics of the test catchments and available data on monthly time step.

No	River	Station	Area (km ²)	Annual quantities (mm)			Period
				Rain	Evap.	Flow	
Tanzania							
1.	Little Ruaha	Ihimbu	2480	1041	1446	232	1966-1975
2.	Little Ruaha	Makawali	759	1244	1449	175	1966-1975
Ethiopia							
3.	Berga	Addis Alem	248	1089	1537	262	1986-1990
4.	Modjo	Modjo	1264	871	1537	98	1985-1989
5.	Awash	Melka Kuntre	4456	1123	1537	180	1986-1991
6.	Awash	Hombole	7656	980	1537	160	1963-1992
Ivory Coast							
7.	Boa	Vialdougou	5770	1285	1458	144	1981-1988
8.	N'zo	Kahin	4300	1618	1309	364	1981-1988
9.	Ferdougouba	N'golod.	5020	1492	1361	330	1981-1988
Guinea							
10.	Niger	Kouroussa	16280	1467	1518	264	1981-1988
Senegal							
11.	Faleme	Fadougou	2370	995	1814	97	1981-1988
12.	Faleme	Moussala	5720	993	1814	84	1981-1988
13.	Bafing	Bafindala	6230	1450	1318	250	1981-1988
Botswana							
14.	Tati	Tati	470	581	1591	87	1985-1991
Zambia							
15.	Mwambashi	Mwambashi	809	1219	1554	273	1978-1989
16.	Lufumpa	Kasempa	1062	951	1564	134	1964-1987
17.	Kafue	Kipushi	440	1120	1734	233	1961-1991
18.	Baluba	Baluba	306	1501	1361	239	1975-1989
China							
19.	SX1	Qianghi Province	809	560	883	206	1957-1970
20.	SX2	Shangxi Province	751	495	873	60	1956-1970

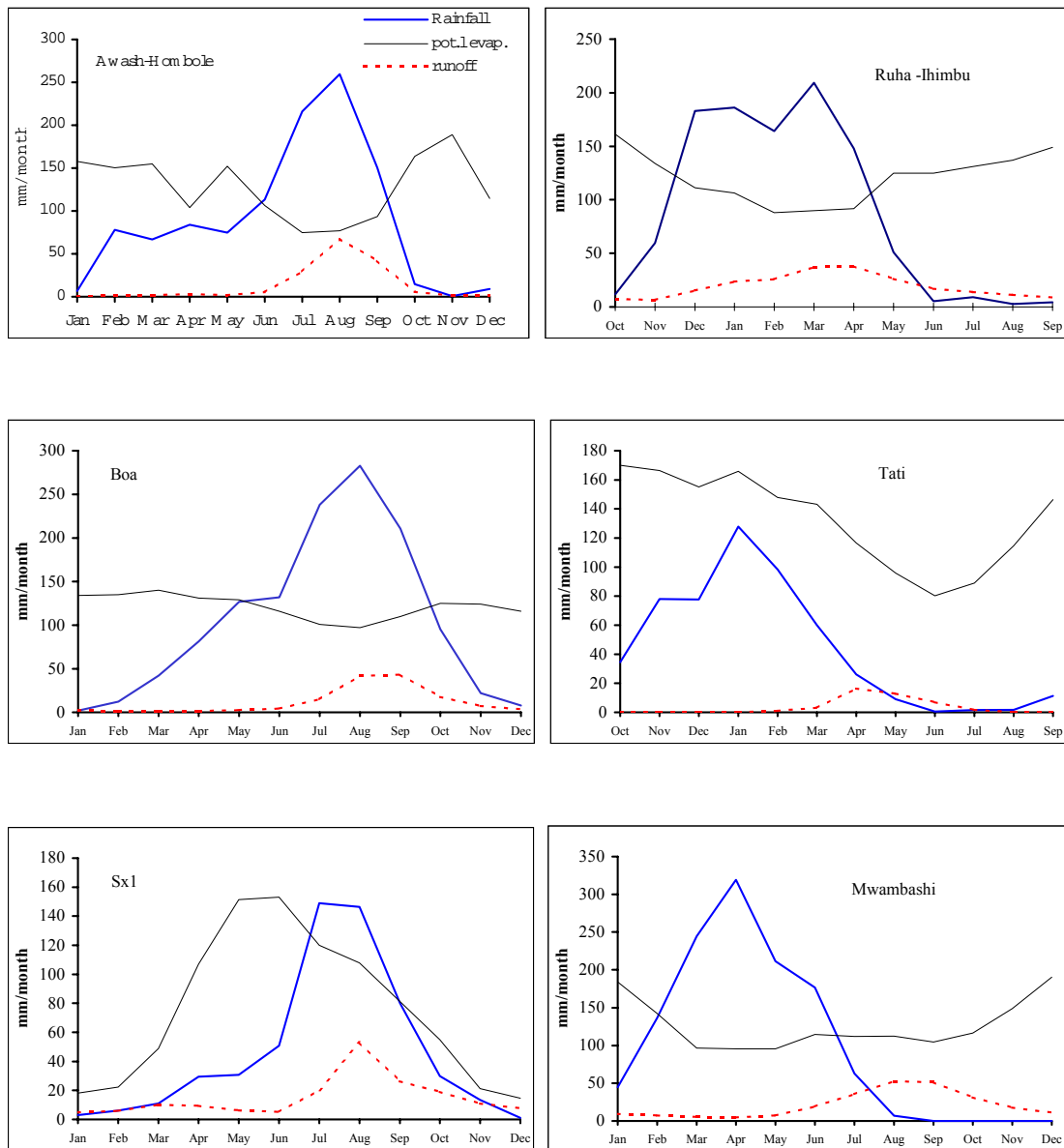


Figure 5.10 Long term monthly pan evaporation, precipitation and flow for some of the study catchments

5.3 Monthly model application

A total of 20 catchments are used to test the monthly water balance models developed in Section 3.2.

5.3.1 Initial soil moisture index

For the models developed, it is shown that the starting moisture index should be approximated. Since this is an average value that indicates the moisture within the catchment in the form of unsaturated and saturated water in the soil, it is rather difficult to measure it. A warming up period would be necessary before the calibration period so that the model results would not be influenced by the approximated initial soil moisture index. It has been suggested that 3 to 6 years may be required for the warming up period in the humid catchments. However in regions where we have strong seasonal variation and extended dry seasons 3 -6 years data of warming up period may not be necessary.

To investigate the warming up period required several catchments are tested by using 1, 2, 3 and 6 years of warming up periods. The calculated soil moisture storages just before the calibration period begins is examined. Table 5.7 shows a procedure to compare the influence of the length of warming up period.

Table 5.7 Representation of different warming up period

Warming up period			Calibration Period	
m_o 1 year			m_{01}	
m_o 2 years			m_{02}	
m_o 3 years			m_{03}	
m_o	6 years		m_{06}	

Table 5.8 indicates that the resulting initial soil moistures are almost the same, regardless of the length of the warming up period. This is mainly due to the fact that during the extended dry season the catchment will exhaust all its storage and consequently will have no carry over for the following years. The implication of this result is that for such regions a rather short warming up period is sufficient. In case of limited length of data one full hydrological year would be sufficient as a warming up period. A hydrological year may be defined as a period

starting from one regime of flow to the next similar regime after 12 months, e.g. (from a low flow regime to the next low flow regime). This definition allows to consider a complete hydrological season for the whole year.

Another possible solution is to append long term mean quantities for a required year before the calibration period. It is worth mentioning that at least one year of observed data should be available as a warming up period to obtain realistic value of initial soil moisture storage.

Table 5.8 Influences of length of warming period on initial soil moisture storage using MWBM-A ($IR=2$, $b_1=2$, $b_2=2$)

Catchment	Starting m_o (mm)	m_{01} (mm)	m_{02} (mm)	m_{03} (mm)	m_{06} (mm)
Awash-Hombole	100	164.7	167.8	168.0	168.0
Baluba	500	593.1	592.1	594.0	597.8
Sx1	100	167.9	169.53	168.8	167.2

5.3.2 Parameter optimization

Two optimization methods, VAO5A and the Shuffled Complex Algorithms, are used to estimate the parameters. For the monthly water balance models (with few parameters) the two methods have given the same results. In general it may therefore be concluded that local optima are not a problem with monthly models. The first method takes a relatively small computation time. In fact computation time for calibration with either of algorithm is not a constraint with the present personal computer capabilities. The order of magnitude of calibration time for a model for a data length of 30 years is 1 to 3 minutes with Pentium-2 machines. Sometimes the Shuffled Complex algorithm was used when good scaling factors are not obtained for the other method

5.3.3 Selection of the forms of the model

Two types of models are considered: The model without imposing an upper limit to the soil moisture, (MWBM-A) and a model with an upper soil moisture limit, (MWBM-B). In each case, because of the 2 evaporation equations ($IR=1,2$) and the 9 combinations of the two

discrete parameters (b_1 and b_2), there are 18 possible forms of a model. Hence, for each catchment, 18 forms of the two models had to be calibrated and analyzed. The details of this analysis are given for the Boa catchment in Ivory Coast. The time series of monthly rainfall, evaporation and flow are shown in Figure 5.11. Table 5.9 and Table 5.10 list the parameter estimates and statistical summary of the results for the three of possible forms for MWBM-A and MWBM-B. The estimated parameters are shown after scaling with appropriate factor as described in Appendix B

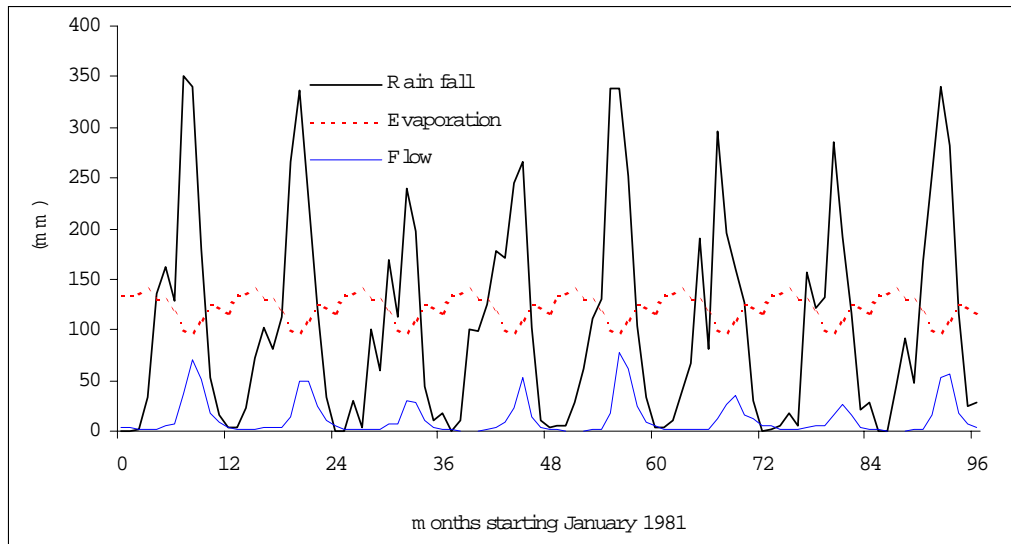


Figure 5.11 Time series of Input data (Boa Catchment, Ivory Coast)

It appears that for most combination of the discrete parameters, the optimum parameters are significant and uncorrelated (the absolute value of correlation coefficient between parameters is not greater than 0.9). This justifies the structure of the model and means that each parameter retains realistic information from the data used for calibration. Global statistics, mean and standard deviation of residuals with the model performance measures are provided for each calibration. Table 5.11 and Table 5.12 summarize the results of all combinations for the two variants of the model.

Table 5.9 Example application of the MWBM-A

	IR=2	IR=2	IR=2
--	------	------	------

	b1=0.5, b2=0.5	b1=1, b2=1	b1=2, b2=2
Parameters			
Evaporation a_1	0.149 ± 0.07	0.789 ± 0.38	0.257 ± 0.07
Slow flow a_2	0.315 ± 0.014	0.177 ± 0.07	0.259 ± 0.01
Fast flow a_3	0.169 ± 0.002	0.671 ± 0.01	0.086 ± 0.03
Max. correlation	$0.49 (a_1, a_2)$	$0.55 (a_1, a_3)$	$0.62(a_1, a_3)$
Results			
Model Quality	2.46	2.47	2.45
Efficiency	85%	95	95
Mean of Residuals	-0.06	0.08	0.03
Standard Deviation	0.65	0.53	0.48

Table 5.10 Example application of the MWBM-B

	IR=2, b1=0.5, b2=0.5	IR=2, b1=1, b2=1	IR=2, b1=2, b2=2
Parameters			
Evaporation a_1	0.140 ± 0.090	0.717 ± 0.30	0.275 ± 0.07
Slow flow a_2	0.315 ± 0.015	0.170 ± 0.07	0.291 ± 0.01
Fast flow a_3	0.118 ± 0.002	0.671 ± 0.01	0.046 ± 0.03
Upper storage a_4	0.948 ± 0.30	0.757 ± 0.10	0.588 ± 0.12
Max. correlation	$0.54(a_1, a_2)$	$0.55.(a_1, a_3)$	$0.63(a_1, a_3)$
Results			
Model Quality	2.46	2.47	2.45
Efficiency	85%	95	95
Mean of Residuals	-0.01	0.08	0.05
Standard Deviation	0.66	0.53	0.49

* Note the parameter and HWCI values are scaled (See Appendix B for appropriate scales)

Table 5.11 Summary of results for all 18 variants of the model WBAM-A. (Boa Catchment, Ivory Coast)

N0.	Discrete parameters			Model Qual.	Eff. %
	IR	b ₁	b ₂		
01	IR=1	0.5	0.5	2.47	85
02			1.0	2.45	93
03			2.0	2.46	94
04		1.0	0.5	2.45	88
05			1.0	2.47	95
06			2.0	2.45	95
07		2.0	0.5	2.45	93
08			1.0	2.22	88
09			2.0	2.45	95

N0.	Discrete parameters			Model Qual.	Eff. %
	IR	b ₁	b ₂		
10	IR=2	0.5	0.5	2.46	85
11			1.0	2.45	95
12			2.0	2.47	94
13		1.0	0.5	2.45	90
14			1.0	2.47	95
15			2.0	2.48	95
16		2.0	0.5	2.40	90
17			1.0	2.17	84
18			2.0	2.48	95

Table 5.12 Summary of results for all 18 variants of the WBAM-B. (Boa Catchment, Ivory Coast)

N0.	Discrete parameters			Model Qual.	Eff. %
	IR	b ₁	b ₂		
01	IR=1	0.5	0.5	2.41	85
02			1.0	2.45	93
03			2.0	2.44	94
04		1.0	0.5	2.46	88
05			1.0	2.12	95
06			2.0	2.45	95
07		2.0	0.5	2.43	93
08			1.0	2.17	86
09			2.0	2.45	95

N0.	Discrete parameters			Model Qual.	Eff. %
	IR	b ₁	b ₂		
10	IR=2	0.5	0.5	2.46	85
11			1.0	2.45	95
12			2.0	2.45	95
13		1.0	0.5	2.44	90
14			1.0	2.47	95
15			2.0	2.48	95
16		2.0	0.5	2.40	90
17			1.0	2.17	84
18			2.0	2.45	95

The task of selecting the best model is not easy since some of the quality criteria sets are often not significantly different for different forms of a given model. The following priority list is suggested to examine the model outputs

1) *Success of the optimization method.* One should at least get the minimum of the objective function in the environment of the optimum values of parameters (Figure 5.12). It is noted that for the model structures with an upper soil moisture limit, one obtains a flat limb of the objective function which indicates that the parameters has no influence on the objective function for values higher than the optimized value (See a_4 in Figure 5.12.)

2) *The significance of the parameters (confidence intervals):* before any analysis on results of a model it is important to check if all the optimized parameters are statistically significant as explained in section 4.4.

3) *Graphical comparison of computed and observed flows:* Visual inspection of the agreement between computed and observed river flows allows the modeler to accept or reject a model. Though this analysis relies on subjective analysis, it is found to be more practical in some cases where other general statistics such as model quality and efficiency do not show variation for the spectrum of model forms.

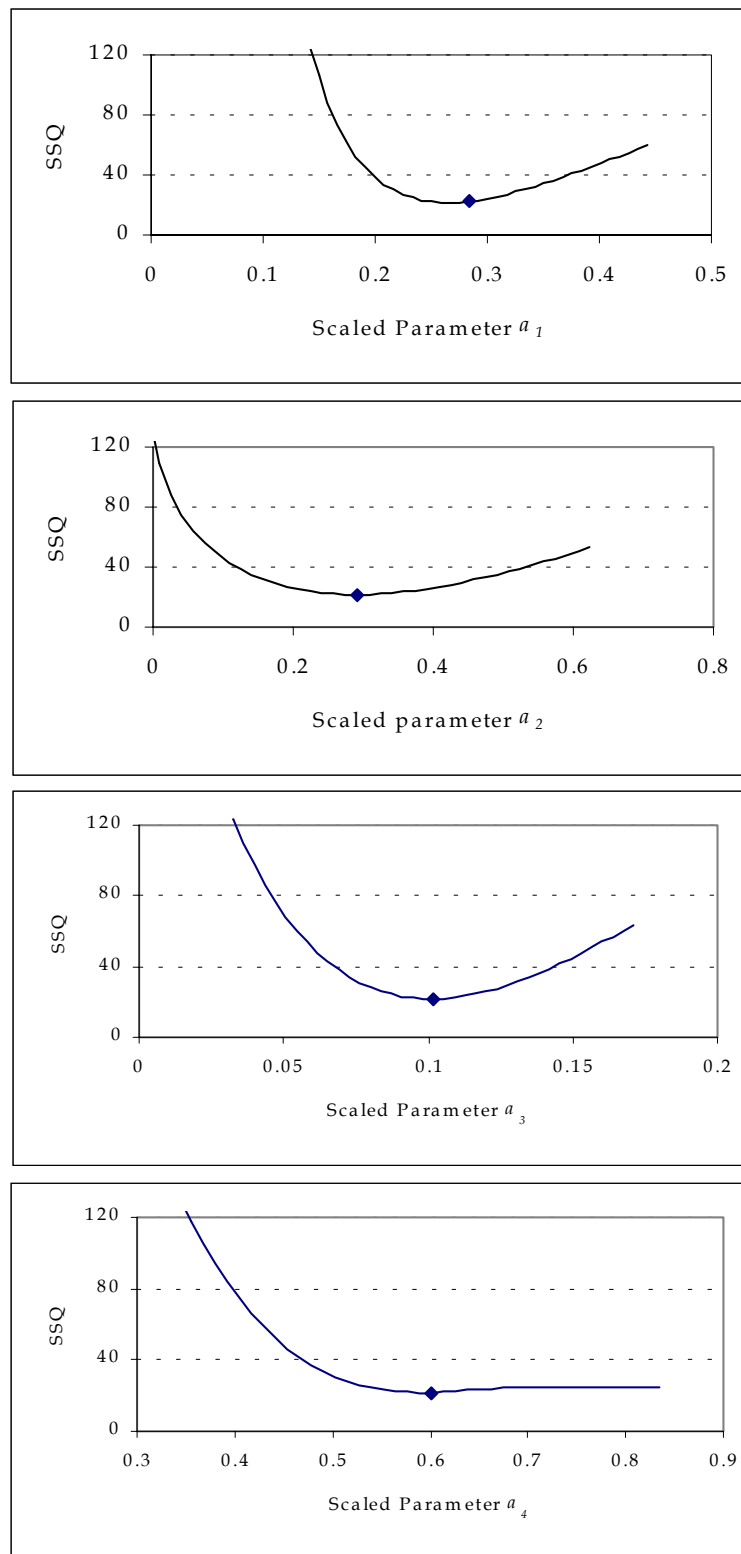


Figure 5.12 Plot of the parameter and the sum of squares of error in the neighborhood of the optimum value. (Boa catchment -modeled with MWBM-B)

Figure 5.13 displays the time series of the observed and calculated flows using the two variants of the model. It can be noted from the graph that both models resulted with good agreement between computed and observed flows.

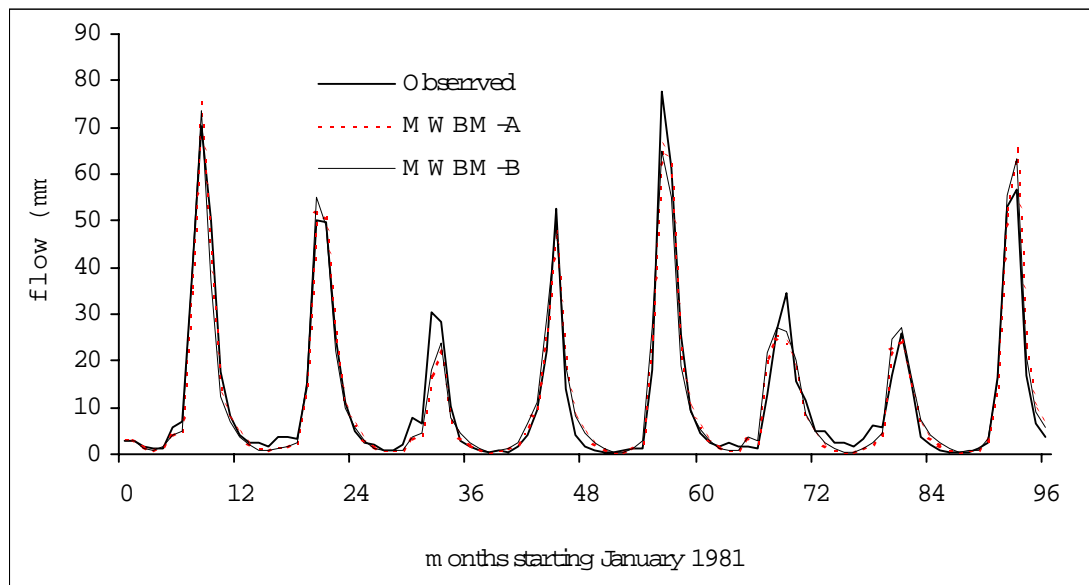


Figure 5.13 Comparison of observed and modeled flow with the two variants of monthly water balance models (Boa catchment)

4) *Comparison of monthly means of observed and computed flow:* The seasonal statistics are essential especially for regions with strong variation of flow in a year. This test reveals mainly the general performance of the model over flow regimes.

5) *Model efficiency and Quality Factor:* These statistics define the overall variance explained by the model. Perhaps the model efficiency is the most used in the hydrology community to evaluate a model and compare its performance with the results of other models. Unlike the previous tests there is no influence of subjectivity. Because of its singular value these tests allow to draw straightforward conclusions. However precaution has to be given if the other tests are also supporting the conclusions. For MWBM-A the model quality factor varies from 2.17-2.48 and the efficiency varies from 84-95% (Table 5.11). For the second variant of the model, MWBM-B the model quality factor ranges from 2.12-2.48 and the efficiency ranges from 85-95% (Table 5.12). From these tables we observe that for the catchment considered

the model quality factor and the model efficiency do not give clear indication of the best model and hence selection of the best model should be supported with other criteria.

6) *Residual analyses*: Various analyses of residuals are implemented in the model as described in Section 4.6. The influence of an input variable can be depicted by plots of residuals versus the input variables. The point of attention is to observe whether the variance of the residual is the same for lower and higher values of input variables. It should be noted that the residuals analyzed are the differences between the square root of observed and square root of computed flows. The residual series versus the rainfall, evaporation and computed flow for both models have showed equal variance over the range of the water balance variables (see Figure 5.14 through Figure 5.19). The independence of the residual series is checked by the autocorrelation function (Figure 5.20). A Time series plot of residuals (Figure 5.21) depicts there is no trend and/or periodicity of residuals. The distribution of the residuals grouped by season is also tested for normality as supposed by the model hypothesis.

In addition to the above tests the evolution of intermediate water balance variables such as soil moisture and actual evaporation should be examined, to analyze whether the values are realistic. For the example catchment considered, the soil moisture fluctuates rapidly. Figure 5.22 and Figure 5.23 show the evolution of the soil moisture and the actual evaporation respectively. According to the model, actual evaporation equals the potential for a few months during the rainy season and remains low for the dry periods. This observation can be generalized for most of the test catchments

One of the features of the model is the separation of the total flow in to 'Fast flow' and 'Slow Flow'. This definition corresponds to direct and base flow components based on classical flow separation methods. The fast flow component comprises large proportion of the flow for the catchment considered (Figure 5.23 and Figure 5.25). It is noticed that the two models show almost a similar proportion of the flow components. However the MWBM-B tends to give a slightly higher percentage of fast flow than MWBM-A.

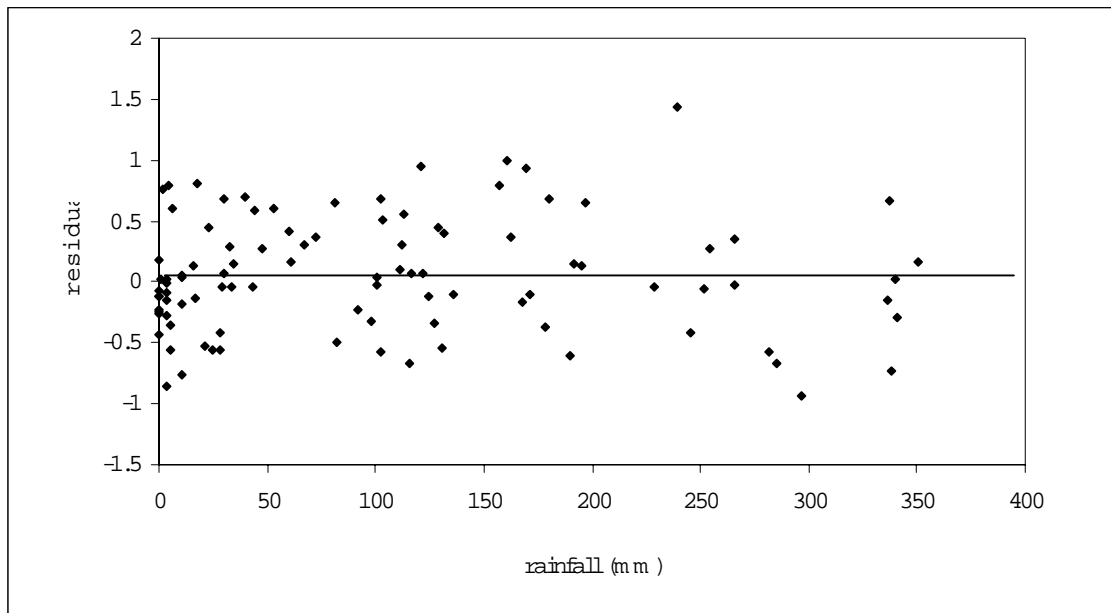


Figure 5.14 Residual versus rainfall MWBM-A. (Boa Catchment, Ivory Coast)

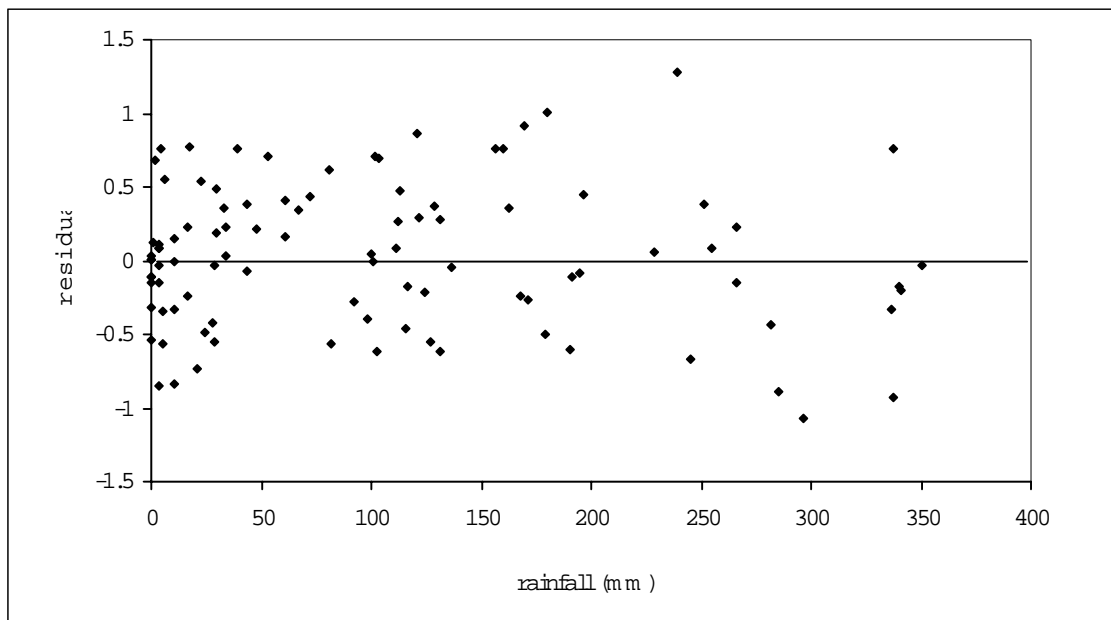


Figure 5.15 Residual versus rainfall MWBM-B (Boa Catchment, Ivory Coast)

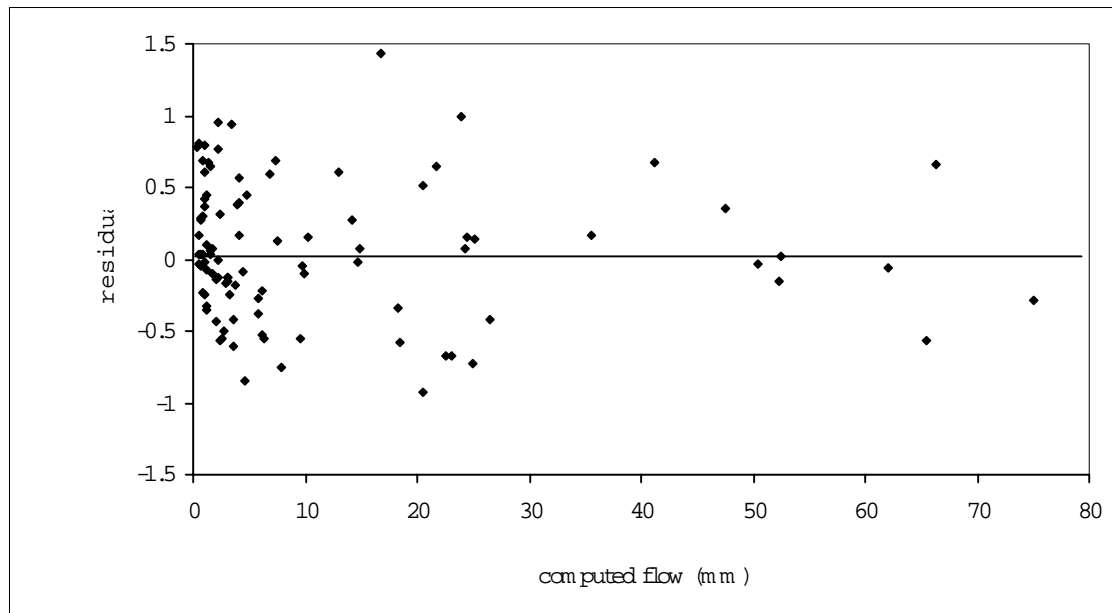


Figure 5.16 Residual versus computed flow MWBM-A. (Boa Catchment, Ivory Coast)

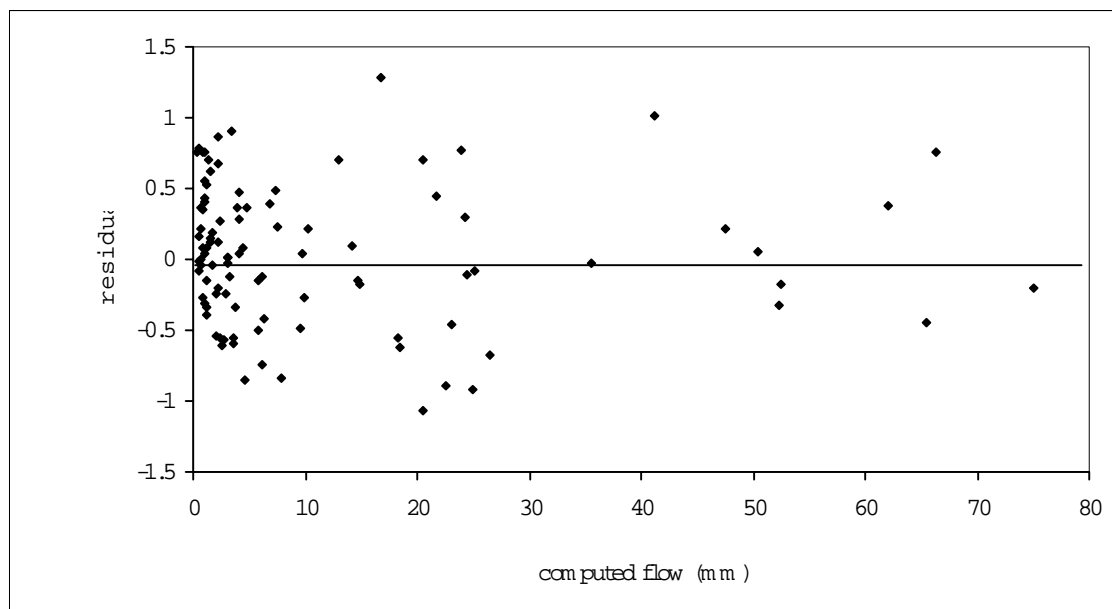


Figure 5.17 Residual versus computed flow MWBM-B. (Boa Catchment, Ivory Coast)

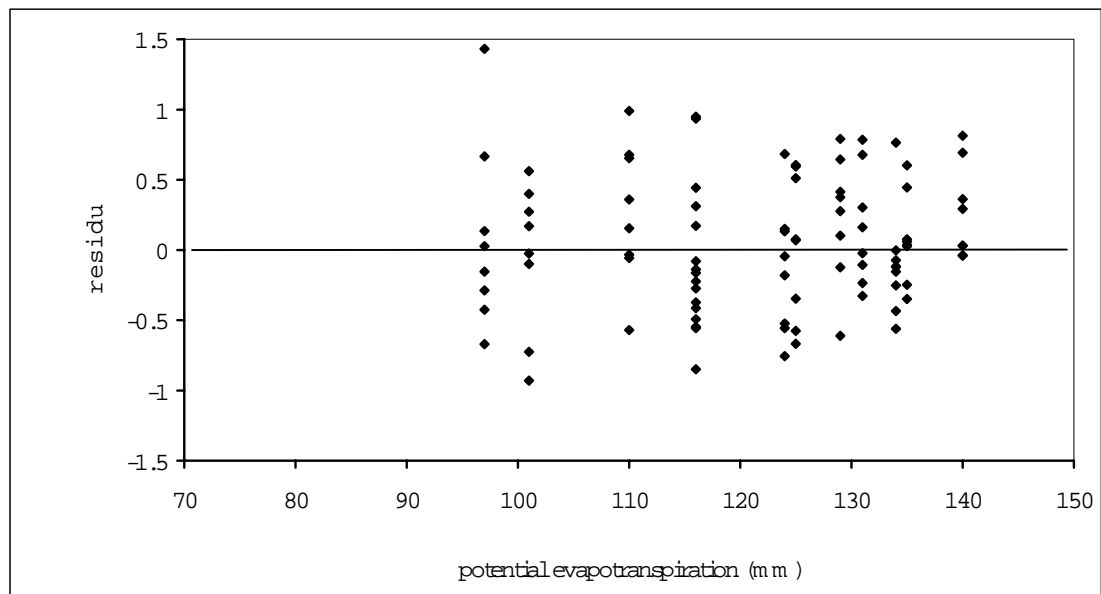


Figure 5.18 Residual versus Potential evapotranspiration MWBM-A. (Boa Catchment, Ivory Coast)

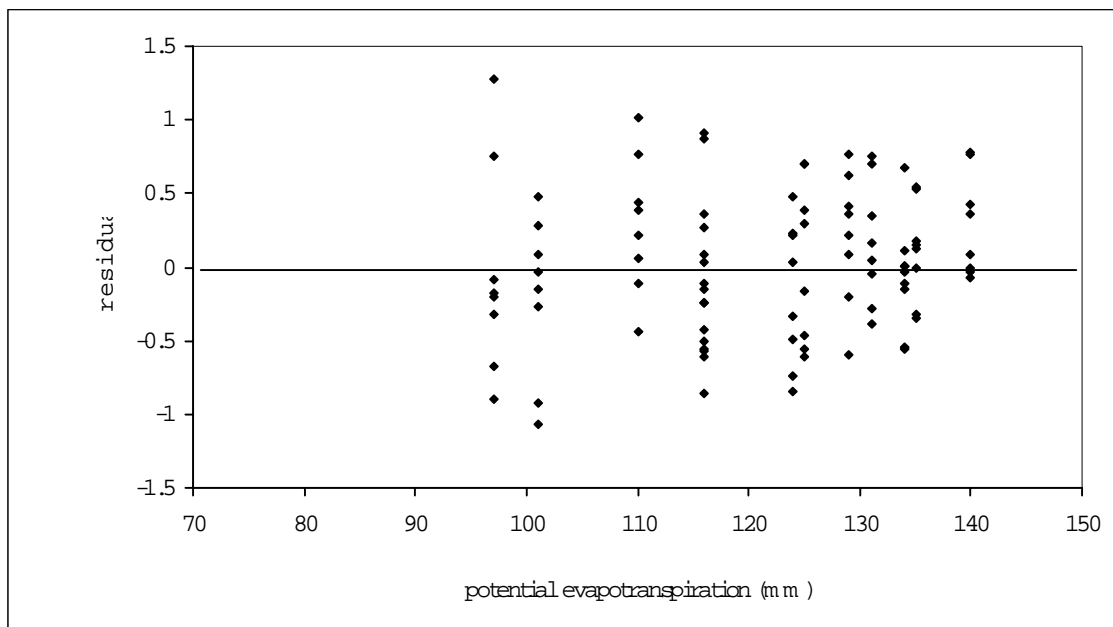


Figure 5.19 Residual versus Potential evapotranspiration MWBM-B. (Boa Catchment, Ivory Coast)

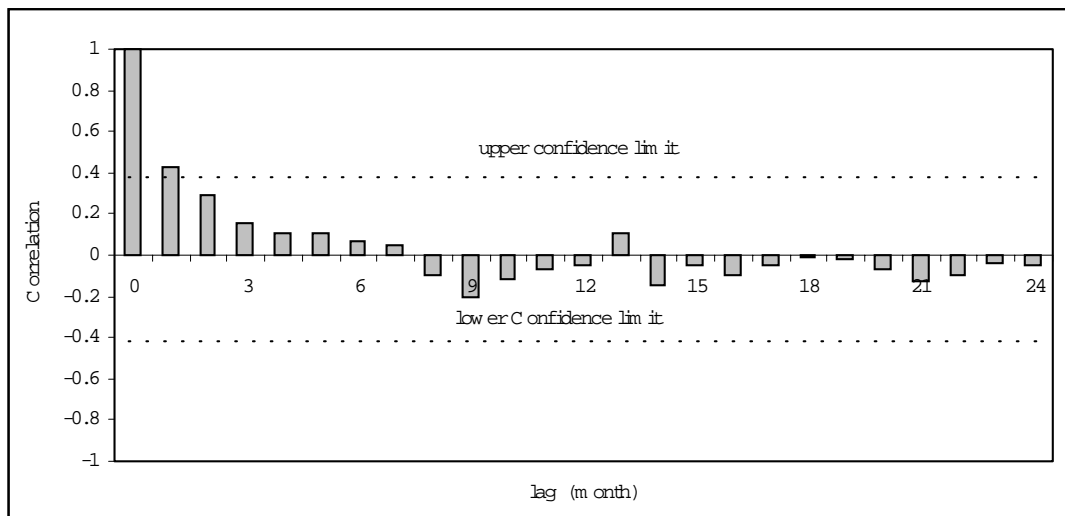


Figure 5.20 Auto correlation of residuals from MWBM-A. (Boa Catchment, Ivory Coast)

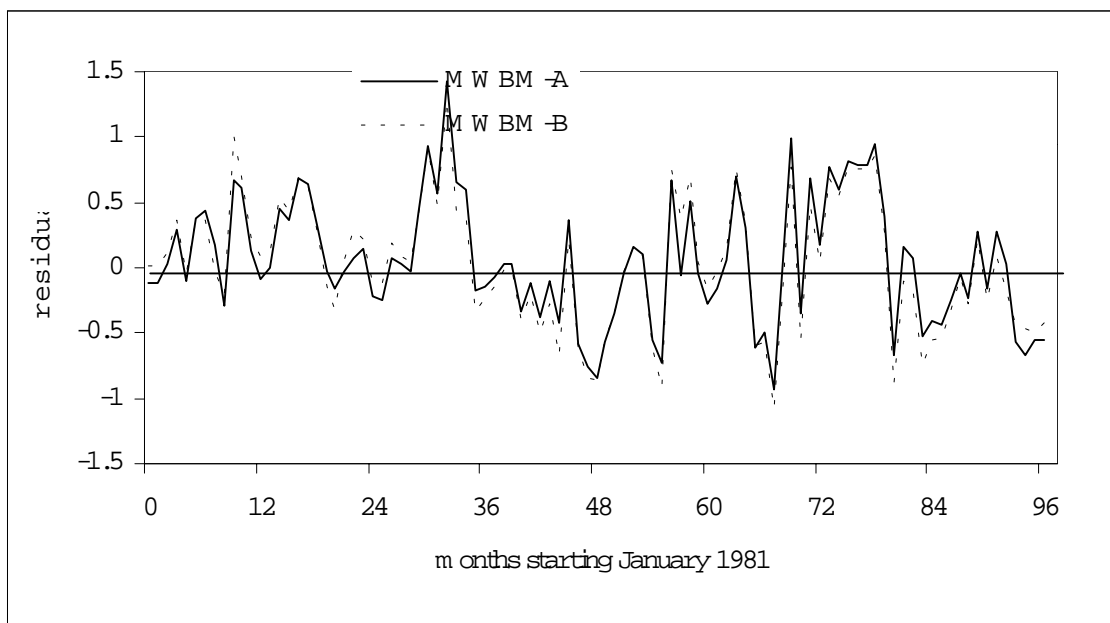


Figure 5.21 Time series plot of residuals. (Boa Catchment, Ivory Coast)

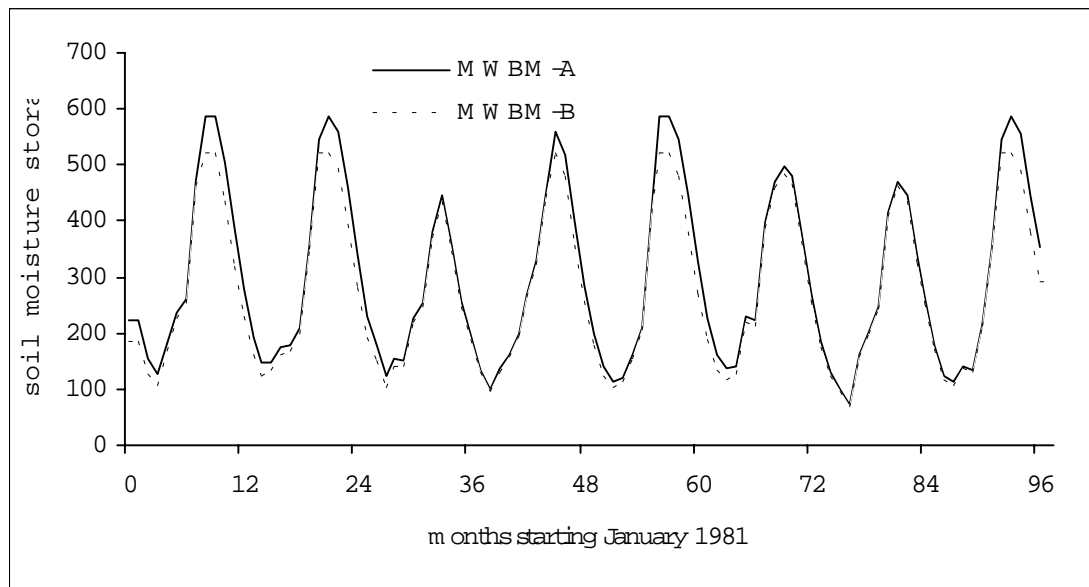


Figure 5.22 Comparison soil moisture evolution flow with the two variants of monthly water balance models (Boa Catchment, Ivory Coast)

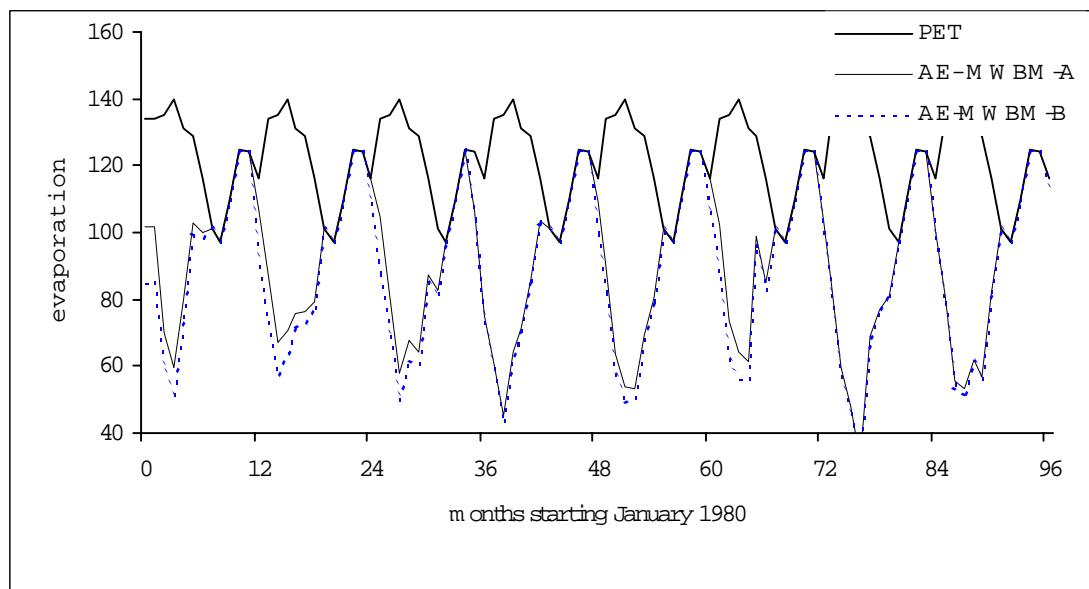


Figure 5.23 Comparison of the actual evaporation with the two variants of monthly water balance models. (Boa Catchment, Ivory Coast)

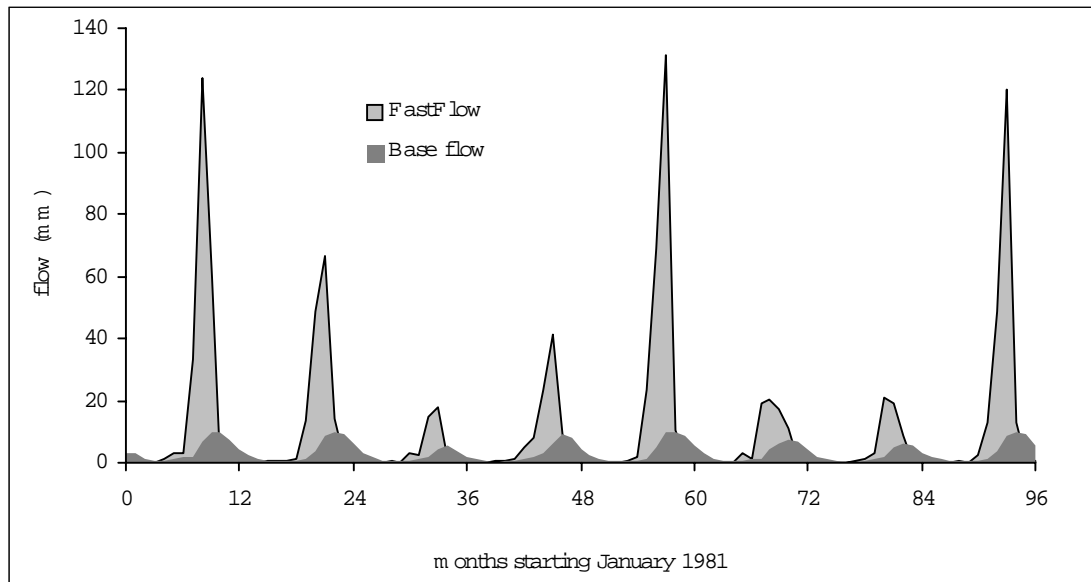


Figure 5.24 Flow components using MWBM-A. (Boa Catchment, Ivory Coast).

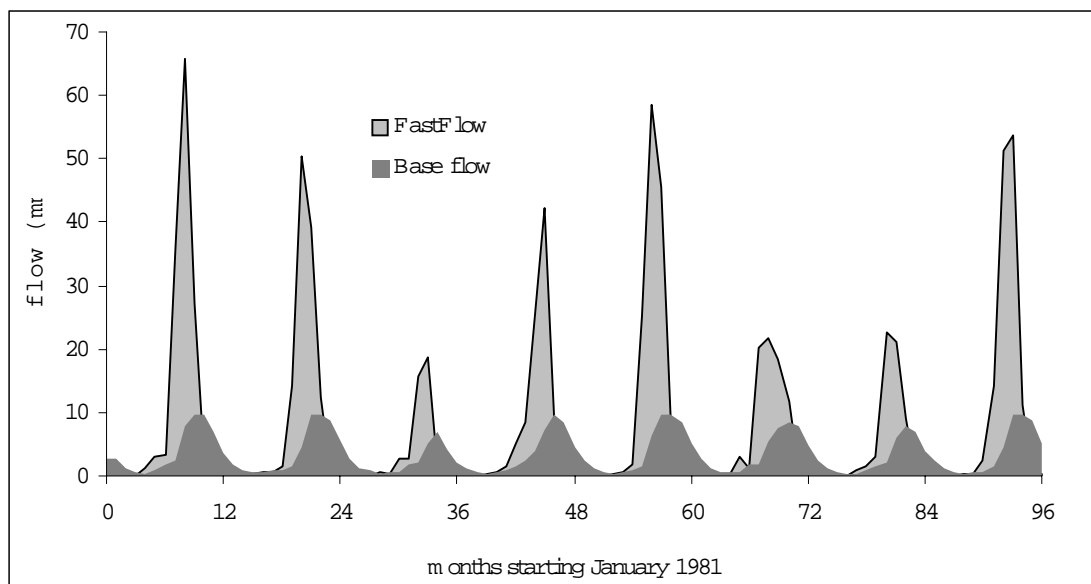


Figure 5.25 Flow components using MWBM-B. (Boa Catchment, Ivory Coast).

5.3.4 Summary of the results for the test catchments

The total number of model calibrations is 20 stations times 2 variants of the model times 18 possible combinations which equals to 360 calibrations

According to the list of tests described in the previous section for individual catchments it is noted that the evaporation equation $IR=2$ yields often better results as compared to $IR=1$. It is also observed that model forms associated to $b_1=0.5$ and $b_2=0.5$ result in a systematic underestimation of both fast and slow flows. The model with the combination of $IR=2$, $b_1=2$ and $b_2=2$ results in a reasonable quality of agreement between simulated and observed flows for all the sub-basins and may therefore be considered as the general model form. In instances where the quality is not acceptable one can try other combinations of the discrete parameters. It is possible in some cases that other forms of the models give a slightly better performance in one of the criteria, however the results of only one combination are reported for even comparison.

The estimates of model parameters with the associated model performance indicated by the efficiency and quality factors are given in Table 5.13 and Table 5.14 for MWBM-A and MWBM-B respectively. For the catchments considered, the model without imposing upper soil moisture has efficiencies that vary from 60-97% and model quality factor ranging from 1.52-3.79. The model with upper soil moisture storage has efficiencies that range from 62-95% and quality factors that vary between 1.57-4.0. The quality factor greater than 1.5 has been classified as good and for ranges above 2.5 the model is considered to be very good for monthly water balance models.

From Table 5.13 and Table 5.14 it is observed that the quality factor has similar magnitudes in a given region. For Example for the Tanzanian catchments, the values are all around of 1.5 while for the west African catchment we have value in the range of 2.5-3.5. This is in consistence with the assertion of Xu (1992) that the quality factor heavily depends on the climatic and physical characteristics of the basin.

Table 5.13 Parameter estimates for without upper limit to storage -MWBM-A (IR=2, $b_1=b_2=2.0$)

Catchment	parameter			Eff. %	MQ
	Evaporation (a_1) $\times 10^{-2}$	Slow flow (a_2) $\times 10^{-4}$	Fast flow (a_3) $\times 10^{-4}$		
1. Ruaha - Ihimbu	.050	.159	.003	75	1.54
2. Ruaha - Mkalala	.071	.208	.002	78	1.52
3. Berga	.230	.571	.004	75	4.00
4. Modjo	.120	.010	.050	62	3.15
5. Awash - Melka	.145	.450	.090	97	3.19
6. Awash - Hombole	.204	.120	.025	88	3.08
7. Boa	.257	.259	.009	95	2.45
8. N'zo	.716	.575	.020	79	3.79
9. Ferdougouba	.278	.502	.012	82	3.09
10. Niger	.431	.804	.010	77	3.04
11. Faleme - Fad.	.809	.717	.038	80	2.92
12. Faleme - Mous.	.855	.589	.030	80	2.64
13. Bafing	.550	.458	.062	61	2.84
14. Tati	.315	.080	.000	73	2.66
15. Mwambashi	.171	.132	.014	79	3.22
16. Lufumpa	.200	.467	.010	65	3.00
17. Kafu	.100	.678	.020	60	2.42
18. Baluba	.240	.794	.030	72	2.75
19. SX1	.254	.160	.600	82	3.19
20. SX2	.204	.255	.028	91	2.01

Table 5.14 Parameter estimates for with upper limit to storage MWBM-B (IR=2, $b_1=b_2=2.0$)

Catchment	parameter				Eff. %	MQ
	Evaporation (a_1) $\times 10^{-2}$	Slow flow (a_2) $\times 10^{-4}$	Fast flow (a_3) $\times 10^{-4}$	Upper limit (a_4)		
1. Ruaha - Ihimbu	.120	.613	.006	.775	68	1.57
2. Ruaha - Mkalala	.130	.606	.002	.545	57	1.68
3. Berga	.23	.429	.050	.414	79	3.93
4. Modjo	.120	.010	.050	.471	67	3.14
5. Awash	.231	.220	.020	.463	93	2.99
6. Awash	.260	.821	.060	.263	83	3.28
7. Boa	.275	.291	.046	.588	95	2.45
8. N'zo	.201	.139	.009	.756	94	2.49
9. Ferdougouba	.572	.575	.029	.554	68	4.00
10. Niger	.330	.572	.019	.635	78	3.13
11. Faleme - Fad.	.315	.579	.011	.000	78	3.03
12. Faleme - Mas.	.442	.368	.038	.418	80	2.93
13. Bafing	.212	.400	.070	.867	62	2.83
14. Tati	.186	.100	.090	.280	71	2.65
15. Mwambashi	.153	.731	.030	.657	70	2.17
16. Lufumpa	.200	.385	.010	.638	65	2.97
17. Kafu	.107	.120	.040	.733	73	2.54
18. Baluba	.138	.177	.040	.818	75	2.47
19. SX1	.138	.544	.027	.470	88	2.82
20. SX2	.162	.159	.020	.451	78	2.07

Introducing the upper limit to the soil moisture marginally improved the model performance only for a few catchments notably for the West African and Zambian catchments.

The variation of estimates of the parameters is shown in Figure 5.26. Because of the limited information on catchment it has not been attempted to relate the parameter values with catchment characteristics.

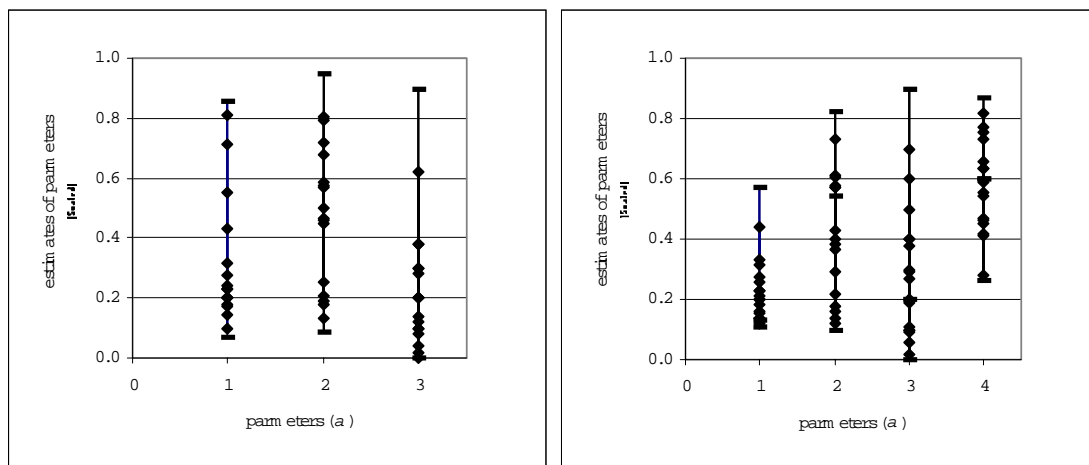


Figure 5.26 Ranges of estimates of parameter for MWBM-A (left) and MWBM-B (right)

5.3.5 Reproducing flow regimes

One of the requirements of a model is to reproduce the flow regimes. The models applied generally conserve the long-term monthly mean flows for the high as well as for the low flow regimes.

Figure 5.27 shows 6 examples of results obtained by using the two variants of the monthly water balance models. The best agreement between the observed and simulated long-term mean is shown for the Awash catchments in Ethiopia and Boa catchment in West Africa. For some catchments as for example Mwambashi the models reproduce well the low flows and medium flow regimes, but that high flows are not well reproduced. These differences may probably be attributed to rainfall events concentrated in few days, which produce exceptionally high flows.

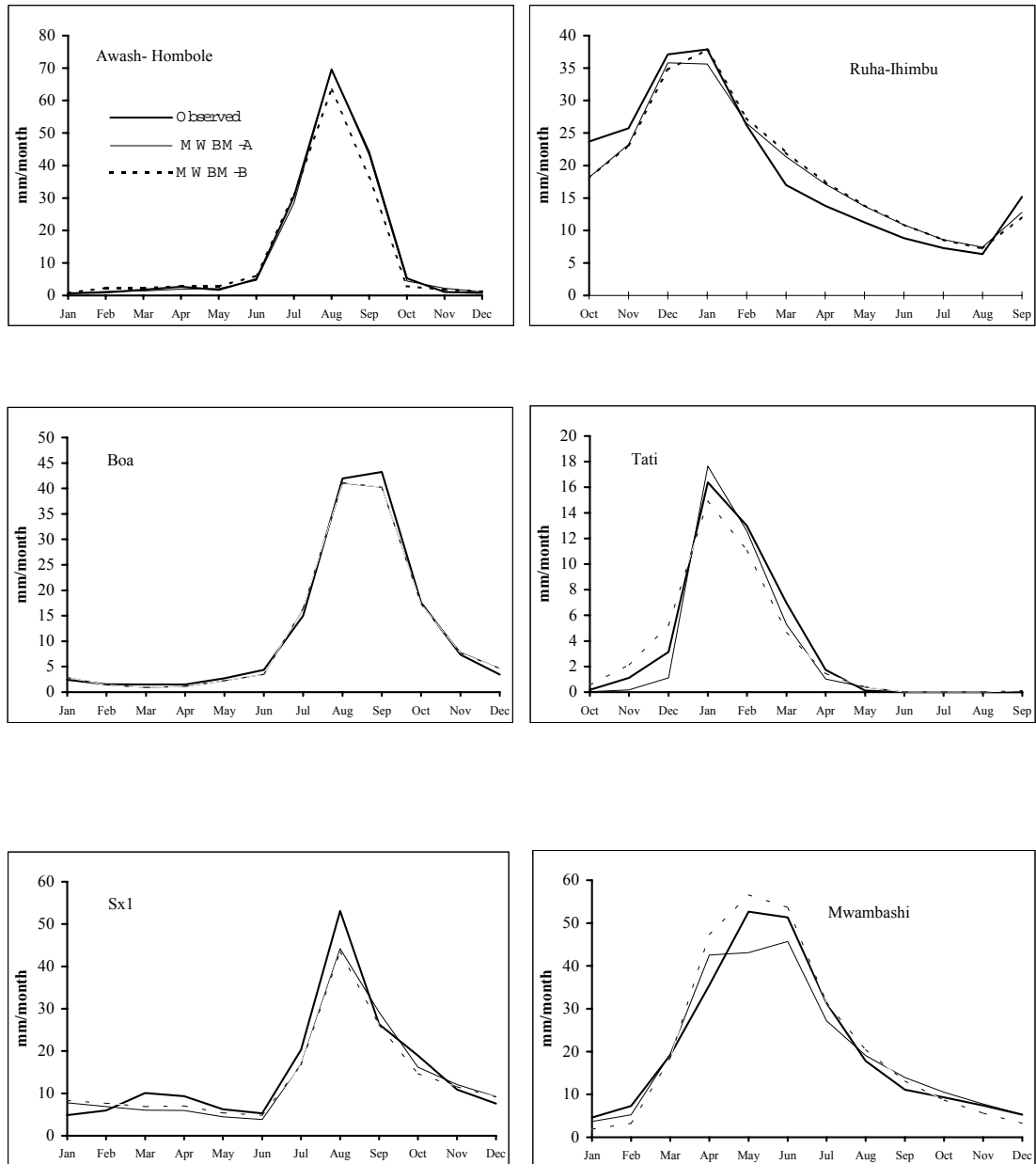


Figure 5.27 Comparison of seasonal observed and simulated monthly flows using MWBM-A and MWBM-B.

As the model implicitly assumes a homogeneous rainfall distribution over the period of one month, the effects of such short duration events are damped out. This phenomenon is linked to the choice of the model time base and could be improved by reducing the time step of the modelling. Similar results are observed for the other catchments.

5.3.6 Water balance variables

Besides establishing the rainfall-runoff relationship, the models compute the actual evapotranspiration and from the simulations the water balance proportions can be obtained. Considering rainfall as input to the system, the model results showed that from 70 to 90 percent of the water goes back to atmosphere through evaporation. Figure 5.28 through Figure 5.31 show the long-term average percentage of fast flow, base flow and actual evaporations for the catchments. The percentage of fast flow and base flow varies greatly. The dominant flow is fast flow for catchments from Ethiopia (Berga and Awash). For Tanzanian catchment Ruaha the flow is dominated by base flow. The extreme case is that for Botswana catchment Tati, where the flow is composed of only fast flow.

The possible reason for the differences of proportion is mainly due to the length of rainfall season. With the exception of the Tati, catchments with longer rainy season have relatively a higher proportion of slow flow components. Other possible reasons could be the type of soil and geological formation of the catchments, this can only be verified by detailed studies of the geology of the catchments.

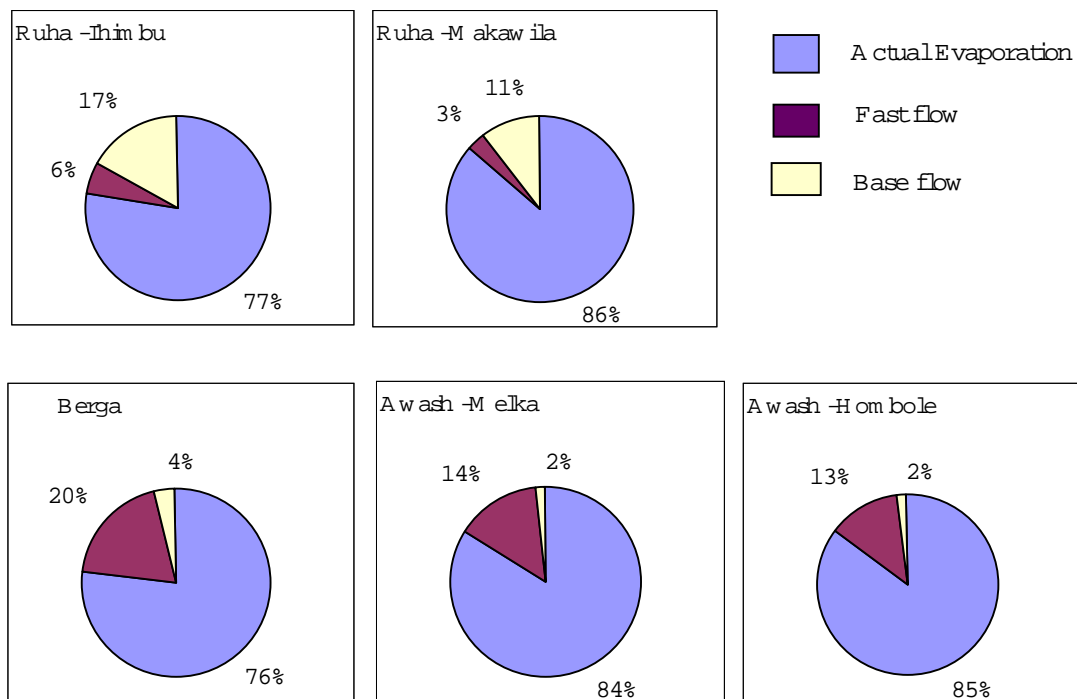


Figure 5.28 Proportion of water balances variables for East African catchments

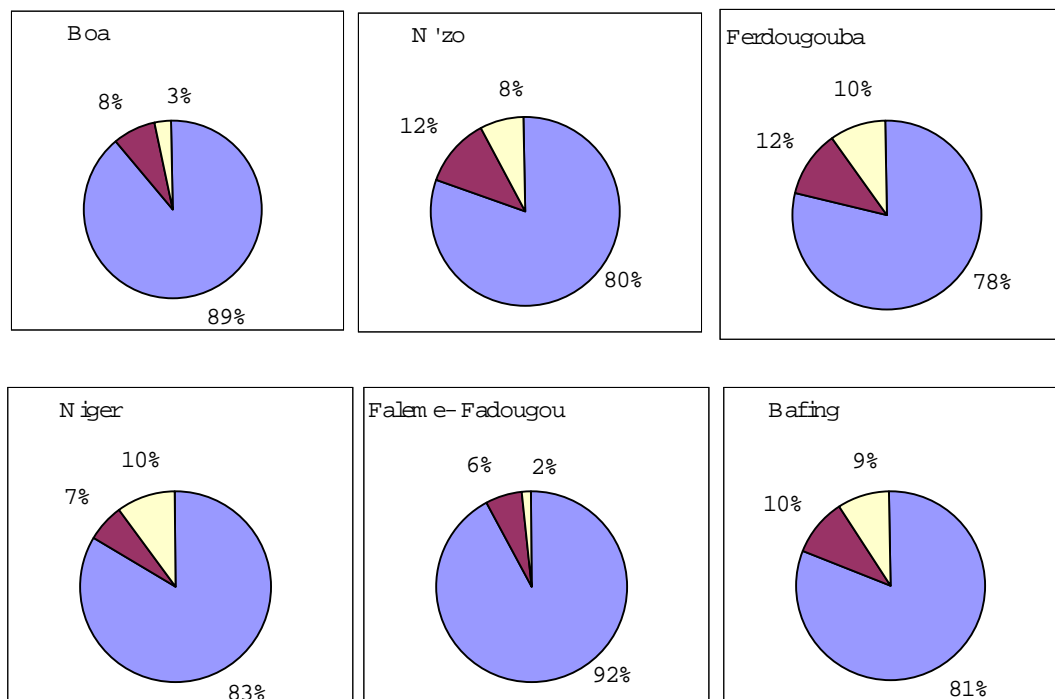


Figure 5. 29 Proportion of water balances for West African catchments

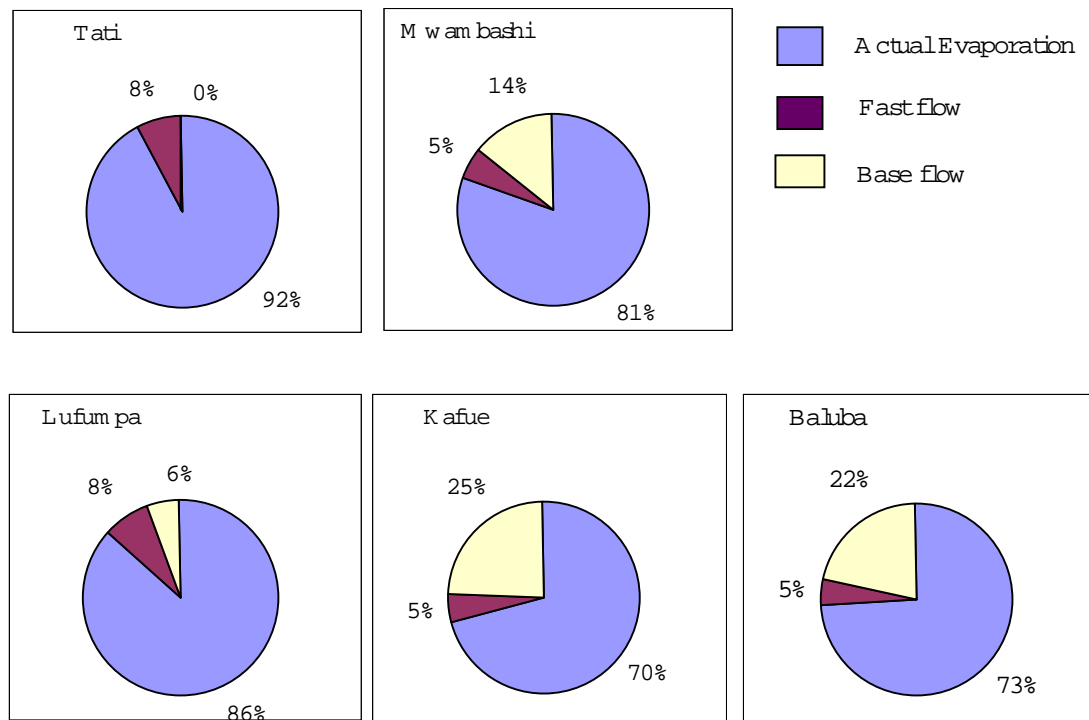


Figure 5. 30 Proportion of water balances for South African catchments

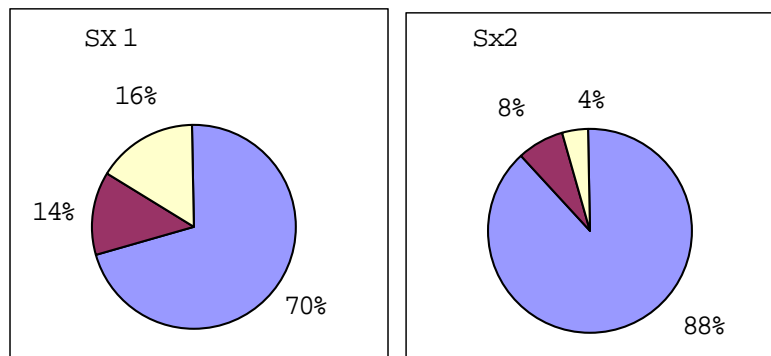


Figure 5.31 Proportion of water balances for Chines catchments

5.3.7 Sensitivity of the parameters for the calibration period and extrapolation test

Many researchers have advocated that model test and validation should be performed using split-sample experiments. This is done by subdividing the input data into two parts. To evaluate the sensitivity of the parameters to the calibration periods, the model is calibrated separately using the entire data and two split parts. Consequently, the parameters obtained from these three sets are compared. An example for a catchment is shown in Table 5.15. As - in this case as well as for the other considered catchments - the confidence intervals for the three sets overlap for all the parameters, it may be concluded that the three sets resulted in comparable parameters and that the parameter values were not biased by the calibration period.

Table 5.15 Comparison of parameter estimates and water balance variables for the three sets of data (Awash catchment the discrete parameters: $b_1=2$, $b_2=2$)

Parameter	Scale Of Par.	Periods		
		1963-1977	1978-1992	1963-1992
Evaporation Par. a_1	100	0.210	0.187	0.204 ± 0.07
Fast Flow Par. a_2	10000	0.148	0.093	0.120 ± 0.09
Slow Flow a_3	10000	0.045	0.053	0.041 ± 0.02
Mean annual water Balance Variables (mm)				
Rainfall		937	933.6	935
P. Evaporation		1794	1794	1794
Actual evaporation		758	777	770
Observed flow		183	165	175
Calculated flow		179	158	167

On the other hand extrapolation test can be performed by calibrating the model with the first half of the data and simulate using the input of the second half. The performance of the model in the two periods is compared. This shows the ability of the model to retain some of the hydrological characteristic of the catchment, independent of the calibration period. The two tests can be performed only if there is a sufficient length of data to obtain acceptable statistics.

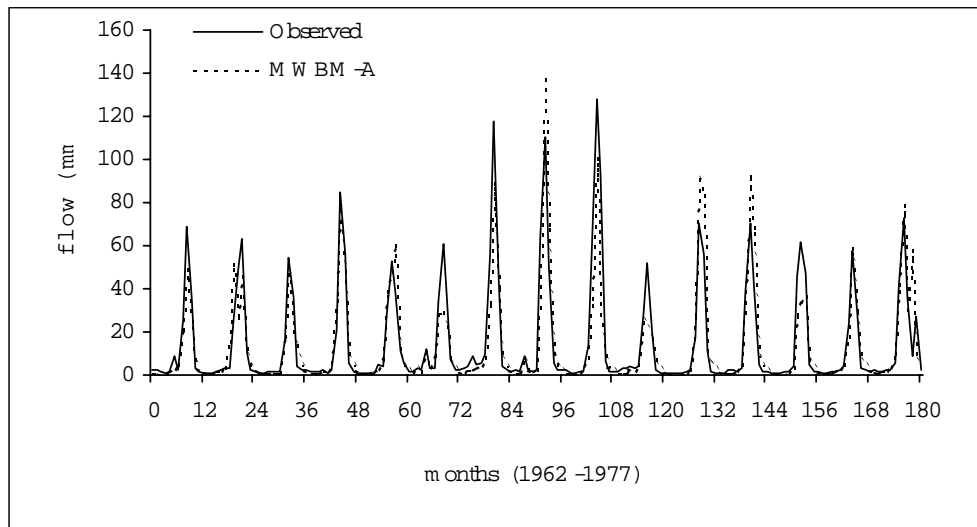


Figure 5.32 Comparison of observed and computed flow for the calibration period (Awash - Hombole)

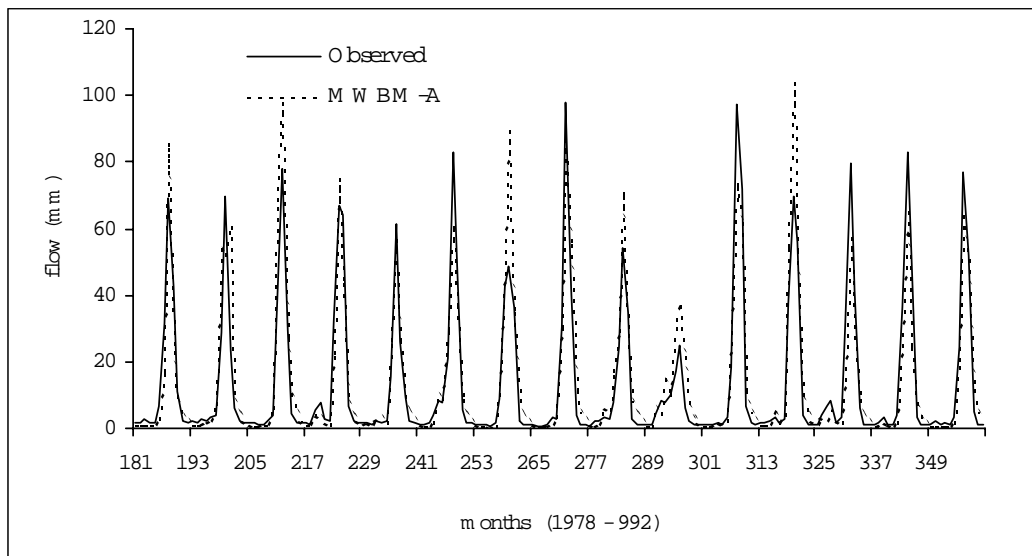


Figure 5.33 Comparison of observed and computed flow for the verification period (Awash - Hombole)

5.4 Conclusions

The conceptual monthly water balance models originally developed and tested for humid regions are applied to arid and semiarid cases with slight modification of the structure of the

model apropos to the temporal variability of the hydrological processes in the latter regions. More over it is shown that a particular representation of the evaporation term is justified and some of the discrete parameters were narrowed to a definite range of values, indicating the possible regionalization of the forms of the general equations governing the models.

The following conclusions may be specifically drawn from the present study:

- For the catchments considered a warming up period of one to three year is sufficient to avoid the influence of initial soil moisture assumption.
- The model structure whereby the fast flow is expressed as a function of the average soil moisture index resulted with good agreement of observed and calculated flow for most of the catchment studied. Introducing an additional parameter such as upper limit of the soil moisture index marginally improved the modelling in few catchments.
- Evaporation Equation $IR=2$ is best suited for the catchments and also the discrete parameters for slow flow and fast flow can be set to $b_1=2$ and $b_2=2$.
- The models seem good enough to represent the rainfall runoff relationship for low flow and medium flow but may over or under estimate the exceptional peaks.
- The model parameters are not biased by the calibration period.
- The seasonal mean flow statistics are well preserved.

The result of the modelling of the study catchments is encouraging for practical applications such as extending and filling missing flow data for the periods where rainfall and evaporation are available to obtain long-term flow data for water resource planning and management.

Chapter 6

6 CASE STUDIES OF THE 10-DAY WATER BALANCE MODEL

6.1	Introduction	140
6.2	Data description.....	140
6.3	Detailed model tests with an example catchment.....	143
6.4	Summary of the results for the test catchments	154
6.5	Concluding remarks	158

6.1 Introduction

In this chapter, the conceptual 10-day water balance model (DWBM), described in section 3.3 is tested. Among the 20 catchments, 8 are selected due to availability of data on a 10-day time step. The model results are compared to the once obtained by using the monthly model structure of the second variant, MWBM-B with 10-day time steps. Since the structure of the two models differs, a one-to-one comparison of the parameters will not be possible, however general statistics of the results are compared.

6.2 Data description

Table 6.1 lists the 8 catchments used to test the models at 10-day time step. The characteristics of the catchments were discussed in chapter 5. The 10-day rainfall and flow data for all test

catchments are obtained by aggregating the daily data. Figure 6.1 shows the mean 10-day variation of rainfall and runoff in a year.

The monthly evaporation data were available for most of the catchments. To obtain the 10-day time step values, the monthly evaporation amount is first divided in to three parts. Next, the evaporation of the first decade of a month and the last decade are adjusted by taking the average of the evaporation obtained by the month before and following. This gives a smooth transition from one month to the next. Only for three catchments (Berga, Awash at Melka Kuntre and Hombole) daily evaporation data at one station for period of two years (1988-1989) were available. The 10-day mean for (36 values of the year) are calculated. These data are used for all the catchments in the Awash River Basin.

Table 6.1 Test catchments for 10-day time step modelling.

No	River	Station	Area	Period
Tanzania				
1.	Little Ruaha	Ihimbu	2480	1966-1975
2.	Little Ruaha	Makawali	759	1966-1975
Ethiopia				
3.	Berga	Addis Alem	248	1986-1990
5.	Awash	Melka Kuntre	4456	1985-1991
6.	Awash	Hombole	7656	1985-1992
Botswana				
14.	Tati	Tati	470	1985-1991
Zambia				
15.	Mwambashi	Mwambashi	809	1978-1989
18.	Baluba	Baluba	306	1975-1989

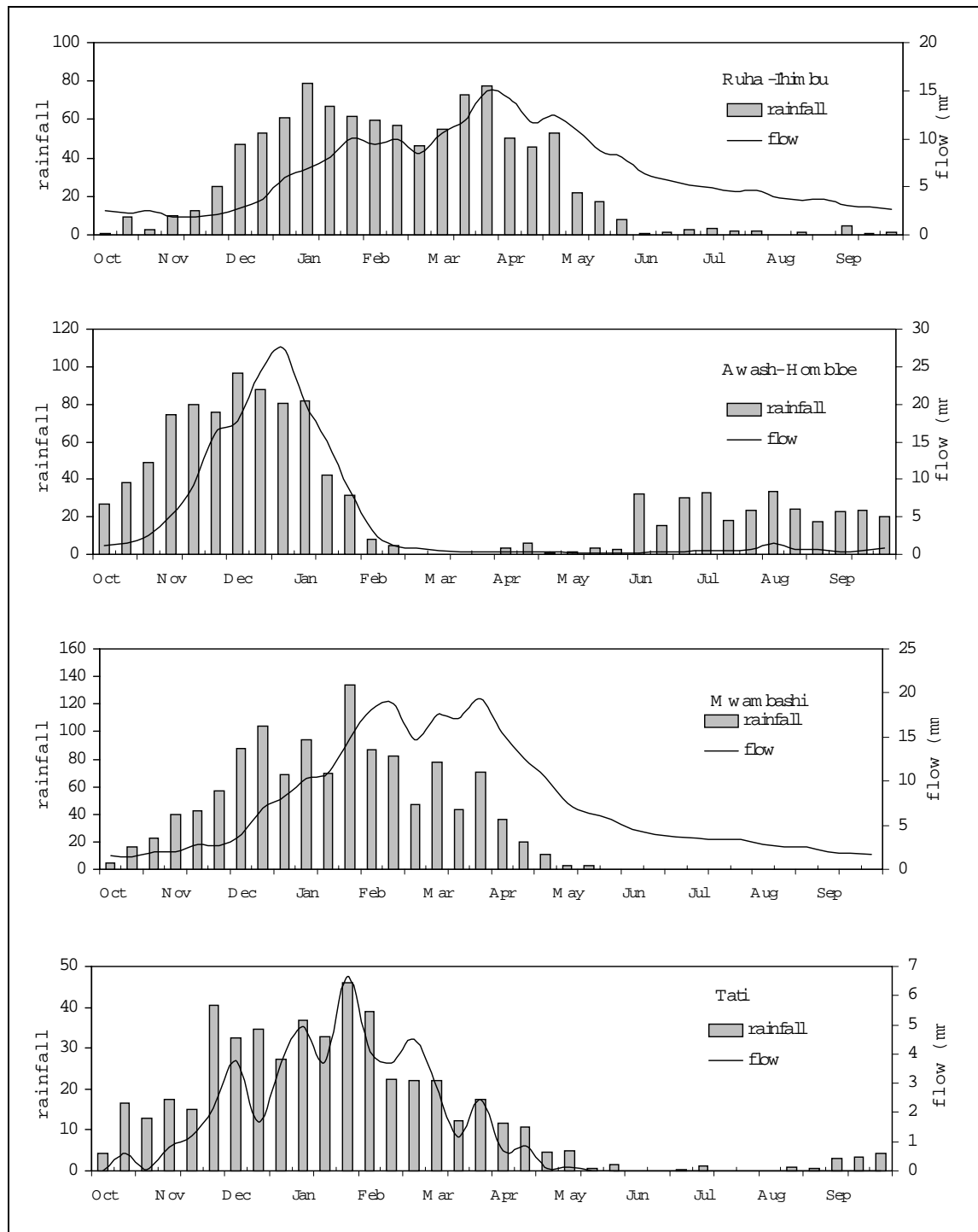


Figure 6.1 10-day long-term mean of rainfall and flow for the study catchments

6.3 Detailed model tests with an example catchment

As in the monthly water balance models the output of the models, is too extensive to report for all the studied catchments. Therefore we present the detailed result of only one catchment (Awash at Hombole). Later, a summary of the results obtained for all the catchments and conclusions derived are presented. Typical seasonal variation of the input variables is shown in Figure 6.2. It is observed that the potential evaporation exceeds the rainfall for most of the period, except during the rainy season. From the time series plot it is noted that peak flows occur latter than the highest rainfall.

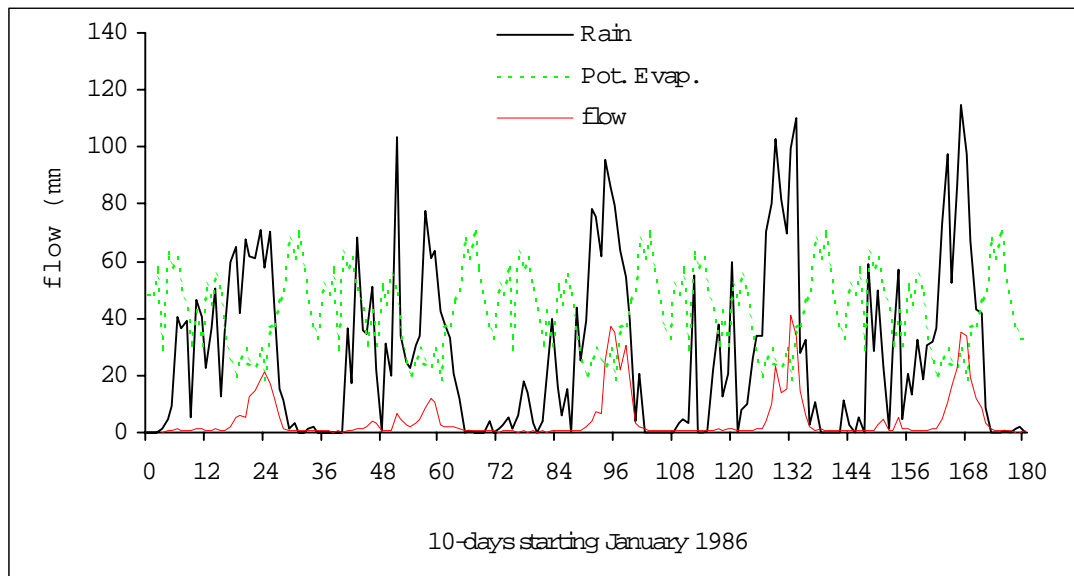


Figure 6.2 Time series of rainfall, evaporation and flow data for calibration (Awash at Hombole)

6.3.1 Parameter optimization

In the process of optimization the limitation of the VAO5A procedure is clearly observed. Specifically for the models studied in here, the problem is in selecting the right scale of individual parameters. The procedure applied is first to use the Shuffled Complex Algorithm by assigning a very wide range of parameters as lower and upper limit. Next, individual parameters are scaled to intervals (0 - 1) and the scaling factor is retained for further call of the VAO5A optimization method. The VAO5A algorithm then provides the necessary

statistics such as correlation between parameters, confidence intervals of individual parameters.

The base flow parameter of the DWBM is estimated using the hydrograph analysis routine incorporated in the model.

Regarding the parameter importance, when the time step of modeling is reduced from the month to 10-day, it appears that the evaporation parameter value of a_1 has no influence on the sum of squares of errors after a certain upper limit (See Figure 6.3). This phenomenon was common for the two models. It has been said that in the second type of evaporation equation the actual evaporation is computed as a function of available soil moisture and limited to the potential evaporation. The physical explanation that follows is that at shorter time steps indeed the potential evaporation is satisfied in most of the time during rainy days and hence the influence of the evaporation parameter of a higher value is minimal. If one assumes the higher value of the evaporation parameter, the model takes always the actual evaporation equal to the potential.

The upper soil moisture limit, parameter a_4 , shows the same behavior as previously noted on the monthly time step modelling. Once the critical maximum value corresponding to minimum of sum of squares is achieved increasing this parameter will increase the sum of errors of square slightly in the neighborhood of the optimum point and the effect will disappear for the higher values. This is expected because for whatever values above the critical point the soil moisture does never exceed this upper limit. In fact in the model calibration process, the first trial is to use models without upper limit and investigate the highest soil moisture attained. This gives an indication of the highest range of this parameter. The other two parameters a_2 and a_3 are found to be fairly stable and significantly representing the model structure.

Table 6.2 Parameter estimates of the MWBM-B and DWBM for Awash -Hombole)

MWBM-B		DWBM	
Parameter	estimates and Confidence interval	Parameters	estimates and Confidence interval
evaporation, $a_1 \times 10^{-2}$	0.78 ± 0.37	evaporation, $a_1 \times 10^{-2}$	0.89 ± 0.85
slow flow, $a_2 \times 10^{-2}$	0.76 ± 0.42	percolation, $a_2 \times 10^{-1}$	0.46 ± 0.28
fast flow, $a_3 \times 10^{-2}$	0.13 ± 0.03	interflow, $a_3 \times 10^{-2}$	0.82 ± 0.3
max. storage, $a_4 \times 10^3$	0.67 ± 0.16	max. storage, $a_4 \times 10^3$	0.51 ± 0.19
Max. Correlation	$0.85 (a_1, a_2)$	base flow, a_5	0.15
		Max. Correlation	$0.677 (a_1, a_3)$

6.3.2 Comparison of observed and computed flow

Generally speaking, the two models reproduce the flow series very well. From the comparison of the observed and computed (Figure 6.4) except for the extreme peak flows the medium flow and low flows are generally modeled quite satisfactorily. The model efficiencies for the catchment considered are 84% and 86% for MWBM-B and DWBM respectively. It is noted that as in the monthly water balance models modelling the peak flows remains the weak point of the whole modelling with the time steps considered.

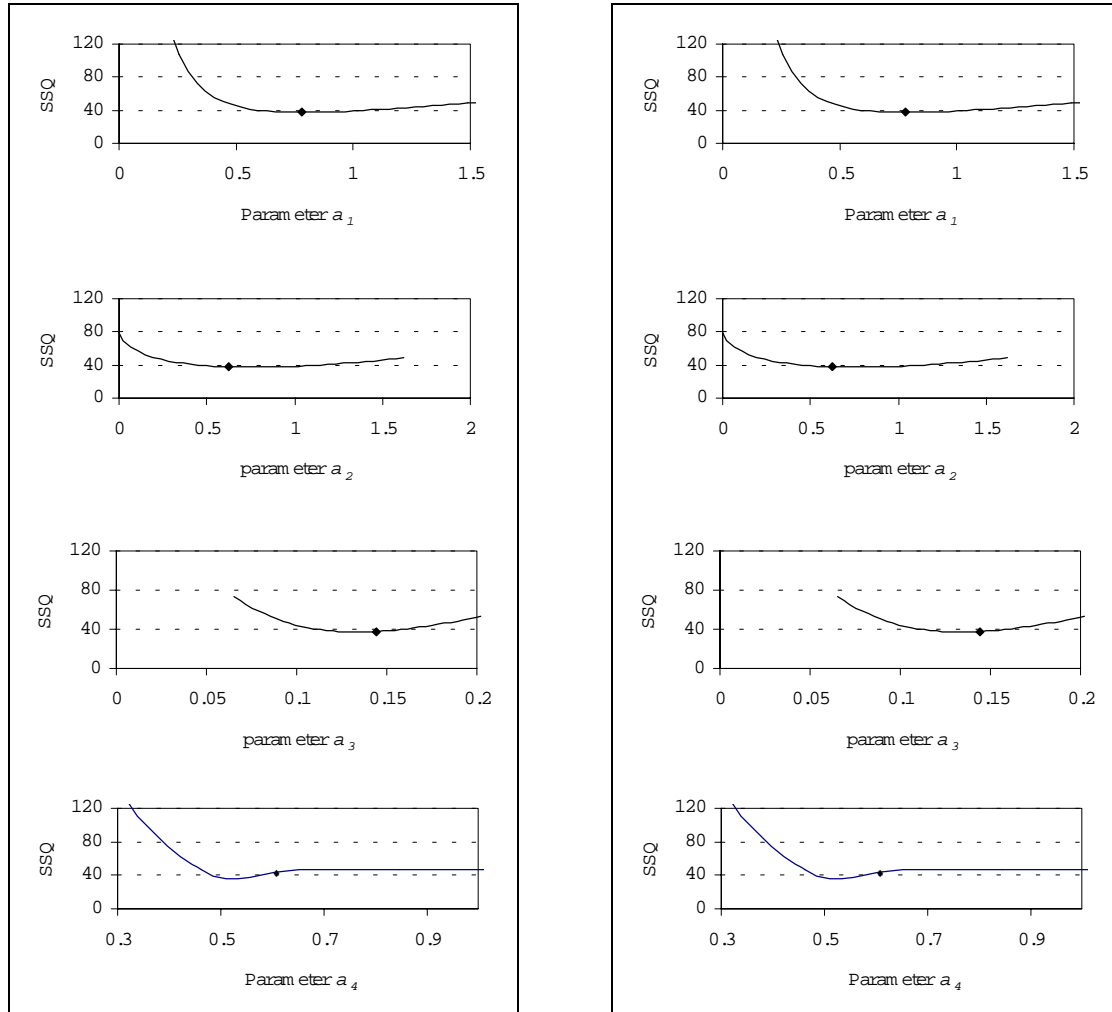


Figure 6.3 Plot of the parameter and the sum of squares of error in the neighborhood of optimum value. (left: MWBM-B, and right DWBM).

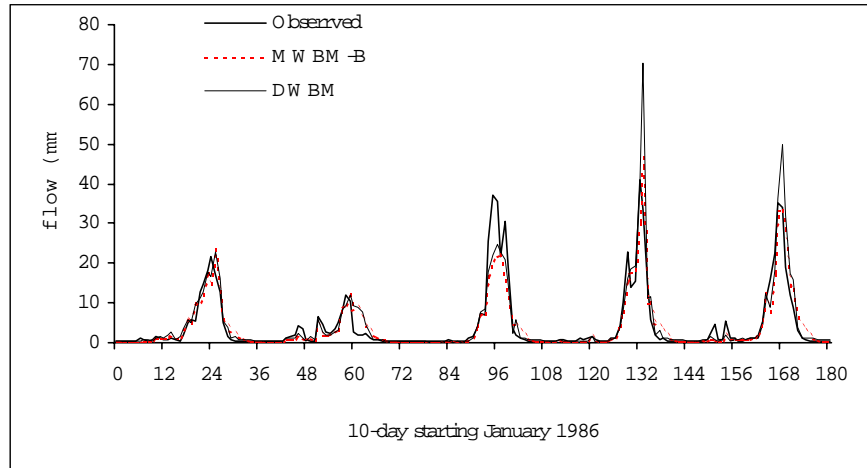


Figure 6.4 Comparison of observed and modeled flow with MWBM and DWBM (Awash-Hombole)

6.3.3 Flow components

The two models have different assumption with regard to the flow components: the MWBM-B classifies the flows into two components (fast and slow flow) while the DWBM adds one more component (interflow). The need for further classification is discussed in the model development. Considering the example case, no fast flow component is generated. It means that at the 10-day time step the intensity of the rainfall is always lower than the infiltration capacity. It is observed that the base flow component is much lower than what is considered as slow flow in the monthly model structure because the former explicitly emerges from the groundwater storage. Therefore for the 10-day model structure the interflow component includes almost all the flow generated except the base flow. The flow classification of the DWBM appears more realistic for the fact that for e.g. the base flow contribution for this catchment is very low (Figure 6. 6). For the MWBM, the flow separation flow the fast flow is the flow that is generated immediately within the time step considered and the slow flow is the flow that arrives with delay often are more than one time step.

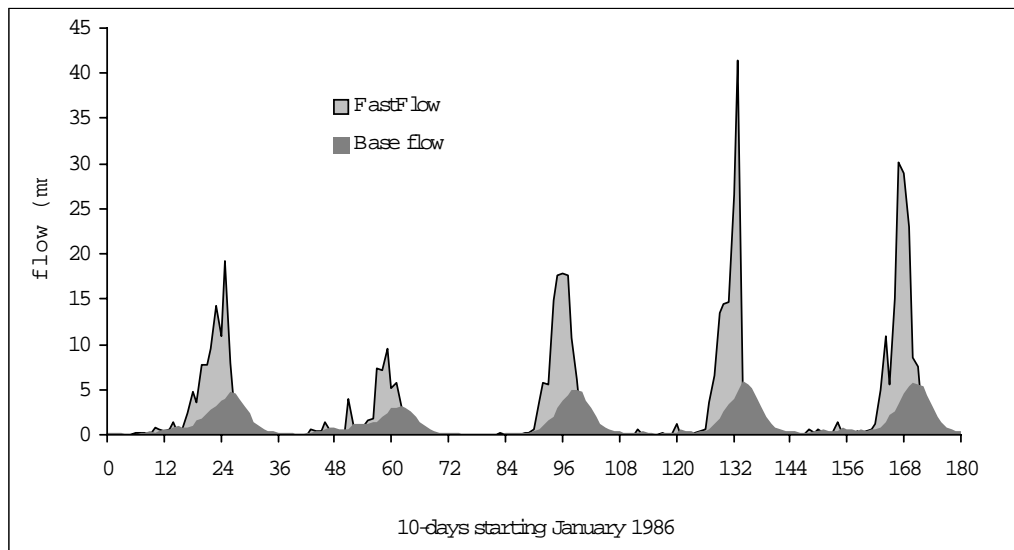


Figure 6. 5 Flow components using MWBM-B. (Awash-Hombole)

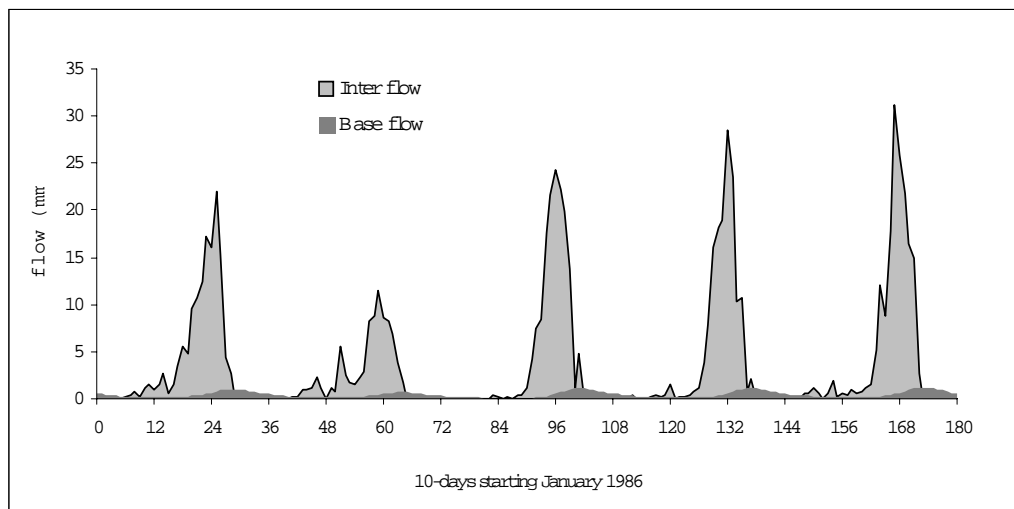


Figure 6. 6 Flow components using DWBM (Awash-Hombole)

6.3.4 Intermediate water balance variables

Apparently, the soil moisture and actual evaporation evolution of the two models agree quite reasonably (Figure 6.7 and Figure 6. 8). For the DWBM the two storages are added together for comparison. Regarding the actual evaporation it is noted that during the rainy season the actual evaporation strictly follows the potential evaporation while during dry season the actual evaporation is controlled by the available water in the catchment as expressed by the soil moisture index.

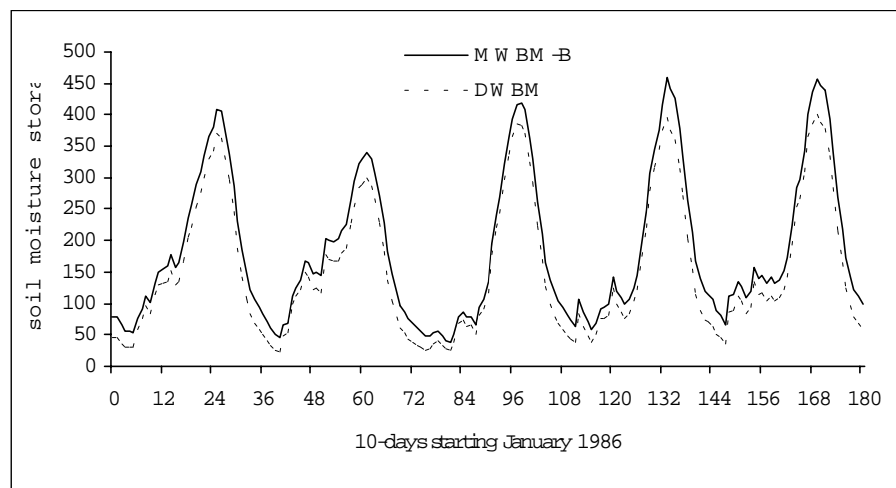


Figure 6.7 Comparison of soil moisture storage evolution with MWBM-B and DWBM. (Awash-Hombole)

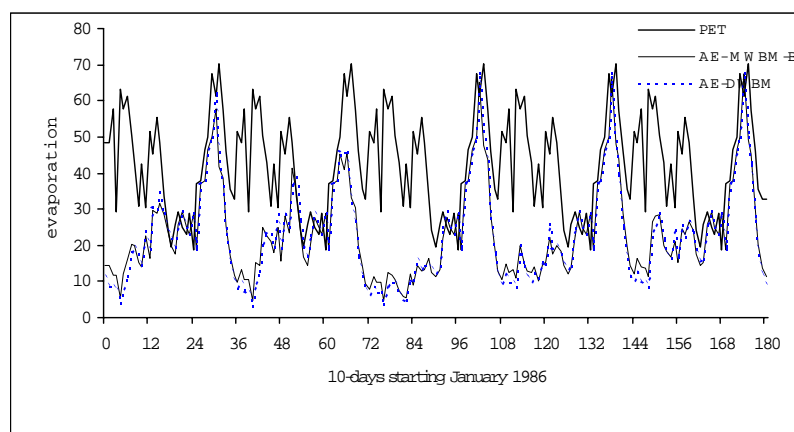


Figure 6. 8 Comparison of 10-day actual evaporation with MWBM-B and DWBM. (Awash-Hombole)

6.3.5 Residual analyses

Residuals obtained from the two models are investigated to verify the effects of the input of the model and also to check the versatility of the model in ranges of the input. Plots of residuals versus rainfall are given in (Figure 6.9). In all the cases the residuals plotted are the difference between the transformed observed and computed flows.

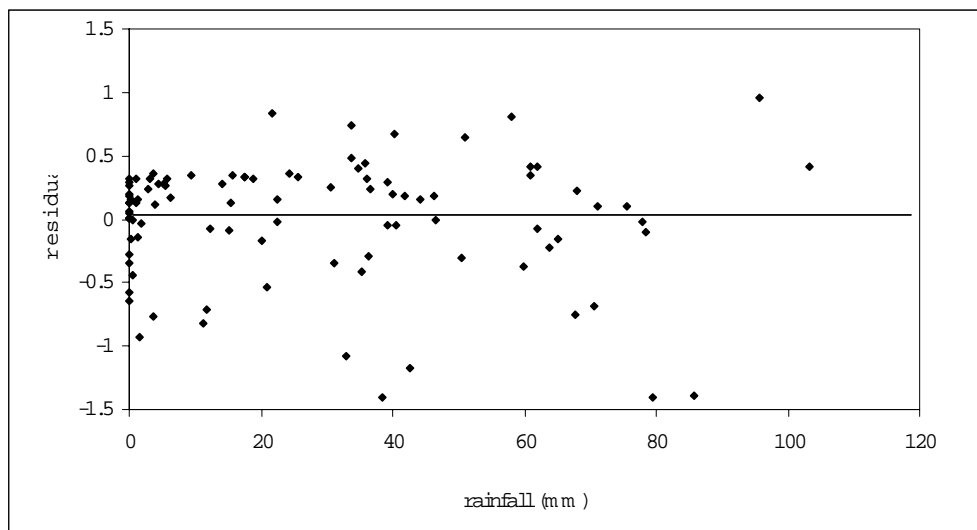


Figure 6.9 Residual versus rainfall using MWBM-B (Awash-Hombole).

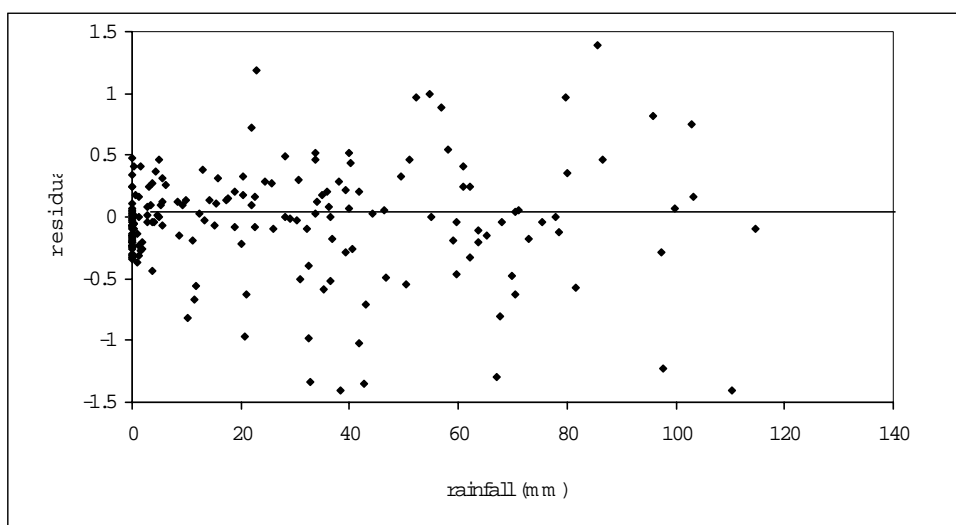


Figure 6.10 Residual versus rainfall using DWBM. (Awash-Hombole)

Plots of residuals versus potential evaporation (Figure 6.11) show that for MWBM-B the residuals have a constant deviation for the range of potential evaporation. For DWBM (Figure 6.12) the residuals show a smaller deviation for the high amounts of evaporation.

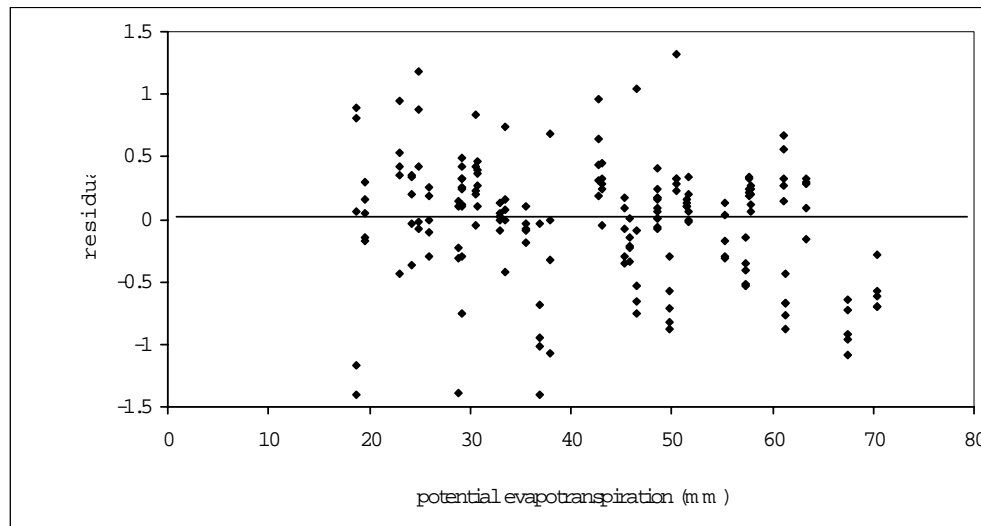


Figure 6.11 Residual versus potential evapotranspiration using MWBM-B. (Awash-Hombole)

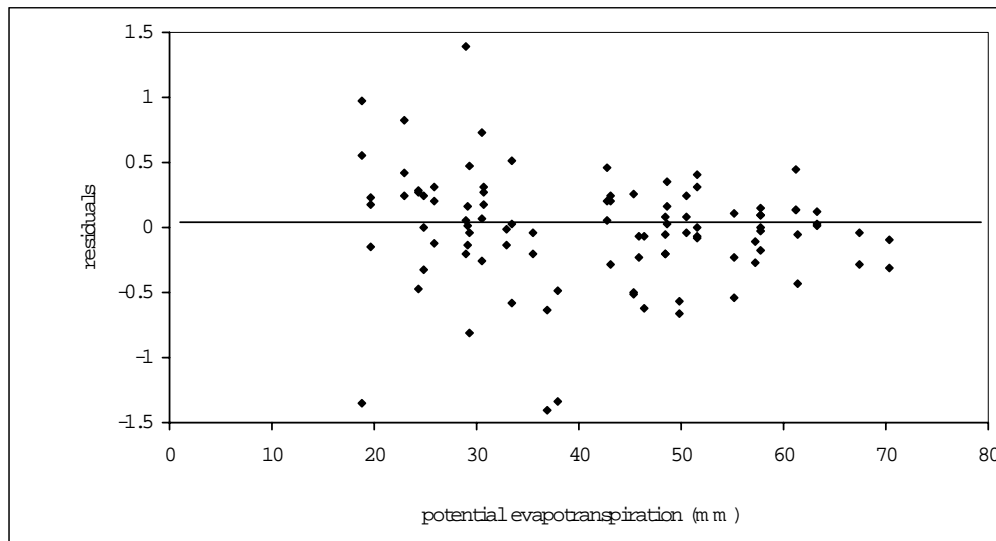


Figure 6.12 Residual versus potential evapotranspiration DWBM. (Awash-Hombole)

Plots of residuals versus computed flow (Figure 6.13 and Figure 6.14) show that for both models the residuals have a constant deviation for the range of computed flows. The scatter is denser around the low flows for the fact that during large periods of time the flow is in the low flow regimes.

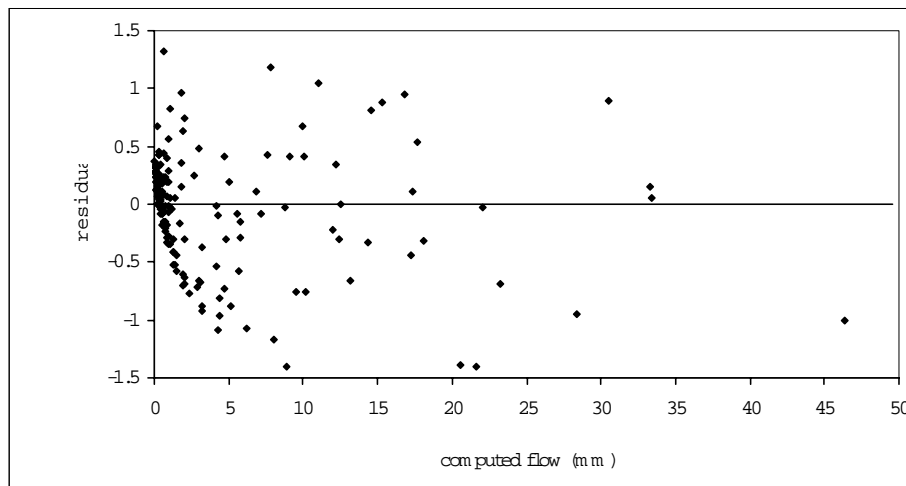


Figure 6.13 Residual versus computed flow using MWBM-B. (Awash-Hombole)

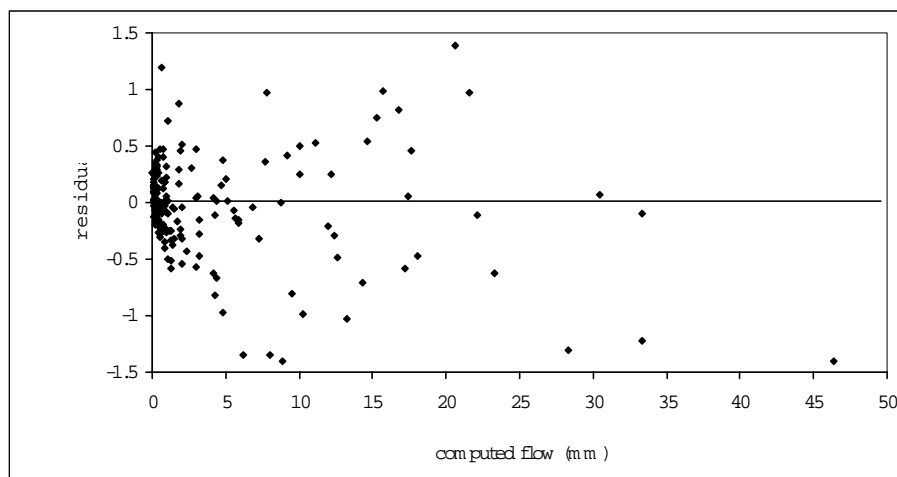


Figure 6.14 Residual versus computed flow using DWBM. (Awash-Hombole).

From the time series plot of the residuals (Figure 6.15), the residuals from both models do not show any trend. The autocorrelation coefficient of the residuals is slightly higher than the 95 confidence limit (Figure 6. 16) for only lag 1 (10-day). For the higher lags the correlation coefficients are not significant. This can also be seen from the time series plot that, there is a tendency of consistent over or under estimation for few periods.

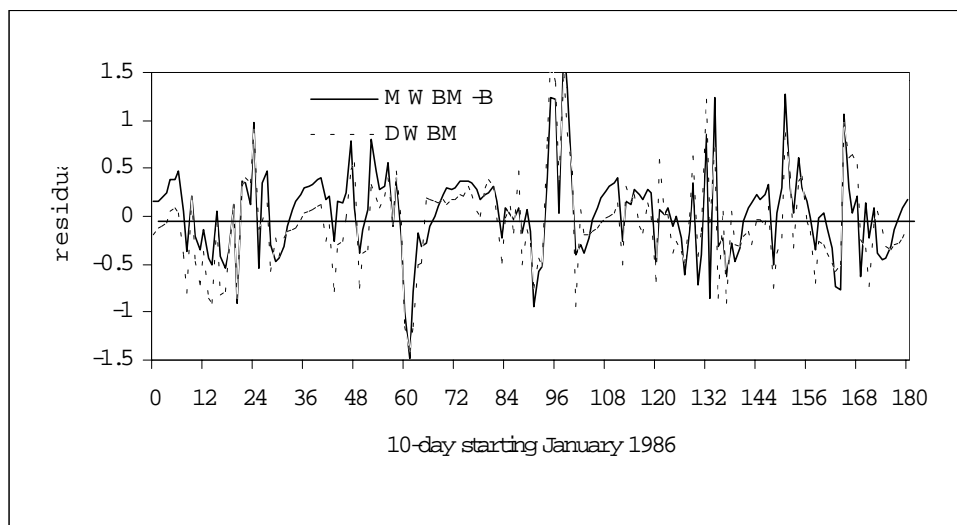


Figure 6.15 Time series plot of residuals. (Awash-Hombole)

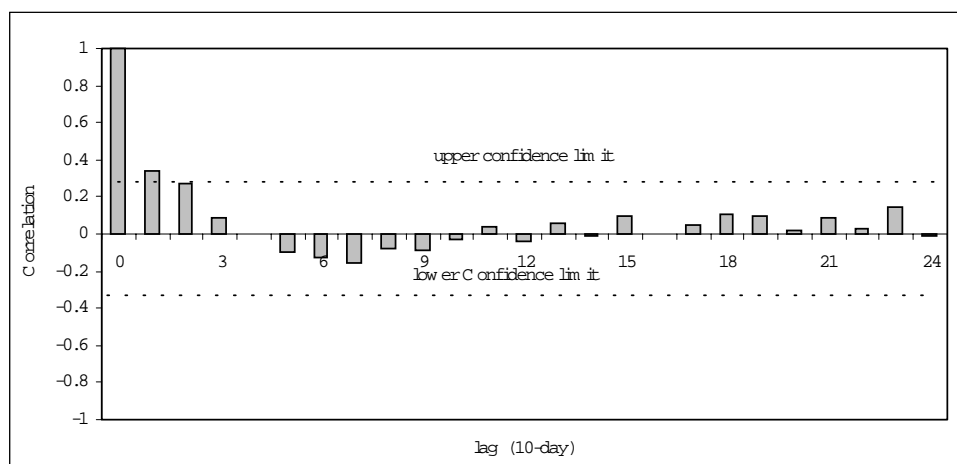


Figure 6. 16 Autocorrelation of residuals for DWBM. (Awash-Hombole)

6.4 Summary of the results for the test catchments

6.4.1 General performance of the models

Table 6.3 lists the estimates of the parameters and the two measures of performance efficiency and model factors for MWBM-B when applied to the test catchments at 10-day time step. The model performed fairly well in reproducing the flows, the model efficiencies vary from 60 % for the Ruaha-Ihimbu catchment to 84 % for the Awash-Hombole catchment. The Model quality factors for the model vary between 0.98 for the Ruaha-Ihimbu catchment to 2.19 for the Tati catchment.

For the DWBM the efficiencies vary from 60% for the Mwambashi catchment to 89 % for The Awash-Hombole catchment. (Table 6. 4). The model quality factor on the other hand varies from 1.54 for the Mwambashi catchment to 2.12 for the Tati catchment.

Considering the two model quality measures, especially the efficiency, the two models explains more than 60 per cent of the variance which is fairly acceptable. Comparison of the two models shows that the difference of their performance is marginal. Nevertheless the new DWBM has not only performed as good as the monthly model structure, the conceptual representation is quite realistic mainly in separating the catchment storage into groundwater and soil moisture storages.

6.4.1 Reproducing flow regimes

In addition to the general performance of a model measured by the efficiency or model quality, the versatility of the model in reproducing the flow regimes is checked by comparing the long term seasonal flows. Figure 6.17 shows good agreement between the observed and model computed long-term 10 days mean flows.

Table 6.3 Table Parameter estimates for the MWBM-B with 10-day time step.

Catchment	Estimates of Parameters				Eff. %	MQ
	Evaporation (a_1) $\times 10^{-2}$	Slow flow (a_2) $\times 10^{-2}$	Fast flow (a_3) $\times 10^{-3}$	Upper limit (a_4) $\times 10^3$		
1. Ruaha -Mak	.196	.169	.209	.811	75	1.00
2. Ruaha - Ih.	.330	.170	.101	.414	60	0.98
3. Berga	.020	.700	.198	.151	74	2.00
5. Awash-M	.800	.630	.103	.572	79	1.89
6. Awash-H	.780	.760	.130	.670	84	1.95
14. Tati	.100	.000	.400	.697	64	2.19
15. Mwambashi	.280	.200	.010	.583	70	1.56
18 Baluba	.300	.200	.940	.900	70	1.53

Table 6. 4 Parameter estimates for the DWBM

Catchment	Estimates of parameters					Eff. %	MQ
	Evaporation (a_1) $\times 10^{-2}$	Percolation (a_2) $\times 10^{-1}$	Interflow (a_3) $\times 10^{-2}$	Upper limit (a_4) $\times 10^3$	Recession a_5		
1. Ruaha -Mak	.317	.300	.080	.612	.070	69	0.98
2. Little -Ih.	.900	.200	.025	.792	.011	70	1.04
3. Berga	.380	.060	.140	.429	.090	66	2.09
5. Awash-M	.240	.540	.080	.679	.198	83	1.90
6. Awash-H	.777	.461	.600	.510	.148	89	1.97
14. Tati	.940	.200	.020	.306	.029	65	2.12
15. Mwambashi	.600	.400	.020	.708	.118	60	1.54
18. Baluba	.300	.030	.030	.790	.090	72	1.59

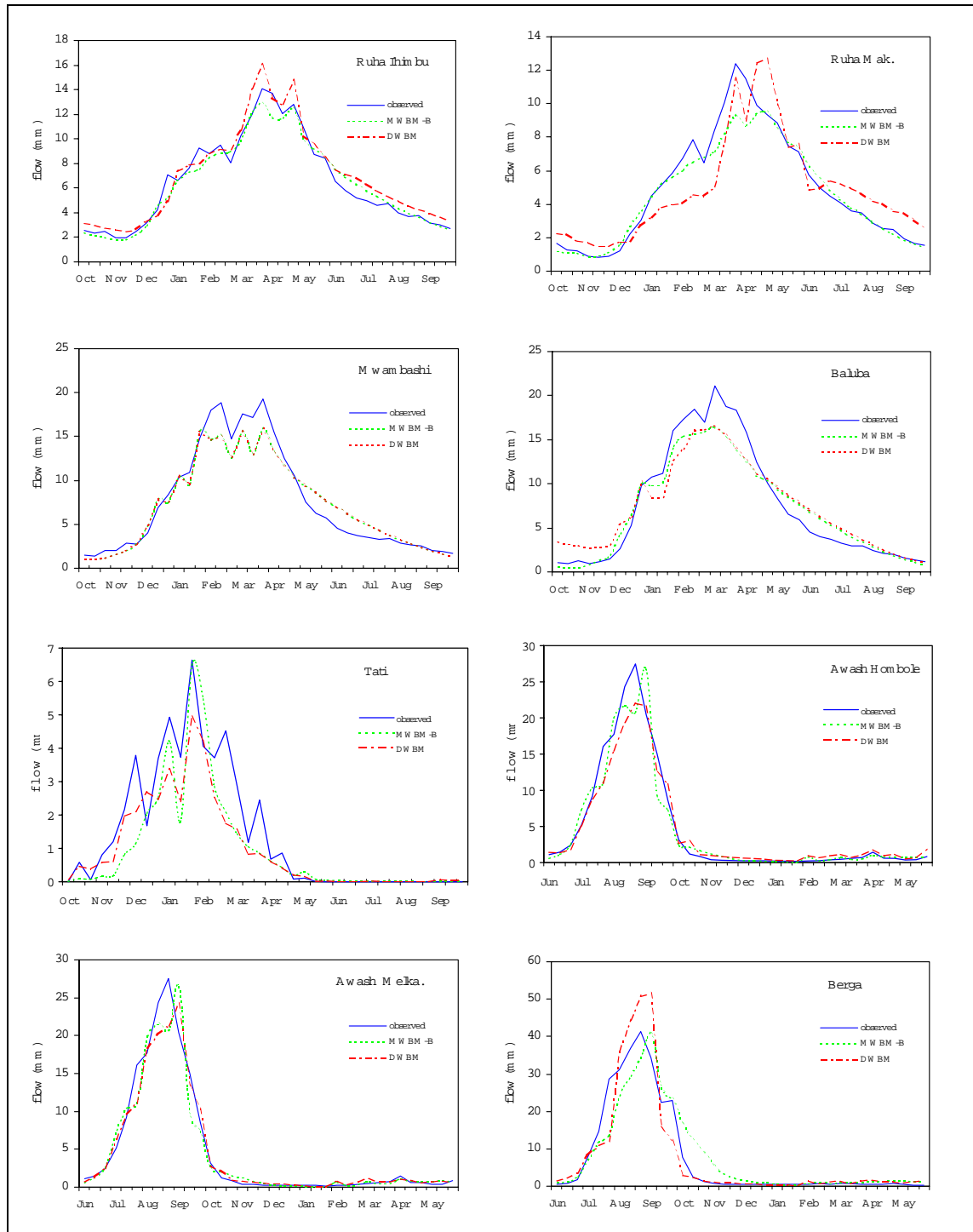


Figure 6.17 Comparison of long-term 10 day mean observed and computed flow using MWBM-A and DWBAM.

6.4.2 Water Balance components

For all the considered catchments the fast flow component (infiltration excess) does not exist, hence the total flow is only composed of interflow and base flow (Figure 6. 8. The reason for this could be that with the 10 day time interval it is likely that the isolated intensive short duration storms are smoothed, and excess runoff can not be generated. For e.g. the Awash River, the base flow component is very low. Although isolated rain events occur during the dry season, it appears that most of the rain is lost by evaporation and only part of it reaches the river as interflow.

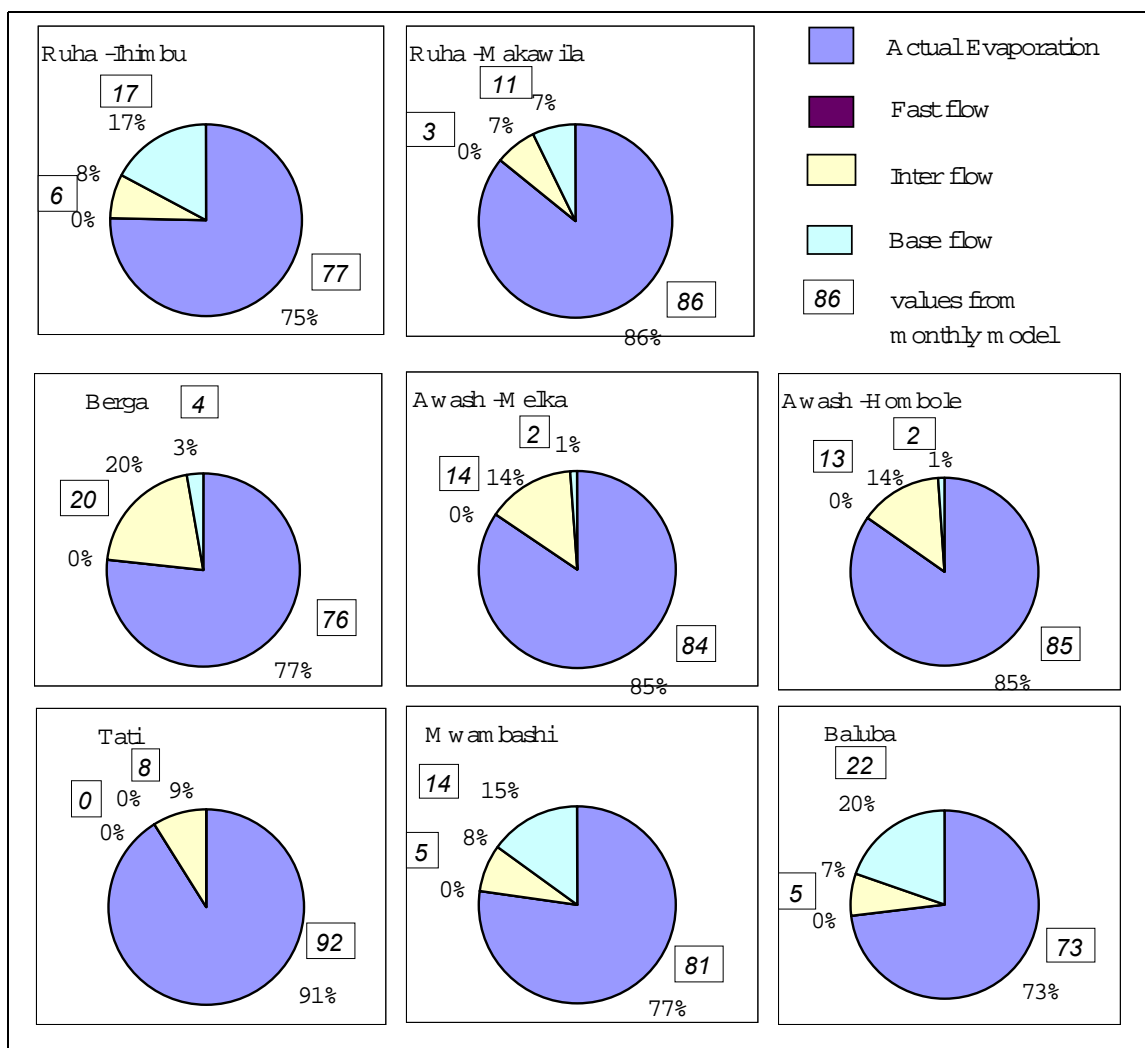


Figure 6.18 Proportion of water balance s using DWBM.

For the Mwambashi, Ruaha and Baluba catchments, on the other hand, a substantial amount of the flow comes as groundwater supply that maintains relatively high base flow. For Tati catchment the flow is totally interflow. The water balance proportion obtained by the 10-day

model is almost the same as for the monthly model with regard to evaporation and flow components.

6.5 Concluding remarks

The comparison between the two models suggests that the new 10-day model structure is as good as the previous monthly one. It is also more realistic as it incorporates more concepts in flow separation as well as flow recessions without increasing the number of parameters to be optimized. The flows computed using the decade time step are aggregated to obtain monthly time series. These time series are compared to the observed monthly flow and time series obtained by using the monthly water balance models (Figure 6.19). The conclusion is that regarding the monthly flow generation the three models (MWBM with monthly time step, MWBM with 10 day-time step and the DWBM) have nearly the same performance. The model structure described for a monthly time step could therefore be used as the first trial in modelling for the reason of simplicity. One can also see that none of the models has overcome the problem of inaccurate estimation of the exceptional peaks.

The present study shows that a relatively small number of parameters are sufficient to represent the rainfall-runoff relations in 10-day time step. Further, it demonstrates that a routine devised to compute the recession coefficient is useful to incorporate *a priori* knowledge of a catchment in hydrological modelling. We believe that the approach of stepwise parameter optimization can be extended to daily rainfall runoff models by hierarchically determining parameters such as the recession coefficient from hydrograph analysis and evaporation parameters from long-term water balance models. This will ease the competition of numerous parameters in minimization the objective function in standard optimization procedures.

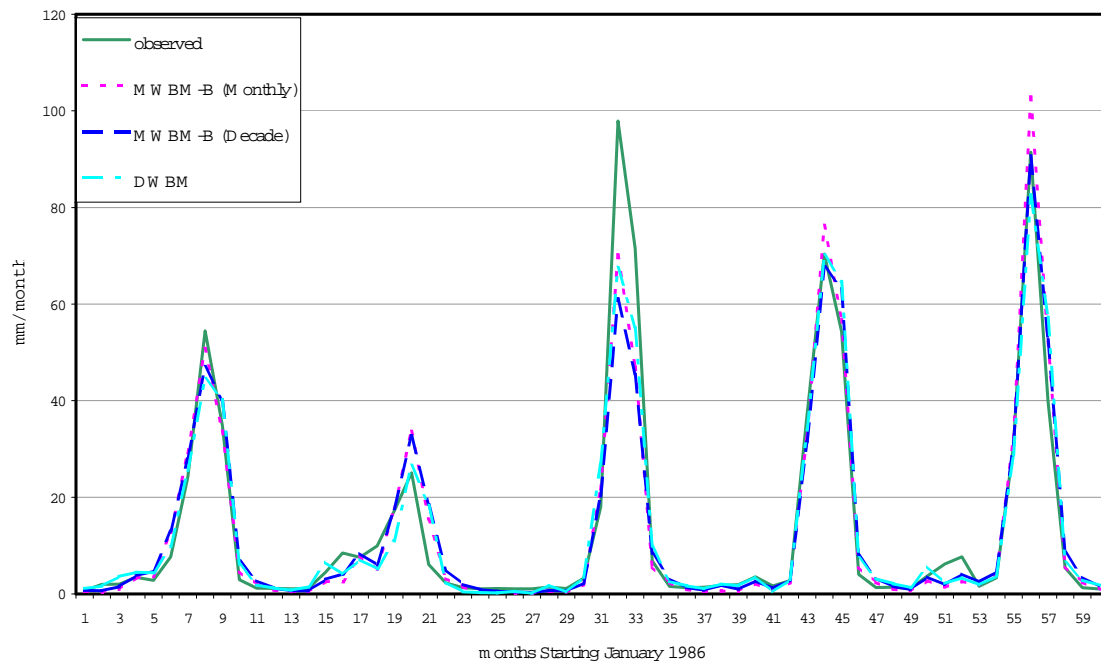


Figure 6.19 Comparison of monthly observed and computed flow using the MWBM and the DWBM. (Awash -Hombole)

Chapter 7

7 CASE STUDIES OF DAILY RAINFALL RUNOFF MODELS

7.1	Introduction	160
7.2	Models from literature.....	161
7.3	Application of the rainfall-runoff models.....	164
7.4	Comparison of the PDRRM with the 10 days and monthly models.....	173
7.5	Concluding remarks	175

7.1 Introduction

The aim of this chapter is to test the parsimonious daily rainfall - runoff model proposed in Section 3.4. The performance of the model is compared to three classical models, which have been applied to a number of catchments in the world. The three candidate models are XINANJIANG (XNJ) (Zhao *et al.*, 1980), SMAR (O'Connell *et al.*, 1970) and NAM (Danish Hydraulic Institute, 1982). The models are selected on the following merits:

- 1) Data requirement as of the available data, all of the models require time series of areal rainfall and evaporation and flow data for calibration.
- 2) The models have equal complexity in conceptualizing rainfall-runoff processes
- 3) The three models have been applied in dry regions before. (see Gan and Biftu 1996; Gan *et al.*, 1997)
- 4) All the model parameters are obtained by automatic optimization procedure.

The chapter begins with a brief description of the conceptual representation and parameters of the three models. The results of the three models and the newly developed model are then discussed. Finally the summary of comparison of the results obtained using daily and coarse time steps i.e. 10-day and monthly models are given. Four catchments (Awash - Melka, Awash-Hombole, Modjo and Berga), from Awash River Basin in Ethiopia are used as a test catchments. The discussion on the quality of data was given in Chapter 5.

7.2 Models from literature

7.2.1 The XNJ model

The XINANJIANG model (XNJ), developed in 1973, has been used to forecast floods flows to the Xinanjiang reservoir (Zhao *et al.*, 1980). Two distinct components are identified as for most of conceptual rainfall runoff models: 1) soil-level water balance and 2) the transfer to the closure section of catchments (Franchini and Pacciani, 1990). The XNJ model represents the soil level water balance components by four interconnected storages, the upper zone tension, the lower tension, deep zone tension and free water storages. Evaporation will take place at potential rate from upper zone and with reduced rate from lower storages. The model takes into account the variable area source concept through a probability distribution. The transfer to the closure is represented by direct overland flow, saturation overland flow, interflow and groundwater flow. A unit hydrograph is used for surface flow and linear reservoir for the base flow routing. The model has 15 parameters that are described in Table 7.1.

7.2.2 The Soil Moisture Accounting and Routing (SMAR) model.

SMAR was developed at the University of Galway (O'Connell *et al.*, 1970). The model assumes that the catchment is analogous to a vertical stack of horizontal soil layers which can contain various amounts of water. Similar to the XNJ, model the evaporation from the top layer occurs at potential rate. Evaporation from second layer occurs only on exhaustion of the

first layer, at the potential rate multiplied by a factor C (whose value is less than unity). On the exhaustion of the second layer, evaporation from third layer occurs at potential rate multiplied by C^2 . Thus a constant potential evaporation applied to the basin would reduce the soil moisture in a roughly exponential manner. Three inter-connected storages are represented: Surface storage, maximum of 5 layers of soil moisture storage and groundwater storage. The model simulates four components of flow: direct overland flow, saturation overland flow, interflow and groundwater flow. The model has 9 parameters that are described in Table 7.2.

Table 7.1 Description of XNJ model parameters (Zhao *et al.*, 1980)

Soil moisture phase	No.	Parameter	Description	Approximate range
Direct runoff	1	WM	Mean areal soil moisture capacity (mm)	30 - 300
Upper zone	2	X	Upper soil moisture storage capacity (mm)	0.0 - 0.5
Lower zone	3	Y	Lower soil moisture storage capacity (mm)	-
	4	KE	Evaporation coefficient	0.5 - 1.0
Upper zone	5	B	Tension water distribution index	0.05 - 0.2
	6	SM	Aerial free water capacity (mm)	0 - 40
	7	EX	Free water distribution index	0.0 - 2.0
	8	CI	Fraction of free water to interflow	0.0 - 1.0
	9	CG	Fraction of free water to ground water	0.0 - 1.0
	10	IMP	Impermeability coefficient	0.0 - 0.5
Lower zone	11	C	Deep layer evaporation coefficient	0.0 - 0.3
	12	KI	Interflow recession coefficient	0.5 - 0.9
	13	KG	Groundwater recession coefficient	0.95 - 1.00
	14	N	Parameter for linear reservoir	1 - 10
	15	NK	Number of time steps	1 - 10

Table 7.2 Description of SMAR model parameters (O' Connell *et al.*, 1970)

Soil Moisture Phase	No.	Parameter	Description	Range
Upper Zone	1	C	Evaporation	0.0 - 1.0
	2	Z	Total soil moisture capacity	50-500
	3	Y	Soil infiltration capacity	20-200
Direct Runoff	4	H	Direct runoff area index	0.0 - 1.0
Groundwater	5	T	Potential evaporation factor	0.0 - 0.0
	6	G	Groundwater runoff coefficient	0.0-1.0
	7	N	Parameter for linear reservoir	0.5-5.0
	8	NK	Number of time step [Parameter nk]	0.5-40
	9	KG	Number of time step groundwater K	5-200

7.2.3 The NAM model

The "Nedbor-Afstromnings Model" NAM (Danish Hydraulic Institute, 1982) is a deterministic, lumped conceptual rainfall-runoff model developed at the Technical University of Denmark. The model is a soil moisture accounting one, utilizing five different, mutually interrelated, moisture storages. The effects of snow are controlled by the temperature conditions. Surface storage is composed of interception and depression storages. The root zone is represented by the lower storage from which vegetation draws water for transpiration.

Rain and snow are subject to surface storage, evaporation and interflow. When maximum surface storage is reached, some of the excess water enters the stream as overland flow and the remainder infiltrates to the lower zone and groundwater. The groundwater recharge is divided into two storages, upper and lower with different time constants. The groundwater storage acts as a linear reservoir draining continuously to the stream as base flow. Overland flow and interflow are routed through one linear reservoir before all the streamflow components are added and routed through a final linear reservoir. The model has 15 parameters described in Table 7.3. For the present study the snow component is not relevant, hence the parameter corresponding to this process is set to zero.

Table 7.3 Parameters of the NAM model (Ref. Danish Hydraulic Institute, 1982)

Soil moisture phase	No.	Parameter	Description	Range
Direct runoff	1	UMAX	Upper zone storage capacity (mm)	1 - 100
	2	LMAX	Lower zone storage capacity (mm)	20 - 500
	3	CMELT	Snow melt coefficient (mm/°C/day)	-
Upper zone	4	CQOF	Overland flow runoff coefficient	0.01 - 1.0
	5	CLOF	Overland flow threshold coefficient	0.0 - 0.8
	6	CQIF	Interflow drainage coefficient	1E-5 - 0.05
	7	CLIF	Interflow threshold coefficient	0.0 - 0.95
Lower zone Ground-water	8	CLG	Recharge threshold coefficient	0.0 - 0.95
	9	CBFL	Groundwater storage recharge	0.0 - 0.95
	10	CK1	Linear reservoir (1) routing constant	6 - 120
	11	CK2	Linear reservoir (2) routing constant	6 - 120
	12	CKBFU	Upper groundwater storage baseflow routing constant	100 - 4000
	13	CKBFL	Lower groundwater storage baseflow routing constant	200 - 9000
	14	CAREA	Permeability constant	1.0
	15	CEVP	Conversion factor from pan evaporation data to potential	0.5 - 1.0

7.3 Application of the rainfall-runoff models

7.3.1 Calibration of the models

With exception of limiting the memory of the unit hydrographs for the flow routing component, all the parameters are obtained by optimization. The five to six years of available data are divided in to two parts to serve as calibration and verification periods as shown in Table 7.4.

Table 7.4 Calibration periods

Catchment	Calibration Period 1	verification Period 2
Berga	1986-1987	1988-1990
Modjo	1985-1987	1988-1989
Awash - Melka	1985-1988	1989-1991
Awash -Hombole	1985-1987	1988-1990

As described in the previous sections the number of model parameters are large for the three models. The optimum values are obtained by automatic optimization of the sum of squares of

errors of square root transformed daily observed and model calculated flows. The optimum parameters for the four models are given in Table 7.5 through 7.8.

Table 7.5 Model parameters: The XNJ Model

No.	Parameter	Catchments			
		Berga	Modjo	Awash M.	Awash H.
1	WM	99.458	407.8	461.0	462.6
2	X	0.125	0.237	0.080	0.128
3	Y	0.331	0.930	0.904	0.640
4	KE	0.599	0.977	0.926	0.925
5	B	0.500	1.804	0.877	1.979
6	SM	20.438	2.229	0.000	7.917
7	EX	1.906	0.131	1.775	1.970
8	CI	0.080	0.246	0.909	0.045
9	CG	0.577	0.020	0.091	0.001
10	IMP	0.173	0.046	0.106	0.132
11	C	0.187	0.114	0.085	0.280
12	KI	0.900	0.509	0.506	0.500
13	KG	0.917	0.700	0.510	0.501
14	N	1.000	1.202	1.236	1.001
15	NK	7.775	6.094	9.137	6.294

Table 7. 6 The SMAR Model parameters:

No.	Parameter	Catchments			
		Berga	Modjo	Awash M.	Awash H.
1	C	0.512	0.934	0.917	0.999
2	Z	274.9	398.1	367.4	380.0
3	Y	167.221	105.4	135.1	101.0
4	H	0.551	0.216	0.587	0.629
5	T	0.695	0.714	0.850	0.638
6	G	0.441	0.609	0.812	0.006
7	N	0.502	0.775	0.718	0.702
8	NK	11.302	39.149	23.58	39.61
9	KG	31.707	199.99	156.11	141.73

Table 7. 7 Model parameters: The NAM Model

No.	Parameter	Catchments			
		Berga	Modjo	Awash M.	Awash H.
1	UMAX	3.120	55.2	30.8	8.947
2	LMAX	281.5	587.3	599.997	446.9
3	CMELT	2.000	2.000	2.000	2.000
4	CQOF	0.503	0.321	0.564	0.860
5	CLOF	0.391	0.000	0.000	0.015
6	CQIF	0.036	0.049	0.036	0.036
7	CLIF	0.432	0.730	0.797	0.803
8	CLG	0.000	0.326	0.137	0.108
9	CBFL	0.266	0.950	0.493	0.582
10	CK1	72.99	95.97	110.72	84.99
11	CK2	10.45	6.24	101.61	85.83
12	CKBFU	407.3	3645	147.7	100
13	CKBEL	5688.4	8999	8988.	8993
14	CAREA	1.0	1.0	1.0	1.0
15	CEVP	0.732	0.874	0.816	1.000

Table 7.8 Model parameters: The PDRRM

No.	Parameter	Catchments			
		Berga	Modjo	Awash M.	Awash H.
a_1	Evaporation	0.023	0.045	0.023	0.028
a_2	Percolation	0.065	0.0042	0.032	0.037
a_3	Interflow	0.0011	0.0005	0.0012	0.0011
a_4	Upperlimit	402.2	896	764.	709.0
a_5	recession	0.069	0.012	0.02	0.010
a_6	k-fast flow UH	1.00	1.01	1.01	1.01
a_7	k-base flow UH	1.20	1.5	2.69	2.05
	Max. correlation	0.86 (a_1, a_2)	-0.82(a_2, a_3)	-0.67 (a_2, a_3)	-0.62($a_2 a_3$)

7.3.2 Comparison of performance of the models

To compare the performance of the models, the Root mean Squares Errors (RMSE) and Bias of residuals are used in addition to the Nash-Sutcliffe model efficiency. The two former indices are widely used in comparison of daily rainfall runoff models. The RMSE is defined as:

$$RMSE = \sqrt{\frac{\sum_{t=1}^n (d_t - q_t)^2}{n}} \quad (7.1)$$

and the Bias of residuals is calculated as:

$$Bias(\%) = \frac{\sum_{t=1}^N (d_t - q_t)}{\sum_{t=1}^N d_t} 100 \quad (7.2)$$

where:

q_t = observed daily flow (mm)

d_t = model computed flow (mm)

N = total number of data points used for calibration or verification.

Since the root mean square is function of the magnitude of the observed flows, only results obtained by different models when applied to the same catchment and for the same period can be compared. The requirement of a good model is to obtain a small root mean square error as much as possible. The bias and efficiency indices allow comparison of model performance when applied to various ranges of catchments. Positive values of the bias indicate over estimation, whereas negative values indicate under estimation of flows.

The model parameters listed in Section 7.3.1 are used to estimate the flows during the calibration and verification periods. Table 7.9 summarises the statistical indices of the four models applied to four catchments. From Table 7.9 it is clearly seen that except for Modjo catchment, all the models resulted with small biases ranging from 2%-7% for the calibration period. Unfortunately this performance is not maintained when the model is used for the period that has not be used for calibration. This can be seen from the scatter plot of observed and estimated flow for the Awash- Hombole (Figure 7. 1).

Table 7.9 Comparison of statistics of the studied models

Catchment	Calibration			Verification		
	Bias %	RMSE (mm)	Ef. %	Bias %	RMSE (mm)	Ef. %
XNJ						
Berga	-4	0.99	68	-39	1.47	25
Modjo	-3	1.25	17	38	2.09	11
Awash M.	-2	0.35	80	5.9	0.58	51
Awash H.	-2	0.33	82	5.8	0.49	77
SMAR						
Berga	3	0.91	69	-9	1.26	20
Modjo	28.	0.85	5	-39	1.58	5
Awash M.	7	0.31	83	17	0.49	59
Awash H.	-1.0	0.23	82	12	0.57	72
NAM						
Berga	-6	0.93	71	-20	1.55	16
Modjo	32	0.23	54	33	0.56	17
Awash M.	2	0.34	81	22	0.61	46
Awash H.	2	0.31	84	-7	0.5	76
PDRRM						
Berga	-3	1.02	56	6	1.19	50
Modjo	-17	1.68	21	25		12
Awash M.	-6	0.47	74	12	0.53	58
Awash H.	-5	0.41	78	7.5	0.54	75

The scatter plots are fairly evenly distributed along the 45-degree line, which shows the fit of the observed and estimated flows for the calibration period. However for the verification period, the scatter plots are widely spread which shows poor representation of the hydrograph.

The above observation is confirmed by the reduction of the RMSE and the Efficiency of each model from the calibration to verification periods. According to the three indices and to the graphical comparisons of the flow hydrographs, the three models (XNJ, SMAR and NAM) have well reproduced the flows for the calibration periods for the Awash River at Hombole and Melka Kuntre. Berga River is also not badly modelled. The result of modelling the Modjo River shows an extremely low performance for all the models.

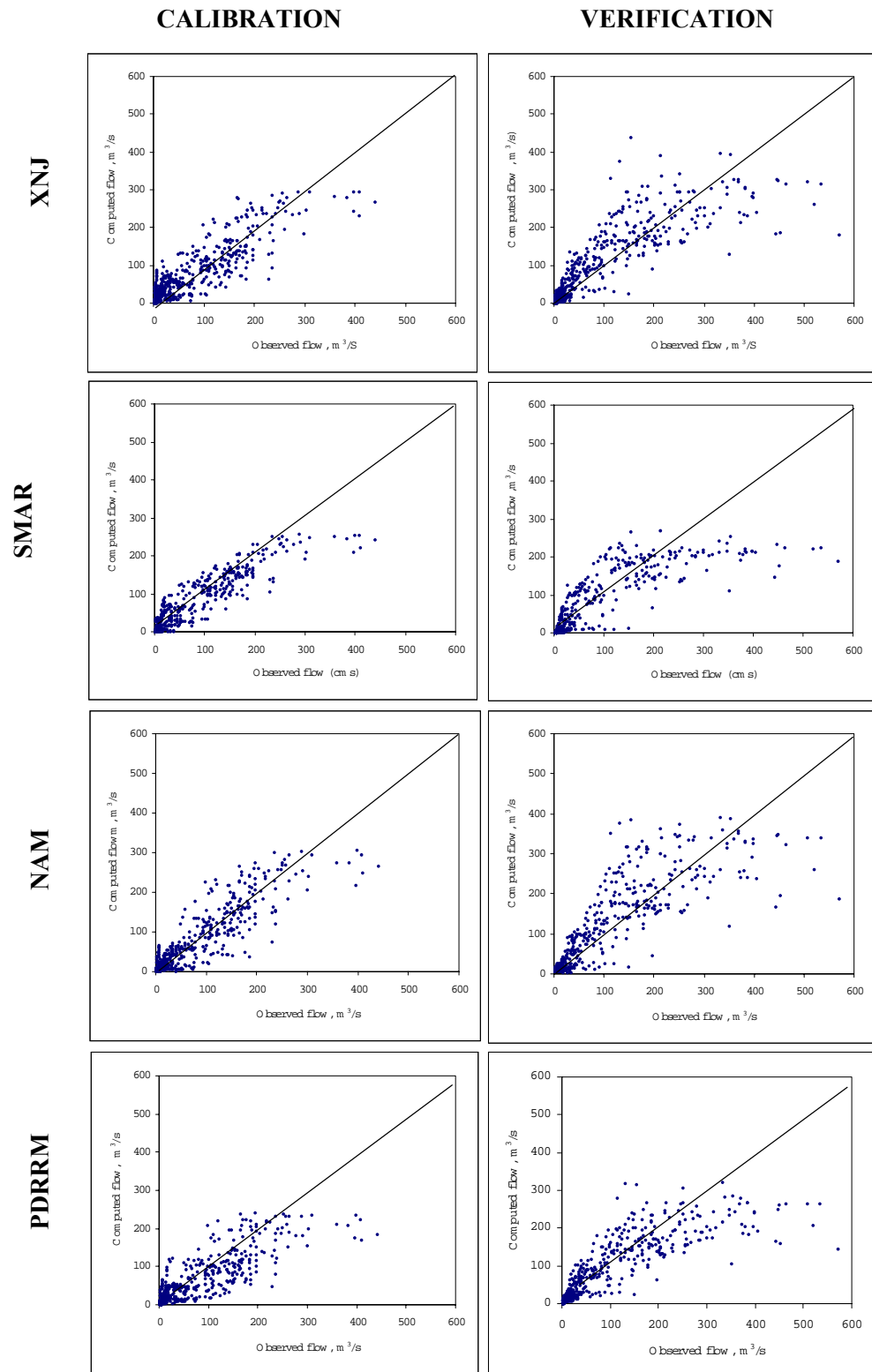


Figure 7. 1 A comparison of scatter plots of the observed and computed flow for the four models (Awash River at Hombole).

The possible explanation for this catchment is the poor quality of data. It has been mentioned in section 5.2 that the flow of Modjo River is questionable due to an inadequate rating curve.

Considering the statistic indices and the scatter plot of the residuals, and excluding the Modjo catchment, the PDRRM shows a lesser efficiency for the calibration periods. Nevertheless the difference is not that significant. For example the efficiency of XNJ model for the Awash-Hombole is 82% while for PDRRM the efficiency is 78%. It can also be seen that the PDRRM model has maintained the performance of the model for verification period, which is not always the case for the other models.

For the purpose of investigating the efficiency of the model in reproducing various flow regimes a typical hydrograph of Awash-Hombole for the year 1986 is compared with the flows estimated by the four models (Figure 7.2). From this comparison, we observe that all the models have attempted to follow the trend of the observed hydrograph. For this particular hydrograph it appears that the rising limb of the hydrograph and the high flows are well modelled. There is an over estimation of the low flows, because of some local peaks that resulted from short storms during the dry season. The recession limb of the hydrograph is also where one observes discrepancies. From calibration point of view and looking into the statistics and the comparison of hydrographs the XNJ model is found to be slightly better than the other models considered.

The PDRRM, in general was able to reproduce well the hydrographs in low and high flow regimes. It should be mentioned that the model under estimates the peaks for almost all the catchments and there is a trend of smoothening erratic daily flows. Figure 7.3 and Figure 7.4 show a comparison of the estimated flow hydrographs for the Awash-Melka and Berga catchments respectively. Like for the other three models, the Modjo catchment was not modelled with acceptable efficiency. It should also be remembered that the model structure used are first tested on a rather larger time steps, further application to other catchments and verification are necessary.

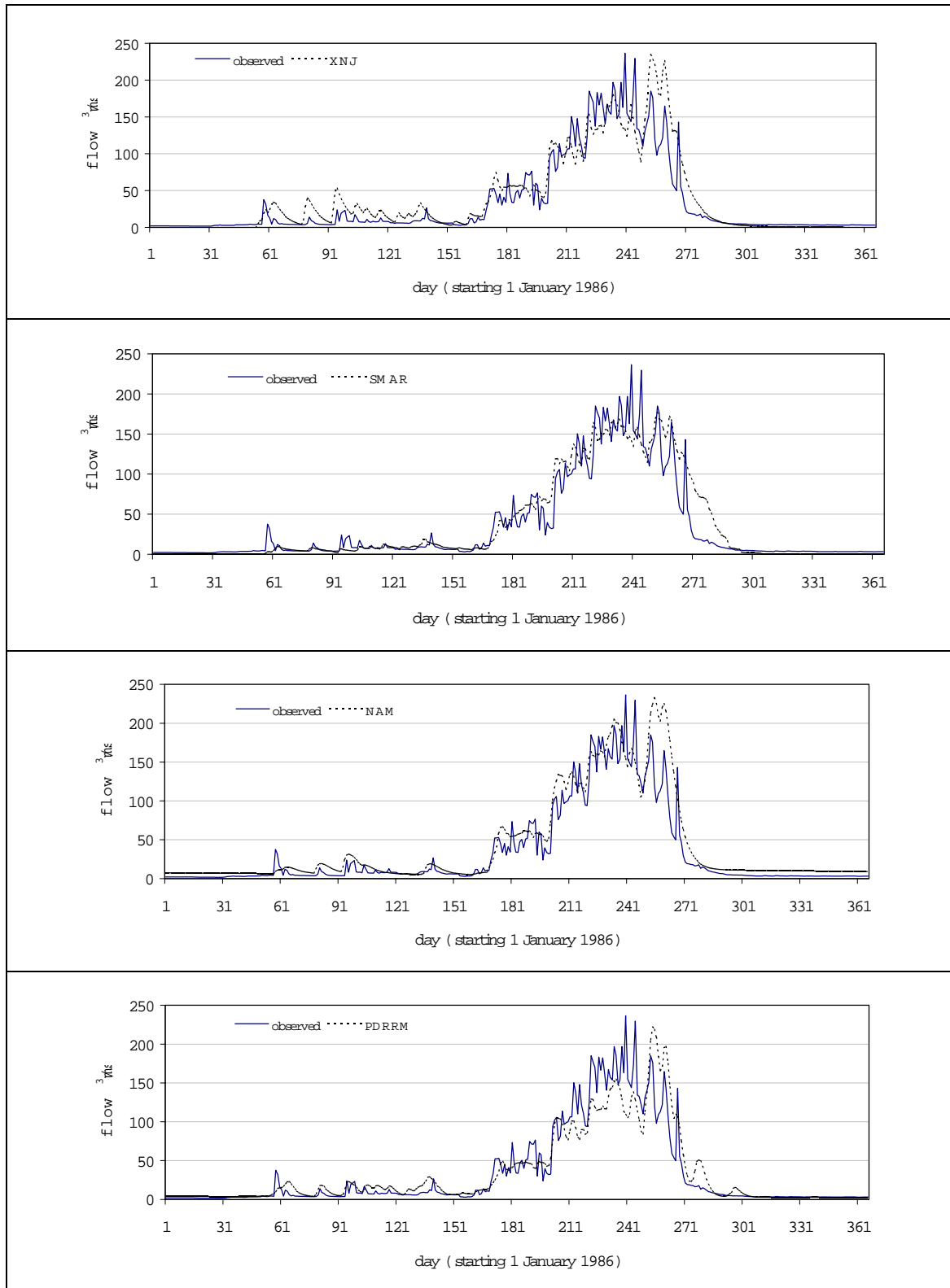


Figure 7.2 Comparison of observed and computed hydrographs for the Awash-Hombole catchment. (Typical year 1986.)

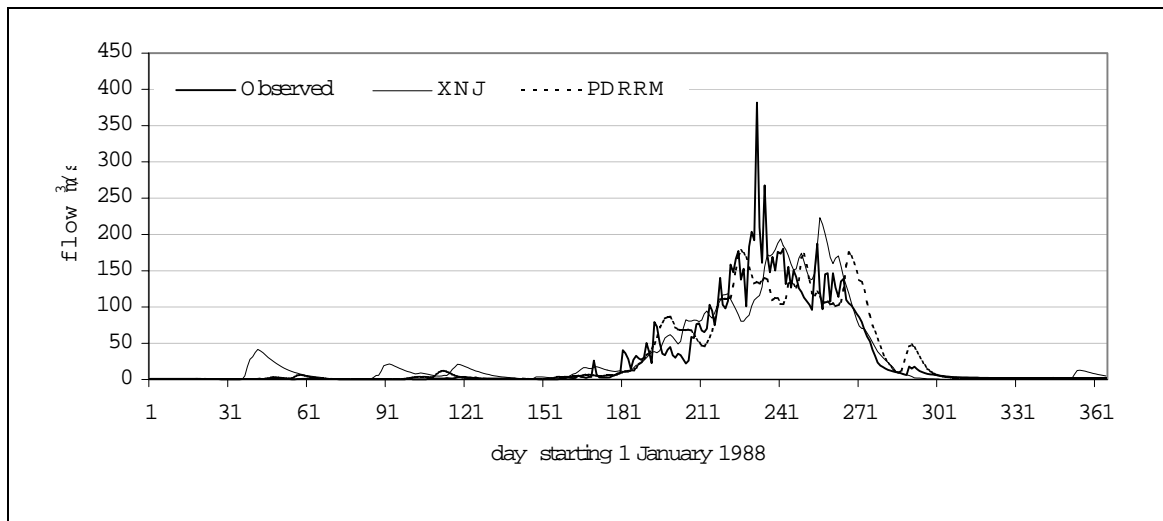


Figure 7.3 Comparison of observed and estimated flows for Awash-Melka catchment

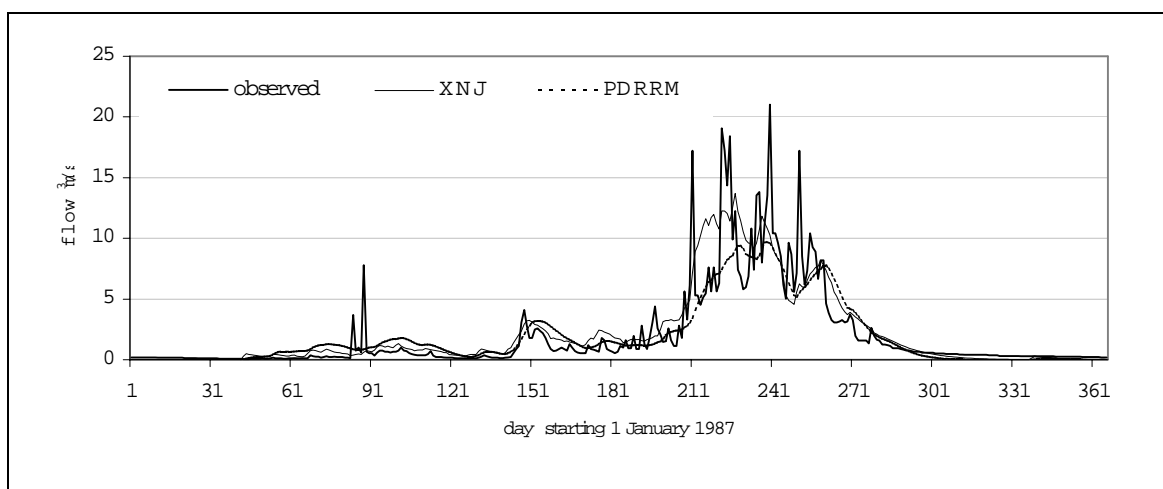


Figure 7.4 Comparison of observed and estimated flows Berga catchment

7.4 Comparison of the PDRRM with the 10 days and monthly models

In chapter 5 and chapter 6, we have reported that simple models are capable of modelling rainfall-runoff relationship at monthly and 10-day time steps. The question that may be asked is that whether shorter time step modelling is beneficial in applications, which require 10-day or monthly flows? An example of such applications is flow extension for reservoir design. The argument is not to undermine the necessity of the short time step modelling, because in applications such as flood forecasting one can not surpass the short time steps models. The problem is mainly that the short time step requires detailed data and the quality of the data is also very important to calibrate these models. For 10-day and monthly time step it is commonly believed that the individual daily errors tend to compensate one another unless there are systematic errors. Moreover some inputs such as potential evaporation are readily available on monthly basis.

Following the above argument, a catchment is modeled using the three time steps. The daily flows estimated by the PDRRM is aggregated to give the 10-day flow to compare it with flows that are estimated by the DWBM. Similarly the 10-day flows obtained by the DWBM and those aggregated from daily model are again grouped on monthly basis to compare them with the estimate of monthly water balance model.

These analyses show that the daily model is only slightly better than the 10-day time step modelling in reproducing the long-term seasonal flows. Both models underestimate the high flow regime and it is observed that the water balance is compensated by a slight over estimation of the recession limb (Figure 7.5). Comparing the mean monthly flows obtained by the PDRRM, the DWBM and MWBM, surprisingly, the MWBM shows the best fit to the mean seasonal flows (Figure 7. 6). The model efficiencies on monthly flow representation for the catchment considered is (90%, 89%, 90%) for MWBM, DWBM and PDRRM respectively.

The implication of this finding is that, given the problem at hand one should start with the simple and larger time step model. The shorter time step models are recommended for those applications, which requires shorter time step and also in cases where reliable and good quality data are available.

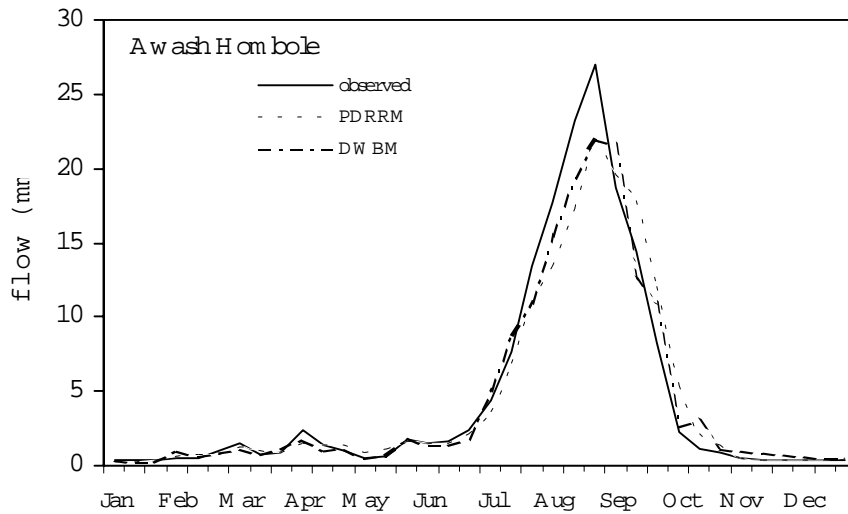


Figure 7.5 Comparison of the daily rainfall-runoff and the 10-day water balance models (Awash-Hombole)

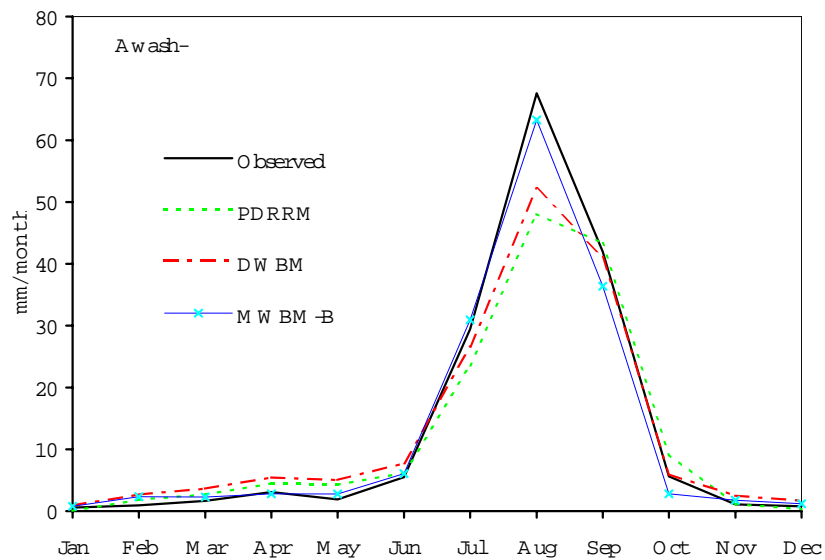


Figure 7.6 Comparison of the daily rainfall-runoff, the 10-day and monthly water balance models (Awash-Hombole)

7.5 Concluding remarks

From the results of calibration of the models the following conclusions can be made:

- 1) Among the four considered models (XNJ, SMAR, NAM and PDRRM) tested on four semi -arid catchments, the XNJ model performs the best for the calibration period considered.
- 2) For all the models, it was observed that the efficiency reduces when the models are applied to a verification period. During the verification period, all the models performed equally well (or bad).
- 3) The results of the PDRRM show that, though the quality of the model is somewhat less than for the other models tested (with more parameters), the general reproduction of the hydrograph is promising. It is the author's opinion that with few refinements of the structure of the model, the performance of the model can be improved.
- 4) Regarding the time step of modelling, it is found that, if the application requires seasonal flows, the first model to try is the monthly water balance model.

Chapter 8

8 PRACTICAL APPLICATION OF THE DEVELOPED MODEL

8.1	Introduction	176
8.2	Influences of the variability of rainfall on flow regimes	179
8.3	Low flow - duration - return period curves	186
8.4	Reservoir capacity design.....	188

8.1 Introduction

In order to make decisions for planning, design and control of water resource systems long runoff series are required. The latter are not often obtained with reasonable length. However, rainfall observations are relatively long. In this chapter, the monthly water balance model is used to extend flow data of a catchment to study long-term influences of variability of rainfall on runoff, development of low flow duration curves and preliminary reservoir capacity design.

For the reason of availability of data, the Awash River basin is used. (See section 5.2 for description of the catchment). The present study focuses only on the water head area of 7560 km² upstream of Hombole. In this sub catchment, a minimum human interference such as dams and diversions on the river flow regime is anticipated. Five rainfall stations with concurrent data length (1980 - 1995) were used to calculate the areal rainfall (Figure 8.1). The station at Addis Ababa has a longer record of rainfall (1900-1995). To assess whether the use of the longer data series of Addis Ababa station is justifiable, the correlation of the calculated areal rainfall and main station is analyzed. Areal monthly rainfall computed using the mean of the five stations and rainfall series at Addis Ababa are well correlated (Figure

8.2). Therefore the rainfall station of Addis Ababa is considered as an index station for further investigation of the temporal variability of the rainfall over the catchment. The linear equation obtained is $R_{area} = 0.794R_{AddisAbaba}$ with a coefficient of determination $R^2 = 0.9$. This equation is used to extrapolate the areal rainfall from the observed data of Addis Ababa.

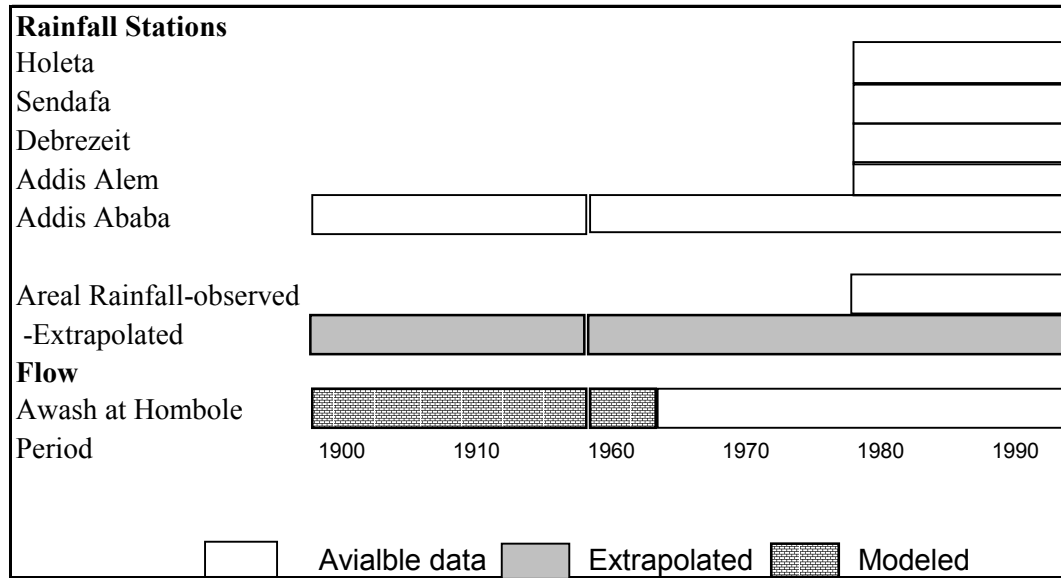


Figure 8.1 Schematic representation of extension of flow.

A monthly water balance model developed in section 3.2 is applied to reconstruct the long-term record of flows from the observed rainfall series. The model requires monthly rainfall, potential evaporation and river flow as inputs. The areal rainfall data obtained from the Addis Ababa rainfall is used. Mean monthly evaporation data at Addis Ababa for the years (1988 and 1987) were available. Due to the fact that evaporation in such region is mainly controlled by the available water, the long-term changes of the potential evaporation over the whole period of simulation may not greatly influence the rainfall run-off processes. Hence, the constant seasonal variation of evaporation is used throughout the simulation period.

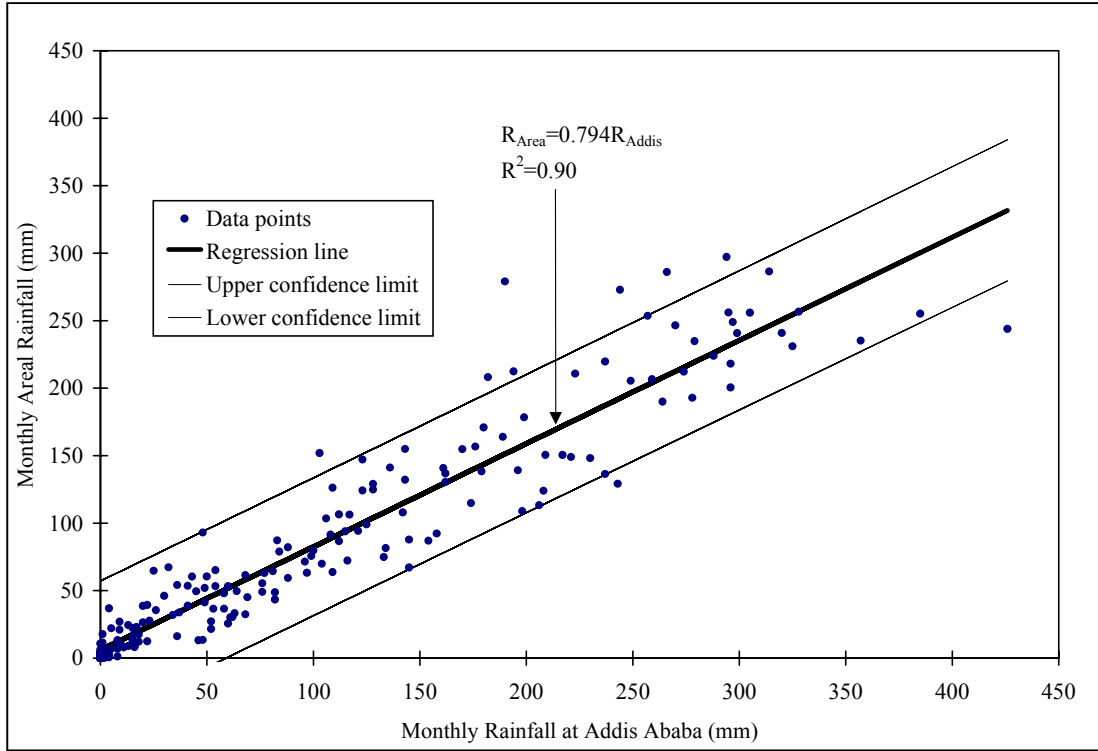


Figure 8.2 Relationship between areal and Addis Ababa monthly rainfall (R^2 is coefficient of determination).

Monthly river flow data of the Awash River at the Hombole gauging site for the years 1963-1992 are used to calibrate the model. The optimum parameters obtained previously in chapter 5 (see section 5.3.7) are used for reconstructing the flow series corresponding to the historical rainfall series. It is further assumed that the catchment characteristics have not altered greatly. Therefore, the parameters are assumed to be time invariant and, consequently, the monthly flows series of the years (1900-1992) is simulated for the analysis in the following sections. Figure 8.3 shows the comparison of the annual historical rainfall and reconstructed flows. One can see good agreement for the segment of the time series where both calculated and observed flows are available (1963-1992).

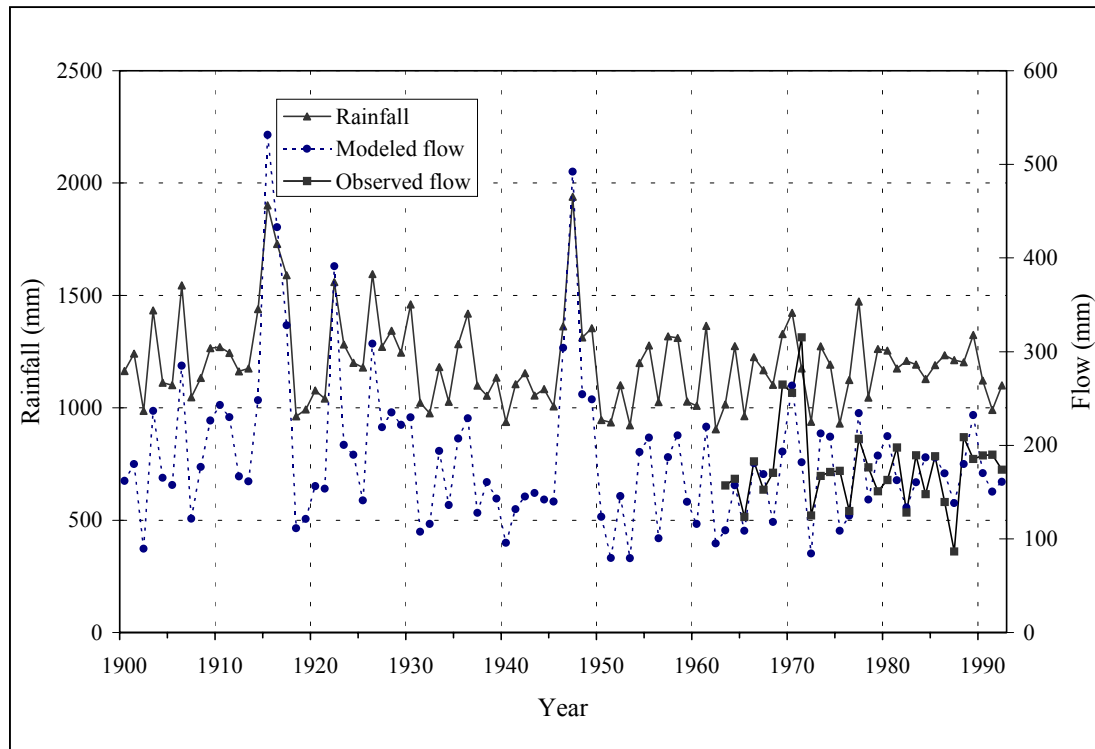


Figure 8.3 Time series comparison of long-term rainfall series and modeled annual flows

8.2 Influences of the variability of rainfall on flow regimes

8.2.1 Introduction

Rainfall variability due to climatic change has remained a concern to hydrological science. Globally one may see two types of rainfall variability: the continuous decline of the amount of annual rainfall (e.g. West Africa since 1960s) and recursive anomalies of annual rainfall (e.g. East and North East of Africa). From hydrological point of view each variability has a different magnitude of influence on the water resource system of a region or a catchment. In this study we investigate the link between the variability of annual runoff and the corresponding annual rainfall and flow regimes by using a water head catchment of the Upper Awash River Basin located in central Ethiopia.

From the annual rainfall record of this century, researchers have shown that there is a shift of the mean annual rainfall in Northeastern Africa since the last half of this century. Seleshi

(1996) reported that there is a decline of mean summer rainfall over this region since the mid of 1960s, which has also been observed for the Sahel regions. Comparing the data of the Blue Nile catchment for two 20 years windows (1946-1965) and (1965-1984) Conway & Hulme (1993) estimated that there is 18 percent of reduction of the mean annual flow corresponding to 8 percent reduction of the annual mean rainfall in the second 20 year period. From analysis of 5 and 10 years moving average of the flow of the Blue Nile at Dongola, Misganaw (1989) asserted that there is a general trend of decline of the annual flows after mid 1960s'.

Due to the high local variability of the rainfall and to the limited number of observations over the large area of a basin like the Blue Nile, it is always difficult to precisely determine the degree of influence of the anomaly of rainfall on the flow regimes. In the present study, a medium size catchment is selected from the central part of Ethiopia with fairly distributed rainfall stations. Because of the limited years of record of runoff (30 years), extension of flow data is achieved through rainfall-runoff modelling of the catchment. It is evident that the decline of the annual rainfall amounts is echoed to the annual flows. However it is important to know the extent of the influences and to study the variability of flow regimes caused by the temporal variability of rainfall on seasonal basis. Hence monthly rainfall and flow data are analyzed to obtain a clearer link between the two variables.

8.2.2 Annual rainfall variability

From the rainfall record at Addis Ababa station, it can be stated (with the exception of the decade of 1930's) that the first half of the twentieth-century has experienced higher rainfall amounts than the second half. The lowest rainfall on the decade basis was observed during the 1950s. The lowest annual rainfall (904 mm) was observed in 1962. From Table 8.1, one can see that there is a persistence of the lower annual mean values during the years after 1960. The linear and polynomial trends fitted to the rainfall and runoff series resulted with a statistically insignificant coefficient of determination ($R^2=0.023$ and 0.004) respectively. However the 5 and 10 years of moving average curves confirms the general decline of the amount of flow and rainfall (Figure 8.4 and Figure 8.5).

Table 8.1 Rainfall Variability during the last 9 decades based on Addis Ababa observations. (+) and (-) indicate values above and below long term mean respectively.

Period	Annual Rainfall (mm)	Summer Rainfall (mm)	Period	Annual Rainfall (mm)	Summer Rainfall (mm)
1901-1910	1213 (+)	886 (+)	1951-1960	1112 (-)	787 (-)
1911-1920	1327 (+)	981 (+)	1961-1970	1176 (-)	807 (-)
1921-1930	1317 (+)	951 (+)	1971-1980	1166 (-)	854 (-)
1931-1940	1113 (-)	803 (-)	1981-1990	1198 (-)	800 (-)
1941-1950	1231 (+)	933 (+)			
Long term Mean (1900-1995) Annual = 1203 mm Summer= 864mm					

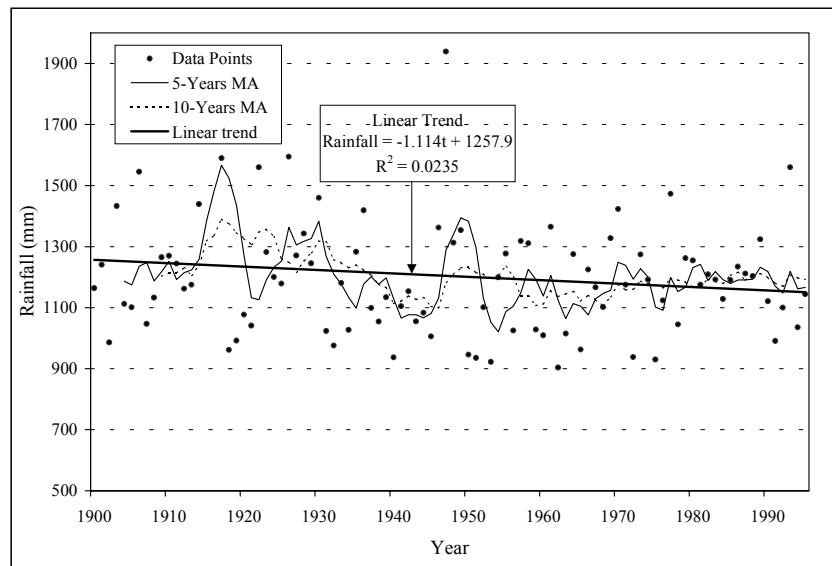


Figure 8.4 Annual variability of rainfall at Addis Ababa station.

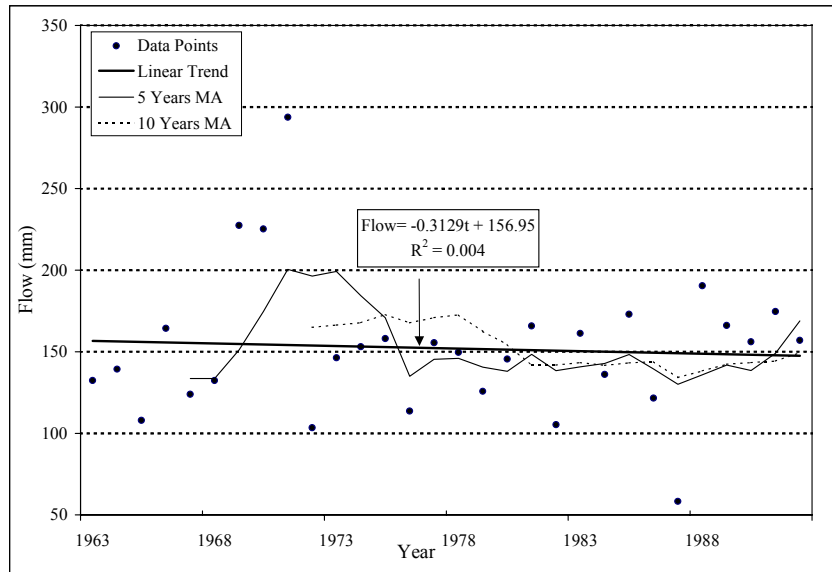


Figure 8.5 Annual variability of Awash River flow at Hombole

8.2.3 Influence of rainfall timing on flow regimes

The correlation coefficient between the annual areal rainfall and the reconstructed flow is 0.6, which indicates that mere annual magnitude anomalies of rainfall can not fully explain the effect on the total generated flow. Hence it is useful to dissociate the rainfalls in to seasons, to study the influence of the timing and length of the rainy season on the flow regimes. It can be argued that in regions with long dry periods, the first arrival of rain on bare soil will generate high flows and leaves little or no water for groundwater supply. Consequently, smaller or no base flow will occur during the non-rainy season. A more favorable condition for higher flow is when there is intense rain during the last days of the rainy season when the upper soil is saturated.

From the cross correlations of monthly rainfall and summer runoff (Table 8.2), it is observed that the rainfall of June is more important than the July rain. The explanation is that the first arrival of rain determines the losses. The most significant cross correlation of monthly rainfall with the summer flow is obtained for the August rainfall. The interpretation is that in August, there is a higher opportunity of flow generation (even for small storms) since the catchment is already moist and the losses are minimal. The total summer rainfall is also well correlated

with the summer flow (correlation coefficient $r = 0.73$). On the other hand, the individual monthly rainfall and also the total summer (June-September) rainfall less influence the low flow regime (November-February), due to fast response of the catchment.

Table 8.2 Cross correlation coefficients of rainfall and flow regimes: Underlined values show significant correlation at 95 % confidence limit = ± 0.2)

Flow regimes	Rainfall					
	June	July	August	September	October	Summer
Summer flow (June-September)	<u>0.43</u>	<u>0.36</u>	<u>0.63</u>	<u>0.46</u>	-0.05	<u>0.73</u>
Low flow (Nov. – February)	-0.01	0.14	0.04	0.16	<u>0.21</u>	0.11

8.2.4 Influence of long-term rainfall variability on flow regimes

The reconstructed annual mean flows of the second half of the century are observed to be below the long-term mean which is consistent with the rainfall variability. It is also noted that there is an amplification of the variability of the flow, especially for the summer flows. For example in the 1950s there was a departure of the flows of 25 % from the long term mean (163 mm), corresponding to only 10 % departure of rainfall from the long term mean (1200mm) (Figure 8.6 and Figure 8.7). On the other hand, during the same decade the base flow component has shown only a departure of 10 % from long term mean of (25 mm) and the annual low flow has only a departure of 7 % (Figure 8. 8). Moreover, the base flow and annual low flow (November-February) does not show high variability during the whole period of analysis.

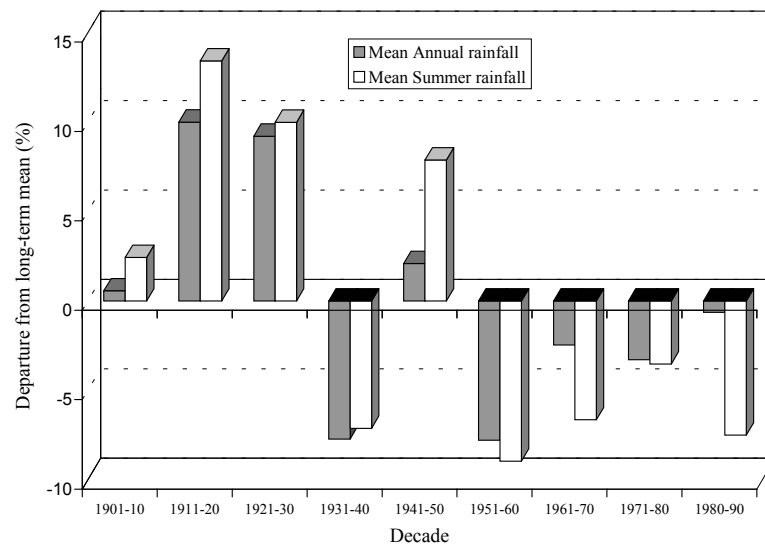


Figure 8.6 Departure of annual and summer rainfall from long term means on decade basis.

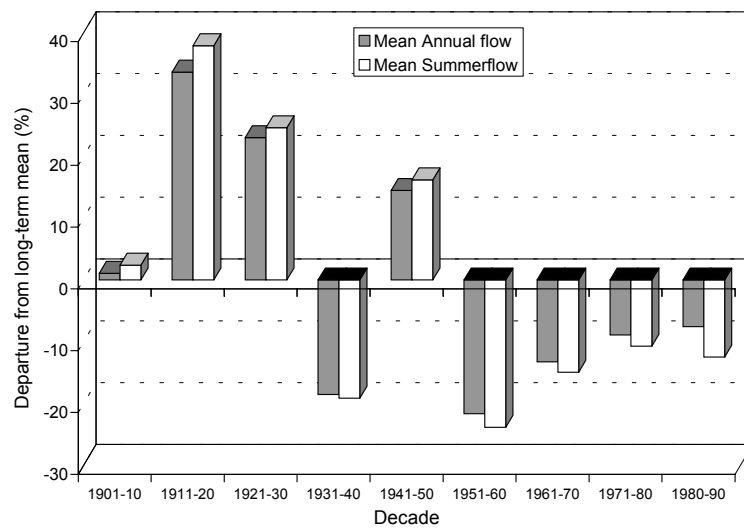


Figure 8.7 Departure of annual and summer flow from long-term means on decade basis.

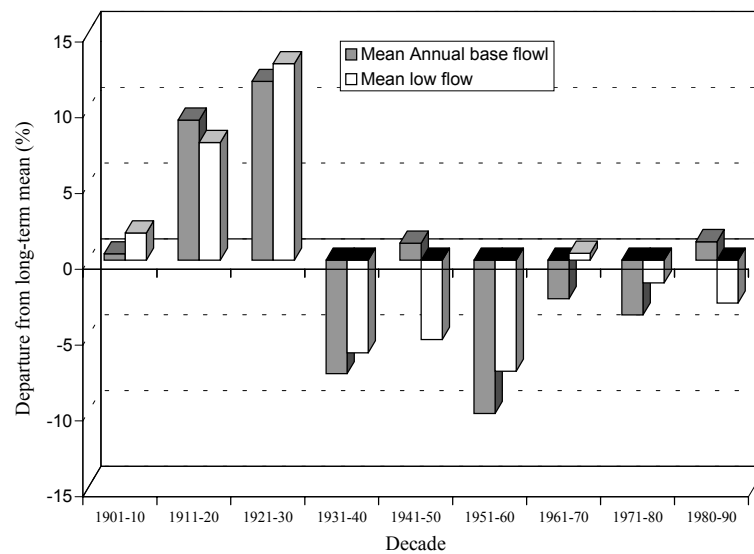


Figure 8. 8 Departure of annual base flow and low flow from long term means on decade basis.

8.2.5 Conclusions

From simple correlation analysis of the available data in the catchment, it is shown that the Addis Ababa rainfall station can be used as an index station to study the long-term temporal variability of rainfall over that upper Awash catchment. It has been observed that the mean annual and summer rainfall amounts have declined since the second half of this century and that this low mean is maintained up to the beginning of the 1990's. However, the linear trend of the decline is found to be not significant.

The study has also shown that the runoff variability is amplified compared to the rainfall variability. It is also demonstrated that the major flow regime (summer flow) is affected greatly by the low anomalies of rainfall and that the low flow, which is normally small, does not show large variation in this century. The analysis on the timing of rainfall showed that June rainfall is significantly important for the total summer flow to the river, though August rainfall is the most significant cause of high summer flows. It should be noted that this study is limited on the causality of rainfall on the flow regimes. Further influence of land use and vegetation cover changes on the flow regimes should be studied with more detail e.g. by means of distributed hydrological models.

8.3 Low flow - duration - return period curves

Low flow frequency analyses use data that are independent and homogeneous and therefore they can be used to determine the probability of occurrence of a flow event of specific magnitude. To obtain an independent series the annual minimum series are used for the analysis.

The procedure to obtain the curves is outlined below

- 1) From n years of monthly streamflow series, minimum flows with a given duration in each year are obtained and ranked with the lowest flow being ranked, $r = 1$.
- 2) The return period of a flow lower or equal to the lowest minimum flow is then n years and for minimum flow at rank r , it is equal to n/r years.
- 3) Flows and corresponding return periods then are plotted..
- 4) Similar curves can be plotted for other duration.

The low flow frequency analysis is performed on the observed flow series (1963-1992) and the extended series (1900-1995) for Awash River at Hombole. The extension of the flow series has allowed computation of higher return periods, which was not possible with the short observed time series. From the analysis it can be concluded that the Awash River at Hombole can cater a limited amount of supply without any regulation of the river. The river can supply at least about 3 and 2 million m^3 per month, with a failure frequency once in 10 and 100 years respectively (Figure 8.10 and Figure 8.9).

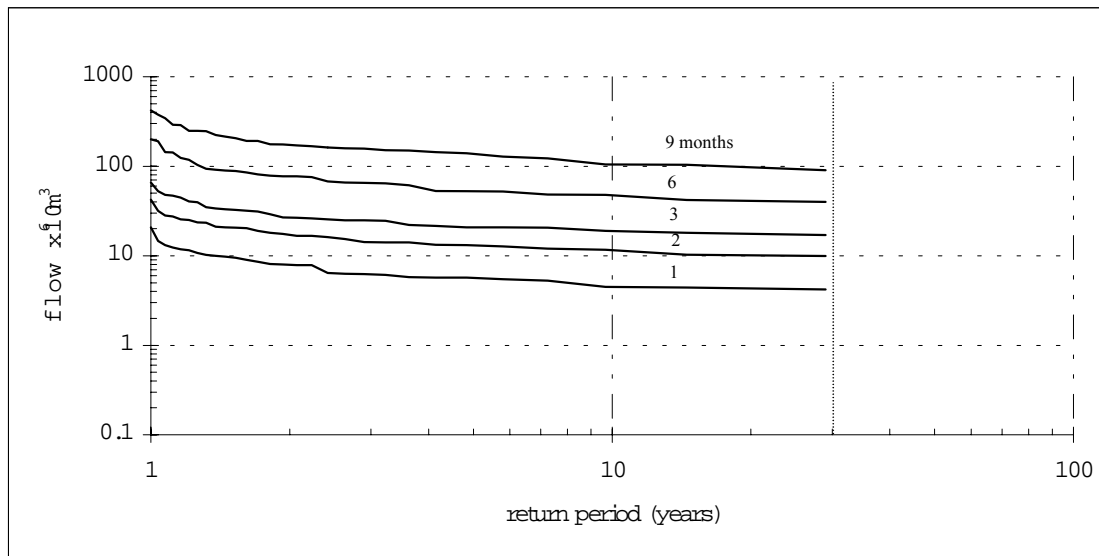


Figure 8.9 Low flow duration -return period relationships for Awash River at Hombole (1963-1992)

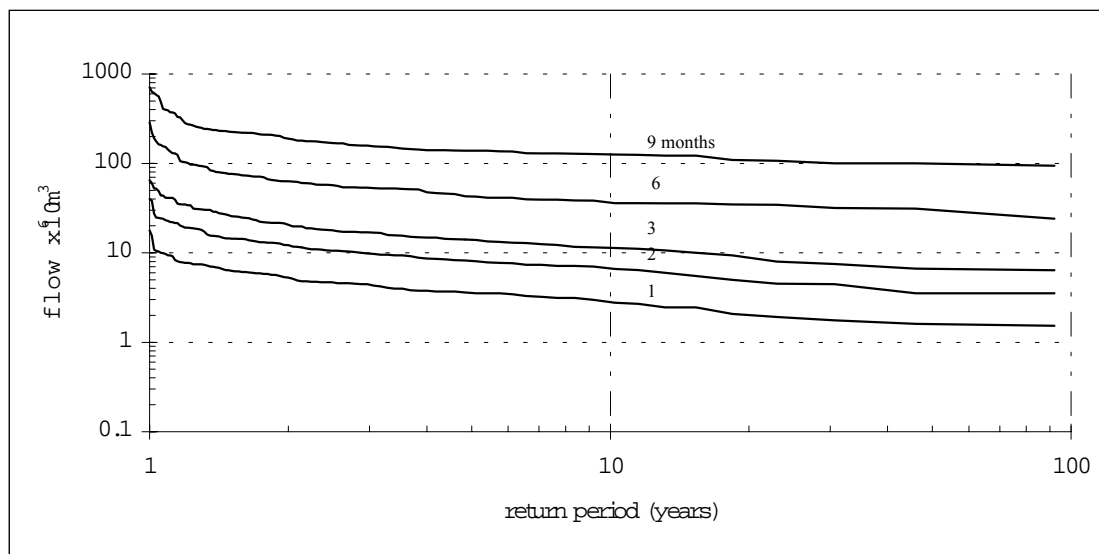


Figure 8.10 Low flow duration -return period relationships for Awash River at Hombole. (1900-1995)

8.4 Reservoir capacity design

McMahon and Mein (1978), give a comprehensive review and classification of most of the currently used reservoir capacity estimation procedures. A critical period defined as a period during which a reservoir goes from a full condition to an empty condition is used in this analysis.

Let S_t = the storage at the beginning of month t ,

K = the capacity of the reservoir,

D_t = the monthly demand and

Q_t = monthly flow,

where all the volumes are in the same units, for example million m^3 . Then the storage at the beginning of month $t+1$ is given as:

$$S_{t+1} = \max(S_t + Q_t - D_t, 0) + \min(0, K - S_t - Q_t + D_t) \quad (8.1)$$

The inflows are monthly river flows obtained from the rainfall of 93 years using the runoff model. In the above equation losses from the reservoir (such as evaporation) are assumed to be incorporated within the demand. Using the above recursive equation the evolution of the content of the reservoir can be computed for the flow series.

There is a shortage during month t whenever $S_{t+1} = 0$. Let s be the number of years amongst the total number of years N during which there is at least one month with shortage, then the estimate of the corresponding return period is given as:

$$R = \frac{N}{s} \quad (8.2)$$

and the inverse $F = 1/R$ is the probability of a shortage. The upper and lower boundaries of the 95% confidence interval are approximately (Vandewiele *et al.*, 1993)

$$\frac{F + \frac{(1.96)^2}{2N} \pm 1.96 \sqrt{\frac{F(1-F)}{N} + \frac{(1.96)^2}{4N^2}}}{1 + \frac{(1.96)^2}{N}} \quad (8.3)$$

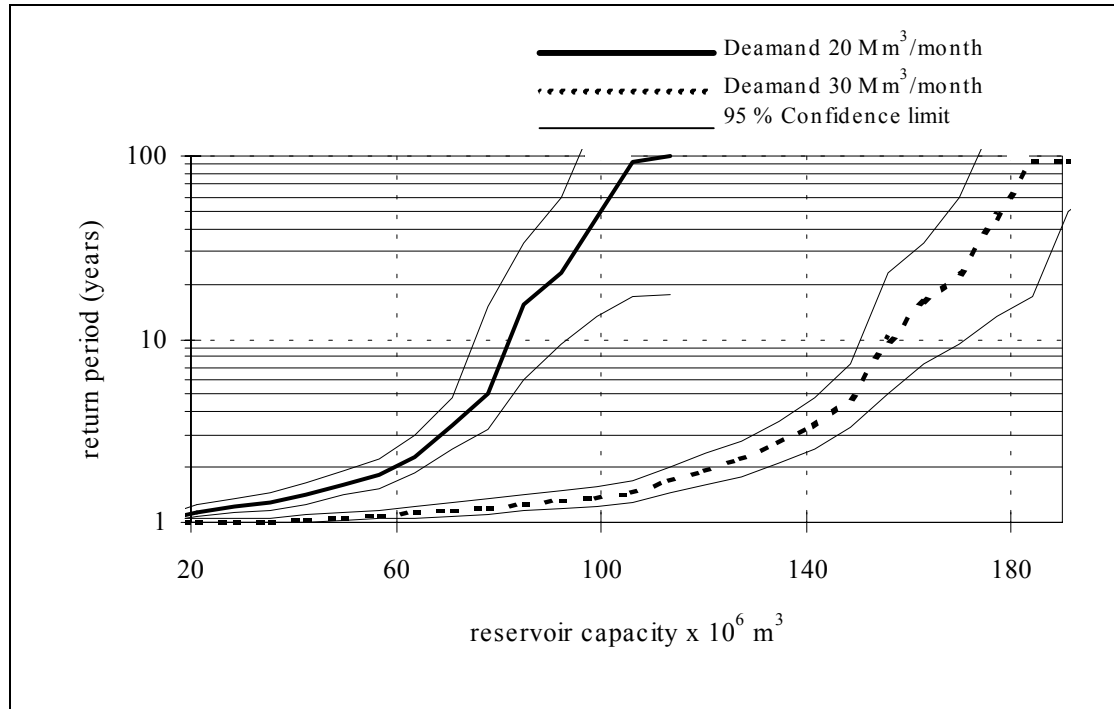


Figure 8.11 Return period versus reservoir capacity using the extended flow series for given demands. (Awash River at Hombole).

Two constant demands, (20 and 30 millions of m^3/month) are considered. Figure 8.11 shows some examples of the reservoir capacities required for the two demands considered, with corresponding return period of shortages for Awash River at Hombole. At this stage it may be noted that, in these figures, the axis of the reservoir capacity can easily be transformed into height of the dam required at a selected dam site which in turn is transformed to the investment required. Hence this relationship is really a very important tool in making decisions at the planning stage both in technical and economical aspects. Moreda, *et al.*, (1998) give similar relationships using long runoff records generated by stochastic pure runoff models.

Chapter 9

9 SUMMARY CONCLUSIONS AND RECOMMENDATIONS

9.1 Summary

The main aim of this research was to contribute to the conceptual rainfall-runoff modelling in regions with limited data. Three time steps (monthly, 10-dayly and daily) rainfall-runoff models were developed systematically and applied to different catchments. The models were coupled with two different optimization algorithms Shuffled Complex Evolution and VOA5A sequentially to efficiently obtain the model parameters and their relevant statistics. The conceptual monthly water balance models originally developed and tested for humid regions were applied to arid and semiarid cases. Modification of the structure of the model was necessary apropos to the temporal variability of the hydrological processes in the latter regions. More over it was shown that a particular representation of the evaporation term is justified and some of the discrete parameters were narrowed to a definite range of values, indicating the possible regionalization of the forms of the general equations governing the models. Based on the experiences on the monthly model, a 10-day water balance models was developed and tested. The concept was extended to develop a daily time step model.

9.2 Conclusions

The following conclusions may be specifically drawn from the development and application of the models:

9.2.1 Monthly water balance models

- For semi-arid and arid catchments considered, a warming up period of one to three year is sufficient to avoid the influence of initial soil moisture assumption.
- The model structure whereby the fast flow is expressed as a function of the average soil moisture index resulted with good agreement of observed and calculated flow for most of the catchment studied. Introducing an additional parameter such as an upper limit of the soil moisture index marginally improved the modelling in a few catchments only.
- Evaporation Equation IR=2 is best suited for the catchments.

$$\text{IR}=2 \quad r_t = \min[w_t(1 - e^{-e_t a_1}), e_t] \quad 0 \leq a_1 < 1$$

where r_t = actual evaporation e_t = Potential evaporation
 w_t = available water a_1 = evaporation parameter

- The discrete parameters for slow and fast flow equations can be set to $b_1=2$ and $b_2=2$.

$$\text{fast flow equation:} \quad f_t = a_3 \bar{m}_t^{b_1} n_t$$

$$\text{Slow flow equation:} \quad s_t = a_2 (\bar{m}_t)^{b_2}$$

where f_t = fast flow
 s_t = slow flow
 \bar{m}_t = soil moisture storage
 a_1, a_2 = slow and fast flow parameters

- No problems of local minima of the objective function were observed during the calibration of the parameters.
- The models well represent the rainfall runoff relationship for low flow and medium flow but may over or under estimate the exceptional peaks.
- The model parameters are not biased by the calibration period.
- The seasonal mean flow statistics are well preserved.

The result of the modelling of the study catchments is encouraging for practical applications such as extending and filling missing flow data for the periods where rainfall and evaporation are available, to obtain long-term flow data for water resource planning and management.

9.2.2 10 days water balance models

The present study shows that a relatively small number of parameters are sufficient to represent the rainfall-runoff relations in 10-day time steps. Further, it demonstrates that a routine devised to compute the recession coefficient is useful to incorporate *a priori* knowledge of a catchment in hydrological modelling. We believe that the approach of stepwise parameter optimization can be extended to daily rainfall runoff models by hierarchically determining parameters such as the recession coefficient from hydrograph analysis and evaporation parameters from long-term water balance models. This will ease the competition of numerous parameters in minimization the objective function in standard optimization procedures.

The comparison of performance the monthly water balance model (MWBM) with 10-day time step and the DWBM (10-day water balance models) suggests that the new 10-day model structure is as good as the previous monthly one. It is also more realistic as it incorporates more concepts in flow separation as well as flow recessions without increasing the number of parameters to be optimized.

9.2.3 Daily rainfall runoff models

The concept of a simple water balance model is extended to develop a parsimonious daily rainfall runoff model, PDRRM. The proposed model and three classical daily rainfall runoff models XNJ, (Zhao *et al.*, 1980), SMAR (O'Connell *et al.*, 1970) and NAM (Danish Hydraulic Institute, 1982) are applied to four semi-arid catchments from Upper Awash River Basin, Ethiopia. Preliminary results comparing the proposed model and three classical daily rainfall run-off models show that, though the quality of the PDRRM results are less than the classical ones, the general reproduction of the hydrographs of the four test catchments is promising. There is a quest for a parsimonious daily rainfall runoff model for flood forecasting and reservoir regulations in small catchments

9.2.4 Practical application of the models

The practical application of the monthly water balance model is demonstrated by extending the flow of the Awash River from the long meteorological records. The extended flows are used to study the influence of temporal rainfall variability on flow regimes, low flow analysis and reservoir capacity design. These analyses were not possible with the short river flow data.

The study on the influence of temporal rainfall variability on the flow regimes for the Awash River Basin during the period of 1900-1995 shows that there is an amplified variability of the annual flow compared to the rainfall variability. For example in the 1950s there was a departure of the annual flows of 25 % from the long term mean (163 mm), corresponding to only 10 % departure of rainfall from the long term mean (1200mm). The major flow regime (summer flow) is affected greatly by the low anomalies of rainfall and that the low flow, which is normally small, does not show large variation in this century. The influence of the on the timing of the rainfall on the flow regimes showed the amount of rainfall that arrives early in the rainy season (rainfall of the month of June), is significantly important for the total summer flow to the river. The August rainfall is the most significant cause of high summer flows.

From low flow analysis the Awash River at Hombole the flow - duration-return period curves were established. From these curves we conclude that the Awash River at Hombole can cater a limited amount of supply without any regulation of the river. The river can supply at least about 3 and 2 million m³ per month, with a failure frequency once in 10 and 100 years

respectively. The reservoir capacity curves, which are important at the feasibility study of water resources projects, were also established.

9.3 Recommendations

- For large catchment, there is a need for water balance modeling based on distributed input variable. Recent work on grid inputs includes e.g. the work of Conway (1997) dealing with a water balance of the Blue Nile.
- For 10-day and daily water balance models, groundwater level data could be incorporated to obtain optimum parameters by using a multi-objective global optimization procedure (Yapo et al. 1998).
- The daily model proposed should be verified with more case studies.
- Good quality data collection should always be encouraged. No model can be calibrated or even used without a good quality of data. The hydrology community should bridge the gap that is existing in the advancement of model development and the data acquisition. The latter is lagging considerably. In addition to the traditional ground observation of hydrometeorological variables derived from satellite images and radar technology can augment the data availability for water resources studies. Of course even these recent technologies can achieve certain goals if and only if they are well calibrated by ground observations.

REFERENCES

- Abayneh, B., 1992. Relationships between physical basin characteristics and parameters of a monthly water balance model, MSc. Thesis. Laboratory of Hydrology, VUB, Brussels, Belgium.
- Abbott, M.B., Bathurst, J.C., Cunge, J. A., O'Connell, P.E. and Rasmussen, J., 1986a. An introduction to the European Hydrological system - Syst \heartsuit m Hydrologique Europ \blacksquare en- "SHE". 1:History and philosophy of a physically based distributed modelling system. *J. Hydrol*, **87**: 45-59.
- Abbott, M.B., Bathurst, J.C., Cunge, J. A., O'Connell, P.E. and Rasmussen, J., 1986b. An introduction to the European Hydrological system - Syst \heartsuit m Hydrologique Europ \blacksquare en- "SHE" 2: Structure of a physically based distributed modelling system. *J. Hydrol*, **87**: 61-77.
- Alem, G., 1989. Monthly pure runoff model for the upper Awash River catchment in Ethiopia. MSc. Thesis, Laboratory of Hydrology, VUB, Brussels, Belgium.
- Alley, W. M., 1984. On the treatment of evaporation, soil moisture accounting and aquifer recharge in water balance models. *Waer Resour. Res.* **20**(11), 37-1149.
- Beven, K.J. and Kirkby, M.J., 1979. A physically based variable contributing area model of basin hydrology. *Hydrol. Sci. Bull.*, **24**:43-69.
- Beven, K.J., Lamb, R., Quinn, P., Romanwicz, R. and Free, J., 1995. TOPMODEL. In: V.P. Sigh (Ed.). Computer Models of Watershed Hydrology. Water Resources Publications, Highlands Ranch, CO, pp 627-668.
- Blaney, H. F. and Crddidle, W.D., 1950. Determining water requirements in irrigated areas from climatological and irrigation data. USDA *Soil Conserv. Serv.* TP - 96, 48pp.
- Bl -- schl, G. and Sivapalan, M., 1995. Scale issues in hydrological modelling: A review. In Scale issues in Hydrological modelling (ed) Kalma, J.D. and Sivapalan, M. John Wiley & Sons. p 9-48.

- Box, G.E.P. and Jenkins, G.M., 1976. "Time series analysis. Forecasting and Cotrol" Holden-day, San Francisco 543p.
- Burnash, R.J.C., 1995. The NWS river forecast system-catchment modelling. In: V.P. Sigh (Ed.). Computer Models of Watershed Hydrology. Water Resources Publications, Highlands Ranch, CO, pp. 311-366.
- Burnash, R.J.C., Ferral , R.L and McGuire , R.A., 1973. A general stream flow simulation system - Conceptual modelling for digital computers. Report by the Joint Federal State River Forecasts Senter, Sacramento, California.
- Chow, V.T., 1964. Hydrology of arid and semiarid regions. In Handbook of Applied Hydrology. 24-1 -24-42. McGrawhill Company. New York.
- Chow, V.T., Maidment, D.R. and Mays, L.W., 1988. Applied Hydrology, McGraw-Hill, New York.
- Clarke, R.T., 1973. 'Mathematical models in hydrology.' *Irrigation Drainage Paper* 19. FAO, Rome
- Conway, D. and Hulme, M., 1993. Recent fluctuations in precipitation and runoff over the Nile subbasins and their impact on main Nile discharge. *Climate Change* **25**:127-151.
- Conway, D., 1997. A water Balance model of the Upper Blue Nile, Ethiopia. *J. Hydrol Sci.* **42**(2) 265-286.
- Crawford, N.H. and Linsley, R.K., 1966. Digital simulation in hydrology. Stanford watershed model IV. Tech. Rep. No 39. Dep. Civ. Eng., Stanford University.
- Danish Hydraulic Institute, 1982. NAM Model Documentation. 82-892, JCR/Skn.
- Dawdy, D.R. and O' Donnel, T., 1965. Mathematical models of catchment behavior. *J. Hydraul. Di. Proc. ASCE*, HY4

- Demaree, G., 1982 Comparison of techniques for the optimization of conceptual hydrological models. *Mathematics and Computers in Simulation XXIV* pp.122-130. North-Holland Publishing Company.
- Dias, P.P.G., 1993. Monthly water balance models for basins in Sir-Lanka and West Africa. MSc. Thesis, Laboratory of Hydrology. VUB, Brussels, Belgium.
- Dooge, J.C.I., 1957. The method for estimating flood peak. *Engineering (London)*, 184:311-374.
- Dooge, J.C.I., 1973. The linear theory of the unit hydrologic systems. Tech. Bull. U.S. Dep. Agric., No. 1468, U.S. Gov. Print. Off., Washington, D.C.
- Duan, Q., Sorooshin, S. S. and Gupta, V.K., 1992. Effective and efficient global optimization for conceptual rainfall runoff models. *Water Resour. Res.*, **28**(4): 1015-1031.
- Dyck, S., 1983. Overview on the present status of concepts of water balance models, in: Van der Beken, A. and Hermann, A. (eds), *New Approaches in Water Balance Computations* (Proceeding of the Hamburg Workshop), IAHS publ. No.148, pp.3-19.
- Franchini, M., Galeati, G. and Berra, S., 1998. Global optimization techniques for calibration of conceptual rainfall-runoff models. *Hydrol. Sci. J.* **43**(3), 443-457.
- Franchini, M. and Pacciani, M., 1991. Comparative analysis of several conceptual rainfall-runoff models. *J.Hydrol.*, **122**:161-219.
- Franchini, M. and Todini, E., 1988. PABL: A parabolic and backwater scheme with lateral inflow and outflow. *5th IAHR Int. Symp. Stochastic Hydraulics, Birmingham, UK*.
- Fuchs, M., 1973. The estimation of evapotranspiration. In B.Yaron, E. Danfors and Y. Vaadia (Eds). *Arid Zone Irrigation*. New York. pp 241-247.
- Gan T. Y., 1988. Application of scientific modelling of hydrological response from hypothetical small catchments to assess a complex conceptual rainfall runoff model. Water Resources Series Technical reports no. 111. Department of Civil Engineering, University of Washington, Seattle, Washington

- Gan, T. Y. and Biftu, G. F., 1996. Automatic calibration of conceptual rainfall-runoff models: Optimization algorithms, catchment conditions, and model structure. *Water Resour. Res.*, **32**(12), 3513-3524.
- Gan, T. Y., Dlamini, E. M. and Biftu, G.F., 1997. Effects of model complexity and structure, data quality, and objective functions on hydrologic modeling, *J. Hydrol.*, **192**: 81-103.
- G*rgens, A. H. M., 1983. Reliability of calibration of monthly rainfall-runoff model: the semiarid case. *Hydrolo. Sci. J.* **28**(4), 485-498
- Haan, C.T., 1972. A water yield model for small watersheds. *Water Resour. Res.* **8**(1), 28-69.
- Harwell Subroutine Library, 1974. Subroutine VA05A, 4p.
- Hassan, A., 1984. Stochastic monthly water balance - Subcatchments of upper Awash Basin. MSc. Thesis, Laboratory of Hydrology VUB, Brussels, Belgium.
- Helsel, D.R. and Hirsch, R.M., 1992. Statistical Methods in Water Resources, Elsevier Sciences Publishers Amsterdam, The Netherlands.
- Holland, J. H., 1975. Adaptation in natural and artificial systems. University of Michigan Press. Ann Arbor, Michigan.
- Hooke, R. and Jeeves, T.A., 1961. Direct search solutions of numerical and statistical problems, *Journ. Assoc. Comput. Mach.*, Vol. 8(2), 212-229.

- Horton, R.E., 1939. The role of infiltration in the hydrologic cycle, *Trans. Am. Geophys. Union*, vol. 14, pp.446-460.
- Hsu, Kuo-Iin, Gupta, H.V. and Sorooshian, S., 1995. Artificial neural network modelling of the rainfall-runoff process. *Water Resour. Res.* **31** (10), 2517-2530.
- Hughes, D. A. and Metzler, 1998. Assessment of three monthly rainfall-runoff models for estimating the water resources yield of semi-arid catchments in Namibia. *Hydrol. Sci. J.* **43**(2), 283-297.
- Hughes, D. A., 1982. Conceptual catchment model parameter transfer studies using monthly data from Southern Cape Coastal Lakes Region. Report 1/82. Hydrological Research Unit, Rhodes University, Grahamstown.
- Hughes, D. A., 1995. Monthly rainfall runoff models applied to arid and semi-arid catchments for water resource estimation purposes. *Hydrol. Sci. J.* **40**(6), 751-769.
- Hughes, D. A., 1997. Southern African "FRIEND"- The application of rainfall-runoff models in SADC Region. WRC Report No. 235/1/97. Institute for Water Research Rhodes University.
- Kalman, R.E., and Bucy, R., 1961. New results in linear filtering prediction *J. Basic Eng., (ASME)*, 83D: p95-108.
- Kalman, R.E., 1960. A new approach to linear filtering and prediction problems. *J. Basic Eng., (ASME)*, 82D: p35-45
- Kohler, M.A. and Linsley, R.K., 1951. Predicting the runoff from storm rainfall. U.S. Weather Bureau Research Paper 34.
- Kuczera, G., 1983. Improved parameter inference in catchment models. 1, Evaluationg parameter uncertainty, *Water Resour. Res.* **19**(5), 1151-1162.
- Li, C., 1995. Further development of monthly water balance models in arid and semi-arid and areas in China. MSc. Thesis, Laboratory of Hydrology. VUB, Brussels, Belgium.

- Makhlouf, Z. and Michel, C., 1994. A Two parameters monthly water balance model for France watersheds, *J. hydrol.* **162**: 299-318.
- Mandeville, A.N., O'connell, P.E., Sutcliffe, J.V. and Nash, J.E. 1970. River Forecasting through conceptual models part III.- The Ray catchment at Grendon Underwood. *J. Hydrol.* **11**: 109-128.
- McMahon, T.A. and Mein, R.G., 1978. Reservoir capacity and yield. Elsevier Scientific publishing company, Amsterdam.
- Misganaw D., 1989. Analysis of Drought in Ethiopia based on Nile River flow records: In the Proceedings of the Sahel Forum - The state- of- the-art of Hydrology and Hydrogeology in the Arid and Semiarid Areas of Africa Ouagadougou, Burkina Faso 18-23 February 1989.
- Moore, R.J., 1989. Hydrological Modelling for water management in arid and semiarid areas of Africa: In the Proceedings of the Sahel Forum - The state- of- the-art of Hydrology and Hydrogeology in the Arid and Semi-arid Areas of Africa Ouagadougou, Burkina Faso 18-23 February 1989.
- Moreda, F. and Bauwens W., 1997. Conceptual monthly water balance models applied to arid and semiarid catchments. Paper presented on 5th Scientific Assembly of IAHS in workshop Flow forecasting under conditions of limited data. Rabat, Morocco. 12p.
- Moreda, F. and Bauwens W., 1998. A conceptual 10-day water balance model for semi-arid catchments. Proceedings of the 18th AGU Annual HYDROLOGY DAYS. Hydrology days publications, 57 Sleby Lane, Antherton, CA. pp 211-221.
- Moreda, F. Vandewiele, G., Demaree, G. and Bauwens, W., 1998. Application of pure run-off models in low flow analysis of Awash River basin in Ethiopia. In Demaree, G. Alexander, J. and De Dapper, M. Proc. of International conference "Tropical Climatology, Meteorology and hydrology." pp. 532-555.
- Mott MacDonald and Partners, 1990. Country report: Zambia Sub Saharan Africa. Hydrological Assessment SADC Countries, UK.

- Nash, J.E., 1958. The form of instantaneous unit hydrograph. IUGG Gen. Assem. Toronto, Vol. III, IAHS Publ.No. 45. p114-121.
- Nash, J.E., 1959. Systematic determination of unit hydrograph parameters. *Journal of Geophysical Research* 64(1): 111-115.
- Nash, J.E., 1960 A unit hydrograph study, with particular reference to British catchments. *Proc. Inst. Civ. Eng. (London)* 249-282.
- Nash, J.E. and Barsi, B.I., 1983. A hybrid model for flow forecasting catchments. *J. Hydrol.* **65**(3):125-137.
- Nash, J.E. and Sutcliffe, J., 1970. River flow forecasting through conceptual models, Part I A discussion of principles. *J. Hydrol.* **10**: 282-290.
- Natale, L. and Todini, E., 1976. A stable estimator for linear models II: real hydrological application. *Water Resour. Res.* **12**(4) 672-676.
- Nedler, J. A and Mead, R., 1965. A simplex method for function minimization. *Computer J.* **7**: 308-313.
- Ni-Lar-Win, 1994. Contribution to rainfall runoff modelling on basin scale. VUB Hydrologie-(26), Brussels.
- O' Connell, P. E. and Todini, E., 1996. Modelling of rainfall, flows transport in hydrological systems: an overview. *J. Hydrol.* **175**: 3-16.
- O'Connell, P.E., Nash, J.E. and Farrell, J.P., 1970. River flow forecasting through conceptual models, Part II . *J. hydrol.* **10**: 317-329.
- Palmer, W.C., 1965. Meteorologic drought. Research Paper U.S. Weather Bur., 45, 58p.
- Philip, J.R., 1957. Theory of infiltration: 1. The infiltration equation and its solution. *Soil Sci.* **83**(5), 345-357.
- Pitman, W.V., 1973. A mathematical Model for Generating River flows from Meteorological Data in South Africa, Report 2/73, Hydrological Research Unit, University of the Witwaterstand, Johannesburg.

- Pitman, W.V., 1978. Flow generation by catchment models of different complexity - a comparison of performance. *J. Hydrol.* **38**: 59-70.
- Price, W.L., 1987. Global optimization algorithm for a CAD workstation, *Journal of Optimization Theory and Applications*, **55**(1), 133-146.
- Refsgaard, J. C. and Storm, B., 1995. MIKE SHE. In: V.P. Singh (Ed.). Computer Models of Watershed Hydrology. Water Resources Publications, Highlands Ranch, CO, pp 809-846.
- Roberts, P.J.T., 1978. A comparison of performance of selected conceptual models of the rainfall runoff process in semi-arid catchments near Grahamstown, Report 1/78, Hydrological Research Unit. Rhodes University, Grahamstown.
- Roberts, P.J.T., 1979. Model FLEXIFIT: A conceptual rainfall-runoff model for extension of monthly runoff records. Dept. of Environment Affairs, Hydrological Research institute, Tech. Report TR98.
- Rockwood, D. M., Davis, E. D. and Anderson, J.A., 1972. User manual for COSSARR model. US Army Engineering Division, North Pacific, Portland, OR.
- Rockwood, D. M. and Nelson, M.L., 1966. Computer application to transform flow synthesis and reservoir regulation. IV Int. Conf. Irrig. Drain.
- Rosenbrock, H.H., 1960. An automatic method for finding the greatest or least value of a function, *Computer Journal*, Vol. 3, 175-184.
- Salas, J.D., Tabios III, G.Q. and Obeyesekere, J.T.B., 1986. Seasonal model for watershed simulation, *Users Manual*, Dept. of Civil Engineering, Colorado State University.
- Seleshi, Y., 1996. Stochastic Predictions of summer rainfall amounts over the northeast African highlands and over India. Ph.D. Thesis, Laboratory of Hydrology Free University Brussels, Belgium. 351p.
- Servat, E. and Dezetter, A., 1993. Rainfall-runoff modelling and water resources assessment in northwestern Ivory Coast. Tentative extension to ungauged catchments. *J. Hydrol.*, **148**: 231-248.

- Singh, V.P. and Xu, C.-Y., 1997. Evaluation and generalization of 13 mass-transfer equations for determining free water evaporation. *Hydrological processes*. **11**: 311-323.
- Singh, V.P., 1992. Elementary Hydrology. Prentice Hall, Englewood Cliffs. 973p.
- Sorooshian, S., 1981. Parameter estimation of rainfall runoff Models with Heteroscedastic streamflow errors: Non informative data case, In: Y. Haimes and J. Knolles (Eds.), Water and related land resources systems, IFAC symposium, Cleveland, Ohio, May 28-31, 1980. Pergamon Press, New York N.Y., pp. 477- 485.
- Sorooshian , S. and Dracup, J.A., 1980. Stochastic parameter estimation procedures for hydrologic rainfall-runoff models: Correlated and heteroscedastic cases, *Water Resour. Res.* **16**(2), 430-442.
- Sorooshian, S., and Gupta, V.K., 1995. Model calibration. In: V.P. Singh (Ed.). Computer Models of Watershed Hydrology. *Water Resources Publications*, Highlands Ranch, CO, pp23-68.
- Sorooshian, S., Gupta, V.K., and Fulton J.L., 1983. Evaluation of maximum likelihood parameter estimation techniques for conceptual rainfall-runoff models- influence of calibration data variability and length on model credibility, *Water Resour. Research*, **19** (1), 251-259.
- Starosolszky, O., 1987. Applied surface hydrology. *Water Resources Publications*, Littleton, CO, p.526.
- Szilagyi, J. and Parlange M. B., 1998. Base flow separation based on analytical solution of the Boussinesq equation. *J. Hydrol.* **204**: 251-260.
- Thornthwaite, and C. W., Mather, J.R., 1955. The water balance. *Publ. Climatol. Lab. Dresel Inst. Technol.* **8**(1), 1-104
- Thornthwaite, C. W. 1948. An approach toward a rational classification of climate. *Geog. Rev.* **38**(1), 55-94.
- Todd, D.K., 1980. Groundwater Hydrology. 2nd ed. John Wiley & Sons, Inc, New York.

- Todini, E. and Wallis, J. R., 1978. A real time rainfall-runoff model for an on-line flood warning system. Proc. AGU Chapman Cof. Appl. Kalman Filtering Tech. Dep. Civ. Eng. University of Pittsburgh, Pa.
- Todini, E., 1978. Mutually interactive state parameters (MISP) estimation. Proc. AGU Chapman Cof. Appl. Kalman Filtering Tech. Dep. Civ. Eng. University of Pittsburgh, Pa.
- Todini, E., 1988. Rainfall-runoff modelling- past, present and future. *J. Hydrol.* **100**:341-352.
- Todini, E., 1996. The ARNO rainfall-runoff model. *J. Hydrol.* **175**:339-382.
- Todini, E., and Bossi, A., 1986. PAB (Parabolic and backwater) an unconditionally stable flow routing scheme particularly suited for real time forecasting and control. *J. Hydraul. Res.* **24**: 405-424.
- UNESCO, 1979. Map of the world distribution of arid regions, MAB Technical note 7. UNESCO.
- Van der Beken, A., 1977. A monthly water balance model applied to two different watersheds 3rd International Symposium Fort Collins. Colorado. pp. 178-189.
- Van der Beken, A., 1977. and J. Byloos, J., 1977. A monthly water balance model including deep infiltration and canal losses. *Hydrol. Sci. Bull.* **22**(3), 341-351.
- Vandewiele, G.L. and Atlabachew, E., 1995. Monthly water Balances of ungauged catchments obtained by geographical regionalization. *J. Hydrol.* **170**: 277-291.
- Vandewiele, G.L. and Ni-Lar-Win, (1998). Monthly water balance models for 55 basins in 10 countries. *Hydrol. Sci. J.* **43**(5), 689-699.
- Vandewiele, G.L. Xu, C.Y and Ni-Lar-Win, 1992. Methodology and comparative study of monthly water balance models in Belgium, China and Burma. *J. Hydrol.*, **134**:315-347.

- Vandewiele, G.L., Xu, C.Y and Ni-Lar-Win, 1993. Methodology for constructing monthly water balance models on basin scale. VUB Hydrologie (20) *Second ed.* Brussels, Belgium.
- Vandewiele, G.L., Xu, C.Y and Huybrechts, W., 1991. Regionalization of physically based water balance models in Belgium. Application to ungauged catchments. *Water Resource Mangement* **5**: 199-208.
- Verma, R.D., 1979. A physical model of the rainfall-runoff relationships for semiarid lands. In The hydrology of areas of low precipitation, (proceedings of the Canberra Symposium). *IAHS Publ. no.* 128.
- Wang, Q.J., 1991. The genetic algorithm and its application to calibrating conceptual rainfall - runoff models. *Water Resour. Res.* **27**(9), 2467-2471.
- WMO, 1975. Inter comparison of hydrological models. *WMO publ.*, Geneva.
- WMO, 1994. Data Review and coding. In Guide to Hydrological Practice. Fifth ed. *WMO - No 168*. pp. 316.339.
- Xu, C. Y. and Singh, V. P. 1998. A review on monthly water balance models for water resources investigations. *Water Resources Management* **12**: 31-50.
- Xu, C. Y., 1988 Regional study of monthly rainfall runoff models. MSc. Thesis. Laboratory of Hydrology, VUB, Brussels, Belgium.
- Xu, C. Y., 1992. Monthly water balance models in different climatic regions. VUB Hydrologie- (22), Brussels, Belgium.
- Xu, C. Y., Seibert, J. and Halldin, S., 1995. Regional water balance modelling in the NOPEX area: development and application of monthly water balance models. *J. Hydrol.* **180**: 211-236.
- Yapo, P.O., Gupta, H.V., and Sorooshian, S., 1996. Automatic calibration of conceptual rainfall - runoff models: Sensitivity to calibration data. *J. Hyrol.* **181**: 23-48.

-
- Yapo, P.O., Gupta, H.V., and Sorooshian, S., 1998. Multi-objective global optimization for hydrological models. *J. Hyrol.* **204**: 83-97.
- Zhao, R.J, Zhaung, Y.L, Fang, L.R., Lui, X.R. and Zhang, Q.S., 1980. The Xinanjiang model. In Hydrological Forecasting, Proceedings of the Oxford Symposium, *IAHS publ. No* 129.

APPENDIX A The VUBMOD for Windows

APPENDIX B Orders of magnitude of the model parameters